University of Oviedo

Instituto Universitario de Oncología del Principado de Asturias

Programa de Doctorado "Investigación en Cáncer"

New animal models and next-generation sequencing approaches for the functional analysis of cancer progression

Doctoral Thesis

Miriam Fanjul Fernández

Oviedo 2013

UNIVERSIDAD DE OVIEDO
Vicerrectorado
de Internacionalización y Postgrado

CENTRO INTERNACIONAL DE POSTGRADO
CAMPUS DE EXCELENCIA INTERNACIONAL

RESUMEN DEL CONTENIDO DE TESIS DOCTORAL

1.- Título de la Tesis	
Español/Otro Idioma:	Inglés: New animal models and next-generation sequencing approaches for the functional analysis of cancer progression

2.- Autor	
Nombre: MIRIAM FANJUL FERNÁNDEZ	
Programa de Doctorado: Investigación en cancer (Mención de Calidad)	
Órgano responsable: INSTITUTO UNIVERSITARIO DE ONCOLOGÍA	

RESUMEN (en español)

Durante esta Tesis doctoral, hemos intentado contribuir al estudio de las claves moleculares que subyacen a la progresión tumoral mediante dos perspectivas diferentes pero complementarias. Así, en la primera parte de este trabajo hemos llevado a cabo una aproximación experimental muy específica centrada en el análisis de la relevancia oncológica *in vivo* de la metaloproteasa Mmp-1a, a través de la generación y caracterización de ratones deficientes en el gen que la codifica. Tras inducir diversos modelos de cáncer en ratones deficientes en *Mmp1a* y en los correspondientes controles, hemos demostrado que esta proteasa desempeña una función pro-tumoral en cáncer de pulmón y hemos descrito los mecanismos moleculares responsables de dicha actividad. No obstante, el cáncer es una enfermedad causada por la acumulación de múltiples daños genéticos en las células tumorales. Por ello, en la segunda parte de esta Tesis doctoral y gracias al desarrollo y puesta a punto de las técnicas de ultrasecuenciación en nuestro laboratorio, nos propusimos abordar desde una perspectiva global el estudio del paisaje mutacional del cáncer de cabeza y cuello. Este trabajo nos ha llevado a describir dos genes implicados en adhesión celular como nuevos supresores tumorales recurrentemente mutados en esta agresiva enfermedad. Finalmente, la integración de los estudios genómicos y funcionales con la información clínica de los pacientes estudiados, nos ha permitido abordar una nueva aproximación a la investigación oncológica que en un futuro puede conducir a terapias personalizadas para cada paciente.

RESUMEN (en Inglés)

In this Thesis, we have tried to contribute to a better understanding of the mechanisms underlying cancer progression through two opposite but complementary perspectives. Thus, in the first part of this work, we have performed a very specific experimental approach focused on the *in vivo* analysis of the oncological relevance of the mouse metalloproteinase Mmp-1a, through the generation and characterization of *Mmp1a*-deficient mice. Based on the results obtained from several cancer-induction protocols in these mutant animals and in their corresponding controls, we have shown that this protease plays a pro-tumorigenic role in lung cancer. Moreover, we have defined the molecular mechanisms responsible for this oncogenic activity of Mmp-1a. Nevertheless, cancer is a genetic disease caused by accumulation of multiple alterations in the genome of somatic cells. Accordingly, in the second part of this work, and by taking advantage of the recent development of new-generation sequencing approaches, we have moved from the functional study of specific genes involved in cancer to the global genomic analysis of aggressive tumors such as head and neck carcinomas. This study has allowed us to identify *CTNNA2* and *CTNNA3* as novel recurrently mutated genes in these human malignancies. The integration of these genomic data with the functional analysis of the mutated genes and with the clinical information of the corresponding patients may serve as a representative example of the forthcoming and necessary personalized medicine for cancer patients.

SRA. DIRECTORA DEL INSTITUTO UNIVERSITARIO DE ONCOLOGÍA/

INTRODUCTION

Genetic instability is a key phenomenon for tumor development and progression. The whole set of point mutations, chromosomal rearrangements and epigenetic variations occurring within a neoplastic cell and leading to changes in gene sequence, structure, copy number and expression, provide transformed cells with a wide range of potent biological abilities that convert them into entities with ability to proliferate autonomously. These functional capabilities include the development of an unlimited proliferative potential, the ability to circumvent negative growth regulation, host-induced cell death and immune destruction, the induction of angiogenesis and the activation of mechanisms of invasion and metastasis (1). Acquisition of these multiple hallmarks largely depends on a succession of random alterations in the genome of neoplastic cells. At the end of this competitive race, mutant genotypes that have conferred the most powerful selective advantages will enable malignant cells to dominate basic physiological processes of the host, finally assuming the control of a local tissue environment or, in a worst scenario, of the whole organism.

Understanding how cancer cells acquire the properties that enable them to survive and proliferate despite the mechanisms that have emerged to constrain them, is critical to develop strategies aimed at recovering the physiological balance. Accordingly, the identification of genes and signaling pathways implicated in cancer progression has been an important focus of research along the last decades in the field of cancer (2).

Tumor progression is a complex multistep genetic process in which both cancer cells and the tumor microenvironment undergo molecular changes that facilitate the invasive properties of malignant cells. Thus, cancer invasion and metastasis are landmark events that transform a locally growing tumor into a systemic, metastatic and life-threatening disease. Most cancer deaths are consequence of the completion of a metastasis program carried out by neoplastic cells (3). The selective process of metastasis requires that cancer cells successfully complete several sequential steps: they must detach from the primary tumor, locally invade the surrounding tissue, intravasate into lymphatic or blood vessels, survive to the host immune defense, spread to the capillary bed of distant

organs, extravasate in a new tissue and finally, adapt to this foreign microenvironment in ways that allow cell proliferation and the formation of a macroscopic secondary tumor **(Figure 1)**. However, tumor cells do not act in isolation, but rather subsist in a rich microenvironment provided by resident fibroblasts, endothelial and immune cells, as well as by the extracellular matrix (4). In fact, tumor cells initiate an active cross-talk with the surrounding stroma, mainly mediated by direct cell-cell contact or paracrine cytokine and growth factor signaling. Such signaling may activate the tumor microenvironment at the primary and secondary tumor sites, generating morphological changes and allowing or even supporting tumor outgrowth, invasion and metastasis. Hence, extracellular matrix turnover is a necessary step for tumor progression and requires the cooperation of multiple proteolytic systems such as cathepsins, serine proteases, ADAMs (a disintegrin and metalloprotease), ADAMTSs (ADAMs with thrombospondin domains) and matrix metalloproteinases (MMPs) (5-7).

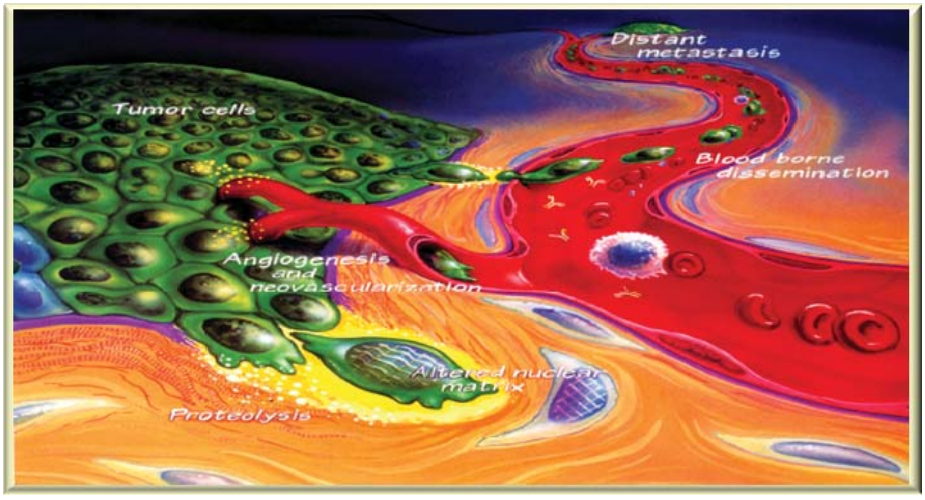

***Figure 1. The** different steps of the metastatic process*

The extracellular matrix (ECM) is a complex meshwork of proteins and proteoglycans that provides structure and support to cells and tissues. In this context, MMPs were initially considered as demolition agents responsible for the matrix degradation to create pores allowing neoplastic cells to reach blood vessels, and facilitating the metastatic process. However, nowadays it is well known that MMPs are implicated in all stages of cancer progression, including

tumor growth, cell migration and invasion and angiogenesis **(Figure 2)** (8). To this aim, MMPs are able to regulate cell-cell and cell-matrix junctions, as well as cell proliferation and apoptosis, either directly or through the processing of a wide variety of bioactive molecules such as growth and angiogenic factors, cytokines or cell receptors (9). As an example of this activity, PAR1 (protease-activated receptor 1) receptor, located at the surface of breast cancer cells, undergoes proteolytic activation mediated by MMP-1 produced by surrounding stromal cells, triggering an intracellular signalling pathway which promotes cell proliferation (10). Notwithstanding, MMPs may also play antitumor roles throughout the different cancer progression steps, being then associated with good clinical evolution. Thus, expression of MMP-8 in breast cancer is associated with a lower incidence of metastasis in lymph nodes (11). Hence, in addition to their classic role as degradative enzymes of the extracellular matrix, MMPs play more specific and subtle functions in tumor progression and metastasis than initially considered. Therefore, the contribution of these proteases to tumor development must be specifically analyzed in each stage of the progression of this disease.

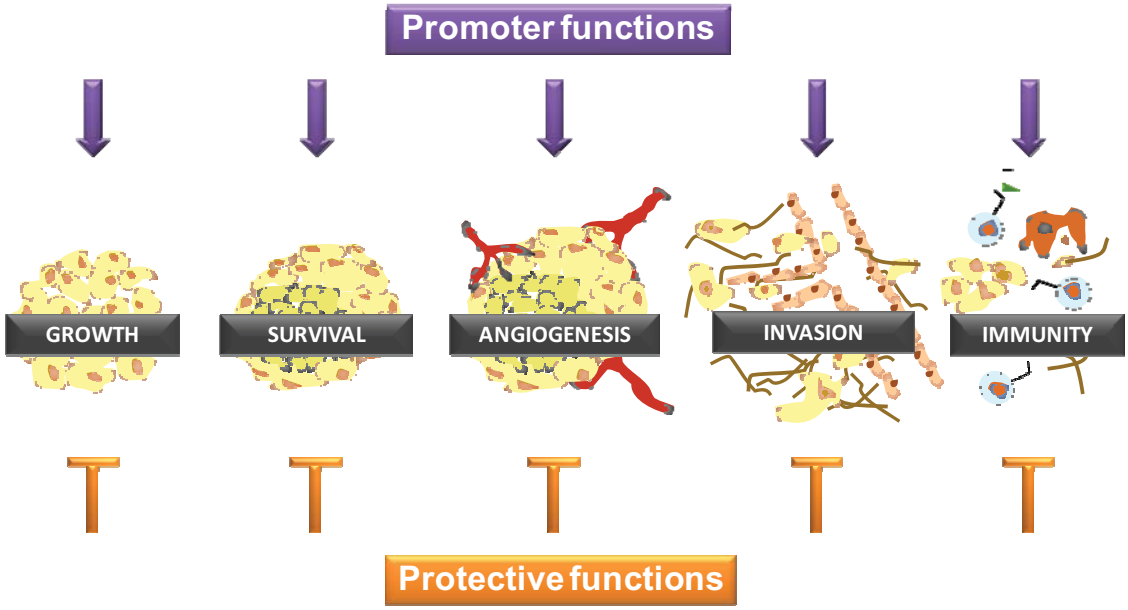

Figure 2. *Dual roles displayed by MMPs during tumor progression*

Matrix metalloproteinases: classification and properties

MMPs comprise a large family of zinc-dependent endoproteinases, collectively capable of degrading all extracellular matrix components. These enzymes are found in all kingdoms of life and belong to the metzincin superfamily of metalloproteinases, which are characterized by the presence of a catalytic zinc atom in their active center followed by a conserved methionine residue (12). To date, at least 25 different vertebrate MMPs have been identified, 24 of which are present in humans, including two recently duplicated genes encoding MMP-23 (13).

MMPs are synthesized as zymogens with a signal peptide which leads them to the secretory pathway. Then, these enzymes can be secreted from the cell or anchored to the plasma membrane, thereby confining their catalytic activity to the extracellular space or to the cell surface, respectively. Interestingly, recent studies have reported that several MMP family members, such as MMP-1 (14), MMP-2 (15), MMP-11 (16) and MMP-13 (17), can be found as intracellular proteins, although their functions at this subcellular location are still unclear. The archetypal MMPs consist of a propeptide with a cysteine-switch motif, a catalytic metalloproteinase domain with the characteristic zinc-binding site, a linker peptide of variable length and a hemopexin domain.

Nevertheless, the family of MMPs has evolved into different groups by removing some domains or by incorporating others that are absent in the previously described basic structural core, highlighting the complexity of this group of enzymes **(Figure 3)**. On the basis of their domain organization, MMPs can be classified in four different groups: archetypal MMPs, matrilysins, gelatinases and furin-activatable MMPs.

Due to the large number of diseases in which MMPs are implicated, production of these enzymes must be strictly controlled in time and space to maintain a proper homeostasis of the extracellular and pericellular environment. To this end, MMP expression and activity can be regulated at different levels

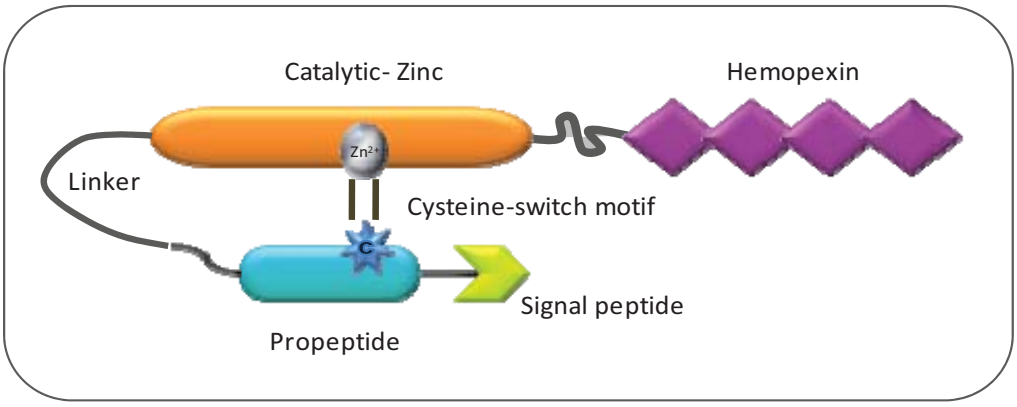

Figure 3. *Characteristic domain arrangement of an archetypal MMP.*

including gene transcription, proenzyme activation and endogenous inhibition, which act in a coordinated manner to confine the diverse MMP proteolytic activities to those conditions and locations where they are necessary. Tissue specificity is achieved through the combination of multiple signaling pathways with a wide repertoire of transcription factors that regulate the expression of MMPs by binding to their promoters (18). Furthermore, epigenetic regulatory mechanisms as DNA methylation (19) or acetylation of histones (20) can also contribute to modulate both activation and repression of *MMP* gene expression. Similarly, mRNA stability, translational efficiency and microRNA-mediated regulatory mechanisms have been described as modulators of MMP expression (21,22). Nevertheless, these stringent regulatory mechanisms are frequently altered in many pathological conditions, contributing to the development of diseases where extracellular matrix is substantially modified, such as pulmonary fibrosis, atherosclerosis or cancer.

Polymorphisms in human *MMP* genes may also modify its expression by altering the interaction between transcription factors and their binding sites located in the corresponding promoter regions. The resulting higher or lower transcriptional activity of *MMP* genes is in turn associated with a higher or lower susceptibility to cancer development and, in some cases, with a better or worse prognosis. A correlation between single nucleotide polymorphisms (SNPs) and susceptibility to cancer has been described for several MMPs (23,24).

Therefore, taking into account the precise and sometimes subtle role that MMPs play in a large number of different diseases, as well as the dual activities they can display, acting as protumor or antitumor proteases, their function should be carefully analyzed. In this regard, it is remarkable that genetically-engineered mouse models have significantly contributed to our understanding of cancer biology. They have been proven to be useful in validating gene functions, identifying novel cancer genes and tumor biomarkers, gaining insight into the molecular and cellular mechanisms underlying tumor initiation and multistage processes of tumorigenesis, and providing better clinical models in which to test novel therapeutic strategies (25).

Mouse models for functional analysis of MMPs

Over the last two decades, the generation of genetically-modified mouse models has become one of the most powerful strategies to study gene function *in vivo*. Genetic engineering approaches have allowed the modulation of gene expression through gain-of-function (*transgenic*) or loss-of-function (*knock-out*) *in vivo* models. To date, many transgenic and knock-out mice have been generated to analyze the effects of altering MMP activity in a variety of physiological and pathological processes. Likewise, these strategies have provided the opportunity to validate candidate substrates, which are the essential partners to uncover protease function (26).

A total of 17 out of the 23 murine *Mmp* genes have already been knocked-out. However, despite this broad landscape of gene targeting, the vast majority of these constitutive knock-out mice display subtle spontaneous phenotypes. Among the collagenases, deficiency in collagenase-3 (Mmp-13) leads to developmental defects characterized by impaired bone formation and remodeling due, in part, to the lack of appropriate type II collagen cleavage (27,28). However, mice deficient in collagenase-2 (Mmp-8) show no overt physiological abnormalities (29). Likewise, the absence of any of the three stromelysins does not cause major alterations, with the exception of *Mmp3*-null mice, whose mammary glands show deficient secondary branching morphogenesis (30). Deficiency in any of the two

gelatinases is also characterized by certain defects in bone biology. Thus, mice deficient in *Mmp9* have delayed long bone growth and development due to impaired vascular invasion in skeletal growth plates (31). *Mmp2* deficiency causes disruption of the osteocytic networks and reduced bone density (32). Interestingly, the most severe phenotype among *Mmp* knock-outs is also associated with defects in skeletal development. In this sense, targeted inactivation of the *Mmp14* gene causes multiple abnormalities in the remodeling of skeletal and connective tissues, as well as defective angiogenesis, leading to premature death by 3-12 weeks after birth (33,34). In addition, mice deficient in *Mmp20* have defects in tooth development due to impaired amelogenin processing (35). Remarkably, these bone abnormalities shown in *Mmp* knock-outs phenocopy the human skeletal syndromes caused by loss-of-function *Mmp* mutations (36-38). The remaining *Mmp*-null mice generated to date show no major physiological alterations, although it is important to emphasize that all available *Mmp* knock-out models are constitutive, thus leading to the possibility of enzymatic compensation as a way to circumvent the absence of the targeted gene. Another possible explanation for the lack of severe phenotypes in *Mmp*-null mice is the enzymatic redundancy among different members of the family, which share many substrates *in vitro*. The recent generation of double *Mmp* mutants has supported this hypothesis, and future studies in this direction may also argue for essential roles of certain MMPs in embryonic development, in addition to their known functions in postnatal tissue remodeling (39,40).

Despite early characterization of *Mmp* knock-outs did not provide major evidences about the biological relevance of this family of proteases, further analyses of these mouse models challenged by a series of pathogenic conditions have revealed the essential contribution of MMPs to a broad number of pathological processes. Among them, over the last 25 years, cancer has been the central disease supporting the promising field of MMP research. The first transgenic mouse models overexpressing different members of the family validated the initial assumption for the contributory effect of these matrix degrading enzymes to tumor progression (41-43), since high levels of MMPs often correlated with poor clinical outcome in cancer patients. However, the generation of new

genetically-modified animal models has demonstrated that certain MMPs, such as MMP-8 or MMP-12, contribute to tumor suppression (29,44-46). Furthermore, it has also been reported that other MMPs, including MMP-3 (47), MMP-9 (48), MMP-11 (49) and MMP-19 (50,51) play dual roles as pro- or anti-tumorigenic enzymes depending on tissue type and stage of the disease. Likewise, gain- or loss-of-function mouse models have allowed the identification of some of the *in vivo* substrates for these enzymes. This is another step forward in the complex relationship between MMPs and cancer, since many non-matrix bioactive molecules, such as growth factor receptors, chemokines, cytokines, apoptotic ligands or angiogenic factors, have been identified as substrates for MMPs (52). Altogether, these findings illustrate the diversity of MMP functions associated with cancer and provide explanations for the disappointing results of the first clinical trials based on the use of broad spectrum MMP inhibitors (53).

The increasing complexity of the *in vivo* functions of MMPs also affects many other pathological contexts, particularly those involving inflammatory conditions where MMP expression is frequently deregulated (54). In this sense, genetically-modified mice have been essential to demonstrate the relevance of these enzymes in prevalent human pathologies, such as rheumatic, pulmonary, cardiovascular and neurodegenerative disorders. Remarkably, these studies have also shown opposing and unexpected effects among different members of the MMP family on the progression of these diseases. Thus, and somewhat surprisingly, mice deficient in *Mmp2* or *Mmp3* develop more severe arthritis than control animals (55,56). Likewise, deficiency in *Mmp3* or *Mmp13* results in more stable atherosclerotic plaques (57,58). By contrast, deletion of *Mmp2* or *Mmp9* reduces the formation of the plaques and attenuates cardiac fibrosis after experimental myocardial infarction (59,60). In neuroinflammatory diseases, such as experimental autoimmune encephalomyelitis, which represents a murine model of human multiple sclerosis, MMPs also show opposite roles. Indeed, certain mouse MMPs, including Mmp-2, Mmp-7, Mmp-8 and Mmp-9 (61-63), contribute to the severity of the clinical symptoms of paralysis, whereas others, such as Mmp-12 (64), play protective functions. Similarly, the role of MMPs in respiratory disorders is very complex, since it is not clear yet whether MMPs up-regulation is

harmful in acute and chronic lung pathologies. Genetically-modified mice have demonstrated that lack of *Mmp2*, *Mmp8* or both *Mmp2*/*Mmp9* (65-67) increases the allergic response in a mouse model of asthma due to the failure in clearing inflammatory cells. Mice deficient in *Mmp10* also show more severe pulmonary inflammation and greater susceptibility to death following bacterial infection (68). By contrast, deletion of *Mmp7* or *Mmp12* is beneficial in chronic lung diseases, such as pulmonary fibrosis or emphysema (69,70).

Overall, the generation of gain- or loss-of-function mouse models has been essential to demonstrate the complex and even paradoxical roles that MMPs play in physiological and pathological processes (71). Likewise, these approaches have allowed the *in vivo* validation and identification of specific substrates, providing a better understanding of the mechanisms involved in the development of the diseases. Therefore, it is necessary to continue the detailed analysis of available *Mmp*-null mice, as well as to generate those *Mmp*-deficient mice that are currently unavailable. In this regard, it is noteworthy that to date, no mutant mice deficient in the mouse ortholog of human MMP-1 have been described. This is especially surprising if we consider that this collagenase was the founder member of the MMP family and many reports have described its strong association with the development and progression of human malignancies (72,73).

MMP-1 as an important mediator of tumorigenesis

Proteolytic remodeling of peritumoral extracellular matrix is an essential process in the development of a malignant tumor. Numerous studies have shown the overexpression of interstitial collagenases in neoplastic tissues, suggesting a possible involvement of these proteases in the ability of such tumors to invade and spread. However, in addition to its participation in the later stages of the disease, we now know that collagenases are also involved in the generation of complex microenvironments that promote malignant transformation at the earliest stages of tumor formation (74).

Among the three identified interstitial collagenases, MMP-1 or collagenase-1 is the most widely expressed and its preferential ECM substrate is collagen type

III. This metalloproteinase is produced by a variety of cell types, including fibroblasts, macrophages, endothelial and epithelial cells, as well as by tumor cells themselves, suggesting the great variety of biological processes in which MMP-1 is involved (75,76). Interestingly, and despite basal expression of MMP-1 is low, multiple tumors produce high levels of this enzyme, being induced by many bioactive molecules, such as phorbol esters, growth factors and inflammatory cytokines (77).

The expression of MMP-1 is increased in colorectal carcinomas (78), esophageal carcinomas (79), metastatic melanomas (80) and lung adenocarcinomas (81). Similarly, several studies have associated its expression with the invasive capacity of breast cancer cells, enhancing the colonization of adjacent lymph nodes (82). Moreover, recent studies have identified *MMP1* as one of the four key genes required for the colonization in lung metastatic breast cancer (83). In all these circumstances, the expression of *MMP1* is associated with poor prognosis. However, the main limitation of these studies correlating MMP-1 levels with cancer progression derives from the lack of *in vivo* models that can contribute to exclude these findings from the list of secondary effects and prove them as the causative agent. The generation of these animal models has been severely hampered by the limited and sometimes contradictory information available on this collagenolytic system in the mouse. For a long time, the murine ortholog gene for human MMP-1 was attributed to a protease mainly expressed in uterine postpartum involution. However, the discovery in our laboratory of human collagenase-3 (MMP-13) completely changed this perspective and inaugurated a new stage in the investigation of the role of matrix metalloproteinases in cancer and other diseases (84). Currently, we know that the murine collagenolityc system is equivalent or even more complex than that of humans and consists of at least four genes located on chromosome 9. Two of these genes are the orthologs of collagenase-2 (MMP-8) and collagenase-3 (MMP-13), whereas surprisingly, detailed studies by Balbin *et al*. (85) showed the existence of two potential mice orthologs of human MMP-1. These genes encode proteins that were initially called McolA and McolB, and are currently known as MMP-1a and MMP-1b, respectively. Both proteins maintain a similar percentage of identities with human MMP-1 (63%

and 58% for the catalytic domain), but the subsequent functional analyses showed that only Mmp-1a has a significant collagenolytic activity.This fact is probably related to substantial changes occurred in MMP-1b at essential residues for the catalytic activity of MMPs. Furthermore, expression analyses of MMP1 revealed that both isoforms showed nearly undetectable levels in virtually all tissues analyzed; however, MMP-1a was clearly detected in placenta (85). Collectively, these results strongly suggested that Mmp-1a was the functional ortholog of human MMP-1, and opened a new avenue for the creation of *in vivo* models that may facilitate the study of the functional relevance of this protease in normal and pathological conditions, including cancer.

Cancer research: from genes to genomes

During the last years, our laboratory has been implicated in the analysis of protease-mediated mechanisms in life and disease, including cancer progression (26). However, the growing information about tumor biology as well as the development of new experimental approaches has prompted the necessity to adopt a new perspective in cancer research. Thus, to further understand the molecular mechanisms underlying tumor pathogenesis, we need to move from the analysis of individual genes to the global landscape offered by the study of cancer genomes.

It is almost forty years since the first studies demonstrating that cancer is a genetic disease, as assessed by the observation of specific chromosomal alterations associated with different types of leukemia (86). However, it is just four years since the first whole-genome sequence of a human malignant tumor was reported (87). Since then, the creation of the International Cancer Genome Consortium and the launching of The Cancer Genome Analysis project, have provided critical insights into the etiology of this complex disease (88,89). The impressive development of the field of cancer genomics has been enormously facilitated by the application of next-generation sequencing technology. Hence, there has been a rapid progression from targeted gene re-sequencing using PCR and Sanger sequencing to either targeted, whole-genome, or whole-transcriptome

sequencing using these massive parallel sequencing platforms. Over the past few years, we have seen next-generation technologies being applied in a variety of contexts, including *de novo* whole-genome sequencing, re-sequencing of genomes for variant identification, profiling mRNAs and other small and non-coding RNAs and methylation patterns. All these experimental approaches have had an extraordinary influence at multiple levels in cancer research.

Next-generation sequencing for cancer genome analysis

The introduction in 1977 of the Sanger method for DNA sequencing, based on the chain-terminating didesoxynucleotide analogues, transformed biomedical research (90). Over the past 30 years, this first-generation sequencing technology has been universally used for elucidating the nucleotide sequence of DNA molecules. However, the launching of new large-scale projects, including those implicating whole-genome sequencing of cancer samples, has made necessary the development of new methods that are widely known as next-generation sequencing technologies (91). These techniques are more sensitive than Sanger methods and can detect somatic mutations even when they are present only in a subset of tumor cells. Moreover, these new sequencing strategies are quantitative and can be used to simultaneously determine both nucleotide and copy number variations. They can also be coupled to other procedures such as those involving paired-ends reads, allowing the identification of multiple structural alterations such as insertions, deletions and rearrangements, commonly occurring in cancer genomes. The aforementioned next-generation or massive parallel DNA sequencing technology is embodied in several different instrument platforms: Roche 454, Illumina/Solexa, Life/APG´s SOLiD3, Helicos BioSciences/Heliscope, and Pacific Bioscience/PacBio RS. The main features of these sequencing platforms are shown in **Table 1**. It is also remarkable the very recent introduction of the Polonator G.007 instrument, an open source platform with freely available software and protocols, the Ion Torrent´s semiconductor sequencer, as well as those involving self-assembling DNA nanoballs or nanopore technologies. These new machines are driving the field toward the era of third-generation sequencing,

which brings enormous clinical interest as it can substantially increase speed and accuracy of analysis at reduced costs and facilitate the possibility of single molecule sequencing of human genomes (92).

***Table 1**. Comparative analysis of next-generation sequencing platforms*

Platform	Library/template preparation	Sequencing method	Average read-length (bases)	Run time (days)	Gb per run	Instrument cost (US$)	Comments
Roche 454 GS FLX	Fragment, Mate-pair Emulsion PCR	Pyrosequencing	400	0.35	0.45	500,000	Fast run times High reagent cost
Illumina HiSeq2000	Fragment, Mate-pair Solid-phase	Reversible terminator	100-125	8 (mate-pair run)	150-200	540,000	Most widely used platform Low multiplexing capability
Life/APG's SOLiD 5500xl	Fragment, Mate-pair Emulsion PCR	Cleavable probe, sequencing by ligation	35-75	7 (mate-pair run)	180-300	595,000	Inherent error correction Long run times
Helicos BioSciences HeliScope	Fragment, Mate-pair Single molecule	Reversible terminator	32	8 (fragment run)	37	999,000	Non-bias template representation High error rates
Pacific Biosciences PacBio RS	Fragment Single molecule	Real-time sequencing	1000	1	0.075	N.A.	Greatest potential for long reads Highest error rates
Polonator G.007	Mate-pair Emulsion PCR	Non-cleavable probe, sequencing by ligation	26	5 (mate-pair run)	12	170,000	Least expensive platform Shortest read lengths

Accordingly, next generation sequencing approaches represent the newest entry into the cancer genome decoding area and have already been widely applied to cancer research. Thus, and as mentioned above, the first group to apply these methodologies to whole cancer genomes was that of Ley *et al.*, who in 2008 reported the sequencing of the entire genome of a patient with acute myeloid leukemia (AML) using the Illumina/Solexa platform (87). The comparison of this sequence with of the one from the normal tissue from the same patient enabled to identify eight genes with point mutations harboured only in the tumor genome. Follow-up whole genome studies for this malignancy, identified three frequently mutated genes (IDH1, IDH2 and DNMT3A) that, either alone or in combination with other recurrent mutated genes, predict poor outcomes for those AML patients whose genomes contain the mutation (93-95). These works established the basic approach to whole-genome somatic mutation studies and since then, numerous whole-genome data from different tumors have been reported for a high variety of human malignancies.

The first solid cancer to undergo whole-genome sequencing was a malignant melanoma that was compared to a lymphoblastoid cell line from the same patient (96). Impressively, a total of 33,345 somatic base substitutions were identified, with 187 non-synonymous substitutions in protein-coding sequences, at least one order of magnitude higher than any other cancer type. Most somatic base substitutions were C>G changes, which is consistent with ultraviolet light exposure mutation signatures previously reported in melanoma. Likewise, lung, prostate, and breast adenocarcinomas (97-99), as well as hematological neoplasias such as chronic lymphocytic leukemia (100), are among the first human tumors for which whole-genome sequence information has been made available. Additionally, the recent introduction of efficient methods of capture and sequencing of whole-exomes has provided an additional dimension to the study of genomic alterations present in cancer (101). In fact, whole-exome sequencing studies have allowed the rapid expansion of data on the mutational landscape characteristic of many different tumors (102,103).

All these works have opened a new avenue to more ambitious initiatives. Thus, recent studies have begun to elucidate the genomic changes that accompany metastasis evolution, through comparative analysis of primary and metastatic lesions. The first study applying next-generation sequencing methods to deciphering the mutation evolution of neoplastic cells throughout different cancer stages involved the analysis of three samples derived from the same patient: the primary basal-like ductal breast carcinoma, a brain metastasis generated eight months after the primary tumor was diagnosed, and a xenograft-propagated tumor derived from the primary lesion (104). The comparative sequence analysis showed a wide range of mutant allele frequencies in the primary tumor, which was narrowed in the metastatic and xenograft samples. These findings suggested that the primary tumor was significantly more heterogeneous in its cell populations compared to its matched metastatic and xenograft samples as these underwent selection processes during metastasis or transplantation (104). The second work aimed at evaluating, under a whole-genomic perspective, the genetic relationship between primary and metastatic lesions in human cancer, was based on sequencing the genomes of seven

pancreatic carcinomas and their corresponding metastatic lesions (105). This study revealed that clonal populations which give rise to distant metastases are mostly represented within the primary carcinoma, concluding that the genetic heterogeneity of metastases reflects the heterogeneity already existing within the primary carcinoma.

Thus, the main lesson learned from these first whole-genome metastasis studies has been that, although metastatic lesions harbour an increased number of genetic alterations, the majority of the alterations are already presented in the primary tumor. However, additional studies along this line are clearly needed to fully understand the potential for metastasis and the roles of specific mutations in the tendency of certain tumors to metastasize. In this regard, it is well-established that malignancies arising from epithelial tissues, such as head and neck carcinomas, progress to higher pathological grades of malignancy, finally resulting in local invasion and metastasis. Unfortunately, the available information about the genomic alterations and molecular mechanisms underlying these events is still very limited.

Molecular pathology of head and neck carcinomas

Head and neck carcinomas are a heterogeneous group of malignancies involving the oral cavity and oropharynx, nasopharynx, hypopharynx, larynx, nasal cavity and paranasal sinuses, as well as ear and salivary glands. Head and neck squamous cell carcinoma (HNSCC) represents more than 90% of all head and neck cancers and arises from the mucosa of the upper aerodigestive tract. With a worldwide incidence exceeding half a million cases annually, HNSCC poses a major health risk and is one of the leading causes of mortality in developing nations (106). The most significant risk factors to develop HNSCC remain tobacco and alcohol abuse. Nevertheless, oncogenic human papillomavirus (HPV) is now considered a potential causative agent in certain HNSCC subsites, specifically the oropharynx (107). In fact, oropharyngeal cancers are becoming more prevalent, which may be related to an increase in oral HPV infections. Other risk factors associated with this disease include dietary deficiencies, poor oral hygiene,

asbestos and indoor air pollution from fossil fuel combustion (108). Notably, and despite several therapeutic advances, survival has remained relatively unchanged over the past few decades. Accordingly, it is expected that a better understanding of the molecular and genetic alterations underlying the pathogenesis of head and neck carcinomas may result in the development of more effective preventative, diagnostic, and treatment strategies.

It is now well established that HNSCC is a heterogeneous disease, both at the molecular and clinical level, which arises from a multistage pathogenesis process (**Figure 4**). Thus, various subclasses of HNSCC can be distinguished at the histological level, from hyperplasia, dysplasia, carcinoma *in situ*, and invasive carcinoma to metastasis (109). Analysis of the genetic alterations underlying this tumor evolution has also convincingly demonstrated the existence of additional subclasses of HNSCCs. The first and most prominent distinction is the difference between tumors that are caused by infection with high-risk types of HPV (20%) and those that do not contain HPV (80%) (110). The HPV contains two oncogenes, E6 and E7, whose expression inactivates p53 and retinoblastoma (RB) respectively, causing perturbation of the cell cycle regulation, which is considered to be the onset of HPV-mediated carcinogenesis. These HNSCC cases usually have wild-type *TP53* and a favourable prognosis (111). The remaining 80% may be in turn split into two subgroups: those tumors that are characterized by many numerical genetic changes caused by high chromosome instability, which have mainly mutated *TP53* and show a poor prognosis, and those characterized by low number of genetic changes with *TP53* found mainly in a wild-type form (112).

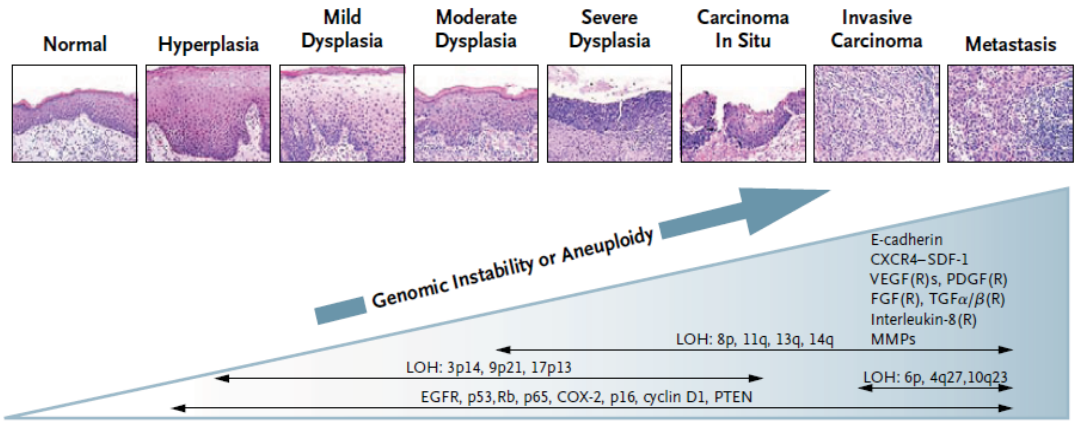

Figure 4. *Multistep progression model in head and neck carcinomas (113)*

A plethora of studies have been published on the identification of candidate cancer genes in the HNSCC pathogenesis. Point mutations, together with chromosomal alterations leading to activation or inhibition and loss or gain of crucial genes involved in the regulation of key cancer pathways, are the principal known genetic events driving this HNSCC-multistep process. Thus, genes involved in the regulation of cell cycle like *TP53* are found recurrently mutated in 60-80% of HNSCC cases (114). The same is true for *CDKN2A* located on chromosome 9p21 and encoding $p16^{INK4A}$, and *PTEN* located on 10q, which are commonly inactivated by mutation or chromosome loss (115,116). These genetic alterations are already frequently found in pre-neoplastic lesions (117). Likewise, *FHIT* mapping at 3p, *SMAD4* and transforming growth factor-β (*TGFβ*) receptor located at 18q, and tyrosine phosphatase receptor S (*PTPRS*) on chromosome 19p13, are other target locus which undergo recurrent loss of heterozygosity (LOH) or inactivating mutations in HNSCCs (118-120). Despite loss of function seems to be the most prominent event in HNSCC carcinogenesis, some oncogenes are also implicated in the process. Among the most common chromosomal amplifications, *CCND1* located at 11q13 and encoding cyclin D1, epithelial growth factor receptor (EGFR) and transforming growth factor-alpha (TGF-α) at 7p12 locus play an important role in the progression and treatment efficiency of this malignancy (121-123). Indeed, *PTPRS* loss promotes EGFR/PI3K pathway activation, modulating resistance to EGFR inhibition treatment, an important molecular therapy introduced for HNSCC (120). Among the most

recurrent activating mutations, those affecting the classical *PIK3CA* gene involved in the PI3K-PTEN-AKT pathway seem to be at the top of the list (124).

There is also a growing body of literature providing mechanistic insights into the molecular pathogenesis of the metastatic process in HNSCC. Down-regulation of genes encoding E-cadherin and catenins has been found in patients with metastatic HNSCC (125). Likewise, up-regulation of integrins has been proposed to be responsible for the increase in cell motility and growth of HNSCC cells (126). Overexpression of MMPs such as collagenase-1 and collagenase-3 has also been associated with invasion, metastasis and poor prognosis (127,128). In addition, several signal transduction pathways, including those mediated by receptor tyrosine kinases (RTKs), signal transducer and activator of transcription 3 (Stat3), Rho GTPases, protein kinase Cε (PKCε), and nuclear factor-κB (NF-κB) have been reported to play critical roles in the evolution of HNSCC (129).

Nevertheless, a more global genomic perspective is still needed to shed light over the whole mutational landscape characteristic of this type of tumor. In this regard, recent works of whole-exome sequencing of HNSCC have been published (130,131). In addition to identifying gene previously known to be involved in HNSCC, such as *TP53*, *CDKN2A*, *PTEN*, *PIK3CA* and *HRAS*, both groups have proposed *NOTCH1* as a possible key tumor suppressor gene in the HNSCC carcinogenic process. Other genes such as *IRF6*, *TP63* and *FBXW7* have also been described in these reports as important HNSCC-mutated genes. However, these next-generation sequencing HNSCC studies have failed to identify novel cancer-related genes. Likewise, metastasis causative genes have not yet been described in these works, thereby making necessary to provide a more comprehensive view of HNSCC mutational evolution along tumor progression from a genomic perspective

.

OBJECTIVES

Despite the many efforts invested in deciphering the molecular clues underlying tumor progression and the large amount of information accumulated during the last decades, the “cancer puzzle” remains still unsolved. In this work, and as part of the long-term studies of our laboratory focused on the functional analysis of protease genes deregulated in human malignancies, we have first proposed to study the *in vivo* role of MMP-1 in cancer development and progression. In addition, and in an attempt to obtain a global perspective of the cancer landscape, we have intended to apply next-generation sequencing techniques to analyze tumor evolution, using as a model head and neck carcinomas.

The specific objectives proposed for this work were the following:

- Generation of mice deficient in *Mmp1a*, as an *in vivo* model to analyze the role of this metalloproteinase in cancer.

- Global study of HNSCC from a genomic perspective, employing next-generation sequencing techniques.

- Functional characterization of relevant genes implicated in HNSCC carcinogenesis.

EXPERIMENTAL PROCEDURES

Molecular Biology Methods

General methods

The basic techniques of molecular biology employed in this work including digestion with restriction enzymes, DNA ligations, agarose gel electrophoresis or Southern blot hybridization, which are not detailed below, were performed following manufacturers' instructions or standard protocols.

Northern blot analysis

Total RNA was isolated from frozen placenta samples obtained from wild-type and knock-out female mice at 13.5 days of embryonic development by using a commercial kit (RNeasy Mini Kit; Qiagen). A total of 15 µg of denatured RNA was separated by electrophoresis on 1.2% agarose gels and transferred to Hybond N+ (Amersham Pharmacia Biotech). Blots were prehybridized at 42 °C for 3 h in 50% formamide, 5X SSPE (1X = 150 mM NaCl, 10 mM NaH_2PO_4, 1 mM EDTA, pH 7.4), 10X Denhardt's solution, 2% SDS, and 100 µg/mL denatured herring sperm DNA, and then hybridized with a random primed ^{32}P-labeled cDNA probe for mouse *Mmp1a* (40090601, Geneservice) for 20 h under the same conditions. Blots were washed with 0.1X SSC, 0.1% SDS for 2 h at 50 °C and exposed to autoradiography. RNA integrity and equal loading was assessed by hybridization with a β-actin cDNA probe.

RT-PCR

Total RNA was reverse-transcribed using the Thermoscript RT-PCR system (Invitrogen). A PCR reaction was then performed with the following *Mmp1a*-specific primers: *Mmp1a*-Exon4, 5´-GGACCTAACTATAAGCTTGCTC ACA-3´; *Mmp1a*-Exon7, 5´-CTGGAAGATTTGGCCAGAGAATAC-3´. The PCR reaction was performed in a GeneAmp 9700 PCR system from Applied Biosystems for 35 cycles of denaturation (95 ºC, 30 s), annealing (60 ºC, 30 s), and extension (72 ºC, 1 min). As a control, *β*-actin was PCR amplified from all samples under the same conditions.

Immunohistochemistry

Lungs samples were fixed in 4% paraformaldehyde and embedded in paraffin. Deparaffined and rehydrated sections were rinsed in PBS (pH 7.5). Endogenous peroxidase activity and nonspecific binding were blocked with peroxidase block buffer (DakoCytomation) and 1% bovine serum albumin, respectively. Sections were incubated overnight at 4 ºC with a rabbit polyclonal antibody anti-mouse CD31 (Abcam), diluted 1:100. Then, sections were incubated with an anti-rabbit EnVision system labeled polymer-HRP (DakoCytomation) for 30 min, washed and visualized with diaminobenzidine. Sections were counterstained with Mayer's hematoxylin, dehydrated and mounted in Entellan®. Sections were examined using a Nikon Eclipse E400 microscope and images were acquired with a Nikon DS-Si1 camera and Nikon NIS-Elements F2.20 software. Paraffin-embedding, sectioning, and immunohistochemistry for von Willebrand Factor (vWF) were performed by the Tufts Medical Center Pathology Department. Quantification of the number of vWF-positive blood vessels was performed in a blinded fashion by counting the number of blood vessels per 50 fields at 40X magnification, in viable/non-necrotic regions of the tumors.

Difference gel electrophoresis

Lungs from WT and KO mice were rinsed in TAM (10 mM Tris pH 8.5, 5 mM magnesium acetate) and homogenized in TUCT (2 M thiourea, 7 M urea, 4% CHAPS, 30 mM Tris pH 8.5). 50 µg of each sample were labeled with 400 pmol of a specific fluorophore (GE Healthcare): CyDye 3 (WT sample), CyDye 5 (KO sample) and CyDye 2 (pool of WT and KO sample 1:1). Labeled samples were combined and UCDA (8 M urea, 4% CHAPS, 130 mM DTT, 2% IEF buffer) was added in a 1:1 ratio. UCda (8 M urea, 4% CHAPS, 13 mM DTT, 1% IEF buffer) was used to reach 450 µL of final volume. Samples were loaded in a strip holder and 24 cm IPG strips, non linear pH gradient 3–11 (GE Healthcare), were placed over them. After strip rehydration, protein isoelectrofocusing was allowed to proceed for 26 h on an IPGphor Unit (GEHealthcare) in the dark at 18 ºC. Then, strips were equilibrated for 15 min in SES-DTT (6 M urea, 30% glycerol, 2% SDS,

75 mM Tris pH 6.8, 0.5% DTT and bromophenol blue) and 15 min in SES-IA (SES with 4.5% iodoacetamide), mounted on top of a 13% SDS–PAGE and electrophoresed at 80 V overnight in the dark at 18 ºC. After SDS–PAGE, cyanine dye-labeled proteins were visualized directly by scanning using a Typhoon™ 9400 imager (GE Healthcare), and analyzed with Progenesis SameSpots software (Nonlinear dynamics) and stained with SYPRO Ruby (Molecular Probes).

Tryptic digestion and MALDI-ToF analysis

Differential spots were manually excised over a transilluminator. Gel pieces were washed twice with 25 mM ammonium bicarbonate/acetonitrile (70:30), dried for 15 min at 90 ºC, and incubated with 12 ng/µL trypsin (Promega) in 25 mM ammonium bicarbonate for 1 h at 60 ºC. Peptides were purified with ZipTip C18 (Millipore) and eluted with 1 µL of CHCA (α-cyano-4-hydroxycinnamic acid) to be placed onto MALDI-ToF´s plate. Once dried, they were analyzed by mass spectrometry on a time-of-flight mass spectrometer equipped with a nitrogen laser source (Voyager-DE STR, Applied Biosystems). Data from 200 laser shots were collected and analyzed with data explorer version 4.0.0.0 (Applied Biosystems).

Western blotting

Samples were electrophoresed and transferred to PVDF (0.45 µm pore size) membranes (Millipore). Blots were blocked with 5% non-fat dry milk in TBS-T buffer (20 mM Tris-HCl pH 7.4, 150 mM NaCl and 0.05% Tween-20), for 1 h at room temperature. 0.2 µg /mL of anti-CHI3L3 (R&D Systems), anti-S100A8 (R&D Systems), anti-CTNNA2 (Origene), anti-CTNNA3 (Proteintech Europe) and 1:1000 anti-RAGE (Cell Signaling) and anti α-actin (Sigma) were used for overnight incubations at 4 ºC with 3% BSA in TBS-T. Finally, blots were incubated for 1 h at room temperature in 2.5% non-fat dry milk in TBS-T buffer with 10 ng/mL of goat anti-rat horseradish peroxidase (GE Healthcare), rabbit anti-goat (Thermo Scientific), and donkey anti-rabbit (GE Healthcare). Then, blots were washed with TBS-T and developed with Immobilon Western chemiluminescent HRP substrate

(Millipore). Chemiluminescent images were taken with a Fujifilm LAS3000 mini apparatus.

Enzymatic assays

For *in vitro* proteolysis assays, we used recombinant S100A8 and S100A9 kindly provided by Dr. P. Tessier, and recombinant CHI3L3 and MMP-1 from R&D Systems. Briefly, 100 ng of rMMP-1 per reaction was activated with 4-aminophenylmercuric acetate (APMA) at 37 ºC for 2 h. Then, purified CHI3L3, S100A8 and S100A9 (1 µg) were incubated with activated MMP-1 at 37 ºC for 24 h, and analyzed by SDS-PAGE and Western-blot.

Analysis of cytokine levels

To evaluate the levels of different Th1/Th2 cytokines, we used a Mouse Th1/Th2/Th17/Th22 13plex FlowCytomix Multiplex kit and a TGF-β1 kit (eBioscience), following manufacturer instructions. Briefly, snap-frozen lungs were homogenized at 4 ºC in T-PER (Tissue Protein Extraction Reagent; Thermo Scientific) containing Complete Mini Protease Inhibitor Cocktail tablets (1 tablet / 50 mL of T-PER stock reagent) and centrifuged at 9,000 x g for 15 min. Total protein concentration in supernatant was determined using BCA kit. A total of 100 µg of each homogenate was incubated with antibody-coated bead complexes and biotinylated secondary antibody for 2 h. After washing, 100 µL streptavidin-phycoerythrin was added to each well and incubated for 1 h. Samples were then transferred to appropriate cytometry tubes and analyzed using the FC500 Celular Cytomics analyzer (Beckman Coulter). A minimum of 300 events (beads) were collected for each cytokine/sample and median fluorescence intensities were obtained. Cytokine concentrations were calculated based on standard curve data using FlowCytomix Pro 3.0 Software (eBioscience). The results were expressed as mean ± SE (n = 5).

DNA isolation from human specimens

We obtained from each patient surgically resected tumor samples and matched blood samples. To obtain tumor genomic DNA, approximately 10 mg of fresh-frozen tumor tissue were lysed in 360 µL of ATL buffer supplemented with 40 µL of proteinase K for 2-16 h. After complete macroscopic digestion, the lysate was mixed with 400 µL of AL buffer to homogeneization, and then 400 µL of 100% EtOH were added, followed by thorough vortexing for 15 s and 5 min incubation at room temperature. Genomic DNA was then precipitated by 10 min centrifugation at 4 ºC and 20,000 x g, washed with 70% EtOH, air-dried and resuspended in 50-100 µL of AE buffer. ATL, AL, proteinase K and AE buffer were from Qiagen. Germline genomic DNA was obtained from blood samples using the Flexigene kit (Qiagen), according to manufacturer's instructions. The experiments were conducted in accordance with the Hospital Universitario Central de Asturias Ethics Committee, and written informed consent was obtained from each individual providing biological samples.

Exome-enrichment

Three µg of genomic DNA from each sample were sheared and used for the construction of a paired-end sequencing library as previously described in the Paired-End sequencing sample preparation protocol provided by Illumina. Enrichment of exonic sequences was then performed for each library using the Sure Select Human All Exon Kit 50 Mb (Agilent Technologies) following the manufacturer´s instructions. Exon-enriched DNA was pulled down by magnetic beads coated with streptavidin (Invitrogen), and was followed by washing, elution and 18 additional cycles of amplification of the captured library. Exon enrichment was validated by real-time PCR in a 7300 Real-Time PCR System (Applied Biosystems) using a set of two pairs of primers to amplify exons and one pair to amplify an intron. Enriched libraries were sequenced using two lanes of an Illumina GAIIx.

Somatic mutation identification in pooled samples (SMIPS)

To discover recurrent somatic mutations in the validation series of genomic analysis, we performed a screening in a set of 86 additional HNSCC cases using a combination of pooled samples, PCR amplification and high-throughput sequencing. We used a modified method for the analysis of pooled samples. Briefly, we amplified each selected exon from two pools containing equal amounts of tumor and normal DNA respectively from the patients. To obtain sufficient coverage, we mixed equal amounts of the resulting amplicons in four pools for each sample. Each pool was sequenced in one lane of an IlluminaGAIIx sequencer for an average coverage of about 10^5 over more than 200,000 bases.

Mutation validation

To deconvolute the sequencing data generated by SMIPS, we analyzed each tumor DNA from the validation set by using SNaPShot (Life Technnologies), according to manufacturer's instructions. We performed two separate SNaPShot reactions per tumor DNA, one for *CTNNA2* and one for *CTNNA3*, using the appropriate primers in each case. The presence of the corresponding mutation identified by SNaPShot was verified by Sanger sequencing using a 3130XL Genetic Analyzer.

Cell Biology Methods

Cells and cell culture conditions

The human squamous cell carcinoma cell line SCC-2 was cultured in complete medium Dulbecco´s Modified Eagle Medium, (DMEM, Invitrogen) containing 10% fetal bovine serum (FBS), 2% HEPES, 1% non-essential amino acids and 1% penicillin-streptomycin-glutamine. For overexpression experiments, cells at 80% confluence were transfected using Lipofectamine 2000 (Invitrogene) with the full-length human cDNA of *CTNNA2* and/or *CTNNA3* (Origene RC208731 and RC226241, respectively). For knockdown experiments, cells were transduced

with a set of four retroviral short-hairpin RNA (shRNA) vectors based on the pLKO.1 vector and designed to specifically target human *CTNNA2* and/or *CTNNA3* transcripts (Origene TG313667 and TG313666,respectively), using HEK-293T cells for virus packaging. *CTNNA2* and *CTNNA3* mutant DNAs were created using a Stratagene Quik Change II Site-Directed Mutagenesis kit (Agilent Technologies). Transfected clones were selected during 5-7 days with 400 µg/mL of G418 for overexpressing clones, and 1.1 µg/mL puromycin for silencing clones. All cell lines were analyzed by Western blot to confirm expression or silencing. Lewis lung carcinoma LLC1 cells were purchased from American Type Culture Collection. Cells were maintained in DMEM supplemented with 10% FBS and 1% penicillin/ streptomycin. To generate mouse embryonic fibroblasts (MEFs), embryos were harvested from *Mmp1a* heterozygote crosses at embryonic day 12.5. Cells were maintained in DMEM supplemented with 10% FBS, 1% Pen-Strep.

Endothelial tube formation

MatTek plates were chilled and coated with 100 µL Matrigel. HUVEC cells (3.5×10^4, p2-5) in EBM2 media with 0.5% BSA were placed on top. The cells were stimulated with MEF conditioned media (diluted 1:2, from 1×10^6 MEFs following 24 h conditioning in 0.5% BSA DMEM). Endothelial tubes were observed after 6 h under phase contrast inverted microscopy (4X magnification). ImageJ software was used to quantify tubal length and branch complexity from digital images.

Cell adhesion assays

The adhesion capacity of different cell pools was analyzed with the ECM Cell Adhesion Array kit (Colorimetric) (EMD Biosciences, ECM540 96 wells) following manufacturer's instructions. Briefly, 6×10^5 cells were incubated in the ECM Array during 3 hours. After cell lysis, the absorbance was measured at 485

nm using a Synergy H4 Hybrid reader. All data were the mean of three independent experiments.

Time-lapse migration assays

For cell migration assays, laminin (15 µg/mL; Sigma L2020) was added for 2 h at 37 ºC on Ibidi uncoated µ-Dishes (Ibidi 81151). 6 x 10^5 cells were seeded 6 h before performance of the experiment on coated dishes with culture inserts (Ibidi 80209) until complete adhesion. Inserts were removed defining a cell free gap of around 500 µm, and cells were covered with 2 mL of culture media. Migration of cells were time-lapse recorded in a Zeiss Axiovert 200 microscope during 12 h, with a XL-multi S1 incubator and using Axiovision software. Migration areas at different time points were calculated using ImageJ.

In vitro invasion assays

The *in vitro* invasion potential of different SCC-2 cell lines was evaluated using Matrigel-coated invasion chambers with an 8-Am pore size (BD Biosciences). For each experiment, 2.5 x 10^5 cells per well were allowed to migrate for 27 h through the Matrigel-coated membranes using 3% FBS as chemoattractant. For LLC1 cells, 2 x 10^4 cells were placed in the upper chamber and allowed to invade for 48 h using MEF conditioned media as a chemoattractant in the lower well. Cells that reached the lower surface of the membrane were stained. The total number of cells in the lower chamber was determined by visible microscopy (magnification 4x).

Cell proliferation assays

To quantify cell proliferation, we used a CellTiter96AQ nonradioactive cell proliferation kit (Promega Corp.). For each experiment, one hundred B16F10 cells were seeded in triplicate in 96-well plates and incubated at 37 ºC, 5% CO_2 for 4 days. Cell proliferation was quantified by measuring the conversion of 3-(4,5-dimethylthiazol-2-yl)-5-(3-carboxyme-thoxyphenyl)-2-(4-sulfophenyl)-2H

tetrazolium, inner salt (MTS) into water-soluble formazan catalyzed by dehydrogenase in living cells. The reaction was monitored by measuring the absorbance at 490 nm using a Synergy H4 Hybrid reader. All experiments were repeated three times independently.

Luciferase reporter gene assay

To measure the transcriptional activity of the β-catenin/Wnt signaling pathway, SCC-2 cell lines transfected with different constructs were seeded in 24-well plates, at 1.0 x 10^5 cells/well. After 24 h, 0.6 μg of TCF/LEF-1 reporter (pTOP-FLASH) or control vector (pFOP-FLASH) were transiently cotransfected with 0.06 μg of TLRK vector and 0.2 μg of each DNA construct (shRNAs, full-length wild-type and mutated cDNAs, respectively for both *CTNNA2* and *CTNNA3*) following the standard Lipofectamine 2000 protocol (Invitrogen). Cells were incubated for 24 h, and then 10 μL out of the 100 μL cell extract were used for measuring luciferase activity using the Dual Luciferase Reporter Assay System kit (Promega).

Animal Model Methods

Generation of mutant mice

To generate *Mmp1a*$^{-/-}$mice, we first isolated a genomic PAC clone encoding *Mmp1a* from a mouse 129/SvJ library (HGMP Resource Centre) by using a murine *Mmp1a* cDNA fragment as a probe. Then, we used the plasmid pKO scrambler V916 (Lexicon Genetics) to construct the *Mmp1a* targeting vector. A 1.4 kb *HindIII* fragment from the 5'-flanking containing exon 2, 3 and part of exon 4 was used as the 5'-homologous region, whereas a 6.8 kb *EcoRI-RsrII* fragment containing part of the exon 6 and exon 7 was used as the 3'-region of homology. The PGK-neo cassette was subcloned into an *AscI* site of the vector with the transcriptional orientation opposite to that of *Mmp1a* and replaced a 1.7 kb fragment containing exons 4, 5 and part of the exon 6 of the gene. The targeting vector was linearized by digestion with *NotI* and electroporated into HM-1 (129/Ola) embryonic stem

cells. Resistant clones were selected for homologous recombination with G418 and ganciclovir, and screened by Southern blot analysis. The heterozygous stem cells were aggregated to CD1 morulas and transferred into uteri of pseudopregnant females to generate chimeras. Chimeric males were mated with C57BL/6J females and the offspring was screened by Southern blot analysis of tail genomic DNA. The heterozygous littermates were mated to generate homozygous mutant mice.

Urethane carcinogenesis model

Mouse experimentation was done in accordance with the guidelines of the Universidad de Oviedo (Spain), regarding the care and use of laboratory animals. For urethane (ethylcarbamate; Sigma) chemical carcinogenesis, 12-week-old mice were injected intraperitoneally with two doses (separated by 48 h) of a freshly prepared solution of 1 mg of urethane/g body weight, dissolved in sterile 0.9% NaCl (saline). Mice were sacrificed 32 weeks after urethane exposure, and their lungs were either snap-frozen in liquid nitrogen for further RNA and protein analysis or fixed in 4% paraformaldehyde and processed for histological studies. After conventional staining with hematoxylin and eosin, cells were morphologically identified by an expert pathologist with no previous knowledge of mice genotypes.

Lewis lung carcinoma model

Six to nine week old female animals were injected with $2x10^5$ LLC1 cells in sterile PBS in the abdominal fat pad (2 inoculations per mouse). Starting at day 12, palpable tumors were measured every other day and tumor volume was calculated using the equation $(LxW^2)/2$. At the day 26 endpoint, animals were sacrificed. Finally, tumors were harvested, weighed, and formalin-fixed for histology.

Other pathological models

For B16F10 melanoma experimental model, mice were injected with 5 × 10^4 cells in the tail vein and mice were sacrificed 3 weeks later. The two-stage chemical skin carcinogenesis induced by DMBA/TPA (9,10-dimethyl-1,2-benzanthracene/12-O-tetradecanoylphorbol-13-acetate) was performed by pipette application of 100 µg of DMBA in 200 µL acetone onto the shaved-back skin of mice. Tumor promotion was performed twice weekly with 25 µg of TPA from week 1 to week 12. Mice were assessed weekly for papilloma development for up to 20 weeks. For MCA-induced fibrosarcoma, 100 µg of MCA (3-methyl-cholanthrene) were subcutaneously injected in each mouse flank in 100 µL of corn oil. Mice were assessed weekly for fibrosarcoma development for up to 30 weeks. For the oral squamous cell carcinogenesis model, 4-NQO (4-nitroquinoline 1-oxide) stock solution was prepared weekly in propylene glycol at 5 mg/mL and then diluted at 100 µg/mL in the drinking water, which was changed once a week. Mice were allowed access to the drinking water at all times during the 16 weeks of 4-NQO treatment. For DEN-induced hepatocarcinoma (N,N-diethylnitrosamine), mice at 15 days of age were treated with a single intraperitoneal injection of 5 mg/kg DEN in 0.1 mL of saline; animals were euthanized after 9 months. For azoxymethane-induced colon carcinomas, mice were intraperitoneally injected with 12.5 mg/kg body weight. After 5 days, dextran sulphate was diluted at 2.5% in the drinking water and administered to the mice during 5 days, following by a free dextran sulphate-water time for 16 days. This cycle was repeated three times and after last 16 days of free-water time, mice were sacrificed. For hepatic fibrosis, mice received 1 mL/kg of CCl_4 diluted 1:4 in olive oil twice a week during 4 weeks and then, animals were sacrificed. Bleomycin lung fibrosis was induced in mice by intratracheal instillation of a sub-lethal dose of bleomycin (2 U/kg dissolved in 400 µL of sterile saline) under fluorane anaesthesia. Mice were sacrificed at 48 h for the acute protocol and 3 weeks later for the chronic model. MMTV-PyMT (mammary tumor virus-polyoma middle T antigen) breast cancer and K14-HPV16 (keratin 14-human papillomavirus type 16) skin cancer samples were kindly provided by Dr. Agnés Noël (University of Liege, Belgium). All these protocols

were performed using as minimum of n=10 mice with ages ranging between 8 and 10 weeks, except for DEN-induced hepatocarcinoma model.

Bioinformatics and Statistical Analysis

Sequence reads mapping and processing

For exome sequencing, reads from each library were mapped to the human reference genome (GRCh37) using BWA with the sampe option, and a BAM file was generated using SAM tools. Reads from the same paired-end libraries were merged and optical or PCR duplicates were removed using Picard (http://picard.sourceforge.net/index.shtml). Statistics about the number of mapped reads and depth of coverage for each sample are shown in the corresponding Thesis manuscripts. For the identification of somatic substitutions, we used the *Sidrón* algorithm, which has been previously described in our laboratory (100). The frequencies of machine error were estimated by examining 3 x 10^5 likely homozygous positions (coverage higher than 15, fraction of non-reference bases lower than 0.1). Due to the contamination of tumor samples with normal tissue, the cutoff S values were lowered to 11 for positions with coverage higher than 20. The validation rate of the somatic mutations detected by *Sidrón* was higher than 90% as assessed by Sanger sequencing.

Statistical analysis

We used the Prism Program (GraphPad) to compare mean samples between groups, applying t-Student or Mann-Whitney U test depending on sample distribution characteristics. The SPSS Statistics 17.0 (SPSS Inc) package was employed to correlate clinical and biological variables by means of Fisher's test or non-parametric test when necessary. Survival curves were analyzed according to the Kaplan and Meier method and compared using the log-rank test. All statistical tests were two-sided and the level of statistical significance was 0.05. The probability of concurrent *CTNNA2* and *CTNNA3* mutations in the validation series was estimated with a Monte Carlo simulation.

RESULTS

I. The complex family of matrix metalloproteinases

Over the last years, the intensive research dedicated to understand the complex proteolytic universe has allowed to characterize, genetically and functionally, a large number of proteolytic systems. Among them, the family of matrix metalloproteinases (MMPs) has achieved a great relevance in both physiological and pathological processes owing to their ability to degrade all extracellular matrix components as well as a high variety of bioactive molecules. The growing interest for this family has generated a significant amount of information. Accordingly, and as a first objective of this thesis, we proposed the collection, revision and integration of the recent literature about this family of metalloproteinases.

Article 1. **Miriam Fanjul-Fernández**, Alicia R. Folgueras, Sandra Cabrera, Carlos López-Otín. "Matrix metalloproteinases: evolution, gene regulation and functional analysis in mouse models".

Biochimica et Biophysica Acta 1803: 3–19 (2010)

Personal contribution to this work

In this work, I was the main responsible for collecting, integrating and summarizing all the current information available about this family of metalloproteinases. I also outlined the main topics which were reviewed in this manuscript, prepared the figures and performed most part of the writing with the collaboration of Drs. Alicia R. Folgueras and Sandra Cabrera, and under the supervision of Dr. Carlos López-Otín.

Biochimica et Biophysica Acta 1803 (2010) 3–19

Contents lists available at ScienceDirect

Biochimica et Biophysica Acta

journal homepage: www.elsevier.com/locate/bbamcr

Review

Matrix metalloproteinases: Evolution, gene regulation and functional analysis in mouse models

Miriam Fanjul-Fernández, Alicia R. Folgueras, Sandra Cabrera, Carlos López-Otín *

Departamento de Bioquímica y Biología Molecular, Facultad de Medicina, Instituto Universitario de Oncología, Universidad de Oviedo, 33006 Oviedo, Spain

ARTICLE INFO

Article history:
Received 24 March 2009
Received in revised form 11 July 2009
Accepted 14 July 2009
Available online 23 July 2009

Keywords:
Degradome
Protease
Cancer
Polymorphism
Cardiovascular disease

ABSTRACT

Matrix metalloproteinases (MMPs) are a large family of zinc-endopeptidases which play important roles in multiple physiological and pathological processes. These enzymes are widely distributed in all kingdoms of life and have likely evolved from a single-domain protein which underwent successive rounds of duplication, gene fusion and exon shuffling events to generate the multidomain architecture and functional diversity currently exhibited by MMPs. Proper regulation of these enzymes is required to prevent their unwanted activity in a variety of disorders, including cancer, arthritis and cardiovascular diseases. Multiple hormones, cytokines and growth factors are able to induce *MMP* expression, although the tissue specificity of the diverse family members is mainly achieved by the combination of different transcriptional control mechanisms. The integration of multiple signaling pathways, coupled with the cooperation between several *cis*-regulatory elements found at the *MMP* promoters facilitates the strict spatiotemporal control of *MMP* transcriptional activity. Additionally, epigenetic mechanisms, such as DNA methylation or histone acetylation, may also contribute to *MMP* regulation. Likewise, post-transcriptional regulatory processes including mRNA stability, protein translational efficiency, and microRNA-based mechanisms have been recently described as modulators of *MMP* gene expression. Parallel studies have led to the identification of *MMP* polymorphisms and mutations causally implicated in the development of different genetic diseases. These genomic analyses have been further extended through the generation of animal models of gain- or loss-of-function for MMPs which have allowed the identification of novel functions for these enzymes and the establishment of causal relationships between MMP dysregulation and development of different human diseases. Further genomic studies of MMPs, including functional analysis of gene regulation and generation of novel animal models will help to answer the multiple questions still open in relation to a family of enzymes which strongly influence multiple events in life and disease.

1. Introduction

Matrix metalloproteinases (MMPs) comprise a large family of zinc-dependent endoproteinases, collectively capable of degrading all extracellular matrix (ECM) components. MMPs (also called matrixins) are found in all kingdoms of life and belong to the metzincin superfamily of metalloproteinases, which is characterized by the presence of a catalytic zinc atom in their active center followed by a conserved methionine residue [1]. To date, at least 25 different vertebrate MMPs have been identified, 24 of which are present in humans, including two recently duplicated genes encoding MMP-23 [2].

The proteolytic activities of MMPs influence essential cellular processes like cell proliferation, migration and adhesion, as well as many fundamental physiological events involving tissue remodeling, such as angiogenesis, bone development, wound healing, and uterine and mammary involution [3,4]. However, the increasing relevance of this family of proteases mainly derives from the high number of pathological conditions where these enzymes have been implicated [5,6]. Thus, upregulation of MMPs has been reported in cancer, vascular diseases and many different types of inflammatory pathologies, supporting the need of a precise spatiotemporal regulation of MMPs to maintain a proper homeostasis of the extracellular and pericellular environment. MMP expression and activity can be regulated at different levels including gene transcription, proenzyme activation and endogenous inhibition, which act in a coordinated manner to confine the diverse MMP proteolytic activities to those conditions and locations where they are necessary. Unfortunately, these restrictive regulatory mechanisms are frequently lost in multiple pathological conditions, as assessed from studies based on the use of gain- or loss-of-function of MMPs in animal models [7]. These models have also provided important clues about the functional relevance of MMPs in a variety of physiological processes taking place in all organisms with ability to produce these proteases. In this review,

* Corresponding author. Tel.: +34 985 104201; fax: +34 985 103564.
E-mail address: clo@uniovi.es (C. López-Otín).

0167-4889/$ – see front matter © 2009 Elsevier B.V. All rights reserved.
doi:10.1016/j.bbamcr.2009.07.004

and after a general introduction to the biochemical properties of MMPs, we will focus on genomic characteristics of this family of proteolytic enzymes, paying special attention to gene organization and evolution. Likewise, we will discuss different levels of *MMP* gene regulation with particular emphasis on the mechanisms responsible for their transcriptional control and on the presentation of data on epigenetic and post-transcriptional regulation of these protease genes. Finally, we will present the most recent information about *MMP* polymorphisms and mutations associated with human pathologies, as well as those mouse models generated by genetic manipulation which have shed light on the functional relevance of these enzymes in life and disease.

2. Matrix metalloproteinases: Classification and biochemical properties

MMPs or matrixins are synthesized as zymogens with a signal peptide which leads them to the secretory pathway. Then, these enzymes can be secreted from the cell or anchored to the plasma membrane, thereby confining their catalytic activity to the extracellular space or to the cell surface, respectively. Interestingly, recent studies have reported that several MMP family members, such as MMP-1 [8], MMP-2 [9], MMP-11 [10] and MMP-13 [11], can be found as intracellular proteins, although their functions at this subcellular location are still unclear. The archetypal MMPs consist of a propeptide (~80 amino acids) with a cysteine-switch motif, a catalytic metalloproteinase domain (~170 amino acids), a linker peptide of variable length and a hemopexin domain (~200 amino acids). Nevertheless, the family of MMPs has evolved into different groups by removing some domains or by incorporating others which are absent in the previously described basic core (Fig. 1). Thus, based on their domain organization, MMPs can be classified in four different groups: archetypal MMPs, matrilysins, gelatinases and furin-activatable MMPs.

2.1. Archetypal MMPs

Within this category, and according to their substrate specificities, we can establish three different subgroups: collagenases, stromelysins and other archetypal MMPs.

2.1.1. Collagenases

This subgroup is composed of three enzymes, MMP-1, MMP-8 and MMP-13 (also known as collagenases-1, 2, and 3, respectively) whose name reflects their ability to cleave the collagen triple helix into characteristic 3/4 and 1/4 fragments. In addition, collagenases are also able to proteolytically process other ECM proteins, as well as a number of bioactive molecules such as interleukin-8 (IL-8) [12], pro-tumor necrosis factor (TNF)-α [13], protease-activated receptor-1 [14], and several insulin-like growth factor binding proteins (IGFBPs) [15]. Removal of the hemopexin domain turns these MMPs into enzymes unable to degrade native collagen, suggesting that the cooperation between the catalytic and hemopexin domains is essential to carry out their collagenolytic activity [16]. A fourth type of collagenase (MMP-18) has been identified in *Xenopus* [17], but it does not have any known orthologue in mammals.

2.1.2. Stromelysins

Stromelysin-1 (MMP-3) and stromelysin-2 (MMP-10) show the same structural design as collagenases and can degrade many different ECM components, but they are not able to cleave native collagen. In addition, stromelysin-1 also processes several bioactive substrates including stromal-cell derived factor-1, E-cadherin, and pro-interleukin-1 beta (IL-1β) [15]. Likewise, stromelysins participate in proMMP activation through their ability to remove the propeptide domain of the three procollagenases [18] and proMMP-9 [19], generating the fully active form of these enzymes. Stromelysins are expressed by both fibroblast and epithelial cells, and are secreted to the extracellular space where they play important roles in biological

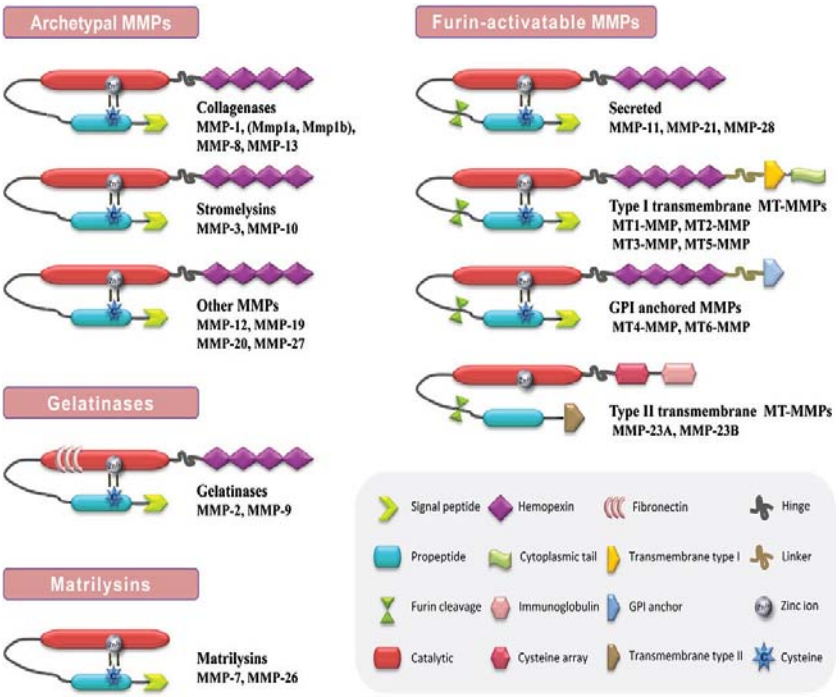

Fig. 1. The mammalian family of matrix metalloproteinases. Structural classification of MMPs based on their domain arrangement.

processes such as mammary gland development, immunity and wound healing [3]. There is another MMP called stromelysin-3 (MMP-11) which shares some structural characteristics with stromelysins but due to the presence of additional features, it is classified into the category of furin-activatable MMPs.

2.1.3. Other archetypal MMPs

There are four matrixins (MMP-12, -19, -20, -27) which cannot be classified in the previous subgroups because of their divergence in sequence and substrate specificity. MMP-12 or metalloelastase is the most potent elastolytic enzyme of the family although, as other MMPs, it can also degrade many other ECM proteins, including aggrecan, fibronectin, laminin, and type IV collagen [15]. MMP-12 is mainly expressed by macrophages [20] but it is also produced by hypertrophic chondrocytes and osteoclasts [21]. MMP-19 was first isolated from human cDNA liver libraries [22] and, afterwards, it was detected in the inflamed synovium from patients with rheumatoid arthritis [23]. This MMP is expressed in a wide variety of human tissues and exhibits a potent degradative activity against components of basement membranes, such as type IV collagen or tenascin, as well as gelatin and aggrecan [24]. MMP-20, also named enamelysin because of its first isolation from a porcine enamel organ, is secreted by ameloblasts and odontoblasts of the dental papila, which are involved in tooth enamel formation [25,26]. MMP-27 was first cloned from a chicken embryo fibroblasts cDNA library [27]. It has been reported that this chicken enzyme is able to degrade gelatin and casein, but little information is available about the activity of its human orthologue, which is highly expressed in B-lymphocytes [28].

2.2. Matrilysins

MMP-7 and MMP-26, also known as matrilysins-1 and -2, are expressed under normal and pathological conditions and have been implicated in the progression of several types of human cancers. Both proteases exhibit the simplest domain arrangement of all MMPs since they lack the carboxy-terminal hemopexin domain [29]. Matrilysins play important roles in the degradation of ECM proteins like type IV collagen, laminin and entactin [15], as well as in the processing of non-ECM proteins. Thus, MMP-7 catalyzes the ectodomain shedding of several cell surface molecules like Fas ligand [30], E-cadherin [31] and syndecan-1 [32], whereas MMP-26 has been reported to be an activator of proMMP-9 under pathological conditions [33]. In addition, matrilysins have been associated with the remodeling of the post-partum uterus and with embryo implantation [34].

2.3. Gelatinases

MMP-2 (gelatinase-A) and MMP-9 (gelatinase-B) are constitutively expressed by many cell types including fibroblasts, keratinocytes, endothelial cells, chondrocytes and monocytes in the case of MMP-2, and alveolar macrophages, polymorphonuclear leukocytes and osteoclasts in the case of MMP-9. These MMPs have an additional fibronectin domain located inside the catalytic domain, which allows the binding and processing of denatured collagen or gelatin [1], suggesting that these enzymes also play a key role in the remodeling of collagenous ECM. Thus, gelatinases degrade a broad spectrum of ECM molecules such as collagen types I, IV, V, VII, X, IX, elastin, fibronectin, aggrecan, vitronectin, laminin [15], but also many non-ECM molecules including pro-TNF-α [13], transforming growth factor (TGF)-β [35], pro-IL-1β, pro-IL-8 and monocyte chemoattractant protein (MCP)-3 [36]. Likewise, these enzymes are able to release or generate several factors with pro- or anti-angiogenic properties [37]. Both gelatinases have been associated with multiple pathologies, including cancer, bone diseases, inflammatory disorders and vascular alterations such as atherosclerosis, aortic aneurysm and myocardial infarction [5].

2.4. Furin-activatable MMPs

All MMPs belonging to this category contain a furin recognition motif inserted between the propeptide and the catalytic domain. This sequence is recognized and cleaved by convertase proteases, providing the basis for furin-dependent activation of latent enzymes prior to secretion. These furin-activatable MMPs include three secreted MMPs, six membrane-type-MMPs and two unusual type II transmembrane MMPs.

2.4.1. Secreted MMPs (MMP-11, -21, and -28)

Unlike the other secreted MMPs, these three furin-activatable enzymes are processed intracellularly by furin-like proteases and secreted as active forms. MMP-11, also known as stromelysin-3, is expressed during embryogenesis, tissue involution and wound healing, and has been proposed to play an important role in cancer [38]. Recent studies have reported that MMP-11 is induced in adipose tissue by cancer cells and contributes to tumor progression through the degradation of collagen VI, suggesting a molecular link between obesity and cancer [39]. MMP-21 is the human orthologue of *Xenopus* XMMP and it has been detected during embryo development in several organs such as kidney, intestine and skin, as well as in various epithelial cancers [40]. MMP-28, also known as epilysin, is expressed in several adult tissues such as testis, lung, heart, colon, intestine, brain and epidermis [41]. MMP-28 is also produced by several carcinomas but its functional role in transformation events has not been clearly defined. In addition, recent data have reported that epilysin may be an important mediator in certain diseases of the central nervous system, such as multiple sclerosis, where it may participate in demyelinating processes [42].

2.4.2. Membrane-type MMPs (MMP-14, -15, -16, -17, -24, and -25)

These MMPs incorporate membrane-anchoring domains that locate them at the cell surface. This feature makes these enzymes as optimal pericellular proteolytic machines, able to control the local environment that surrounds normal and tumoral cells. On the basis of their type of attachment to the plasma membrane, MT-MMPs can be classified into two groups: type I transmembrane MT-MMPs and glycosylphosphatidylinositol (GPI) MT-MMPs [43]. The first group comprises MT1-, MT2-, MT3-, and MT5-MMP (MMP-14, -15, -16 and -24, respectively). These enzymes are characterized by a long hydrophobic sequence followed by a short cytoplasmic tail which is involved in numerous cellular events, such as the activation of MERK/ERK and src-tyrosine kinase pathways or the protein trafficking to discrete regions of the cell surface [44,45]. Moreover, it has been reported that the cytoplasmic domain of MT1-MMP is essential for the regulation of protease activity through a dynamin-mediated process of internalization in clathrin-coated vesicles [46]. Besides their capacity to cleave a variety of substrates including ECM components, these membrane-associated MMPs are the major physiological activators of proMMP-2 [47]. MT-MMPs are expressed by different tissues under normal conditions, but they are also frequently upregulated in tumors. Thus, MT1-MMP expression has been associated with poor prognosis in several types of cancer [48, 49] and its overexpression strongly promotes cellular invasion and experimental metastasis [50,51]. Likewise, MT-MMPs have been involved in the formation of new blood vessels in both physiological and pathological conditions [47]. On the other hand, MT4-MMP and MT6-MMP (MMP-17 and -25, respectively) constitute the second subgroup of membrane-type MMPs which are bound to the cell surface via a GPI-anchor. MT4-MMP is expressed in brain, colon, ovary, testis, and leukocytes [52], whereas MT6-MMP is predominantly expressed in leukocytes, lung and spleen [53]. MT4-MMP has shown a low enzymatic activity against ECM components, and its contribution to ECM turnover seems to be indirectly mediated by its ability to activate aggrecanase-1 (ADAMTS-4) [54]. In contrast, MT6-MMP is able to process gelatin, collagen IV, fibronectin, fibrin, and proteoglycans [55].

Although little is known about the *in vivo* function of these proteases, recent data have detected the expression of MT4-MMP and MT6-MMP in breast and colon cancer, respectively, and, in both cases, these MMPs appear to be associated with tumor growth [56].

2.4.3. Type II transmembrane MMPs (MMP-23A and -23B)

MMP-23A and MMP-23B have identical amino acid sequence, but are encoded by distinct genes in the human genome. These proteases are unique among the matrixin family because they lack the signal peptide, the cysteine-switch motif and the hemopexin domain characteristic of all MMPs, but contain cysteine-array (CA) and immunoglobulin (Ig) domains in their shortened C-terminal tail. Besides, their type II transmembrane domain is located at the N-terminal of the propeptide. Expression analysis has demonstrated that MMP-23 is predominantly produced by ovary, testis, and prostate, suggesting that this MMP may play a specialized role in reproductive processes [57]; however, the *in vivo* functions of this protease still remain undetermined.

3. Gene evolution and genomic organization of MMPs

Comparative genomic analyses have indicated that the impressive diversity characteristic of the family of vertebrate *MMP* genes mainly derives of a series of evolutionary events that occurred during early stages of vertebrate emergence. Nevertheless, these comparative studies have also revealed a more ancient origin for these endopeptidases which predates the emergence of vertebrates. Thus, the identification of plant MMPs orthologues to both vertebrate and invertebrate MMPs clearly supports the proposal of an ancient evolutionary history for these enzymes. Moreover, the finding that MMPs in plants and invertebrates have a closer relationship between them than with vertebrate MMPs, coupled with the absence of hemopexin domains in their structure, suggests that they could be modern representatives of an ancient MMP ancestor, common to the three groups [58]. Likewise, it is tempting to speculate that the earliest forms of MMPs were based on very simple architectural designs conformed by catalytic devices without any ancillary domains. These primitive MMPs were subsequently increasing their complexity through gene fusion events that led to the incorporation of the variety of modules currently exhibited by most family members. It is also remarkable that most *MMP* genes found in vertebrates have an orthologue in *Ciona intestinalis*, one of the closest invertebrate relatives of vertebrates [59]. Thus, these enzymes likely evolved before the divergence between the vertebrate and urochordate lineages (Fig. 2). Prior to the emergence of vertebrates, the *MMP* family had remained relatively stable throughout evolution as assessed by the low number of conserved *MMP* genes present in protostomes (2 *MMP*s in *Drosophila melanogaster*) [60] and urochordates (5 *MMP*s in *C. intestinalis*) [59]. Nevertheless, it is noteworthy the presence in the sea urchin genome of at least 26 *MMP* genes with significant similarity to vertebrate *MMP*s, although they are clustered together and separated from vertebrate MMP groups. These findings suggest that *MMP* genes found in the last common ancestor to vertebrates and echinoderms underwent independent duplication and divergence, following separation of these two groups [61]. Thus, and as discussed above, it appears that *MMP* vertebrate genes were amplified from a common protostome-deuterostome ancestor (Fig. 2).

The major evolutionary event in the generation of the *MMP* gene repertoire of vertebrates was the widespread duplication of pre-existing genes (Fig. 2). In particular, most MMP subfamilies show a further expansion along the early teleost lineage. Nevertheless, it should be noted that both teleost- and tetrapod-specific duplications have occurred after the divergence of both lineages. The expansion in teleosts of *MMP* orthologues related to human *MMP7* and *MMP20*, an evolutionary event likely linked to the continuous teeth replacement in these vertebrates, is remarkable. Similarly, *MT-MMP* genes underwent

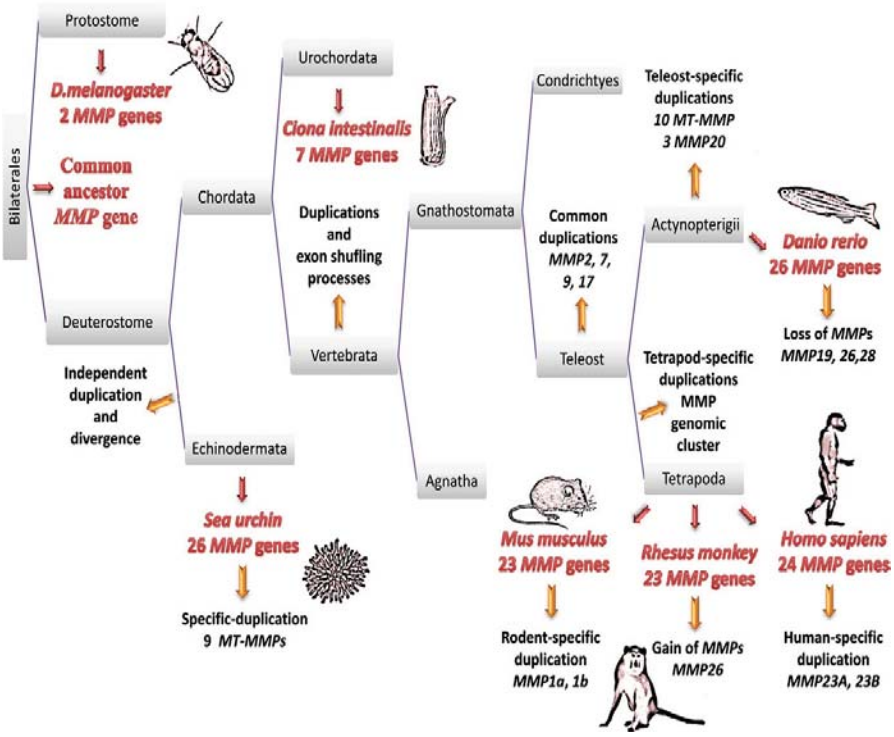

Fig. 2. Evolution of MMPs. Schematic representation of key events occurring throughout the evolutionary history of MMPs.

Although little is known about the *in vivo* function of these proteases, recent data have detected the expression of MT4-MMP and MT6-MMP in breast and colon cancer, respectively, and, in both cases, these MMPs appear to be associated with tumor growth [56].

2.4.3. Type II transmembrane MMPs (MMP-23A and -23B)

MMP-23A and MMP-23B have identical amino acid sequence, but are encoded by distinct genes in the human genome. These proteases are unique among the matrixin family because they lack the signal peptide, the cysteine-switch motif and the hemopexin domain characteristic of all MMPs, but contain cysteine-array (CA) and immunoglobulin (Ig) domains in their shortened C-terminal tail. Besides, their type II transmembrane domain is located at the N-terminal of the propeptide. Expression analysis has demonstrated that MMP-23 is predominantly produced by ovary, testis, and prostate, suggesting that this MMP may play a specialized role in reproductive processes [57]; however, the *in vivo* functions of this protease still remain undetermined.

3. Gene evolution and genomic organization of MMPs

Comparative genomic analyses have indicated that the impressive diversity characteristic of the family of vertebrate *MMP* genes mainly derives of a series of evolutionary events that occurred during early stages of vertebrate emergence. Nevertheless, these comparative studies have also revealed a more ancient origin for these endopeptidases which predates the emergence of vertebrates. Thus, the identification of plant MMPs orthologues to both vertebrate and invertebrate MMPs clearly supports the proposal of an ancient evolutionary history for these enzymes. Moreover, the finding that MMPs in plants and invertebrates have a closer relationship between them than with vertebrate MMPs, coupled with the absence of hemopexin domains in their structure, suggests that they could be modern representatives of an ancient MMP ancestor, common to the three groups [58]. Likewise, it is tempting to speculate that the earliest forms of MMPs were based on very simple architectural designs conformed by catalytic devices without any ancillary domains. These primitive MMPs were subsequently increasing their complexity through gene fusion events that led to the incorporation of the variety of modules currently exhibited by most family members. It is also remarkable that most *MMP* genes found in vertebrates have an orthologue in *Ciona intestinalis*, one of the closest invertebrate relatives of vertebrates [59]. Thus, these enzymes likely evolved before the divergence between the vertebrate and urochordate lineages (Fig. 2). Prior to the emergence of vertebrates, the *MMP* family had remained relatively stable throughout evolution as assessed by the low number of conserved *MMP* genes present in protostomes (2 *MMP*s in *Drosophila melanogaster*) [60] and urochordates (5 *MMP*s in *C. intestinalis*) [59]. Nevertheless, it is noteworthy the presence in the sea urchin genome of at least 26 *MMP* genes with significant similarity to vertebrate *MMP*s, although they are clustered together and separated from vertebrate MMP groups. These findings suggest that *MMP* genes found in the last common ancestor to vertebrates and echinoderms underwent independent duplication and divergence, following separation of these two groups [61]. Thus, and as discussed above, it appears that *MMP* vertebrate genes were amplified from a common protostome-deuterostome ancestor (Fig. 2).

The major evolutionary event in the generation of the *MMP* gene repertoire of vertebrates was the widespread duplication of pre-existing genes (Fig. 2). In particular, most MMP subfamilies show a further expansion along the early teleost lineage. Nevertheless, it should be noted that both teleost- and tetrapod-specific duplications have occurred after the divergence of both lineages. The expansion in teleosts of *MMP* orthologues related to human *MMP7* and *MMP20*, an evolutionary event likely linked to the continuous teeth replacement in these vertebrates, is remarkable. Similarly, *MT-MMP* genes underwent

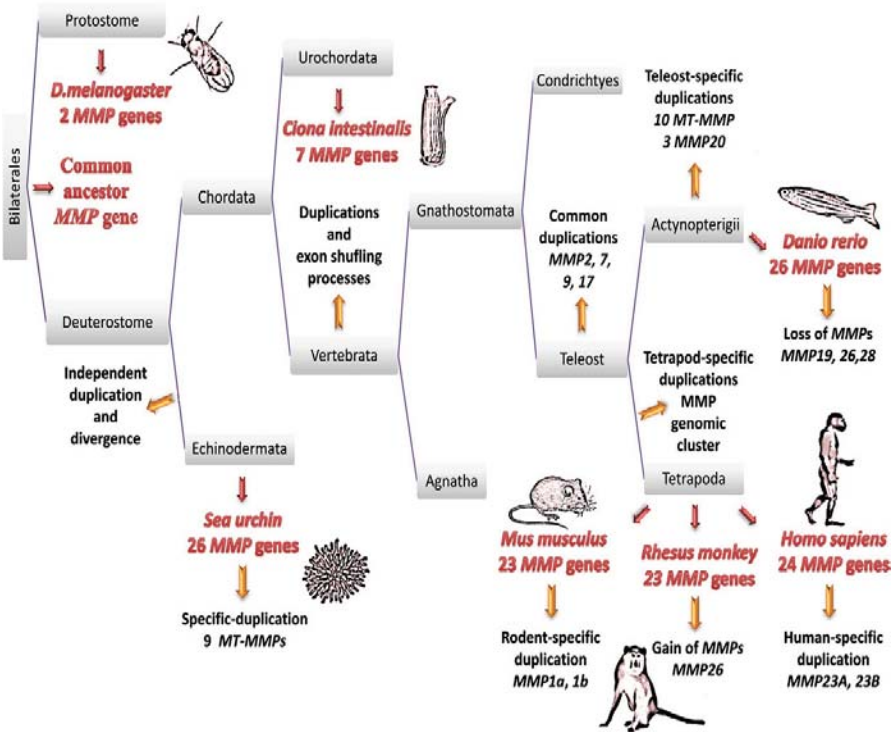

Fig. 2. Evolution of MMPs. Schematic representation of key events occurring throughout the evolutionary history of MMPs.

a greater amplification along teleost lineage, reaching a number of 10 *MT-MMPs* compared to 6 *MT-MMPs* in humans [59]. In contrast, there are no orthologues to human *MMP19*, *-26* and *-28* in the zebrafish genome, although the presence of these genes in some invertebrates strongly suggests that they have been specifically lost in the teleost lineage. Interestingly, there are several tetrapod-specific innovations within the *MMP* gene family. This is the case of *MMP26* which has only been detected in humans and other primates like chimpanzee, orangutan and rhesus monkey genomes, strongly suggesting that this small MMP is the result of a recent evolutionary event circumscribed to the primate lineage [62]. Another remarkable innovation occurred during early evolution of tetrapods is the introduction of CA and Ig-like domains in both human *MMP23* genes, since zebrafish has an orthologue for this gene which lacks these C-terminal domains. Furthermore, the identification of a single *MMP23* copy in rodent and chimpanzee genomes, suggests that the two human copies evolved from a recent duplication event in the human lineage. The presence of two almost-identical genes (*CDC2L1* and *CDC2L2*) adjacent to both human *MMP23* genes provides additional support to the idea that this region has been specifically duplicated in the human lineage [62]. Interestingly, recent studies have also found two putative *MMP23* copies in the *Xenopus* genome. The observation that one of these genes is closer to its human orthologue than to its *Xenopus* paralogue, has suggested that *MMP23* might have duplicated before the separation of amphibians and mammals, an event that was then followed by the loss of one copy of this mammalian gene, which emphasizes the relevance of genomic losses during the evolutionary history of mammals [63,64].

In any case, and beyond these specific changes affecting individual *MMP* genes, the most prominent evolutionary event among those giving rise to the current *MMP* gene families was an extensive gene tandem duplication in the tetrapod lineage (Fig. 2). Accordingly, several members of the *MMP* family have likely evolved from a single gene similar to zebrafish *MMPLe* which, in successive rounds of duplications, led to the formation of a genomic cluster of *MMPs* whose organization is preserved from amphibians to mammals. The synteny of the common *MMP* genes within this cluster is also conserved among all species of sequenced mammals to date, from platypus to human [65]. This *MMP* cluster is not composed of the same members in the different organisms, as there are species-specific enzymes encoded in the cluster and distinct events involving loss- and gain-of-certain *MMPs* have occurred in the different genomes. Thus, the gene encoding collagenase-4 (*MMP18*) has only been identified in frog, whereas *MMP20* (coding for enamelysin) has not been found in chicken because its lack of teeth makes unnecessary the occurrence of an enzyme involved in enamel formation. Likewise, a rodent-specific duplication event has generated two *MMP1* copies, *MMP1a* and *MMP1b* [2,66]. The human cluster is located at chromosome 11q22 and contains *MMP13*, *MMP12*, *MMP3*, *MMP1*, *MMP10*, *MMP8*, *MMP27*, *MMP20*, and *MMP7* (Fig. 3). The fact that most of these MMPs are able to target protein components of the ECM, coupled with the wide number of ECM components present in most vertebrates, suggests that a co-evolution event could have played a role in this process [67]. As an illustrative example supporting this idea, there are three collagenolytic enzymes encoded in this cluster (MMP-1, MMP-8 and MMP-13) which have preferential activity against one of the three major types of fibrillar collagen: MMP-1 is mainly active against type III collagen, MMP-8 targets type I collagen and MMP-13 preferentially cleaves type II collagen [68]. *MMP* genes are not exclusively clustered in a few regions of the vertebrate genomes as they are widely distributed along the different chromosomes. This is the case of human *MMPs* which are distributed in 10 distinct chromosomes (Fig. 3). It is also noteworthy the localization of functionally related *MMP* genes in different chromosomes, as illustrated for the two gelatinase genes *MMP2* and *MMP9* which map at chromosomes 16 and 20, respectively. Moreover, the sequences encoding the catalytic and hemopexin domains of both gelatinases are not clustered together. Collectively, these observations suggest that these MMPs likely evolved in parallel, indicating that the selection pressure was distinct in the course of the diversification of this family of metalloproteinases [58].

In addition to mechanisms based on gene duplication, the evolution of *MMP* genes has also been driven by exon shuffling and duplication of protein modules to form new arrangements. In this regard, it is well known that proteases link their catalytic domains to a range of specialized functional modules generating an extraordinary diversity of specialized enzymes [69]. In the case of MMPs, some of these modules, including the hemopexin, Ig-like and fibronectin domains, act as ancillary domains that allow these enzymes to interact with other proteins and expand their functional relevance (Fig. 1). Nevertheless, evolution has also progressed in the reverse direction as illustrated by the case of the hemopexin domain which is present in most MMPs, but was specifically lost in both members of the matrilysin subfamily (MMP-7 and MMP-26) [2].

In summary, genomic studies are consistent with the idea that most part of the large complexity currently observed in MMP families of tetrapods arose during early stages of vertebrate evolution. It is also likely that these enzymes first appeared as simple proteins with a catalytic domain that, after several rounds of duplication, gene fusion and exon shuffling events, acquired a more complex structural architecture based on the introduction of additional functional domains of diverse sizes and shapes. The incorporation of ancillary domains, coupled with the subsequent parallel evolution of each member of the family, originated the increasingly specialization of these proteases. The amplification in the number of genes that has occurred from *C. intestinalis* to *H. sapiens*, together with the presence of duplicated genes in paralogous regions of the genome, suggests that one or two rounds of whole genome duplication took place. In the case of mammalian *MMP* genes, these processes of duplication and reorganization have led to a wide distribution of these genes into different chromosomes, although a number of them are clustered in a specific genome region. The large complexity arisen during *MMP* evolution made also necessary the evolutionary incorporation of precise mechanisms of regulation to control the expression and activity of these enzymes. These regulatory mechanisms, which are only partially understood, will be discussed in the next sections of this review.

4. Regulation of *MMP* gene expression

MMP gene expression is primarily regulated at the transcriptional level, which usually results in low basal levels of these enzymes in normal physiology. Most members of the *MMP* family share common *cis*-elements in their promoter sequences, which allow a tight control of cell-specific expression. As a result, *MMPs* are often co-expressed or co-repressed in response to multiple stimuli, including inflammatory cytokines, growth factors, glucocorticoids or retinoids [70]. This response at the transcriptional level occurs several hours after exposure to a stimulus, suggesting that *MMP* promoters are downstream targets within signaling pathways of early response genes, which are induced shortly after cellular stimulation and in the absence of new protein synthesis. These early response genes encode signaling proteins that phosphorylate the different transcription factors, which are then able to bind the promoters of *MMP* genes. These signaling intermediates involved in the activation of transcription factors include the nuclear factor kappa B (NF-κB), the mitogen activated protein kinases (MAPK), the signal transducers and activators of transcription (STAT) and the Smad family of proteins. These intermediates belong to signaling pathways that are activated by a large variety of ligands, such as IL-1β, TNF-α and oncostatin M. The blockade of these signaling pathways by decreasing the synthesis of some downstream mediators, by sequestering the transcription factors to prevent their binding or by inhibiting their phosphorylation, may repress the expression of *MMP* genes [71]. Some of the key transcription-binding

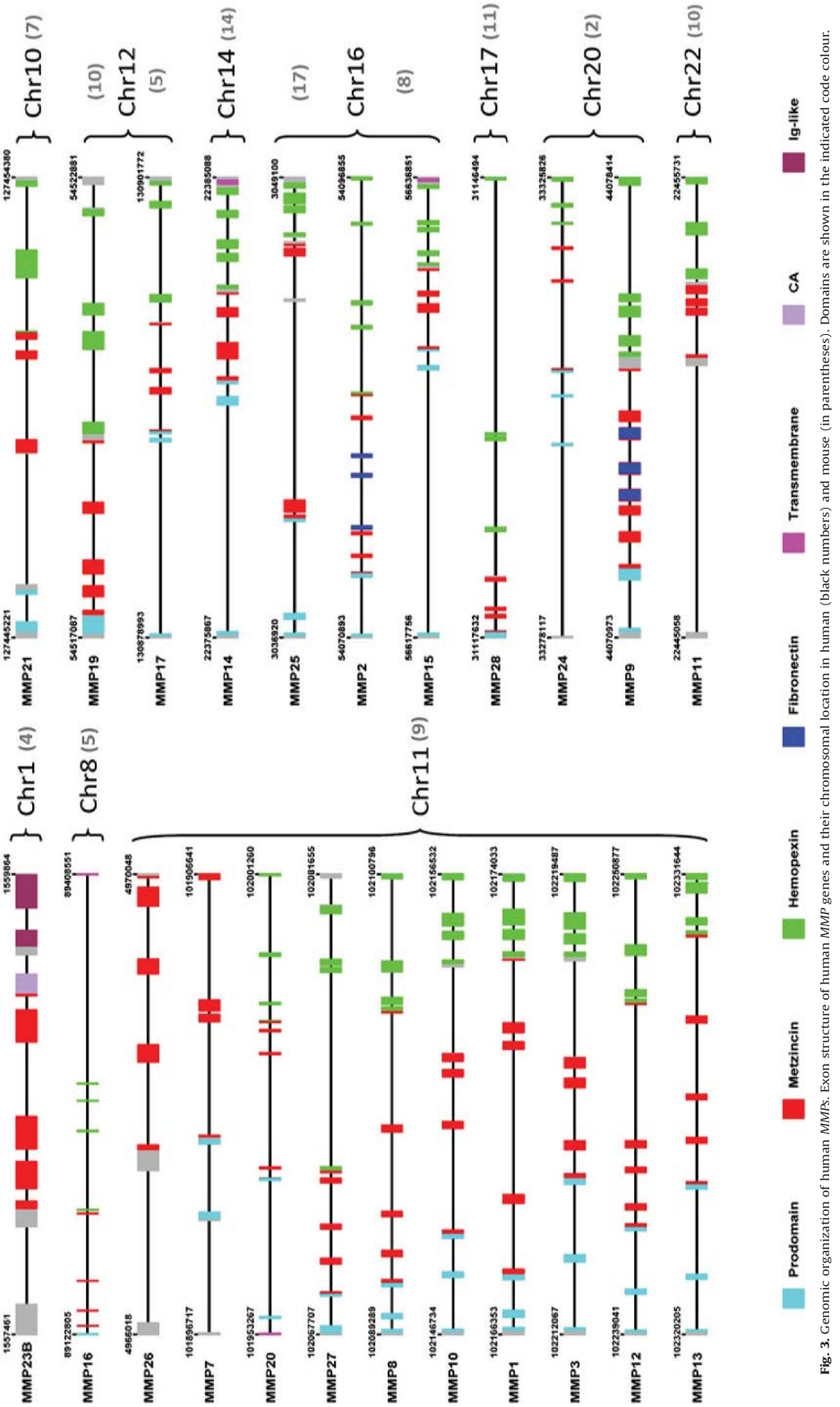

Fig. 3. Genomic organization of human *MMPs*. Exon structure of human *MMP* genes and their chromosomal location in human (black numbers) and mouse (in parentheses). Domains are shown in the indicated code colour.

sites involved in the regulation of *MMP* genes are: the activator proteins (AP) -1 and -2 sites, the polyomavirus enhancer-A binding protein-3 (PEA3) site, the NF-κB site, and the STAT site [72]. Interestingly, *MMP*s that are co-regulated in their expression under certain conditions share several transcription-binding sites in their promoter sequences, whilst functionally related MMPs, such as gelatinases (MMP-2 and -9) or collagenases (MMP-1 and -8), differ greatly in the composition of the *cis*-elements present in their respective promoter regions (Fig. 4).

4.1. AP-1 response elements

The AP-1 site appears to be the major mediator of the regulation of *MMP* genes. Thus, most *MMP* promoters harbor an AP-1 site in the proximal promoter, located close to a typical TATA box (Fig. 4). However, the composition of the AP-1 complex itself, as well as the juxtaposition of transcription factor binding sites, may determine the specificity among different genes [73]. An example of AP-1 regulation can be found in the *MMP1* promoter. Thus, it has been reported that inflammatory cytokines enhance the *trans*-activation of *MMP1* through the MAPK signaling pathway, by increasing the levels of different AP-1 proteins, such as c-*jun*, jun-B and c-*fos* [74]. In this sense, c-Jun has been described to be an independent activator of *MMP1* expression as demonstrated by its capacity to induce minimal *MMP1* promoter activity as a Jun/Jun homodimer. However, jun-B requires the interaction with other members of the AP-1 family, such as c-*fos*, to promote *MMP1* transcription [75]. Likewise, these heterodimers may form ternary complexes with additional transcription factors, thus increasing their binding capacity to the regulatory *cis*-elements [76].

4.2. PEA3 response elements

The PEA3 site binds members of the Ets family of oncoproteins. In several *MMP*s, the PEA3 site is located adjacent to the AP-1 site, and both may act cooperatively to promote MMP production by cancer cells, allowing their migration and invasiveness [77]. In this sense, although PEA3 proteins have been shown to *trans*-activate artificial promoter constructs only containing the PEA3 element, they do not usually dimerize and bind to DNA alone, but prefer to form complexes with other transcription factors, thereby enhancing their effect [78]. Consistently, PEA3 sites are able to bind multiple Ets factors and these proteins contribute to provide the required specificity. For example, Ets1 increases *MMP1* expression through c-Jun, whereas ErgB enhances the *trans*-activation of this promoter only via JunB, and Pu1 represses its induction by both c-Jun and JunB. These examples of functional interaction between Ets and AP-1 factors indicate that *MMP* gene expression may be specifically modulated in situations such as tumor cell growth and invasion, where both types of factors can be simultaneously induced [79, 80].

4.3. NF-κB response elements

The NF-κB pathway is involved in the regulation of several *MMP*s, upon activation by a number of growth factors and cytokines in pathological conditions, such as arthritis, muscular disorders and cancer [81–83]. In addition, this family of transcription factors, including NF-κB1 and 2, RelA, c-Rel, and Rel-B, can interact with other proteins to increase *MMP* expression. Thus, IL-1β-induced *MMP1* gene expression in chondrocytes requires NF-κB homodimers binding to Bcl-3 to activate *MMP1* transcription [84]. Likewise, interaction between juxtaposed sites allows the specific expression of this *MMP* in osteosarcoma and hepatoma cells after its stimulation with TNF-α, which increases the activity of both NF-κB and Sp-1 transcription factors [85].

4.4. STAT response elements

STAT proteins are transcription factors that translocate to the nucleus following tyrosine phosphorylation and dimerization [86]. This family of proteins frequently collaborates with different factors to promote gene-specific expression. Thus, epidermal growth factor (EGF)-mediated-*MMP1* transcription through STAT-3 is stimulated by the binding of c-Jun to the AP-1 element, which is located close to the STAT site [87]. It seems that the stimulation of the STAT pathway is an

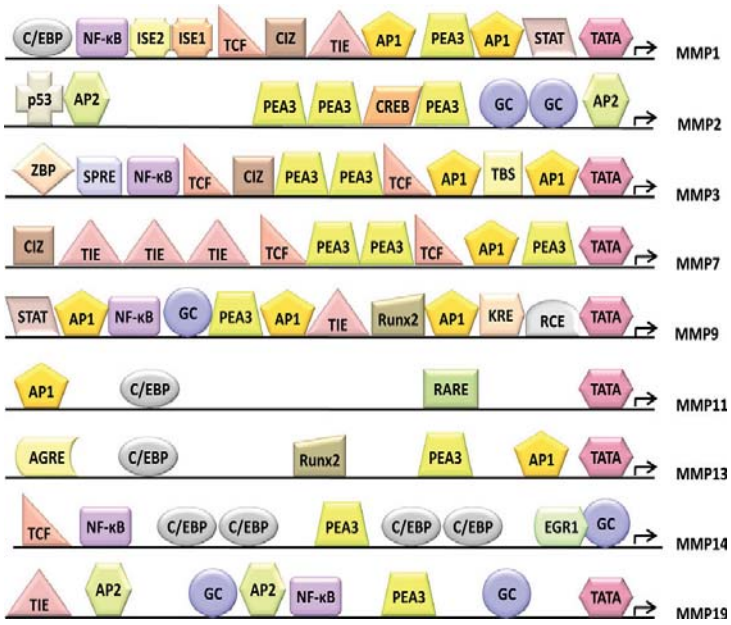

Fig. 4. Regulatory elements in the promoter regions of human *MMP* genes. Transcription start sites are indicated with a bent arrow and the main functionally validated *cis*-elements are represented within boxes. The relative positions of the different binding sites are not drawn to scale.

additional mechanism for increasing the transcription of *MMP1* in pathological conditions [71]. Similarly, a complex composed of c-Jun/Fra-1 and STAT-3 proteins has been shown to bind the promoter-proximal AP-1 site of *MMP9*, thereby confirming the existence of a STAT binding site in juxtaposition with the AP-1 site [88]. Interestingly, activation of STAT proteins does not always induce *MMP* gene expression. Thus, *MMP9* and *MMP13* expression can be repressed as a result of sequestration of co-activators, such as CBP/p300, by STAT proteins, which impair their binding to *cis*-elements on the promoters [89].

4.5. Other regulated cis-elements

MMP7 is regulated by Wnt signaling through the binding of beta-catenin and its partners like Tcf/Lef-1, to its promoter region [90]. Tcf/Lef-1 also synergizes with other factors, particularly those that bind to PEA3 or AP-1 sites, to enhance the expression of *MMP7* in colorectal tumors [91]. Similarly, soluble E-cadherin fragments increase *MMP14* expression in lung cancer cells under the control of the beta-catenin pathway [92]. On the other hand, *MMP13* expression is stimulated by p38 signaling through the recruitment of AP-1 proteins and the chondrocyte/osteoblast-specific transcription factor Runx-2, emphasizing the tissue-specific mechanisms regulating *MMP13* gene expression [93,94]. *MMP9* expression is also regulated by Runx2 binding elements, which agrees with its proposed role in bone remodeling during endochondral ossification [95]. *MMPs* are also regulated by Smads, a small family of co-regulatory proteins that can enhance or inhibit TGF-β-mediated gene expression, providing a mechanism by which TGF-β may play a dual role in the regulation of *MMP* genes during connective tissue remodeling and cancer [96–98]. As mentioned above, TGF-β counteracts the IL-1β-induced *MMP1* transcription through activation of Smad2 and Smad3, which, in turn, are able to block the binding of the CBP/p300 co-activator [99]. Opposite to *MMP1*, *MMP13* gene expression is induced by TGF-β in connective tissue cells, through the activation of Smad3 and the participation of MAPK signaling pathways [96,100]. It is also remarkable that the proximal promoters of several *MMPs* have multiple GC boxes with ability to bind Sp-1 and Sp-3 transcription factors (Fig. 4). Interestingly, some genes such as *MMP2*, *MMP14* and *MMP28*, do not harbor TATA box or other *MMP*-characteristic *cis*-regulatory elements in their proximal promoters, which can explain the fact that they are constitutively expressed and can only be occasionally induced by certain growth factors or cytokines [70]. In summary, the integration of multiple signaling pathways controlling *MMP* transcriptional regulation, provides a wide range of potential interactions between transcription factors, which may explain how tissue specificity is achieved among the different members of the MMP family.

5. Epigenetic regulation of *MMPs*

In general, MMPs have been considered as inducible genes on the basis of a series of experiments that have demonstrated that their expression is transient upon exposure to external stimuli. However, in cancer, both tumor and peritumor cells constitutively express high levels of MMPs, indicating that additional mechanisms are involved in their regulation. Thus, epigenetic mechanisms, such as DNA methylation or histone acetylation, may contribute to modulate both activation and repression of *MMP* gene expression.

Methylation of CpG islands in the promoter region of multiple genes has been widely recognized as an efficient mechanism of repressing transcription. Thus, an inverse correlation between promoter methylation of *MMP9* and expression levels has been found in lymphoma cells, providing evidence that methylation of the promoter region is functionally relevant for *MMP9* gene expression [101]. Likewise, *MMP2* hypomethylation increases its expression and contributes to cancer cell invasiveness and tumorigenesis [102]. Similarly, a colon cancer cell line defective in two key DNA methytransferases (Dmt-1 and Dmt3b) showed increased expression of *MMP3*. In addition, treatment of normal colorectal cells with DNA methyltransferase inhibitors recapitulated this effect, whereas *in vitro* methylation of the *MMP3* promoter suppresses its transcriptional activity. However, this increased expression of *MMP3* appears to be cell-specific since treatment with the same demethylating agent failed to induce *MMP3* transcription in a lymphoma cell line [103].

An additional level of epigenetic control of gene expression derives from post-translational modifications of histones through acetylation processes. Histone acetyl transferases (HAT) are the enzymes responsible for the reversible union of acetyl groups to histones (mainly H3 and H4), leaving the chromatin in a more relaxed state that allows the access of transcription factors and other transcriptional machinery to promoter regions [104]. The effect of the chromatin remodeling in the control of *MMP* expression has been reported for some *MMP* genes. Thus, Yan et al. [105] first showed that MTA1, a component of the NuRD repression complex, binds to the *MMP9* promoter causing the recruitment of histone deacetylase (HDAC) 2 and the decrease of H3/H4 acetylation levels, which finally results in a reduction of DNA accessibility and gene expression. Likewise, *MMP10* expression is repressed as a result of the recruitment of HDAC7–MEF2 complex to the MEF2-binding site present in the *MMP10* promoter [106]. Similarly, the induction of *MMP1* and *MMP13* by IL-1α and oncostatin M is almost completely abolished by two independent HDAC inhibitors [107]. Nevertheless, acetylation *per se* is not sufficient to induce *MMP1* expression in human glioblastoma cells, since treatment with HDAC inhibitors had no effect in *MMP1* mRNA levels despite an increase in local H3 acetylation at the *MMP1* promoter is observed. This finding suggests that *MMP1* transcription requires a prior activation of certain transcription factors, such as c-Jun, c-Fos, TBP, RNAPII and SET9, that bind the *MMP1* promoter and recruit CBP/p300 and RSK2 histone acetyltransferases, finally leading to a permissive state of DNA for transcription initiation [108]. In this sense, the histone acetyltransferase p300 has been recently demonstrated to play a key role in ultraviolet-induced *MMP1* promoter activity [109]. Likewise, analysis of the sequential assembly of transcription complexes on *MMP9* promoter has revealed that, after PMA-induced *MMP9* expression, transcription factors, chromatin-remodeling complexes, and co-activators are recruited to the pre-assembled *MMP9* promoter in a stepwise and coordinated manner, which is dependent on the activation of the MEK-1/ERK and NF-κB signaling pathways. Interestingly, both HDAC1 and HDAC3 are pre-assembled on the *MMP9* promoter as repressive complexes in a basal cell state, being removed upon PMA stimulation [110]. Additional studies have supported the role of transcription factors in the control of gene expression by recruiting chromatin-remodeling complexes to the promoters and the synergy among these co-activators [111,112]. Taken together, these findings show the interconnection between the diverse *MMP* gene regulatory mechanisms operating at the transcriptional level, and confirm that this complexity is increased by cell-specific induction. Nevertheless, further studies will be required to fully understand the epigenetic mechanisms that control *MMP* gene expression.

6. Post-transcriptional regulation of MMPs

Although MMPs are mainly regulated at the transcriptional level, a series of post-transcriptional events have been recently described as relevant mechanisms in the regulation of *MMP* expression. *MMP* transcripts harbor specific sequences in their 5′- or 3′-untranslated regions (UTRs), which are potential targets of different UTR-binding proteins with ability to stabilize or destabilize these mRNAs. Thus, the rat *MMP9* transcript contains several copies of AU-rich elements (ARE) within its 3′-UTR, which are important determinants for RNA turnover [113]. In this regard, it has been reported that IL-1β-induced *MMP9* expression is enhanced by the ATP analog ATPγS through an increase in the binding of the HuR stabilizing factor to the ARE motifs present in the 3′-UTR of the *MMP9* mRNA, providing protection against rapid degradation [114]. Likewise, oncogenic Ras-dependent MERK/ERK signaling maintains

high levels of MMP-9 production in transformed cells, by cooperating with α3β1 integrin which promotes mRNA stability [115]. In contrast, a decline in the *MMP9* mRNA levels has been reported to be caused by nitric oxid in mesangial cells, which is responsible for the reduction of the HuR protein content and its subsequent binding to the 3′-UTR of *MMP9* transcripts [113]. Recent studies have also shown that IL-10 contributes to improve the fibrotic processes that follow acute myocardial infarction, by reduction of *MMP9* expression via repression of HuR protein [116]. Parallel studies have revealed that cortisol induces *MMP13* steady state mRNA in osteoblasts by increasing protein binding to ARE elements in its 3′-UTR region [117].

In addition to mRNA stability, regulation of translational efficiency may be also a mechanism for controlling *MMP* expression. Thus, elevated binding of nucleolin to the 3′-UTR of human *MMP9* mRNA has been observed in fibrosarcoma cells in response to an iron chelator. Nucleolin recruits inactive *MMP9*-mRNA complexes into the rough endoplasmic reticulum, enhancing the efficiency of *MMP9* translation [118]. Likewise, more rapid *MMP9* translation has been described in murine prostate carcinoma cells where an increase in the binding of mRNA to polysomes results in elevated MMP-9 protein levels [119].

Finally, recent experimental work has demonstrated that microRNAs (miRNAs) may also participate in *MMP* regulation. Studies on the role of miRNAs in the regulation of eukaryotic genes have impressively increased over the last few years. These small RNA molecules are capable of negatively regulating gene expression at the post-transcriptional level through either translation repression or degradation of their mRNA targets. Bioinformatic analyses have predicted potential miRNA-binding sites in the 3′-UTR regions of certain *MMP*s [120]; however, to date, only one study has demonstrated that *MMP*s may be direct targets of miRNAs [121]. Indeed, the remaining reports in this field have only shown how *MMP* expression is modulated indirectly through miRNAs that target genes involved in different signaling pathways responsible for *MMP* activation. For instance, *MMP2* expression is upregulated by mir-21 in response to the high levels of phospho-Akt caused by the knockdown of *PTEN* mRNA, which is targeted by this miRNA after myocardial infarction in mice [122]. Similarly, mir-21 downregulates *TIMP3* (tissue inhibitor of metalloproteinase 3), which, in turn, leads to the activation of MMPs and the subsequent promotion of cancer cell invasiveness [123]. Likewise, MMP-13 secretion is modulated by mir-9 in human osteoarthritic processes, through the reduction of TNF-α [124]. Nevertheless, and based on the growing relevance of miRNAs in the regulation of biological processes, it is tempting to speculate that further work in this field will reveal the occurrence of additional miRNAs with ability to target specific MMPs, thus contributing to regulate their functions in the different physiological and pathological contexts in which they are implicated.

7. Mutations in *MMP* genes and human diseases

There are several hereditary disorders caused by autosomal mutations in human *MMP* genes. All of them result from the loss-of-function of the corresponding protease activity, which finally leads to marked deficiencies in the turnover of specific ECM components. The first *MMP* mutation associated with a human inherited disease was identified in two consanguineous Saudi Arabian families with nodulosis–arthropathy–osteolysis syndrome (NAO), an autosomal-recessive form of multicentric osteolysis. A genome-wide analysis had previously identified the chromosome 16 as carrier of the disease gene, and subsequent studies narrowed the critical region close to the gene encoding MMP-2 [125]. To date, several *MMP2* mutations have been reported in three different skeletal disorders, collectively known as inherited osteolysis syndromes and characterized by progressive resorption of bones. The common pathogenic mechanism in the three genetic disorders seems to be the loss of MMP-2 activity, as no detectable MMP-2 enzymatic activity can be found in serum and fibroblasts from patients homozygous for mutations in this gene. Thus, the Y244X mutation described in the above mentioned NAO syndrome introduces a premature stop codon that removes most functional protein domains [125]. The E404K mutation observed in patients with Winchester syndrome changes the key glutamate residue in the catalytic domain of the MMP-2 protein and leads to a complete loss of its peptidase activity [126]. Additionally, two *MMP2* heterozygous mutations have been reported in a patient with Torg syndrome. The first mutation, R101H, has also been found in patients with NAO syndrome and affects a residue adjacent to the key cysteine in the propeptide, thereby resulting in destabilization of the cysteine-zinc interaction. The second mutation, 1957delC, causes a frameshift which creates a truncated nonfunctional protein. In combination, the two mutations should cause the complete loss of MMP-2 activity in this patient with Torg syndrome [127]. Based on the finding that all these mutations abolish MMP-2 proteolytic activity, NAO, Winchester and Torg syndromes have been considered allelic disorders that form a continuous clinical spectrum.

Parallel studies have revealed that another genetic disease of bone metabolism is caused by mutations in a human *MMP* gene. Thus, mutations in the *MMP13* gene are responsible for the Missouri type of human spondyloepimetaphyseal dysplasia (SEMD), an autosomal dominant disorder characterized by defective growth and remodeling of vertebrae and long bones. The F56S missense mutation results in an abnormal intracellular autoactivation and autodegradation of the mutant MMP-13 protein, with the resulting MMP-13 deficiency. Nevertheless, before it is fully proteolytically degraded, the mutant protein intracellularly degrades the MMP-13 product of the wild-type allele, explaining the haploinsufficiency of the gene and thereby, the dominant phenotype of the disorder [128].

Finally, MMP-20 or enamelysin is the third MMP family member that has been implicated in a human inherited disease: autosomal-recessive amelogenesis imperfecta (ARAI). The ARAIs are a group of clinically and genetically heterogeneous disorders that affect enamel development, resulting in abnormalities in the amount, composition, and structure of enamel. To date, at least three different *MMP20* mutations have been reported in families with ARAI. The first identified mutation was found at the 3′-end of intron 6, where AG changed to TG, causing defective splicing events that introduce an upstream translation termination codon in the transcript [129]. Likewise, the W34X mutation is a single nucleotide substitution that generates a stop codon in exon 1 of *MMP20* [130]. The third characterized mutation in this gene (H226Q) changes one of the three-conserved histidine residues in the catalytic domain, thereby destroying the zinc-ligand site required for metal binding [131]. Thus, all *MMP20* mutations described to date lead to complete lack of proteolytic activity on amelogenin, the *in vivo* substrate for enamelysin.

In addition to these interesting cases of *MMP* alterations in inherited human diseases, very recent studies have shown that these genes can also be target of sporadic mutations in cancer. The first indication that *MMP*s could be mutated in cancer derived from the observation that *MMP2* was one of the so-called CAN genes found to be mutated in a small set of breast and colorectal cancers [132]. Further studies have extended the mutational analysis of *MMP*s to other malignant tumors with the finding that some family members including *MMP8*, *MMP14* and *MMP27* are mutated albeit at low frequency in different malignancies including lung carcinomas and melanoma (http://www.sanger.ac.uk/genetics/CGP/cosmic/). These yet unpublished results, together with those recently obtained in the ADAMTS family of metalloproteinases, have supported the innovative proposal that extracellular proteases are direct target of genetic mutations in cancer [6, 133]. Nevertheless, to date, no functional analysis have been reported to validate these preliminary genetic findings and further studies will be necessary to provide functional support to the putative relevance of *MMP* mutations during cancer progression.

8. *MMP* polymorphisms and human disease susceptibility

Polymorphisms in human *MMP*s can modify gene expression by altering the interaction between transcription factors and transcription-

binding sites in the corresponding promoters, resulting in higher or lower transcriptional activity and having dual roles in disease. A number of functional polymorphisms have been identified in the promoters of *MMP* genes and several of them are associated with increased susceptibility to the development of different pathologies and their prognosis (Table 1). Thus, correlations between single nucleotide polymorphisms (SNPs) and cancer susceptibility have been reported for several MMPs.

The first described SNP for *MMP1* is an insertion of a G residue at −1607 in the *MMP1* promoter which creates a binding site for Ets transcription factors adjacent to an AP-1 site located at −1602. The 2G allele leads to higher levels of *MMP1* mRNA and protein in several tumors, and is associated with increased lung and colorectal cancer susceptibility [134,135]. The association between 2G/2G genotype and poor prognosis in patients with melanoma or breast and ovarian carcinomas has also been observed, although data are inconsistent for all tumor types [136–138]. Furthermore, the −1607 1G/2G polymorphism has been implicated in other non-tumor pathologies, such as fibrotic disorders. Thus, *MMP1* is overexpressed in idiopathic pulmonary fibrosis and the frequency of 2G/2G genotype is higher in patients with this disease [139]. The 2G/2G genotype may also contribute to cirrhosis [140].

In the case of *MMP2*, three functional SNPs have been mapped in its promoter region. Two of them are C to T transitions located at −735 and −1306, which abolish Sp1 binding, with the T allele being associated with diminished promoter activity. Interestingly, these SNPs are in linkage disequilibrium with the −1306 T/−735 T haplotype resulting in a lower promoter activity comparing with the single −1306 or −735 T allele haplotypes. High risk of developing lung and esophageal cancer for −1306CC or −735 CC genotype carriers has been reported, suggesting a protective role for −1306 T and −735 T alleles. Importantly, a greater risk of lung and esophageal cancer has been associated with −1306 C/−735C haplotype [141,142]. The third SNP found in the *MMP2* promoter is a G to A transition at −1576, which disrupts estrogen receptor α binding, and also results in lower transcriptional activity [143].

A functional SNP in the *MMP3* promoter has also been described, but in this case, the insertion of an A residue at −1171 generates a 6A allele that enhances the affinity for the repressor ZBP-89 and decreases MMP-3 protein levels. This 6A allele would play a protective role in lung, oral and breast cancer, whereas the 5A *MMP3* allele is linked with an increased risk for these cancers [144–146]. Additional studies have suggested that the 6A/6A *MMP3* genotype is associated with worse rheumatoid arthritis outcome as well as with atherosclerotic processes [147,148]. On the other hand, two polymorphisms have been found in the *MMP7* promoter region, an A to G substitution at position −181 and a C to T substitution at position −153, both of them increasing the promoter activity [149]. A relationship of the −181 G allele with increased susceptibility for gastric, cervical, lung, oral and esophageal cancer has also been described [150–153].

For the *MMP8* gene, three functional SNPs (−799C/T, −381A/G and +17C/G) have been identified. The haplotype with the three less frequent alleles of these SNPs increases *MMP8* promoter activity in trophoblast cells and is associated with higher risk of preterm premature rupture of membranes [154]. Individually, the G allele of the +17 C/G SNP is linked to a decreased risk for lung cancer, and the −799 T to lower susceptibility to metastasis and better survival in breast cancer patients [155,156]. These results are in agreement with the proposal that MMP-8 has antitumor properties [157–159]. With respect to *MMP9*, a polymorphism has been observed in the promoter region located at position −1562. This variant is a C/T transition which leads to a higher promoter activity in the T allele which has been associated with increased susceptibility to atherosclerosis [160], abdominal aortic aneurysm [161] and myocardial ischemia [162]. Additionally, a microsatellite polymorphism of variable number of CA repeats (from 14 to 25 at position −131) and localized immediately adjacent to the proximal AP-1 binding site, has been described to increase the transcriptional activity of the *MMP9* gene in a manner proportional to the number of CA repeats. The *MMP9* microsatellite (≥24 CA repeats) has been associated with a higher risk of bladder cancer invasiveness [163]. This polymorphism has also been associated with susceptibility to a number of conditions, including atherosclerosis [164], multiple sclerosis [165], aneurysmal disease [166], and age-related macular degeneration [167]. For *MMP12*, an A to G substitution at position −82, located in the AP-1 binding site, has been linked to decreased expression *in vitro*. Several studies have also shown that the GG genotype is associated with increased bladder cancer invasiveness and this has been attributed to the loss of putative angiostatic effects of MMP-12 [163]. Finally, it is important to consider that *MMP* polymorphisms may not occur as independent events and could be associated with other polymorphisms in the genome.

9. Transgenic models for functional analysis of MMPs

Over the last two decades, the generation of genetically modified mouse models has become one of the most powerful strategies for studying gene function *in vivo*. Genetic engineering approaches have allowed the modulation of gene expression through gain-of-function (*transgenic*) or loss-of-function (*knock-out*) *in vivo* models. To date, many transgenic and knock-out mice (Table 2) have been generated to analyze the effects of altering MMP activity in a variety of physio-

Table 1
Functional polymorphisms in *MMP* promoters.

Gene	Polymorphism	Promoter activity	Associated pathology	
			Tumor-disease	Non-tumor disease
MMP1	−1607 1G/2G	Higher	↑ Risk: lung [134] and colorectal [135] cancer Poor prognosis: breast [136] and ovarian [137] cancer, cutaneous malignant melanoma [138]	↑ Risk: idiopathic pulmonary fibrosis [139] Poor prognosis: cirrhosis [140]
MMP2	−1575 G/A	Lower	Breast cancer [143] (*in vitro* MCF-7 cells)	
	−1306 C/T	Lower	↓ Risk: esophageal [141] and lung [142] cancer, gastric cardia adenocarcinoma [204], oral squamous cell carcinoma [205]	↓ Risk: lumbar disc disease [206]
	−735 C/T	Lower	↓ Risk: esophageal [141] and lung [142] cancer	
MMP3	−1171 5A/6A	Lower	↓ Risk: lung [144] breast [145] and oral [146] cancer	↑ Risk: atherosclerosis [147] Poor prognosis: rheumatoid arthritis [148]
MMP7	−181 A/G	Higher	↑ Risk: gastric [150], cervical [151] and oral [152] cancer, esophageal squamous cell carcinoma and non-small cell lung carcinoma [153]	Poor prognosis: atherosclerosis [149]
MMP8	−799C/T	Higher	Better prognosis: breast cancer [155]	↑ Risk: preterm premature rupture of membranes (haplotype) [154]
	−381A/G	Higher		↑ Risk: preterm premature rupture of membranes (haplotype) [154]
	+17C/G	Higher	↓ Risk: lung cancer [156]	↑ Risk: preterm premature rupture of membranes (haplotype) [154]
MMP9	−1562 C/T	Higher	↑ Risk: oral cancer [207]	↑ Risk: atherosclerosis [160, 162], abdominal aortic aneurysm [161]
	(CA)n microsatellite	Higher≥20 CA repeats	↑ Risk: bladder cancer [163]	↑ Risk: carotid atherosclerosis [164], multiple sclerosis [165], cerebral aneurysm [166], age-related macular degeneration [167]
MMP12	−82A/G	Lower	Poor prognosis: bladder cancer [163]	

Table 2
Genetically modified mouse models of MMPs.

Genetically modified mice	Spontaneous phenotype	Pathological-induced phenotype	
		Tumoral	Non-tumoral
Haptoglobin-MMP1	Hyperkeratosis [178]	↑ Skin carcinogenesis [178]	
	Pulmonary emphysema [208]		
TypeIγ-GT-MMP2/cmyc	Chronic kidney disease [209]		
WAP-MMP3	Mammary carcinogenesis [180]		
K5-MMP3*$^{301.24}$		↓ Skin carcinogenesis [210]	
SREP-MMP9			↓ Pulmonary fibrosis [211]
MMTV-MMP14	Mammary carcinogenesis [179]		
Mmp2$^{-/-}$*/RIP-TAg*		↓ Pancreatic carcinogenesis [212]	
Mmp2$^{-/-}$*/ApoE*$^{-/-}$			↓ Atherosclerotic plaques [192]
Mmp3$^{-/-}$*/ApoE*$^{-/-}$			↑ Atherosclerotic plaques [190]
			↓ Aneurism formation [190]
Mmp7$^{-/-}$*/Apc*^{Min}		↓ Intestinal adenomas [213]	
Mmp9$^{-/-}$*/ApoE*$^{-/-}$			↓ Atherosclerotic plaques [191]
Mmp9$^{-/-}$*/K14-HPV16*		↓ Skin carcinogenesis [183]	
Mmp9$^{-/-}$*/RIP-TAg*		↓ Pancreatic carcinogenesis [212]	
Mmp11$^{-/-}$*/MMTV-ras*		↓ Mammary carcinogenesis [184]	
		↑ Number of metastasis [184]	
Mmp13$^{-/-}$*/ApoE*$^{-/-}$			↑ Atherosclerotic plaques [189]
Mmp14$^{-/-}$*/MMTV-PyMT*		↓ Lung metastasis [214]	
Mmp1a$^{-/-}$	No overt phenotype (C. Lopez-Otin, unpublished)		
Mmp2$^{-/-}$	↓ Body size [215]	↓ Tumor growth [216]	↑ Arthritis [187]
	↓ Bone density [172]	↓ Angiogenesis [216]	↓ Resolution of lung allergic inflammation [197]
	Altered mammary branching [170]	↓ Acute hepatitis [217]	
Mmp2$^{-/-}$*/Mmp9*$^{-/-}$			↓ Resolution of lung allergic inflammation [198]
Mmp2$^{-/-}$*/Mmp14*$^{-/-}$	Death at birth [176]		Resistance to EAE [193]
Mmp3$^{-/-}$	Altered mammary branching [170]	↑ Skin carcinogenesis [218]	Impaired contact dermatitis [219]
			↓ Acute hepatitis [217]
			↑ Arthritis [188]
Mmp7$^{-/-}$	↓ Innate intestinal immunity [220]		Impaired tracheal wound repair [222]
	Defective prostate involution [221]		↓ Pulmonary fibrosis [202]
			↓ EAE [195]
Mmp8$^{-/-}$		↑ Skin carcinogenesis [157]	↑ Asthma [199]
		↑ Experimental metastasis [158]	↓ Acute hepatitis [223]
			↓ EAE [194]
Mmp9$^{-/-}$	Delayed growth plate vascularization [171]	↓ Experimental metastasis [225]	↓ Aortic aneurysms [226]
	Defective endochondral ossification [171]		↓ Arthritis [187]
	Delayed myelinization [224]		↓ Acute hepatitis [217]
			Prolonged contact dermatitis [219]
			↓ Colitis [227]
Mmp9$^{-/-}$*/Mmp13*$^{-/-}$	Shortened bones [169]		
Mmp10$^{-/-}$			↑ Pulmonary inflammation and mortality [200]
Mmp11$^{-/-}$			Accelerated neointima formation after vessel injury [228]
Mmp12$^{-/-}$	Delayed myelinization [224]		↓ Pulmonary emphysema [201]
			↑ EAE [196]
Mmp13$^{-/-}$	Bone remodeling defects [168, 169]		↓ Hepatic fibrosis [229]
Mmp14$^{-/-}$	Severe abnormalities in bone and connective tissue [173]		
	Defective angiogenesis [174]		
	Premature death [173]		
Mmp14$^{-/-}$*/Mmp16*$^{-/-}$	Perinatal lethality [177]		
Mmp16$^{-/-}$	Growth retardation [177]		
Mmp17$^{-/-}$	No overt phenotype [230]		
Mmp19$^{-/-}$		↓ Skin carcinogenesis [185]	↑ Induced obesity [185]
		↑ Angiogenesis [186]	
Mmp20$^{-/-}$	Amelogenesis imperfecta [175]		
Mmp24$^{-/-}$			Absence of mechanical allodynia [231]
Mmp28$^{-/-}$			↑ Macrophage recruitment in lung [232]

logical and pathological processes. Likewise, these strategies have provided the opportunity to validate candidate substrates, which are the essential partners to uncover protease function [69].

A total of 17 out of the 23 murine *Mmp* genes have already been knocked-down. However, despite this broad landscape of gene targeting, the vast majority of these constitutive knock-out mice display subtle spontaneous phenotypes (Table 2). Among the three collagenases, only the deficiency in collagenase-3 leads to developmental defects characterized by impaired bone formation and remodeling due, in part, to the lack of appropriate type II collagen cleavage [168, 169]. However, mice deficient in collagenase-1 (C. López-Otín, unpublished data) or collagenase-2 show no overt physiological abnormalities [157]. Likewise, the absence of any of the three stromelysins does not produce major alterations, with the exception of *Mmp3*-null mice whose mammary glands show deficient secondary branching morphogenesis [170]. Deficiency in any of the two gelatinases is also characterized by certain defects in bone biology. Thus, mice deficient in *Mmp9* have delayed long bone growth and development due to impaired vascular invasion in skeletal growth plates [171]. In addition, *Mmp2* deficiency causes disruption of the osteocytic networks and reduced bone density [172]. Interestingly, the most severe phenotype among MMP knock-outs is also associated with defects in skeletal development. In this sense, targeted inactivation of the *Mmp14* gene causes multiple abnormalities in the remodeling of skeletal and connective tissues, as well as defective angiogenesis, leading to premature death by 3–12 weeks after birth

[173,174]. In addition, mice deficient in *Mmp20* have defects in tooth development due to impaired amelogenin processing [175]. Remarkably, these bone abnormalities shown in MMP knock-outs phenocopy the human skeletal syndromes caused by loss-of-function MMP mutations [125,128,129]. The remaining *Mmp*-null mice generated to date show no major physiological alterations, although it is important to emphasize that all available MMP knock-out models are constitutive, thus leading to the possibility of enzymatic compensation as a way to circumvent the absence of the targeted gene. Another possible explanation for the lack of severe phenotypes in *Mmp*-null mice is the enzymatic redundancy among different members of the family, which share many substrates *in vitro*. The recent generation of double MMP mutants has supported this hypothesis, and future studies in this direction may also argue for essential roles of certain MMPs in embryonic development, in addition to their known functions in postnatal tissue remodeling [176,177].

Despite early characterization of MMP knock-outs did not provide major evidence about the biological relevance of this family of proteases, further analyses of these mouse models challenged by a series of pathogenic conditions have revealed the essential contribution of MMPs to a broad number of pathological processes. Among them, over the last 25 years, cancer has been the central disease supporting the promising field of MMPs research. In this sense, the first transgenic mouse models overexpressing different members of the family (Table 2) validated the initial assumption for the contributory effect of these ECM degrading enzymes to tumor progression [178–180], since high levels of MMPs often correlated with poor clinical outcome in cancer patients. However, the generation of new genetically modified animal models has demonstrated that certain MMPs, such as MMP-8 or MMP-12, contribute to tumor suppression [6,157,158,181]. Furthermore, it has also been reported that other MMPs, including MMP-3 [182], MMP-9 [183], MMP-11 [184] or MMP-19 [185,186] play dual roles as pro- or anti-tumorigenic enzymes depending on tissue type and stage of the disease (Table 2). Likewise, gain- or loss-of-function mouse models have allowed the identification of some of the *in vivo* substrates for these enzymes. This is another step forward in the complex relationship between MMPs and cancer, since many non-matrix bioactive molecules, such as growth factor receptors, chemokines, cytokines, apoptotic ligands or angiogenic factors, have been identified as substrates for MMPs [37]. Altogether, these findings illustrate the diversity of MMP functions associated with cancer and provide explanations for the disappointing results of the first clinical trials based on the use of broad spectrum MMP inhibitors [72].

The increasing complexity of the *in vivo* functions of MMPs also affects many other pathological contexts, particularly those involving inflammatory conditions where MMP expression is frequently deregulated [5]. In this sense, genetically modified mice have been essential to demonstrate the relevance of these enzymes in prevalent human pathologies, such as rheumatic, pulmonary, cardiovascular and neurodegenerative disorders. Remarkably, these studies have also shown opposing and unexpected effects among different members of the MMP family on the progression of these diseases (Table 2). Thus, and somewhat surprisingly, mice deficient in *Mmp2* or *Mmp3* develop more severe arthritis than control animals [187,188]. Likewise, deficiency in *Mmp3* or *Mmp13* results in more stable atherosclerotic plaques [189,190]. By contrast, deletion of *Mmp2* or *Mmp9* reduces the formation of the plaques and attenuates cardiac fibrosis after experimental myocardial infarction [191,192]. In neuroinflammatory diseases, such as experimental autoimmune encephalomyelitis (EAE), the murine model of multiple sclerosis, MMPs also show opposite roles. Indeed, certain mouse MMPs, including Mmp-2, Mmp-7, Mmp-8 and Mmp-9 [193–195], contribute to the severity of the clinical symptoms of paralysis whereas others, such as Mmp-12 [196], play protective functions. Similarly, the role of MMPs in respiratory disorders is very complex, since it is not clear yet whether MMPs upregulation is harmful in acute and chronic lung pathologies. Genetically modified mice have demonstrated that lack of *Mmp2*, *Mmp8* or both *Mmp2*/*Mmp9* [197–199] increases the allergic response in a mouse model of asthma due to the failure in clearing inflammatory cells. In this sense, mice deficient in *Mmp10* also show more severe pulmonary inflammation and greater susceptibility to death following bacterial infection [200]. By contrast, deletion of *Mmp7* or *Mmp12* [201,202] resulted beneficial in chronic lung diseases, such as pulmonary fibrosis or emphysema.

Overall, the generation of gain- or loss-of-function mouse models has been essential to demonstrate the complex and even paradoxical roles that MMPs play in physiological and pathological processes [203]. Likewise, these approaches have allowed the *in vivo* validation and identification of specific substrates, providing a better understanding of the mechanisms involved in the development of the diseases. Therefore, it is necessary to continue analyzing and generating the remaining MMP knock-outs, but also to improve the experimental approaches through the creation of new biological models with the crossing of *Mmp*-targeted mice and transgenic animals overexpressing oncogenes that mimic human malignancies. Nevertheless, it is important to emphasize that a constitutive deletion of a gene may not have the same effect as inhibiting the enzyme in a specific spatiotemporal context during the adult life. Thus, additional *in vivo* strategies able to modulate MMPs activity, such as conditional targeting or RNA interference delivery, will be required in order to improve the extrapolation of mice experimentation to therapeutic advances in human diseases.

10. Conclusions and perspectives

The availability of the complete genome sequences of different organisms has recently allowed the identification of their entire protease complements including that of MMPs, and the establishment of novel insights into their evolutionary diversification in all kingdoms of life. The family portrait of this group of metalloproteinases has revealed that, beyond an archetypal design, they exhibit a structural diversity which allows them to participate in multiple biological and pathological functions. Over the last years, there has been a substantial change in our view of these MMP functions. Thus, the initial concept that MMPs were mainly implicated in the demolition of the structural groundwork that supports cells and generates tissue barriers has been replaced by a new vision of these enzymes as signaling scissors controlling multiple processes. The generation of animal models of gain- or loss-of-function for MMPs has been crucial for the identification of some novel and unexpected functions of these metalloproteinases. Likewise, these models have been very useful for the identification of *in vivo* substrates of MMPs and for the establishment of causal relationships between dysregulation of these enzymes and development of different human diseases. Nevertheless, the generation of new animal models is still necessary to evaluate the function of several MMP family members such as MMP-23, MMP-27 or MT6-MMP which are largely uncharacterized yet. Some of these new models will require the generation of double or even triple knock-out models to minimize the putative occurrence of functional redundancy or compensatory mechanisms between members of the MMP family. The generation of conditional mouse models to better understand the role of some enzymes, and especially MT1-MMP, in the diverse conditions in which they are presumably involved is also urgent. These genetic approaches to MMP function will also need to be complemented with strategies derived from the application of RNA interference methods to the MMP field. Genomic studies coupled to functional analysis of promoter regions of *MMP* genes have already provided important information about the molecular mechanisms controlling their expression in health and disease. Nevertheless, it will be necessary to complete these regulatory studies on MMPs and extend them to other levels of control including those based on epigenetic or miRNA-mediated mechanisms, which have acquired a great relevance in many eukaryotic genes but whose influence on the *MMP* gene family is still largely unknown. Likewise, and despite the recent progress in the identification of *MMP* mutations and polymorphisms associated with different genetic

diseases, further functional analysis will be necessary to clarify the relevance of these alterations in the context of the multiple genetic and epigenetic changes detected in complex diseases such as cancer. Hopefully, all these studies will provide new insights into the multiple questions still open in relation to a family of enzymes which had a modest irruption into the protease scene owing to their implication in tail resorption of tadpoles, and now are considered essential mediators of multiple events in all living organisms.

Acknowledgments

We thank Drs. J.P. Freije, G. Velasco, V. Quesada, and G. Ordoñez for helpful comments. Our work is supported by grants from the Ministerio de Ciencia e Innovación-Spain, Fundación "M. Botín", and the European Union (FP7 MicroEnviMet.). S.C. is supported by a fellowship from CONACYT (Mexico). The Instituto Universitario de Oncología is supported by Obra Social Cajastur and Acción Transversal del Cáncer-RTICC.

References

[1] F.X. Gomis-Ruth, Catalytic domain architecture of metzincin metalloproteases, J. Biol. Chem. (2009).
[2] X.S. Puente, L.M. Sanchez, C.M. Overall, C. Lopez-Otin, Human and mouse proteases: a comparative genomic approach, Nat. Rev. Genet. 4 (2003) 544–558.
[3] A. Page-McCaw, A.J. Ewald, Z. Werb, Matrix metalloproteinases and the regulation of tissue remodelling, Nat. Rev. Mol. Cell Biol. 8 (2007) 221–233.
[4] R.G. Rowe, S.J. Weiss, Breaching the basement membrane: who, when and how? Trends Cell Biol. 18 (2008) 560–574.
[5] J. Hu, P.E. Van den Steen, Q.X. Sang, G. Opdenakker, Matrix metalloproteinase inhibitors as therapy for inflammatory and vascular diseases, Nat. Rev. Drug Discov. 6 (2007) 480–498.
[6] C. López-Otín, L.M. Matrisian, Emerging roles of proteases in tumour suppression, Nat. Rev. Cancer 7 (2007) 800–808.
[7] A.R. Folgueras, A.M. Pendas, L.M. Sanchez, C. Lopez-Otin, Matrix metalloproteinases in cancer: from new functions to improved inhibition strategies, Int. J. Dev. Biol. 48 (2004) 411–424.
[8] G.A. Limb, K. Matter, G. Murphy, A.D. Cambrey, P.N. Bishop, G.E. Morris, P.T. Khaw, Matrix metalloproteinase-1 associates with intracellular organelles and confers resistance to lamin A/C degradation during apoptosis, Am. J. Pathol. 166 (2005) 1555–1563.
[9] A. Ruta, B. Mark, B. Edward, P. Jawaharlal, Z. Jianliang, Nuclear localization of active matrix metalloproteinase-2 in cigarette smoke-exposed apoptotic endothelial cells, Exp. Lung Res. 35 (2009) 59–75.
[10] D. Luo, B. Mari, I. Stoll, P. Anglard, Alternative splicing and promoter usage generates an intracellular stromelysin 3 isoform directly translated as an active matrix metalloproteinase, J. Biol. Chem. 277 (2002) 25527–25536.
[11] E. Cuadrado, A. Rosell, M. Borrell-Pages, L. Garcia-Bonilla, M. Hernandez-Guillamon, A. Ortega-Aznar, J. Montaner, Matrix metalloproteinase-13 is activated and is found in the nucleus of neural cells after cerebral ischemia, J. Cereb. Blood Flow Metab. 29 (2009) 398–410.
[12] A.M. Tester, J.H. Cox, A.R. Connor, A.E. Starr, R.A. Dean, X.S. Puente, C. Lopez-Otin, C.M. Overall, LPS responsiveness and neutrophil chemotaxis in vivo require PMN MMP-8 activity, PLoS ONE 2 (2007) e312.
[13] A.J. Gearing, P. Beckett, M. Christodoulou, M. Churchill, J. Clements, A.H. Davidson, A.H. Drummond, W.A. Galloway, R. Gilbert, J.L. Gordon, Processing of tumour necrosis factor-alpha precursor by metalloproteinases, Nature 370 (1994) 555–557.
[14] A. Boire, L. Covic, A. Agarwal, S. Jacques, S. Sherifi, A. Kuliopulos, PAR1 is a matrix metalloprotease-1 receptor that promotes invasion and tumorigenesis of breast cancer cells, Cell 120 (2005) 303–313.
[15] C.M. Overall, Molecular determinants of metalloproteinase substrate specificity: matrix metalloproteinase substrate binding domains, modules, and exosites, Mol. Biotechnol. 22 (2002) 51–86.
[16] G. Murphy, V. Knauper, Relating matrix metalloproteinase structure to function: why the "hemopexin" domain? Matrix Biol. 15 (1997) 511–518.
[17] M.A. Stolow, D.D. Bauzon, J. Li, T. Sedgwick, V.C. Liang, Q.A. Sang, Y.B. Shi, Identification and characterization of a novel collagenase in *Xenopus laevis*: possible roles during frog development, Mol. Biol. Cell 7 (1996) 1471–1483.
[18] H.E. Barksby, J.M. Milner, A.M. Patterson, N.J. Peake, W. Hui, T. Robson, R. Lakey, J. Middleton, T.E. Cawston, C.D. Richards, A.D. Rowan, Matrix metalloproteinase 10 promotion of collagenolysis via procollagenase activation: implications for cartilage degradation in arthritis, Arthritis Rheum. 54 (2006) 3244–3253.
[19] N. Geurts, E. Martens, I. Van Aelst, P. Proost, G. Opdenakker, P.E. Van den Steen, Beta-hematin interaction with the hemopexin domain of gelatinase B/MMP-9 provokes autocatalytic processing of the propeptide, thereby priming activation by MMP-3, Biochemistry 47 (2008) 2689–2699.
[20] S.D. Shapiro, D.K. Kobayashi, T.J. Ley, Cloning and characterization of a unique elastolytic metalloproteinase produced by human alveolar macrophages, J. Biol. Chem. 268 (1993) 23824–23829.
[21] P. Hou, T. Troen, M.C. Ovejero, T. Kirkegaard, T.L. Andersen, I. Byrjalsen, M. Ferreras, T. Sato, S.D. Shapiro, N.T. Foged, J.M. Delaisse, Matrix metalloproteinase-12 (MMP-12) in osteoclasts: new lesson on the involvement of MMPs in bone resorption, Bone 34 (2004) 37–47.
[22] A.M. Pendás, V. Knauper, X.S. Puente, E. Llano, M.G. Mattei, S. Apte, G. Murphy, C. López-Otín, Identification and characterization of a novel human matrix metalloproteinase with unique structural characteristics, chromosomal location, and tissue distribution, J. Biol. Chem. 272 (1997) 4281–4286.
[23] C. Kolb, S. Mauch, H.H. Peter, U. Krawinkel, R. Sedlacek, The matrix metalloproteinase RASI-1 is expressed in synovial blood vessels of a rheumatoid arthritis patient, Immunol. Lett. 57 (1997) 83–88.
[24] J.O. Stracke, M. Hutton, M. Stewart, A.M. Pendas, B. Smith, C. Lopez-Otin, G. Murphy, V. Knauper, Biochemical characterization of the catalytic domain of human matrix metalloproteinase 19. Evidence for a role as a potent basement membrane degrading enzyme, J. Biol. Chem. 275 (2000) 14809–14816.
[25] E. Llano, A.M. Pendas, V. Knauper, T. Sorsa, T. Salo, E. Salido, G. Murphy, J.P. Simmer, J.D. Bartlett, C. Lopez-Otin, Identification and structural and functional characterization of human enamelysin (MMP-20), Biochemistry 36 (1997) 15101–15108.
[26] Y. Lu, P. Papagerakis, Y. Yamakoshi, J.C. Hu, J.D. Bartlett, J.P. Simmer, Functions of KLK4 and MMP-20 in dental enamel formation, Biol. Chem. 389 (2008) 695–700.
[27] M. Yang, M. Kurkinen, Cloning and characterization of a novel matrix metalloproteinase (MMP), CMMP, from chicken embryo fibroblasts. CMMP, *Xenopus* XMMP, and human MMP19 have a conserved unique cysteine in the catalytic domain, J. Biol. Chem. 273 (1998) 17893–17900.
[28] A. Bar-Or, R.K. Nuttall, M. Duddy, A. Alter, H.J. Kim, I. Ifergan, C.J. Pennington, P. Bourgoin, D.R. Edwards, V.W. Yong, Analyses of all matrix metalloproteinase members in leukocytes emphasize monocytes as major inflammatory mediators in multiple sclerosis, Brain 126 (2003) 2738–2749.
[29] J.A. Uria, C. Lopez-Otin, Matrilysin-2, a new matrix metalloproteinase expressed in human tumors and showing the minimal domain organization required for secretion, latency, and activity, Cancer Res. 60 (2000) 4745–4751.
[30] W.S. Wang, P.M. Chen, H.S. Wang, W.Y. Liang, Y. Su, Matrix metalloproteinase-7 increases resistance to Fas-mediated apoptosis and is a poor prognostic factor of patients with colorectal carcinoma, Carcinogenesis 27 (2006) 1113–1120.
[31] J.K. McGuire, Q. Li, W.C. Parks, Matrilysin (matrix metalloproteinase-7) mediates E-cadherin ectodomain shedding in injured lung epithelium, Am. J. Pathol. 162 (2003) 1831–1843.
[32] Q. Li, P.W. Park, C.L. Wilson, W.C. Parks, Matrilysin shedding of syndecan-1 regulates chemokine mobilization and transepithelial efflux of neutrophils in acute lung injury, Cell 111 (2002) 635–646.
[33] Y.G. Zhao, A.Z. Xiao, H.I. Park, R.G. Newcomer, M. Yan, Y.G. Man, S.C. Heffelfinger, Q.X. Sang, Endometase/matrilysin-2 in human breast ductal carcinoma in situ and its inhibition by tissue inhibitors of metalloproteinases-2 and -4: a putative role in the initiation of breast cancer invasion, Cancer Res. 64 (2004) 590–598.
[34] W. Qiu, S.X. Bai, M.R. Zhao, X.Q. Wu, Y.G. Zhao, Q.X. Sang, Y.L. Wang, Spatiotemporal expression of matrix metalloproteinase-26 in human placental trophoblasts and fetal red cells during normal placentation, Biol. Reprod. 72 (2005) 954–959.
[35] Q. Yu, I. Stamenkovic, Cell surface-localized matrix metalloproteinase-9 proteolytically activates TGF-beta and promotes tumor invasion and angiogenesis, Genes Dev. 14 (2000) 163–176.
[36] G.A. McQuibban, J.H. Gong, J.P. Wong, J.L. Wallace, I. Clark-Lewis, C.M. Overall, Matrix metalloproteinase processing of monocyte chemoattractant proteins generates CC chemokine receptor antagonists with anti-inflammatory properties in vivo, Blood 100 (2002) 1160–1167.
[37] M. Egeblad, Z. Werb, New functions for the matrix metalloproteinases in cancer progression, Nat. Rev. Cancer 2 (2002) 161–174.
[38] M.C. Rio, From a unique cell to metastasis is a long way to go: clues to stromelysin-3 participation, Biochimie 87 (2005) 299–306.
[39] E.R. Motrescu, S. Blaise, N. Etique, N. Messaddeq, M.P. Chenard, I. Stoll, C. Tomasetto, M.C. Rio, Matrix metalloproteinase-11/stromelysin-3 exhibits collagenolytic function against collagen VI under normal and malignant conditions, Oncogene 27 (2008) 6347–6355.
[40] K. Ahokas, J. Lohi, H. Lohi, O. Elomaa, M.L. Karjalainen-Lindsberg, J. Kere, U. Saarialho-Kere, Matrix metalloproteinase-21, the human orthologue for XMMP, is expressed during fetal development and in cancer, Gene 301 (2002) 31–41.
[41] J. Lohi, C.L. Wilson, J.D. Roby, W.C. Parks, Epilysin, a novel human matrix metalloproteinase (MMP-28) expressed in testis and keratinocytes and in response to injury, J. Biol. Chem. 276 (2001) 10134–10144.
[42] S.R. Werner, J.E. Dotzlaf, R.C. Smith, MMP-28 as a regulator of myelination, BMC Neurosci. 9 (2008) 83.
[43] S. Zucker, D. Pei, J. Cao, C. Lopez-Otin, Membrane type-matrix metalloproteinases (MT-MMP), Curr. Top. Dev. Biol. 54 (2003) 1–74.
[44] D. Gingras, N. Bousquet-Gagnon, S. Langlois, M.P. Lachambre, B. Annabi, R. Beliveau, Activation of the extracellular signal-regulated protein kinase (ERK) cascade by membrane-type-1 matrix metalloproteinase (MT1-MMP), FEBS Lett. 507 (2001) 231–236.
[45] N.E. Sounni, C. Roghi, V. Chabottaux, M. Janssen, C. Munaut, E. Maquoi, B.G. Galvez, C. Gilles, F. Frankenne, G. Murphy, J.M. Foidart, A. Noel, Up-regulation of vascular endothelial growth factor-A by active membrane-type 1 matrix metalloproteinase through activation of Src-tyrosine kinases, J. Biol. Chem. 279 (2004) 13564–13574.
[46] T. Uekita, Y. Itoh, I. Yana, H. Ohno, M. Seiki, Cytoplasmic tail-dependent internalization of membrane-type 1 matrix metalloproteinase is important for its invasion-promoting activity, J. Cell Biol. 155 (2001) 1345–1356.

[47] N.E. Sounni, A. Noel, Membrane type-matrix metalloproteinases and tumor progression, Biochimie 87 (2005) 329–342.
[48] M. Uchibori, Y. Nishida, T. Nagasaka, Y. Yamada, K. Nakanishi, N. Ishiguro, Increased expression of membrane-type matrix metalloproteinase-1 is correlated with poor prognosis in patients with osteosarcoma, Int. J. Oncol. 28 (2006) 33–42.
[49] Y.C. Ip, S.T. Cheung, S.T. Fan, Atypical localization of membrane type 1-matrix metalloproteinase in the nucleus is associated with aggressive features of hepatocellular carcinoma, Mol. Carcinog. 46 (2007) 225–230.
[50] K. Wolf, Y.I. Wu, Y. Liu, J. Geiger, E. Tam, C. Overall, M.S. Stack, P. Friedl, Multi-step pericellular proteolysis controls the transition from individual to collective cancer cell invasion, Nat. Cell Biol. 9 (2007) 893–904.
[51] R.A. Bartolome, S. Ferreiro, M.E. Miquilena-Colina, L. Martinez-Prats, M.L. Soto-Montenegro, D. Garcia-Bernal, J.J. Vaquero, R. Agami, R. Delgado, M. Desco, P. Sanchez-Mateos, J. Teixido, The chemokine receptor CXCR4 and the metalloproteinase MT1-MMP are mutually required during melanoma metastasis to lungs, Am. J. Pathol. 174 (2009) 602–612.
[52] X.S. Puente, A.M. Pendas, E. Llano, G. Velasco, C. Lopez-Otin, Molecular cloning of a novel membrane-type matrix metalloproteinase from a human breast carcinoma, Cancer Res. 56 (1996) 944–949.
[53] D. Pei, Leukolysin/MMP25/MT6-MMP: a novel matrix metalloproteinase specifically expressed in the leukocyte lineage, Cell Res. 9 (1999) 291–303.
[54] G. Gao, A. Plaas, V.P. Thompson, S. Jin, F. Zuo, J.D. Sandy, ADAMTS4 (aggrecanase-1) activation on the cell surface involves C-terminal cleavage by glycosylphosphatidyl inositol-anchored membrane type 4-matrix metalloproteinase and binding of the activated proteinase to chondroitin sulfate and heparan sulfate on syndecan-1, J. Biol. Chem. 279 (2004) 10042–10051.
[55] G. Velasco, S. Cal, A. Merlos-Suarez, A.A. Ferrando, S. Alvarez, A. Nakano, J. Arribas, C. Lopez-Otin, Human MT6-matrix metalloproteinase: identification, progelatinase A activation, and expression in brain tumors, Cancer Res. 60 (2000) 877–882.
[56] A. Sohail, Q. Sun, H. Zhao, M.M. Bernardo, J.A. Cho, R. Fridman, MT4-(MMP17) and MT6-MMP (MMP25), A unique set of membrane-anchored matrix metalloproteinases: properties and expression in cancer, Cancer Metastasis Rev. 27 (2008) 289–302.
[57] G. Velasco, A.M. Pendas, A. Fueyo, V. Knauper, G. Murphy, C. Lopez-Otin, Cloning and characterization of human MMP-23, a new matrix metalloproteinase predominantly expressed in reproductive tissues and lacking conserved domains in other family members, J. Biol. Chem. 274 (1999) 4570–4576.
[58] I. Massova, L.P. Kotra, R. Fridman, S. Mobashery, Matrix metalloproteinases: structures, evolution, and diversification, FASEB J. 12 (1998) 1075–1095.
[59] J. Huxley-Jones, T.K. Clarke, C. Beck, G. Toubaris, D.L. Robertson, R.P. Boot-Handford, The evolution of the vertebrate metzincins; insights from *Ciona intestinalis* and *Danio rerio*, BMC Evol. Biol. 7 (2007) 63.
[60] A. Page-McCaw, Remodeling the model organism: matrix metalloproteinase functions in invertebrates, Semin. Cell Dev. Biol. 19 (2008) 14–23.
[61] L. Angerer, S. Hussain, Z. Wei, B.T. Livingston, Sea urchin metalloproteases: a genomic survey of the BMP-1/tolloid-like, MMP and ADAM families, Dev. Biol. 300 (2006) 267–281.
[62] X.S. Puente, A. Gutierrez-Fernandez, G.R. Ordonez, L.W. Hillier, C. Lopez-Otin, Comparative genomic analysis of human and chimpanzee proteases, Genomics 86 (2005) 638–647.
[63] X.S. Puente, C. Lopez-Otin, A genomic analysis of rat proteases and protease inhibitors, Genome Res. 14 (2004) 609–622.
[64] L. Fu, B. Das, S. Mathew, Y.B. Shi, Genome-wide identification of *Xenopus* matrix metalloproteinases: conservation and unique duplications in amphibians, BMC Genomics 10 (2009) 81.
[65] G.R. Ordonez, L.W. Hillier, W.C. Warren, F. Grutzner, C. Lopez-Otin, X.S. Puente, Loss of genes implicated in gastric function during platypus evolution, Genome Biol. 9 (2008) R81.
[66] M. Balbin, A. Fueyo, V. Knauper, J.M. Lopez, J. Alvarez, L.M. Sanchez, V. Quesada, J. Bordallo, G. Murphy, C. Lopez-Otin, Identification and enzymatic characterization of two diverging murine counterparts of human interstitial collagenase (MMP-1) expressed at sites of embryo implantation, J. Biol. Chem. 276 (2001) 10253–10262.
[67] J. Huxley-Jones, D.L. Robertson, R.P. Boot-Handford, On the origins of the extracellular matrix in vertebrates, Matrix Biol. 26 (2007) 2–11.
[68] V. Knauper, C. Lopez-Otin, B. Smith, G. Knight, G. Murphy, Biochemical characterization of human collagenase-3, J. Biol. Chem. 271 (1996) 1544–1550.
[69] C. Lopez-Otin, J.S. Bond, Proteases: multifunctional enzymes in life and disease, J. Biol. Chem. 283 (2008) 30433–30437.
[70] C. Yan, D.D. Boyd, Regulation of matrix metalloproteinase gene expression, J. Cell Physiol. 211 (2007) 19–26.
[71] M.P. Vincenti, C.E. Brinckerhoff, Signal transduction and cell-type specific regulation of matrix metalloproteinase gene expression: can MMPs be good for you? J. Cell Physiol. 213 (2007) 355–364.
[72] C.M. Overall, C. López-Otín, Strategies for MMP inhibition in cancer: innovations for the post-trial era, Nat. Rev. Cancer 2 (2002) 657–672.
[73] I.M. Clark, T.E. Swingler, C.L. Sampieri, D.R. Edwards, The regulation of matrix metalloproteinases and their inhibitors, Int. J. Biochem. Cell Biol. 40 (2008) 1362–1378.
[74] X. Wang, Z. Bi, W. Chu, Y. Wan, IL-1 receptor antagonist attenuates MAP kinase/AP-1 activation and MMP1 expression in UVA-irradiated human fibroblasts induced by culture medium from UVB-irradiated human skin keratinocytes, Int. J. Mol. Med. 16 (2005) 1117–1124.
[75] S. Chakraborti, M. Mandal, S. Das, A. Mandal, T. Chakraborti, Regulation of matrix metalloproteinases: an overview, Mol. Cell. Biochem. 253 (2003) 269–285.
[76] D. Kumar, A. Ray, B.K. Ray, Transcriptional synergy mediated by SAF-1 and AP-1: critical role of N-terminal polyalanine and two zinc finger domains of SAF-1, J. Biol. Chem. 284 (2009) 1853–1862.
[77] J. Yan, H. Erdem, R. Li, Y. Cai, G. Ayala, M. Ittmann, L.Y. Yu-Lee, S.Y. Tsai, M.J. Tsai, Steroid receptor coactivator-3/AIB1 promotes cell migration and invasiveness through focal adhesion turnover and matrix metalloproteinase expression, Cancer Res. 68 (2008) 5460–5468.
[78] L. Qin, L. Liao, A. Redmond, L. Young, Y. Yuan, H. Chen, B.W. O'Malley, J. Xu, The AIB1 oncogene promotes breast cancer metastasis by activation of PEA3-mediated matrix metalloproteinase 2 (MMP2) and MMP9 expression, Mol. Cell. Biol. 28 (2008) 5937–5950.
[79] J.Y. Wu, H. Lu, Y. Sun, D.Y. Graham, H.S. Cheung, Y. Yamaoka, Balance between polyoma enhancing activator 3 and activator protein 1 regulates Helicobacter pylori-stimulated matrix metalloproteinase 1 expression, Cancer Res. 66 (2006) 5111–5120.
[80] J. Westermarck, A. Seth, V.M. Kahari, Differential regulation of interstitial collagenase (MMP-1) gene expression by ETS transcription factors, Oncogene 14 (1997) 2651–2660.
[81] M.P. Vincenti, C.E. Brinckerhoff, Transcriptional regulation of collagenase (MMP-1, MMP-13) genes in arthritis: integration of complex signaling pathways for the recruitment of gene-specific transcription factors, Arthritis Res. 4 (2002) 157–164.
[82] K. Hnia, J. Gayraud, G. Hugon, M. Ramonatxo, S. De La Porte, S. Matecki, D. Mornet, L-arginine decreases inflammation and modulates the nuclear factor-kappaB/matrix metalloproteinase cascade in mdx muscle fibers, Am. J. Pathol. 172 (2008) 1509–1519.
[83] Z. Wang, D. Kong, S. Banerjee, Y. Li, N.V. Adsay, J. Abbruzzese, F.H. Sarkar, Down-regulation of platelet-derived growth factor-D inhibits cell growth and angiogenesis through inactivation of Notch-1 and nuclear factor-kappaB signaling, Cancer Res. 67 (2007) 11377–11385.
[84] S.F. Elliott, C.I. Coon, E. Hays, T.A. Stadheim, M.P. Vincenti, Bcl-3 is an interleukin-1-responsive gene in chondrocytes and synovial fibroblasts that activates transcription of the matrix metalloproteinase 1 gene, Arthritis Rheum. 46 (2002) 3230–3239.
[85] H. Sato, M. Seiki, Regulatory mechanism of 92 kDa type IV collagenase gene expression which is associated with invasiveness of tumor cells, Oncogene 8 (1993) 395–405.
[86] W.X. Li, Canonical and non-canonical JAK-STAT signaling, Trends Cell Biol. 18 (2008) 545–551.
[87] M. Itoh, T. Murata, T. Suzuki, M. Shindoh, K. Nakajima, K. Imai, K. Yoshida, Requirement of STAT3 activation for maximal collagenase-1 (MMP-1) induction by epidermal growth factor and malignant characteristics in T24 bladder cancer cells, Oncogene 25 (2006) 1195–1204.
[88] Y. Song, L. Qian, S. Song, L. Chen, Y. Zhang, G. Yuan, H. Zhang, Q. Xia, M. Hu, M. Yu, M. Shi, Z. Jiang, N. Guo, Fra-1 and Stat3 synergistically regulate activation of human MMP-9 gene, Mol. Immunol. 45 (2008) 137–143.
[89] X. Zhao, S. Nozell, Z. Ma, E.N. Benveniste, The interferon-stimulated gene factor 3 complex mediates the inhibitory effect of interferon-beta on matrix metalloproteinase-9 expression, FEBS J. 274 (2007) 6456–6468.
[90] M.D. Gustavson, H.C. Crawford, B. Fingleton, L.M. Matrisian, Tcf binding sequence and position determines beta-catenin and Lef-1 responsiveness of MMP-7 promoters, Mol. Carcinog. 41 (2004) 125–139.
[91] H.C. Crawford, B. Fingleton, M.D. Gustavson, N. Kurpios, R.A. Wagenaar, J.A. Hassell, L.M. Matrisian, The PEA3 subfamily of Ets transcription factors synergizes with beta-catenin-LEF-1 to activate matrilysin transcription in intestinal tumors, Mol. Cell. Biol. 21 (2001) 1370–1383.
[92] M. Takahashi, T. Tsunoda, M. Seiki, Y. Nakamura, Y. Furukawa, Identification of membrane-type matrix metalloproteinase-1 as a target of the beta-catenin/Tcf4 complex in human colorectal cancers, Oncogene 21 (2002) 5861–5867.
[93] J.A. Mengshol, M.P. Vincenti, C.E. Brinckerhoff, IL-1 induces collagenase-3 (MMP-13) promoter activity in stably transfected chondrocytic cells: requirement for Runx-2 and activation by p38 MAPK and JNK pathways, Nucleic Acids Res. 29 (2001) 4361–4372.
[94] M.J. Jimenez, M. Balbin, J. Alvarez, T. Komori, P. Bianco, K. Holmbeck, H. Birkedal-Hansen, J.M. Lopez, C. Lopez-Otin, A regulatory cascade involving retinoic acid, Cbfa1, and matrix metalloproteinases is coupled to the development of a process of perichondrial invasion and osteogenic differentiation during bone formation, J. Cell Biol. 155 (2001) 1333–1344.
[95] N. Ortega, D.J. Behonick, Z. Werb, Matrix remodeling during endochondral ossification, Trends Cell Biol. 14 (2004) 86–93.
[96] J.A. Uria, M.G. Jimenez, M. Balbin, J.M. Freije, C. Lopez-Otin, Differential effects of transforming growth factor-beta on the expression of collagenase-1 and collagenase-3 in human fibroblasts, J. Biol. Chem. 273 (1998) 9769–9777.
[97] C. Van Themsche, I. Mathieu, S. Parent, E. Asselin, Transforming growth factor-beta3 increases the invasiveness of endometrial carcinoma cells through phosphatidylinositol 3-kinase-dependent up-regulation of X-linked inhibitor of apoptosis and protein kinase c-dependent induction of matrix metalloproteinase-9, J. Biol. Chem. 282 (2007) 4794–4802.
[98] Y.C. Kuo, C.H. Su, C.Y. Liu, T.H. Chen, C.P. Chen, H.S. Wang, Transforming growth factor-beta induces CD44 cleavage that promotes migration of MDA-MB-435s cells through the up-regulation of membrane type 1-matrix metalloproteinase, Int. J. Cancer (2009).
[99] W. Yuan, J. Varga, Transforming growth factor-beta repression of matrix metalloproteinase-1 in dermal fibroblasts involves Smad3, J. Biol. Chem. 276 (2001) 38502–38510.
[100] S.K. Leivonen, A. Chantry, L. Hakkinen, J. Han, V.M. Kahari, Smad3 mediates

transforming growth factor-beta-induced collagenase-3 (matrix metalloproteinase-13) expression in human gingival fibroblasts. Evidence for cross-talk between Smad3 and p38 signaling pathways, J. Biol. Chem. 277 (2002) 46338–46346.
[101] E. Chicoine, P.O. Esteve, O. Robledo, C. Van Themsche, E.F. Potworowski, Y. St-Pierre, Evidence for the role of promoter methylation in the regulation of MMP-9 gene expression, Biochem. Biophys. Res. Commun. 297 (2002) 765–772.
[102] N. Shukeir, P. Pakneshan, G. Chen, M. Szyf, S.A. Rabbani, Alteration of the methylation status of tumor-promoting genes decreases prostate cancer cell invasiveness and tumorigenesis in vitro and in vivo, Cancer Res. 66 (2006) 9202–9210.
[103] J. Couillard, M. Demers, G. Lavoie, Y. St-Pierre, The role of DNA hypomethylation in the control of stromelysin gene expression, Biochem. Biophys. Res. Commun. 342 (2006) 1233–1239.
[104] T. Kouzarides, Chromatin modifications and their function, Cell 128 (2007) 693–705.
[105] C. Yan, H. Wang, Y. Toh, D.D. Boyd, Repression of 92-kDa type IV collagenase expression by MTA1 is mediated through direct interactions with the promoter via a mechanism, which is both dependent on and independent of histone deacetylation, J. Biol. Chem. 278 (2003) 2309–2316.
[106] S. Chang, B.D. Young, S. Li, X. Qi, J.A. Richardson, E.N. Olson, Histone deacetylase 7 maintains vascular integrity by repressing matrix metalloproteinase 10, Cell 126 (2006) 321–334.
[107] D.A. Young, R.L. Lakey, C.J. Pennington, D. Jones, L. Kevorkian, D.R. Edwards, T.E. Cawston, I.M. Clark, Histone deacetylase inhibitors modulate metalloproteinase gene expression in chondrocytes and block cartilage resorption, Arthritis Res. Ther. 7 (2005) R503–R512.
[108] J.H. Martens, M. Verlaan, E. Kalkhoven, A. Zantema, Cascade of distinct histone modifications during collagenase gene activation, Mol. Cell. Biol. 23 (2003) 1808–1816.
[109] M.K. Kim, J.M. Shin, H.C. Eun, J.H. Chung, The role of p300 histone acetyltransferase in UV-induced histone modifications and MMP-1 gene transcription, PLoS ONE 4 (2009) e4864.
[110] Z. Ma, R.C. Shah, M.J. Chang, E.N. Benveniste, Coordination of cell signaling, chromatin remodeling, histone modifications, and regulator recruitment in human matrix metalloproteinase 9 gene transcription, Mol. Cell. Biol. 24 (2004) 5496–5509.
[111] X. Zhao, E.N. Benveniste, Transcriptional activation of human matrix metalloproteinase-9 gene expression by multiple co-activators, J. Mol. Biol. 383 (2008) 945–956.
[112] I. Robert, M. Aussems, A. Keutgens, X. Zhang, B. Hennuy, P. Viatour, G. Vanstraelen, M.P. Merville, J.P. Chapelle, L. de Leval, F. Lambert, E. Dejardin, A. Gothot, A. Chariot, Matrix Metalloproteinase-9 gene induction by a truncated oncogenic NF-kappaB2 protein involves the recruitment of MLL1 and MLL2 H3K4 histone methyltransferase complexes, Oncogene (2009).
[113] S. Akool el, H. Kleinert, F.M. Hamada, M.H. Abdelwahab, U. Forstermann, J. Pfeilschifter, W. Eberhardt, Nitric oxide increases the decay of matrix metalloproteinase 9 mRNA by inhibiting the expression of mRNA-stabilizing factor HuR, Mol. Cell Biol. 23 (2003) 4901–4916.
[114] A. Huwiler, S. Akool el, A. Aschrafi, F.M. Hamada, J. Pfeilschifter, W. Eberhardt, ATP potentiates interleukin-1 beta-induced MMP-9 expression in mesangial cells via recruitment of the ELAV protein HuR, J. Biol. Chem. 278 (2003) 51758–51769.
[115] V. Iyer, K. Pumiglia, C.M. DiPersio, Alpha3beta1 integrin regulates MMP-9 mRNA stability in immortalized keratinocytes: a novel mechanism of integrin-mediated MMP gene expression, J. Cell. Sci. 118 (2005) 1185–1195.
[116] P. Krishnamurthy, J. Rajasingh, E. Lambers, G. Qin, D.W. Losordo, R. Kishore, IL-10 inhibits inflammation and attenuates left ventricular remodeling after myocardial infarction via activation of STAT3 and suppression of HuR, Circ. Res. 104 (2009) e9–e18.
[117] S. Rydziel, A.M. Delany, E. Canalis, AU-rich elements in the collagenase 3 mRNA mediate stabilization of the transcript by cortisol in osteoblasts, J. Biol. Chem. 279 (2004) 5397–5404.
[118] M. Fahling, A. Steege, A. Perlewitz, B. Nafz, R. Mrowka, P.B. Persson, B.J. Thiele, Role of nucleolin in posttranscriptional control of MMP-9 expression, Biochim. Biophys. Acta 1731 (2005) 32–40.
[119] Y. Jiang, R.J. Muschel, Regulation of matrix metalloproteinase-9 (MMP-9) by translational efficiency in murine prostate carcinoma cells, Cancer Res. 62 (2002) 1910–1914.
[120] T. Dalmay, D.R. Edwards, MicroRNAs and the hallmarks of cancer, Oncogene 25 (2006) 6170–6175.
[121] H. Xia, Y. Qi, S.S. Ng, X. Chen, S. Chen, R. Ge, S. Jiang, G. Li, Y. Chen, M.L. He, H.F. Kung, L. Lai, M.C. Lin, microRNA-146b inhibits glioma cell migration and invasion by targeting MMPs, Brain Res. (2009).
[122] S. Roy, S. Khanna, S.R. Hussain, S. Biswas, A. Azad, C. Rink, S. Gnyawali, S. Shilo, G.J. Nuovo, C.K. Sen, MicroRNA expression in response to murine myocardial infarction: miR-21 regulates fibroblast metalloprotease-2 via phosphatase and tensin homologue, Cardiovasc. Res. 82 (2009) 21–29.
[123] G. Gabriely, T. Wurdinger, S. Kesari, C.C. Esau, J. Burchard, P.S. Linsley, A.M. Krichevsky, MicroRNA 21 promotes glioma invasion by targeting matrix metalloproteinase regulators, Mol. Cell. Biol. 28 (2008) 5369–5380.
[124] S.W. Jones, G. Watkins, N. Le Good, S. Roberts, C.L. Murphy, S.M. Brockbank, M.R. Needham, S.J. Read, P. Newham, The identification of differentially expressed microRNA in osteoarthritic tissue that modulate the production of TNF-alpha and MMP13, Osteoarthritis Cartilage 17 (2009) 464–472.
[125] J.A. Martignetti, A.A. Aqeel, W.A. Sewairi, C.E. Boumah, M. Kambouris, S.A. Mayouf, K.V. Sheth, W.A. Eid, O. Dowling, J. Harris, M.J. Glucksman, S. Bahabri, B.F. Meyer, R.J. Desnick, Mutation of the matrix metalloproteinase 2 gene (MMP2) causes a multicentric osteolysis and arthritis syndrome, Nat. Genet. 28 (2001) 261–265.
[126] A. Zankl, L. Bonafe, V. Calcaterra, M. Di Rocco, A. Superti-Furga, Winchester syndrome caused by a homozygous mutation affecting the active site of matrix metalloproteinase 2, Clin. Genet. 67 (2005) 261–266.
[127] A. Zankl, L. Pachman, A. Poznanski, L. Bonafe, F. Wang, Y. Shusterman, D.A. Fishman, A. Superti-Furga, Torg syndrome is caused by inactivating mutations in MMP2 and is allelic to NAO and Winchester syndrome, J. Bone Miner. Res. 22 (2007) 329–333.
[128] A.M. Kennedy, M. Inada, S.M. Krane, P.T. Christie, B. Harding, C. Lopez-Otin, L.M. Sanchez, A.A. Pannett, A. Dearlove, C. Hartley, M.H. Byrne, A.A. Reed, M.A. Nesbit, M.P. Whyte, R.V. Thakker, MMP13 mutation causes spondyloepimetaphyseal dysplasia, Missouri type (SEMD(MO)), J. Clin. Invest. 115 (2005) 2832–2842.
[129] J.W. Kim, J.P. Simmer, T.C. Hart, P.S. Hart, M.D. Ramaswami, J.D. Bartlett, J.C. Hu, MMP-20 mutation in autosomal recessive pigmented hypomaturation amelogenesis imperfecta, J. Med. Genet. 42 (2005) 271–275.
[130] P. Papagerakis, H.K. Lin, K.Y. Lee, Y. Hu, J.P. Simmer, J.D. Bartlett, J.C. Hu, Premature stop codon in MMP20 causing amelogenesis imperfecta, J. Dent. Res. 87 (2008) 56–59.
[131] D. Ozdemir, P.S. Hart, O.H. Ryu, S.J. Choi, M. Ozdemir-Karatas, E. Firatli, N. Piesco, T.C. Hart, MMP20 active-site mutation in hypomaturation amelogenesis imperfecta, J. Dent. Res. 84 (2005) 1031–1035.
[132] T. Sjoblom, S. Jones, L.D. Wood, D.W. Parsons, J. Lin, T.D. Barber, D. Mandelker, R.J. Leary, J. Ptak, N. Silliman, S. Szabo, P. Buckhaults, C. Farrell, P. Meeh, S.D. Markowitz, J. Willis, D. Dawson, J.K. Willson, A.F. Gazdar, J. Hartigan, L. Wu, C. Liu, G. Parmigiani, B.H. Park, K.E. Bachman, N. Papadopoulos, B. Vogelstein, K.W. Kinzler, V.E. Velculescu, The consensus coding sequences of human breast and colorectal cancers, Science 314 (2006) 268–274.
[133] C.G. Viloria, A.J. Obaya, A. Moncada-Pazos, M. Llamazares, A. Astudillo, G. Capella, S. Cal, C. Lopez-Otin, Genetic inactivation of ADAMTS15 metalloprotease in human colorectal cancer, Cancer Res. 69 (2009) 4926–4934.
[134] Y. Zhu, M.R. Spitz, L. Lei, G.B. Mills, X. Wu, A single nucleotide polymorphism in the matrix metalloproteinase-1 promoter enhances lung cancer susceptibility, Cancer Res. 61 (2001) 7825–7829.
[135] M. Woo, K. Park, J. Nam, J.C. Kim, Clinical implications of matrix metalloproteinase-1, -3, -7, -9, -12, and plasminogen activator inhibitor-1 gene polymorphisms in colorectal cancer, J. Gastroenterol. Hepatol. 22 (2007) 1064–1070.
[136] K. Przybylowska, A. Kluczna, M. Zadrozny, T. Krawczyk, A. Kulig, J. Rykala, A. Kolacinska, Z. Morawiec, J. Drzewoski, J. Blasiak, Polymorphisms of the promoter regions of matrix metalloproteinases genes MMP-1 and MMP-9 in breast cancer, Breast Cancer Res. Treat. 95 (2006) 65–72.
[137] L. Six, C. Grimm, S. Leodolter, C. Tempfer, R. Zeillinger, G. Sliutz, P. Speiser, A. Reinthaller, L.A. Hefler, A polymorphism in the matrix metalloproteinase-1 gene promoter is associated with the prognosis of patients with ovarian cancer, Gynecol. Oncol. 100 (2006) 506–510.
[138] S. Ye, S. Dhillon, S.J. Turner, A.C. Bateman, J.M. Theaker, R.M. Pickering, I. Day, W.M. Howell, Invasiveness of cutaneous malignant melanoma is influenced by matrix metalloproteinase 1 gene polymorphism, Cancer Res. 61 (2001) 1296–1298.
[139] M. Checa, V. Ruiz, M. Montano, R. Velazquez-Cruz, M. Selman, A. Pardo, MMP-1 polymorphisms and the risk of idiopathic pulmonary fibrosis, Hum. Genet. 124 (2008) 465–472.
[140] K. Okamoto, K. Mimura, Y. Murawaki, I. Yuasa, Association of functional gene polymorphisms of matrix metalloproteinase (MMP)-1, MMP-3 and MMP-9 with the progression of chronic liver disease, J. Gastroenterol. Hepatol. 20 (2005) 1102–1108.
[141] C. Yu, Y. Zhou, X. Miao, P. Xiong, W. Tan, D. Lin, Functional haplotypes in the promoter of matrix metalloproteinase-2 predict risk of the occurrence and metastasis of esophageal cancer, Cancer Res. 64 (2004) 7622–7628.
[142] Y. Zhou, C. Yu, X. Miao, Y. Wang, W. Tan, T. Sun, X. Zhang, P. Xiong, D. Lin, Functional haplotypes in the promoter of matrix metalloproteinase-2 and lung cancer susceptibility, Carcinogenesis 26 (2005) 1117–1121.
[143] S. Harendza, D.H. Lovett, U. Panzer, Z. Lukacs, P. Kuhnl, R.A. Stahl, Linked common polymorphisms in the gelatinase a promoter are associated with diminished transcriptional response to estrogen and genetic fitness, J. Biol. Chem. 278 (2003) 20490–20499.
[144] S. Fang, X. Jin, R. Wang, Y. Li, W. Guo, N. Wang, Y. Wang, D. Wen, L. Wei, J. Zhang, Polymorphisms in the MMP1 and MMP3 promoter and non-small cell lung carcinoma in North China, Carcinogenesis 26 (2005) 481–486.
[145] G. Ghilardi, M.L. Biondi, M. Caputo, S. Leviti, M. DeMonti, E. Guagnellini, R. Scorza, A single nucleotide polymorphism in the matrix metalloproteinase-3 promoter enhances breast cancer susceptibility, Clin. Cancer Res. 8 (2002) 3820–3823.
[146] E. Vairaktaris, C. Yapijakis, S. Vasiliou, S. Derka, E. Nkenke, Z. Serefoglou, E. Vorris, A. Vylliotis, V. Ragos, F.W. Neukam, E. Patsouris, Association of −1171 promoter polymorphism of matrix metalloproteinase-3 with increased risk for oral cancer, Anticancer Res. 27 (2007) 4095–4100.
[147] T. Djuric, M. Zivkovic, D. Radak, D. Jekic, S. Radak, L. Stojkovic, R. Raicevic, A. Stankovic, D. Alavantic, Association of MMP-3 5A/6A gene polymorphism with susceptibility to carotid atherosclerosis, Clin. Biochem. 41 (2008) 1326–1329.
[148] D.L. Mattey, N.B. Nixon, P.T. Dawes, W.E. Ollier, A.H. Hajeer, Association of matrix metalloproteinase 3 promoter genotype with disease outcome in rheumatoid arthritis, Genes Immun. 5 (2004) 147–149.
[149] S. Jormsjo, C. Whatling, D.H. Walter, A.M. Zeiher, A. Hamsten, P. Eriksson, Allele-specific regulation of matrix metalloproteinase-7 promoter activity is associated with coronary artery luminal dimensions among hypercholesterolemic patients, Arterioscler Thromb. Vasc. Biol. 21 (2001) 1834–1839.

[150] F.J. Kubben, C.F. Sier, M.J. Meijer, M. van den Berg, J.J. van der Reijden, G. Griffioen, C.J. van de Velde, C.B. Lamers, H.W. Verspaget, Clinical impact of MMP and TIMP gene polymorphisms in gastric cancer, Br. J. Cancer 95 (2006) 744–751.
[151] H. Singh, M. Jain, B. Mittal, MMP-7 (−181A>G) promoter polymorphisms and risk for cervical cancer, Gynecol. Oncol. 110 (2008) 71–75.
[152] E. Vairaktaris, Z. Serefoglou, C. Yapijakis, A. Vylliotis, E. Nkenke, S. Derka, S. Vassiliou, D. Avgoustidis, F.W. Neukam, E. Patsouris, High gene expression of matrix metalloproteinase-7 is associated with early stages of oral cancer, Anticancer Res. 27 (2007) 2493–2498.
[153] J. Zhang, X. Jin, S. Fang, R. Wang, Y. Li, N. Wang, W. Guo, Y. Wang, D. Wen, L. Wei, Z. Dong, G. Kuang, The functional polymorphism in the matrix metalloproteinase-7 promoter increases susceptibility to esophageal squamous cell carcinoma, gastric cardiac adenocarcinoma and non-small cell lung carcinoma, Carcinogenesis 26 (2005) 1748–1753.
[154] H. Wang, S. Parry, G. Macones, M.D. Sammel, P.E. Ferrand, H. Kuivaniemi, G. Tromp, I. Halder, M.D. Shriver, R. Romero, J.F. Strauss, Functionally significant SNP MMP8 promoter haplotypes and preterm premature rupture of membranes (PPROM), Hum. Mol. Genet. 13 (2004) 2659–2669.
[155] J. Decock, J.R. Long, R.C. Laxton, X.O. Shu, C. Hodgkinson, W. Hendrickx, E.G. Pearce, Y.T. Gao, A.C. Pereira, R. Paridaens, W. Zheng, S. Ye, Association of matrix metalloproteinase-8 gene variation with breast cancer prognosis, Cancer Res. 67 (2007) 10214–10221.
[156] P. Gonzalez-Arriaga, M.F. Lopez-Cima, A. Fernandez-Somoano, T. Pascual, M.G. Marron, X.S. Puente, A. Tardon, Polymorphism + 17 C/G in matrix metalloprotease MMP8 decreases lung cancer risk, BMC Cancer 8 (2008) 378.
[157] M. Balbin, A. Fueyo, A.M. Tester, A.M. Pendas, A.S. Pitiot, A. Astudillo, C.M. Overall, S.D. Shapiro, C. Lopez-Otin, Loss of collagenase-2 confers increased skin tumor susceptibility to male mice, Nat. Genet. 35 (2003) 252–257.
[158] A. Gutierrez-Fernandez, A. Fueyo, A.R. Folgueras, C. Garabaya, C.J. Pennington, S. Pilgrim, D.R. Edwards, D.L. Holliday, J.L. Jones, P.N. Span, F.C. Sweep, X.S. Puente, C. Lopez-Otin, Matrix metalloproteinase-8 functions as a metastasis suppressor through modulation of tumor cell adhesion and invasion, Cancer Res. 68 (2008) 2755–2763.
[159] J.T. Korpi, V. Kervinen, H. Maklin, A. Vaananen, M. Lahtinen, E. Laara, A. Ristimaki, G. Thomas, M. Ylipalosaari, P. Astrom, C. Lopez-Otin, T. Sorsa, S. Kantola, E. Pirila, T. Salo, Collagenase-2 (matrix metalloproteinase-8) plays a protective role in tongue cancer, Br. J. Cancer 98 (2008) 766–775.
[160] A.R. Morgan, B. Zhang, W. Tapper, A. Collins, S. Ye, Haplotypic analysis of the MMP-9 gene in relation to coronary artery disease, J. Mol. Med. 81 (2003) 321–326.
[161] G.T. Jones, V.L. Phillips, E.L. Harris, J.I. Rossaak, A.M. van Rij, Functional matrix metalloproteinase-9 polymorphism (C-1562T) associated with abdominal aortic aneurysm, J. Vasc. Surg. 38 (2003) 1363–1367.
[162] T.L. Medley, T.J. Cole, A.M. Dart, C.D. Gatzka, B.A. Kingwell, Matrix metalloproteinase-9 genotype influences large artery stiffness through effects on aortic gene and protein expression, Arterioscler Thromb. Vasc. Biol. 24 (2004) 1479–1484.
[163] A.K. Kader, J. Liu, L. Shao, C.P. Dinney, J. Lin, Y. Wang, J. Gu, H.B. Grossman, X. Wu, Matrix metalloproteinase polymorphisms are associated with bladder cancer invasiveness, Clin. Cancer Res. 13 (2007) 2614–2620.
[164] N. Fiotti, N. Altamura, M. Fisicaro, N. Carraro, R. Adovasio, V.M. Sarra, L. Uxa, G. Guarnieri, B.T. Baxter, C. Giansante, MMP-9 microsatellite polymorphism: association with the progression of intima-media thickening and constrictive remodeling of carotid atherosclerotic plaques, Atherosclerosis 182 (2005) 287–292.
[165] N. Fiotti, R. Zivadinov, N. Altamura, D. Nasuelli, A. Bratina, M.A. Tommasi, A. Bosco, L. Locatelli, A. Grop, G. Cazzato, G. Guarnieri, C. Giansante, M. Zorzon, MMP-9 microsatellite polymorphism and multiple sclerosis, J. Neuroimmunol. 152 (2004) 147–153.
[166] D.G. Peters, A. Kassam, P.L. St Jean, H. Yonas, R.E. Ferrell, Functional polymorphism in the matrix metalloproteinase-9 promoter as a potential risk factor for intracranial aneurysm, Stroke 30 (1999) 2612–2616.
[167] N. Fiotti, M. Pedio, M. Battaglia Parodi, N. Altamura, L. Uxa, G. Guarnieri, C. Giansante, G. Ravalico, MMP-9 microsatellite polymorphism and susceptibility to exudative form of age-related macular degeneration, Genet. Med. 7 (2005) 272–277.
[168] M. Inada, Y. Wang, M.H. Byrne, M.U. Rahman, C. Miyaura, C. López-Otín, S.M. Krane, Critical roles for collagenase-3 (Mmp13) in development of growth plate cartilage and in endochondral ossification, Proc. Natl. Acad. Sci. U. S. A. 101 (2004) 17192–17197.
[169] D. Stickens, D.J. Behonick, N. Ortega, B. Heyer, B. Hartenstein, Y. Yu, A.J. Fosang, M. Schorpp-Kistner, P. Angel, Z. Werb, Altered endochondral bone development in matrix metalloproteinase 13-deficient mice, Development 131 (2004) 5883–5895.
[170] B.S. Wiseman, M.D. Sternlicht, L.R. Lund, C.M. Alexander, J. Mott, M.J. Bissell, P. Soloway, S. Itohara, Z. Werb, Site-specific inductive and inhibitory activities of MMP-2 and MMP-3 orchestrate mammary gland branching morphogenesis, J. Cell Biol. 162 (2003) 1123–1133.
[171] T.H. Vu, J.M. Shipley, G. Bergers, J.E. Berger, J.A. Helms, D. Hanahan, S.D. Shapiro, R. M. Senior, Z. Werb, MMP-9/gelatinase B is a key regulator of growth plate angiogenesis and apoptosis of hypertrophic chondrocytes, Cell 93 (1998) 411–422.
[172] K. Inoue, Y. Mikuni-Takagaki, K. Oikawa, T. Itoh, M. Inada, T. Noguchi, J.S. Park, T. Onodera, S.M. Krane, M. Noda, S. Itohara, A crucial role for matrix metalloproteinase 2 in osteocytic canalicular formation and bone metabolism, J. Biol. Chem. 281 (2006) 33814–33824.
[173] K. Holmbeck, P. Bianco, J. Caterina, S. Yamada, M. Kromer, S.A. Kuznetsov, M. Mankani, P.G. Robey, A.R. Poole, I. Pidoux, J.M. Ward, H. Birkedal-Hansen, MT1-MMP-deficient mice develop dwarfism, osteopenia, arthritis, and connective tissue disease due to inadequate collagen turnover, Cell 99 (1999) 81–92.
[174] Z. Zhou, S.S. Apte, R. Soininen, R. Cao, G.Y. Baaklini, R.W. Rauser, J. Wang, Y. Cao, K. Tryggvason, Impaired endochondral ossification and angiogenesis in mice deficient in membrane-type matrix metalloproteinase I, Proc. Natl. Acad. Sci. U. S. A. 97 (2000) 4052–4057.
[175] J.J. Caterina, Z. Skobe, J. Shi, Y. Ding, J.P. Simmer, H. Birkedal-Hansen, J.D. Bartlett, Enamelysin (matrix metalloproteinase 20)-deficient mice display an amelogenesis imperfecta phenotype, J. Biol. Chem. 277 (2002) 49598–49604.
[176] J. Oh, R. Takahashi, E. Adachi, S. Kondo, S. Kuratomi, A. Noma, D.B. Alexander, H. Motoda, A. Okada, M. Seiki, T. Itoh, S. Itohara, C. Takahashi, M. Noda, Mutations in two matrix metalloproteinase genes, MMP-2 and MT1-MMP, are synthetic lethal in mice, Oncogene 23 (2004) 5041–5048.
[177] J. Shi, M.Y. Son, S. Yamada, L. Szabova, S. Kahan, K. Chrysovergis, L. Wolf, A. Surmak, K. Holmbeck, Membrane-type MMPs enable extracellular matrix permissiveness and mesenchymal cell proliferation during embryogenesis, Dev. Biol. 313 (2008) 196–209.
[178] J. D'Armiento, T. DiColandrea, S.S. Dalal, Y. Okada, M.T. Huang, A.H. Conney, K. Chada, Collagenase expression in transgenic mouse skin causes hyperkeratosis and acanthosis and increases susceptibility to tumorigenesis, Mol. Cell. Biol. 15 (1995) 5732–5739.
[179] H.Y. Ha, H.B. Moon, M.S. Nam, J.W. Lee, Z.Y. Ryoo, T.H. Lee, K.K. Lee, B.J. So, H. Sato, M. Seiki, D.Y. Yu, Overexpression of membrane-type matrix metalloproteinase-1 gene induces mammary gland abnormalities and adenocarcinoma in transgenic mice, Cancer Res. 61 (2001) 984–990.
[180] M.D. Sternlicht, A. Lochter, C.J. Sympson, B. Huey, J.P. Rougier, J.W. Gray, D. Pinkel, M.J. Bissell, Z. Werb, The stromal proteinase MMP3/stromelysin-1 promotes mammary carcinogenesis, Cell 98 (1999) 137–146.
[181] M.J. Gorrin-Rivas, S. Arii, M. Furutani, M. Mizumoto, A. Mori, K. Hanaki, M. Maeda, H. Furuyama, Y. Kondo, M. Imamura, Mouse macrophage metalloelastase gene transfer into a murine melanoma suppresses primary tumor growth by halting angiogenesis, Clin. Cancer Res. 6 (2000) 1647–1654.
[182] J.P. Witty, T. Lempka, R.J. Coffey, L.M. Matrisian, Decreased tumor formation in 7,12-dimethylbenzanthracene-treated stromelysin-1 transgenic mice is associated with alterations in mammary epithelial cell apoptosis, Cancer Res. 55 (1995) 1401–1406.
[183] L.M. Coussens, C.L. Tinkle, D. Hanahan, Z. Werb, MMP-9 supplied by bone marrow-derived cells contributes to skin carcinogenesis, Cell 103 (2000) 481–490.
[184] K.L. Andarawewa, A. Boulay, R. Masson, C. Mathelin, I. Stoll, C. Tomasetto, M.P. Chenard, M. Gintz, J.P. Bellocq, M.C. Rio, Dual stromelysin-3 function during natural mouse mammary tumor virus-ras tumor progression, Cancer Res. 63 (2003) 5844–5849.
[185] A.M. Pendas, A.R. Folgueras, E. Llano, J. Caterina, F. Frerard, F. Rodriguez, A. Astudillo, A. Noel, H. Birkedal-Hansen, C. Lopez-Otin, Diet-induced obesity and reduced skin cancer susceptibility in matrix metalloproteinase 19-deficient mice, Mol. Cell. Biol. 24 (2004) 5304–5313.
[186] M. Jost, A.R. Folgueras, F. Frerart, A.M. Pendas, S. Blacher, X. Houard, S. Berndt, C. Munaut, D. Cataldo, J. Alvarez, L. Melen-Lamalle, J.M. Foidart, C. Lopez-Otin, A. Noel, Earlier onset of tumoral angiogenesis in matrix metalloproteinase-19-deficient mice, Cancer Res. 66 (2006) 5234–5241.
[187] T. Itoh, H. Matsuda, M. Tanioka, K. Kuwabara, S. Itohara, R. Suzuki, The role of matrix metalloproteinase-2 and matrix metalloproteinase-9 in antibody-induced arthritis, J. Immunol. 169 (2002) 2643–2647.
[188] K.M. Clements, J.S. Price, M.G. Chambers, D.M. Visco, A.R. Poole, R.M. Mason, Gene deletion of either interleukin-1beta, interleukin-1beta-converting enzyme, inducible nitric oxide synthase, or stromelysin 1 accelerates the development of knee osteoarthritis in mice after surgical transection of the medial collateral ligament and partial medial meniscectomy, Arthritis Rheum. 48 (2003) 3452–3463.
[189] J.O. Deguchi, E. Aikawa, P. Libby, J.R. Vachon, M. Inada, S.M. Krane, P. Whittaker, M. Aikawa, Matrix metalloproteinase-13/collagenase-3 deletion promotes collagen accumulation and organization in mouse atherosclerotic plaques, Circulation 112 (2005) 2708–2715.
[190] J. Silence, F. Lupu, D. Collen, H.R. Lijnen, Persistence of atherosclerotic plaque but reduced aneurysm formation in mice with stromelysin-1 (MMP-3) gene inactivation, Arterioscler Thromb. Vasc. Biol. 21 (2001) 1440–1445.
[191] A. Luttun, E. Lutgens, A. Manderveld, K. Maris, D. Collen, P. Carmeliet, L. Moons, Loss of matrix metalloproteinase-9 or matrix metalloproteinase-12 protects apolipoprotein E-deficient mice against atherosclerotic media destruction but differentially affects plaque growth, Circulation 109 (2004) 1408–1414.
[192] M. Kuzuya, K. Nakamura, T. Sasaki, X.W. Cheng, S. Itohara, A. Iguchi, Effect of MMP-2 deficiency on atherosclerotic lesion formation in apoE-deficient mice, Arterioscler Thromb. Vasc. Biol. 26 (2006) 1120–1125.
[193] S. Agrawal, P. Anderson, M. Durbeej, N. van Rooijen, F. Ivars, G. Opdenakker, L.M. Sorokin, Dystroglycan is selectively cleaved at the parenchymal basement membrane at sites of leukocyte extravasation in experimental autoimmune encephalomyelitis, J. Exp. Med. 203 (2006) 1007–1019.
[194] A.R. Folgueras, A. Fueyo, O. Garcia-Suarez, J. Cox, A. Astudillo, P. Tortorella, C. Campestre, A. Gutierrez-Fernandez, M. Fanjul-Fernandez, C.J. Pennington, D.R. Edwards, C.M. Overall, C. Lopez-Otin, Collagenase-2 deficiency or inhibition impairs experimental autoimmune encephalomyelitis in mice, J. Biol. Chem. 283 (2008) 9465–9474.
[195] L.A. Buhler, R. Samara, E. Guzman, C.L. Wilson, L. Krizanac-Bengez, D. Janigro, D.W. Ethell, Matrix metalloproteinase-7 facilitates immune access to the CNS in experimental autoimmune encephalomyelitis, BMC Neurosci. 10 (2009) 17.
[196] A. Weaver, A. Goncalves da Silva, R.K. Nuttall, D.R. Edwards, S.D. Shapiro, S. Rivest, V.W. Yong, An elevated matrix metalloproteinase (MMP) in an animal model of multiple sclerosis is protective by affecting Th1/Th2 polarization, FASEB J. 19 (2005) 1668–1670.
[197] D.B. Corry, K. Rishi, J. Kanellis, A. Kiss, L.Z. Song Lz, J. Xu, L. Feng, Z. Werb, F.

Kheradmand, Decreased allergic lung inflammatory cell egression and increased susceptibility to asphyxiation in MMP2-deficiency, Nat. Immunol. 3 (2002) 347–353.
[198] K.J. Greenlee, D.B. Corry, D.A. Engler, R.K. Matsunami, P. Tessier, R.G. Cook, Z. Werb, F. Kheradmand, Proteomic identification of in vivo substrates for matrix metalloproteinases 2 and 9 reveals a mechanism for resolution of inflammation, J. Immunol. 177 (2006) 7312–7321.
[199] M.M. Gueders, M. Balbin, N. Rocks, J.M. Foidart, P. Gosset, R. Louis, S. Shapiro, C. Lopez-Otin, A. Noel, D.D. Cataldo, Matrix metalloproteinase-8 deficiency promotes granulocytic allergen-induced airway inflammation, J. Immunol. 175 (2005) 2589–2597.
[200] S.Y. Kassim, S.A. Gharib, B.H. Mecham, T.P. Birkland, W.C. Parks, J.K. McGuire, Individual matrix metalloproteinases control distinct transcriptional responses in airway epithelial cells infected with *Pseudomonas aeruginosa*, Infect. Immun. 75 (2007) 5640–5650.
[201] R.D. Hautamaki, D.K. Kobayashi, R.M. Senior, S.D. Shapiro, Requirement for macrophage elastase for cigarette smoke-induced emphysema in mice, Science 277 (1997) 2002–2004.
[202] F. Zuo, N. Kaminski, E. Eugui, J. Allard, Z. Yakhini, A. Ben-Dor, L. Lollini, D. Morris, Y. Kim, B. DeLustro, D. Sheppard, A. Pardo, M. Selman, R.A. Heller, Gene expression analysis reveals matrilysin as a key regulator of pulmonary fibrosis in mice and humans, Proc. Natl. Acad. Sci. U. S. A. 99 (2002) 6292–6297.
[203] A. Kruger, Functional genetic mouse models: promising tools for investigation of the proteolytic internet, Biol. Chem. 390 (2009) 91–97.
[204] X. Miao, C. Yu, W. Tan, P. Xiong, G. Liang, W. Lu, D. Lin, A functional polymorphism in the matrix metalloproteinase-2 gene promoter (−1306C/T) is associated with risk of development but not metastasis of gastric cardia adenocarcinoma, Cancer Res. 63 (2003) 3987–3990.
[205] S.C. Lin, S.S. Lo, C.J. Liu, M.Y. Chung, J.W. Huang, K.W. Chang, Functional genotype in matrix metalloproteinases-2 promoter is a risk factor for oral carcinogenesis, J. Oral. Pathol. Med. 33 (2004) 405–409.
[206] D.M. Dong, M. Yao, B. Liu, C.Y. Sun, Y.Q. Jiang, Y.S. Wang, Association between the −1306C/T polymorphism of matrix metalloproteinase-2 gene and lumbar disc disease in Chinese young adults, Eur. Spine J. 16 (2007) 1958–1961.
[207] E. Vairaktaris, S. Vassiliou, E. Nkenke, Z. Serefoglou, S. Derka, C. Tsigris, A. Vylliotis, C. Yapijakis, F.W. Neukam, E. Patsouris, A metalloproteinase-9 polymorphism which affects its expression is associated with increased risk for oral squamous cell carcinoma, Eur. J. Surg. Oncol. 34 (2008) 450–455.
[208] J. D'Armiento, S.S. Dalal, Y. Okada, R.A. Berg, K. Chada, Collagenase expression in the lungs of transgenic mice causes pulmonary emphysema, Cell 71 (1992) 955–961.
[209] S. Cheng, A.S. Pollock, R. Mahimkar, J.L. Olson, D.H. Lovett, Matrix metalloproteinase 2 and basement membrane integrity: a unifying mechanism for progressive renal injury, FASEB J. 20 (2006) 1898–1900.
[210] L.J. McCawley, J. Wright, B.J. LaFleur, H.C. Crawford, L.M. Matrisian, Keratinocyte expression of MMP3 enhances differentiation and prevents tumor establishment, Am. J. Pathol. 173 (2008) 1528–1539.
[211] S. Cabrera, M. Gaxiola, J.L. Arreola, R. Ramirez, P. Jara, J. D'Armiento, T. Richards, M. Selman, A. Pardo, Overexpression of MMP9 in macrophages attenuates pulmonary fibrosis induced by bleomycin, Int. J. Biochem. Cell Biol. 39 (2007) 2324–2338.
[212] G. Bergers, R. Brekken, G. McMahon, T.H. Vu, T. Itoh, K. Tamaki, K. Tanzawa, P. Thorpe, S. Itohara, Z. Werb, D. Hanahan, Matrix metalloproteinase-9 triggers the angiogenic switch during carcinogenesis, Nat. Cell Biol. 2 (2000) 737–744.
[213] C.L. Wilson, K.J. Heppner, P.A. Labosky, B.L. Hogan, L.M. Matrisian, Intestinal tumorigenesis is suppressed in mice lacking the metalloproteinase matrilysin, Proc. Natl. Acad. Sci. U. S. A. 94 (1997) 1402–1407.
[214] L. Szabova, K. Chrysovergis, S.S. Yamada, K. Holmbeck, MT1-MMP is required for efficient tumor dissemination in experimental metastatic disease, Oncogene 27 (2008) 3274–3281.
[215] T. Itoh, T. Ikeda, H. Gomi, S. Nakao, T. Suzuki, S. Itohara, Unaltered secretion of beta-amyloid precursor protein in gelatinase A (matrix metalloproteinase 2)-deficient mice, J. Biol. Chem. 272 (1997) 22389–22392.
[216] T. Itoh, M. Tanioka, H. Yoshida, T. Yoshioka, H. Nishimoto, S. Itohara, Reduced angiogenesis and tumor progression in gelatinase A-deficient mice, Cancer Res. 58 (1998) 1048–1051.
[217] B. Wielockx, K. Lannoy, S.D. Shapiro, T. Itoh, S. Itohara, J. Vandekerckhove, C. Libert, Inhibition of matrix metalloproteinases blocks lethal hepatitis and apoptosis induced by tumor necrosis factor and allows safe antitumor therapy, Nat. Med. 7 (2001) 1202–1208.
[218] L.J. McCawley, H.C. Crawford, L.E. King Jr., J. Mudgett, L.M. Matrisian, A protective role for matrix metalloproteinase-3 in squamous cell carcinoma, Cancer Res. 64 (2004) 6965–6972.
[219] M. Wang, X. Qin, J.S. Mudgett, T.A. Ferguson, R.M. Senior, H.G. Welgus, Matrix metalloproteinase deficiencies affect contact hypersensitivity: stromelysin-1 deficiency prevents the response and gelatinase B deficiency prolongs the response, Proc. Natl. Acad. Sci. U. S. A. 96 (1999) 6885–6889.
[220] C.L. Wilson, A.J. Ouellette, D.P. Satchell, T. Ayabe, Y.S. Lopez-Boado, J.L. Stratman, S.J. Hultgren, L.M. Matrisian, W.C. Parks, Regulation of intestinal alpha-defensin activation by the metalloproteinase matrilysin in innate host defense, Science 286 (1999) 113–117.
[221] W.C. Powell, B. Fingleton, C.L. Wilson, M. Boothby, L.M. Matrisian, The metalloproteinase matrilysin proteolytically generates active soluble Fas ligand and potentiates epithelial cell apoptosis, Curr. Biol. 9 (1999) 1441–1447.
[222] S.E. Dunsmore, U.K. Saarialho-Kere, J.D. Roby, C.L. Wilson, L.M. Matrisian, H.G. Welgus, W.C. Parks, Matrilysin expression and function in airway epithelium, J. Clin. Invest. 102 (1998) 1321–1331.
[223] P. Van Lint, B. Wielockx, L. Puimege, A. Noel, C. Lopez-Otin, C. Libert, Resistance of collagenase-2 (matrix metalloproteinase-8)-deficient mice to TNF-induced lethal hepatitis, J. Immunol. 175 (2005) 7642–7649.
[224] P.H. Larsen, A.G. DaSilva, K. Conant, V.W. Yong, Myelin formation during development of the CNS is delayed in matrix metalloproteinase-9 and -12 null mice, J. Neurosci. 26 (2006) 2207–2214.
[225] T. Itoh, M. Tanioka, H. Matsuda, H. Nishimoto, T. Yoshioka, R. Suzuki, M. Uehira, Experimental metastasis is suppressed in MMP-9-deficient mice, Clin. Exp. Metastasis 17 (1999) 177–181.
[226] G.M. Longo, W. Xiong, T.C. Greiner, Y. Zhao, N. Fiotti, B.T. Baxter, Matrix metalloproteinases 2 and 9 work in concert to produce aortic aneurysms, J. Clin. Invest. 110 (2002) 625–632.
[227] F.E. Castaneda, B. Walia, M. Vijay-Kumar, N.R. Patel, S. Roser, V.L. Kolachala, M. Rojas, L. Wang, G. Oprea, P. Garg, A.T. Gewirtz, J. Roman, D. Merlin, S.V. Sitaraman, Targeted deletion of metalloproteinase 9 attenuates experimental colitis in mice: central role of epithelial-derived MMP, Gastroenterology 129 (2005) 1991–2008.
[228] H.R. Lijnen, B. Van Hoef, I. Vanlinthout, M. Verstreken, M.C. Rio, D. Collen, Accelerated neointima formation after vascular injury in mice with stromelysin-3 (MMP-11) gene inactivation, Arterioscler Thromb. Vasc. Biol. 19 (1999) 2863–2870.
[229] H. Uchinami, E. Seki, D.A. Brenner, J. D'Armiento, Loss of MMP 13 attenuates murine hepatic injury and fibrosis during cholestasis, Hepatology 44 (2006) 420–429.
[230] A. Rikimaru, K. Komori, T. Sakamoto, H. Ichise, N. Yoshida, I. Yana, M. Seiki, Establishment of an MT4-MMP-deficient mouse strain representing an efficient tracking system for MT4-MMP/MMP-17 expression in vivo using beta-galactosidase, Genes Cells 12 (2007) 1091–1100.
[231] K. Komori, T. Nonaka, A. Okada, H. Kinoh, H. Hayashita-Kinoh, N. Yoshida, I. Yana, M. Seiki, Absence of mechanical allodynia and Abeta-fiber sprouting after sciatic nerve injury in mice lacking membrane-type 5 matrix metalloproteinase, FEBS Lett. 557 (2004) 125–128.
[232] A.M. Manicone, T.P. Birkland, M. Lin, T. Betsuyaku, N. van Rooijen, J. Lohi, J. Keski-Oja, Y. Wang, S.J. Skerrett, W.C. Parks, Epilysin (MMP-28) restrains early macrophage recruitment in *Pseudomonas aeruginosa* pneumonia, J. Immunol. 182 (2009) 3866–3876.

II. MMP-19: a paradigm of dual protease in cancer

For many years, MMPs were widely considered as demolition agents in cancer due to their ability to degrade all major components of extracellular matrix and basement membranes. However, a growing body of literature has indicated that these enzymes can also play protective roles during tumor progression. Even more, some recent works have provided conclusive evidence that some specific MMPs may exert dual roles in cancer, acting as pro- or anti-tumor enzymes depending on the context, cell of origin or microenvironmental changes. On this basis, and as a previous step to the experimental work on MMPs performed in this Thesis, we performed an exhaustive revision of the structural and functional properties of MMP-19, a paradigm of proteolytic enzyme with dual roles in cancer.

Article 2. **Miriam Fanjul-Fernández** and Carlos López-Otín. "MMP-19".

Handbook of Proteolytic Enzymes, 3ª edition. Editors: A J. Barret, N. D. Rawlings and J. F. Woessner. Editorial: Academic Press (London); 2012. in press.

Personal contribution to this work

In this work, I was the main responsible for compiling and integrating all the available literature about structural and functional aspects of MMP-19. Likewise, I defined the outline of this article, prepared the figures and wrote the manuscript under the supervision of Dr. Carlos López-Otín.

Chapter 170

Matrix metallopeptidase-19

Miriam Fanjul-Fernández and Carlos López-Otín

Departamento de Bioquímica y Biología Molecular, Instituto Universitario de Oncología, IUOPA. Universidad de Oviedo. 33006-Oviedo, Spain

Name and History

Matrix metallopeptidase 19 (MMP-19) belongs to the Matrix Metalloproteinase (MMP) family, a large group of zinc-endopeptidases, also known as matrixins, collectively capable of degrading all extracellular matrix components. To date, at least 25 different vertebrate MMPs have been identified and their activities have been implicated in a broad range of biological functions like cell proliferation, migration and adhesion as well as in the regulation of many fundamental physiological events including angiogenesis, inflammation and apoptosis (1-3). MMP-19 was first isolated from human cDNA liver libraries (4) and, afterwards, it was detected as an autoantigen in blood vessels from inflamed synovium of a patient with rheumatoid arthritis (5), suggesting that it may be involved in inflammatory processes and angiogenesis. This peptidase exhibits the archetypal domain structure characteristic of the MMP family. However, due to the lack of several structural features common to members of the diverse MMP subclasses, it presents a low sequence homology to any other known MMP and it cannot be classified in previously defined subgroups. The *MMP19* gene maps to chromosome 12q14 and harbours nine exons along 7.6 kb (6). All of them are highly conserved across mammalian species. However, no orthologues to human MMP-19 are found in zebra finch genome although the presence of this gene in some invertebrates suggests that it has been specifically lost in the bird lineage. In addition to its distinctive structural features, MMP-19 also shows an atypical tissue expression. Thus, in contrast to most MMPs, which are only strongly induced under matrix remodelling or pathological processes, MMP-19 is detected in several normal tissues like placenta, lung, pancreas, ovary, spleen, and intestine under normal quiescent conditions (4). Therefore, according to its unusual characteristics, MMP-19 was proposed to represent the first member of a new MMP subfamily with a putative novel role in physiological or pathological circumstances (4).

Activity and Specificity

Like all members of the MMP family, MMP-19 is synthesized as a zymogen with a signal peptide that leads the protein to the secretory pathway. Once the latent form is located at the extracellular matrix (ECM), the proMMP-19 requires a

proenzyme activation process, although it also has a tendency to self–activation. Biochemical studies have revealed that MMP-19 may be a potent player in the degradation of basement membrane components. Thus, MMP-19 is able to cleave collagen type IV, a major component of basement membranes, into two main high molecular mass fragments of 94 and 56 kDa (7). Interestingly, this enzyme was found to be co-expressed with collagen type IV in the tunica media of blood vessels of RA synovium (8). Additionally, laminin and nidogen, another two components of the basement membrane network, are cleaved by MMP-19 in a highly efficient manner. Moreover, since nidogen is thought to stabilize microvessels, MMP-19 might act as an inhibitory factor of the formation or stabilization of blood capillaries. In addition to these proteolytic activities, MMP-19 is also capable of degrading other ECM proteins, such as tenascin-C and fibronectin, as well as two cartilage components, namely, cartilage oligomeric matrix protein and aggrecan, supporting the substantial role of this metalopeptidase in the turnover of ECM and tissue remodelling processes (7, 9). Beyond this classical role in ECM disruption, the identification of novel non-matrix substrates for MMPs including MMP-19, has converted these proteases in sophisticated modulators of more specific processes. Thus, MMP-19 cleaves *in vitro* insulin-like growth factor binding protein-3 (IGFBP-3) suggesting that it could control the activity of insulin-like growth factors and thereby regulate cancer cell growth (10). Unlike other MMPs, MMP-19 catalytic domain is not able to activate most of the latent MMPs tested *in vitro*, with the exception of proMMP-9. Finally, the active form of the enzyme is strongly inhibited by tissue inhibitors of MMPs (TIMPs) –2, -3, and weakly blocked by TIMP-1 (7).

Structural Chemistry

MMP-19 is secreted as a 58 kDa proform presenting the typical domain organization of soluble MMPs including a prodomain region with the essential cysteine residue for maintaining enzyme latency, a catalytic domain of about 160 residues with the conserved zinc-binding motif HEXGHXXXXXHS, a linker region, and a COOH-terminal fragment of about 200 amino acids with sequence similarity to hemopexin (Fig 1A). However, as mentioned above, this matrixin does not display the structural features distinctive of the main MMP subfamilies such as the fibronectin-like repeats of

gelatinases, the Asp, Tyr, and Gly residues near the active site of collagenases, the furin activation consensus sequence between the propeptide and the catalytic domain typical of furin-activatable MMPs, or the COOH-terminal extension rich in hydrophobic residues characteristic of MT-MMPs. In contrast, MMP-19 presents unique structural variations within the MMP family (Fig 1B). Thus, MMP-19 shows a) an insertion of glutamic acid residues in the linker region joining the catalytic and hemopexin domains that are not found in other MMPs, b) an unusual latency motif in the propeptide domain, c) an additional cysteine residue in the catalytic region, and d) a 36 residue threonine-rich region following the final conserved cysteine at the COOH-terminal of the

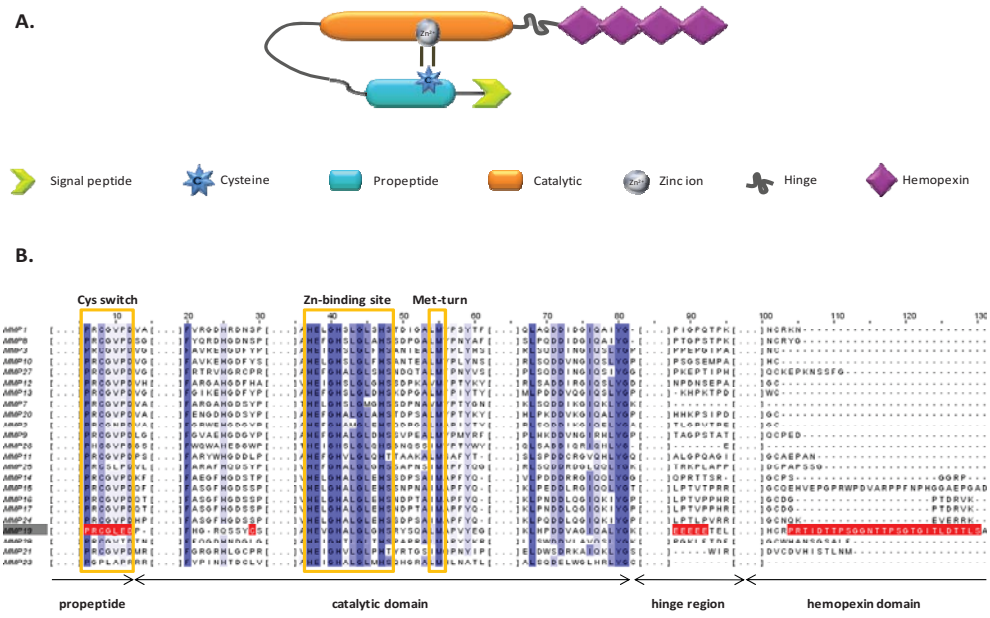

Structural features of the MMP-19. ***A)*** *Domain arrangement of the MMP-19 showing the archetypal assembly of the MMPs.* ***B)*** *Alignment of the main motifs of the MMPs where is shown the unusual amino acid variations of the MMP-19 (red box).*

hemopexin domain that has not sequence similarity to equivalent regions in other human MMPs. Furthermore, MMP-19 contains two potential N-linked glycosylation sites within the hemopexin domain which are absent in all other MMPs (4). On this

basis, MMP-19 does not fit in any previously defined MMP subclass and is classified together with other unusual MMPs in the category of "other MMPs" (1).

Preparation

Human recombinant MMP-19 can be obtained from cultured medium conditioned by NS0 mouse myeloma cells that have been transfected with MMP-19 cDNA, essentially as described previously (11). Briefly, serum-free culture medium from cells expressing high levels of proMMP-19 was dialyzed and loaded onto a S-Sepharose fast flow column. The column was washed three times to remove impurities. After elution, a silver-stained SDS-PAGE was performed to check the purity. A final purification step was achieved by gel filtration chromatography using Sephacryl S-200.

Biological Aspects

The functional relevance of MMP-19 can be deduced from a series of studies aimed at evaluating the implication of this metallopeptidase in tumor progression as well as in other pathological conditions. Some remarkable aspects in this regard are the following:

MMP-19 and cancer.

The MMPs play a complex role in cancer development due to their ability to participate in the proteolytic processing of a wide variety of substrates. MMPs are generally considered as pro-oncogenic factors, since they can degrade the ECM molecules to facilitate tumor cell migration and invasion. However, this pro-oncogenic role of MMPs has been challenged by the emerging antitumor properties reported for some MMPs (12). The role of MMP-19 in cancer is controversial. Thus, *MMP19* is upregulated during the later stages of melanoma progression facilitating the vertical migration of tumor cells (13). However, *MMP19* is downregulated in basal and squamous cell carcinoma during neoplastic dedifferentiation as well as in colon and nasopharyngeal cancers (14-16). In this regard, recent studies have proposed allelic deletion and promoter hypermethylation as mechanisms for *MMP19* silencing during

tumor progression. Moreover, it has proposed that MMP-19 has anti-angiogenic properties that can be responsible for its tumor suppressor activity (16). Additionally, different *in vivo* studies of cancer susceptibility performed in mutant mice deficient in *Mmp19* have confirmed the dual role of this metallopeptidase in cancer. Thus, in a methylcholanthrene-induced fibrosarcoma model, *Mmp19*-null mice develop less fibrosarcomas and with longer latency period than their control littermates whereas, conversely, they exhibit an early onset of angiogenesis and tumor invasion after transplantation of malignant murine PDVA keratinocytes (17, 18). Altogether, these data suggest that MMP-19 negatively regulates early stages of tumor cell invasion, but cancer cells could become less sensitive to MMP-19 activity once tumor develops. These apparently paradoxical results may reflect different roles of MMP-19 in the evolution of various cancer types as well as throughout different steps of cancer progression, highlighting the requirement to understand the individual functions of each MMP to improve anticancer strategies.

MMP-19 and inflammation

Several works have also suggested that MMP-19 may also play a role driving inflammatory processes. Thus, this enzyme was initially identified as an autoantigen in patients with rheumatoid arthritis (19). More recently, it has been shown that MMP-19 acts as a molecular mediator of the airway inflammation, preventing the deposition in the airway walls of tenascin-C, a glycoprotein that promotes inflammatory cell adhesion and accumulation through their capacity to interact with integrins (20, 21). Moreover, the lack of MMP-19 increases the levels of interleukin-13 (IL-13), a prototypic Th2 cytokine that induces eosinophilic inflammation in the airways, suggesting a link between MMP-19 and the Th2 proinflammatory response (22). In this sense, Beck and colleagues (23), have proposed that MMP-19 is also an important factor in cutaneous immune responses and influences the development of T cells. Nevertheless, in the skin context, the lack of MMP-19 reduces the influx of inflammatory cells, decreases keratinocyte proliferation and diminishes activation of $CD8^+$ T cells, which are responsible for this type of reaction. *MMP19* has also been reported to be expressed in myeloid cells (24) and is upregulated under inflammatory conditions such as arthritis and multiple sclerosis, where the expression of the protease by microglia may contribute

to the formation of new lesions by enhancing leucocyte migration, axonal damage and ECM remodeling (24-26).

MMP-19 and other pathological conditions

MMP-19 has been implicated in several skin disorders in which proliferation and differentiation of keratinocytes is disturbed. Thus, in both tinea corporis and eczema, MMP-19 is expressed in the stratum basale and in the healthy epidermis, but also in the spinous layers (27). Likewise, it has been reported that *MMP19* is upregulated in psoriasis, a disease characterized by keratinocyte hyperproliferation, angiogenesis, and infiltration of inflammatory cells (28). MMP-19 is also dysregulated in chronic wounds where is induced in the proliferating epithelium. However, its expression is lost during malignant transformation of the epithelium cells, being absent from invasive areas of squamous cell carcinoma (SCC) (14). Finally, MMP-19 has also been implicated in a panoply of diseases such as renal dysplasia, Dupuytren's disease, Paget's disease, chronic limb ischemia or Henoch-Schönlein purpura (29-33).

Related Peptidases

MMPs comprise a large family of endopeptidases belonging to the superfamily of metzincins, which are characterized by the HExxHxxxGxxH/D consensus zinc-binding sequence in their active centre. They are widely distributed in all kingdoms of life and have likely evolved from a single-domain protein which underwent successive rounds of duplication, gene fusion and exon shuffling events to generate the multidomain architecture and functional diversity currently exhibited by MMPs. It appears conceivable that the domain assemblies occurred at an early stage of the diversification of different MMPs and that they progressed through the evolutionary process independent of one another, and perhaps parallel to each other (1). Between all members of MMPs, MMP-28 seems to be the closest peptidase to MMP-19. Thus, and despite they are classified into distinct MMP subgroup as MMP-28 is a furin-activatable enzyme, both MMPs have the highest percentage of amino acid sequence identities among all secreted MMPs, as well as similar expression pattern. Thus, MMP-28, also known as epilysin, is highly expressed in the skin and in a number of other normal human tissues and is also implicated in the development and regeneration of the nervous

system (34, 35). Also similar to MMP-19, epilysin is found in both cartilage and synovium tissues where the expression is increased in patients with osteoarthritis (36). Likewise, MMP-28 expression is increased in demyelinating lesions in multiple sclerosis and strikingly, all tested forms of MMP-28 increased expression of MMP-19 (37, 38). Finally, both proteins have been shown to associate with the surface of some cells in a C-terminal domain-dependent manner (24, 39).

Further reading

1. Fanjul-Fernandez M, Folgueras AR, Cabrera S, Lopez-Otin C. Matrix metalloproteinases: evolution, gene regulation and functional analysis in mouse models. Biochim Biophys Acta, 2010, *1803*: 3-19.
2. Puente XS, Sanchez LM, Overall CM, Lopez-Otin C. Human and mouse proteases: a comparative genomic approach. Nat Rev Genet, 2003, *4*: 544-58.
3. Page-McCaw A, Ewald AJ, Werb Z. Matrix metalloproteinases and the regulation of tissue remodelling. Nat Rev Mol Cell Biol, 2007, *8*: 221-33.
4. Pendas AM, Knauper V, Puente XS, Llano E, Mattei MG, Apte S, Murphy G, Lopez-Otin C. Identification and characterization of a novel human matrix metalloproteinase with unique structural characteristics, chromosomal location, and tissue distribution. J Biol Chem, 1997, *272*: 4281-6.
5. Kolb C, Mauch S, Peter HH, Krawinkel U, Sedlacek R. The matrix metalloproteinase RASI-1 is expressed in synovial blood vessels of a rheumatoid arthritis patient. Immunol Lett, 1997, *57*: 83-8.
6. Mueller MS, Mauch S, Sedlacek R. Structure of the human MMP-19 gene. Gene, 2000, *252*: 27-37.
7. Stracke JO, Hutton M, Stewart M, Pendas AM, Smith B, Lopez-Otin C, Murphy G, Knauper V. Biochemical characterization of the catalytic domain of human matrix metalloproteinase 19. Evidence for a role as a potent basement membrane degrading enzyme. J Biol Chem, 2000, *275*: 14809-16.
8. Kolb C, Mauch S, Krawinkel U, Sedlacek R. Matrix metalloproteinase-19 in capillary endothelial cells: expression in acutely, but not in chronically, inflamed synovium. Exp Cell Res, 1999, *250*: 122-30.
9. Stracke JO, Fosang AJ, Last K, Mercuri FA, Pendas AM, Llano E, Perris R, Di Cesare PE, Murphy G, Knauper V. Matrix metalloproteinases 19 and 20 cleave aggrecan and cartilage oligomeric matrix protein (COMP). FEBS Lett, 2000, *478*: 52-6.
10. Sadowski T, Dietrich S, Koschinsky F, Sedlacek R. Matrix metalloproteinase 19 regulates insulin-like growth factor-mediated proliferation, migration, and adhesion in human keratinocytes through proteolysis of insulin-like growth factor binding protein-3. Mol Biol Cell, 2003, *14*: 4569-80.
11. Crabbe T, Willenbrock F, Eaton D, Hynds P, Carne AF, Murphy G, Docherty AJ. Biochemical characterization of matrilysin. Activation conforms to the stepwise mechanisms proposed for other matrix metalloproteinases. Biochemistry, 1992, *31*: 8500-7.
12. Lopez-Otin C, Matrisian LM. Emerging roles of proteases in tumour suppression. Nat Rev Cancer, 2007, *7*: 800-8.

13. Muller M, Beck IM, Gadesmann J, Karschuk N, Paschen A, Proksch E, Djonov V, Reiss K, Sedlacek R. MMP19 is upregulated during melanoma progression and increases invasion of melanoma cells. Mod Pathol, 2010, *23*: 511-21.
14. Impola U, Jeskanen L, Ravanti L, Syrjanen S, Baldursson B, Kahari VM, Saarialho-Kere U. Expression of matrix metalloproteinase (MMP)-7 and MMP-13 and loss of MMP-19 and p16 are associated with malignant progression in chronic wounds. Br J Dermatol, 2005, *152*: 720-6.
15. Bister VO, Salmela MT, Karjalainen-Lindsberg ML, Uria J, Lohi J, Puolakkainen P, Lopez-Otin C, Saarialho-Kere U. Differential expression of three matrix metalloproteinases, MMP-19, MMP-26, and MMP-28, in normal and inflamed intestine and colon cancer. Dig Dis Sci, 2004, *49*: 653-61.
16. Chan KC KJ, Lung HL, Sedlacek R, Zhang ZF, Luo DZ, Feng ZB, Chen S, Chen H, Chan KW, Tsao SW, Chua DT, Zabarovsky ER, Stanbridge EJ, Lung ML. Catalytic activity of matrix metalloproteinase-19 is essential for tumor suppressor and anti-angiogenic activities in nasopharyngeal carcinoma. Int J Cancer, 2010,
17. Jost M, Folgueras AR, Frerart F, Pendas AM, Blacher S, Houard X, Berndt S, Munaut C, Cataldo D, Alvarez J, Melen-Lamalle L, Foidart JM, Lopez-Otin C, Noel A. Earlier onset of tumoral angiogenesis in matrix metalloproteinase-19-deficient mice. Cancer Res, 2006, *66*: 5234-41.
18. Pendas AM, Folgueras AR, Llano E, Caterina J, Frerard F, Rodriguez F, Astudillo A, Noel A, Birkedal-Hansen H, Lopez-Otin C. Diet-induced obesity and reduced skin cancer susceptibility in matrix metalloproteinase 19-deficient mice. Mol Cell Biol, 2004, *24*: 5304-13.
19. Sedlacek R, Mauch S, Kolb B, Schatzlein C, Eibel H, Peter HH, Schmitt J, Krawinkel U. Matrix metalloproteinase MMP-19 (RASI-1) is expressed on the surface of activated peripheral blood mononuclear cells and is detected as an autoantigen in rheumatoid arthritis. Immunobiology, 1998, *198*: 408-23.
20. Nishio T, Kawaguchi S, Yamamoto M, Iseda T, Kawasaki T, Hase T. Tenascin-C regulates proliferation and migration of cultured astrocytes in a scratch wound assay. Neuroscience, 2005, *132*: 87-102.
21. Taooka Y, Chen J, Yednock T, Sheppard D. The integrin alpha9beta1 mediates adhesion to activated endothelial cells and transendothelial neutrophil migration through interaction with vascular cell adhesion molecule-1. J Cell Biol, 1999, *145*: 413-20.
22. Gueders MM, Hirst SJ, Quesada-Calvo F, Paulissen G, Hacha J, Gilles C, Gosset P, Louis R, Foidart JM, Lopez-Otin C, Noel A, Cataldo DD. Matrix metalloproteinase-19 deficiency promotes tenascin-C accumulation and allergen-induced airway inflammation. Am J Respir Cell Mol Biol, 2010, *43*: 286-95.
23. Beck IM, Ruckert R, Brandt K, Mueller MS, Sadowski T, Brauer R, Schirmacher P, Mentlein R, Sedlacek R. MMP19 is essential for T cell development and T cell-mediated cutaneous immune responses. PLoS One, 2008, *3*: e2343.
24. Mauch S, Kolb C, Kolb B, Sadowski T, Sedlacek R. Matrix metalloproteinase-19 is expressed in myeloid cells in an adhesion-dependent manner and associates with the cell surface. J Immunol, 2002, *168*: 1244-51.
25. Behera AK, Hildebrand E, Scagliotti J, Steere AC, Hu LT. Induction of host matrix metalloproteinases by Borrelia burgdorferi differs in human and murine lyme arthritis. Infect Immun, 2005, *73*: 126-34.
26. van Horssen J, Vos CM, Admiraal L, van Haastert ES, Montagne L, van der Valk P, de Vries HE. Matrix metalloproteinase-19 is highly expressed in active multiple sclerosis lesions. Neuropathol Appl Neurobiol, 2006, *32*: 585-93.

27. Sadowski T, Dietrich S, Muller M, Havlickova B, Schunck M, Proksch E, Muller MS, Sedlacek R. Matrix metalloproteinase-19 expression in normal and diseased skin: dysregulation by epidermal proliferation. J Invest Dermatol, 2003, *121*: 989-96.
28. Suomela S, Kariniemi AL, Impola U, Karvonen SL, Snellman E, Uurasmaa T, Peltonen J, Saarialho-Kere U. Matrix metalloproteinase-19 is expressed by keratinocytes in psoriasis. Acta Derm Venereol, 2003, *83*: 108-14.
29. Jain S, Suarez AA, McGuire J, Liapis H. Expression profiles of congenital renal dysplasia reveal new insights into renal development and disease. Pediatr Nephrol, 2007, *22*: 962-74.
30. Johnston P, Larson D, Clark IM, Chojnowski AJ. Metalloproteinase gene expression correlates with clinical outcome in Dupuytren's disease. J Hand Surg Am, 2008, *33*: 1160-7.
31. Kuivanen T, Tanskanen M, Jahkola T, Impola U, Asko-Seljavaara S, Saarialho-Kere U. Matrilysin-1 (MMP-7) and MMP-19 are expressed by Paget's cells in extramammary Paget's disease. J Cutan Pathol, 2004, *31*: 483-91.
32. Baum O, Ganster M, Baumgartner I, Nieselt K, Djonov V. Basement membrane remodeling in skeletal muscles of patients with limb ischemia involves regulation of matrix metalloproteinases and tissue inhibitor of matrix metalloproteinases. J Vasc Res, 2007, *44*: 202-13.
33. Shin JI, Song KS, Kim H, Cho NH, Kim J, Kim HS, Lee JS. The gene expression profile of matrix metalloproteinases and their inhibitors in children with Henoch-Schonlein purpura. Br J Dermatol, 2011, *164*: 1348-55.
34. Lohi J, Wilson CL, Roby JD, Parks WC. Epilysin, a novel human matrix metalloproteinase (MMP-28) expressed in testis and keratinocytes and in response to injury. J Biol Chem, 2001, *276*: 10134-44.
35. Werner SR, Mescher AL, Neff AW, King MW, Chaturvedi S, Duffin KL, Harty MW, Smith RC. Neural MMP-28 expression precedes myelination during development and peripheral nerve repair. Dev Dyn, 2007, *236*: 2852-64.
36. Davidson RK, Waters JG, Kevorkian L, Darrah C, Cooper A, Donell ST, Clark IM. Expression profiling of metalloproteinases and their inhibitors in synovium and cartilage. Arthritis Res Ther, 2006, *8*: R124.
37. Werner SR, Dotzlaf JE, Smith RC. MMP-28 as a regulator of myelination. BMC Neurosci, 2008, *9*: 83.
38. Rodgers UR, Kevorkian L, Surridge AK, Waters JG, Swingler TE, Culley K, Illman S, Lohi J, Parker AE, Clark IM. Expression and function of matrix metalloproteinase (MMP)-28. Matrix Biol, 2009, *28*: 263-72.
39. Illman SA, Lehti K, Keski-Oja J, Lohi J. Epilysin (MMP-28) induces TGF-beta mediated epithelial to mesenchymal transition in lung carcinoma cells. J Cell Sci, 2006, *119*: 3856-65.

III. Generation and characterization of Mmp1a-deficient mice

The matrix metalloproteinase MMP-1 has emerged as a potential new target in a variety of human cancers. Previous studies from our laboratory, confirmed and extended by other groups, have demonstrated that Mmp-1a is the mouse ortholog of human MMP-1. However, more than 10 years after the discovery of Mmp-1a, minimal information is still available about its functional role in mouse physiology and pathology, including cancer. This is especially puzzling since human MMP-1 was cloned and associated with tumor invasion and metastasis more than two decades ago, despite these cancer-related functions have not been formally demonstrated *in vivo*. One possibility to explain this lack of information about MMP-1 in cancer is the absence of an *in vivo* model of MMP-1 deficiency, an aspect which has been largely attributed to the wide assumption that no MMP-1 ortholog was present in rodents. Here, we report the first mouse strain genetically deficient in *Mmp1a* and demonstrate that Mmp-1a plays a critical role in lung cancer.

Miriam Fanjul-Fernández, Alicia R. Folgueras, Antonio Fueyo, Milagros Balbín, María F. Suárez, M. Soledad Fernández-García, Steven D. Shapiro and Carlos López-Otín. "Mice deficient in matrix metalloproteinase Mmp-1a show decreased susceptibility to chemically-induced lung cancer**".**

Journal of Biological Chemistry (2012, under revision).

Personal contribution to this work

After my incorporation to López-Otín laboratory and in close collaboration with Dr. Alicia R. Folgueras, I first contributed to the establishment, management and genotyping of the colony of *Mmp1a*-ko mice. Subsequently, I performed most of the experimental work aimed at evaluating lung-cancer susceptibility of these mice and carried out all studies of the molecular mechanisms underlying the pro-tumorigenic activity of this metalloproteinase. Finally, I wrote the manuscript under Dr. Carlos López-Otín's supervision.

Mice deficient in matrix metalloproteinase Mmp-1a show decreased susceptibility to chemically-induced lung cancer

Miriam Fanjul-Fernández[1], Alicia R. Folgueras[1], Antonio Fueyo[2], Milagros Balbín[3], María F. Suárez[1], M. Soledad Fernández-García[4], Steven D. Shapiro[5] and Carlos López-Otín[1]

[1]Departamento de Bioquímica y Biología Molecular, and [2]Biología Funcional, Facultad de Medicina, Instituto Universitario de Oncología, Universidad de Oviedo, Oviedo, Spain;[3]Servicio de Oncología Molecular and [4]Anatomía Patológica, Hospital Universitario Central de Asturias, Oviedo, Spain;[5]Department of Medicine, University of Pittsburgh School of Medicine, Pittsburgh, USA.

Running title: *Mmp1a* deficiency protects against lung carcinoma

To whom correspondence should be addressed: Carlos Lopez-Otin. Departamento de Bioquímica y Biología Molecular, Facultad de Medicina, Universidad de Oviedo, 33006 Oviedo, Spain. Telephone: +34 985104201. E-mail: clo@uniovi.es

Key words: degradome, protease, invasion, metastasis, carcinogenesis.

Background: *MMP1* is overexpressed in malignant tumors and is levels are associated with poor prognosis.
Results: Mice deficient in Mmp-1a, the ortholog of human MMP-1, develop less lung carcinomas than controls and show a Th1 anti-inflammatory response.
Conclusion: Mmp-1a is a protumoral protease which alters Th1/Th2 cytokine balance.
Significance: *Mmp1a*-deficient mice are a new model for the functional analysis of this metalloproteinase in cancer.

ABSTRACT

Human MMP-1 is a matrix metalloproteinase repeatedly associated with many pathological conditions including cancer. Thus, *MMP1* overexpression is a poor prognosis marker in a variety of advanced cancers, including colorectal, breast and lung carcinomas. Moreover, MMP-1 plays a key role in the metastatic behavior of melanoma, breast and prostate cancer cells. However, functional and mechanistic studies on the relevance of MMP-1 in cancer have been hampered by the absence of an *in vivo* model. In this work, we have generated mice deficient in *Mmp1a*, the murine ortholog of human *MMP1*. *Mmp1a*$^{-/-}$ mice are viable and fertile and do not exhibit obvious abnormalities, which has facilitated studies of cancer susceptibility. These studies have shown a decreased susceptibility to develop lung carcinomas induced by chemical carcinogens in *Mmp1a*$^{-/-}$ mice. Histopathological analysis indicated that tumors generated in *Mmp1a*$^{-/-}$ mice are smaller and less angiogenic than those of wild-type mice, both characteristics being consistent with the idea that the absence of Mmp-1a hampers tumor progression. Proteomic analysis revealed decreased levels of chitinase-3 like 3 (CHI3L3) and accumulation of the receptor for advanced glycation end-products (RAGE) and its ligand S100A8 in lung samples from *Mmp1a*$^{-/-}$ mice compared to those from wild-type. These findings suggest that Mmp-1a could play a role in tumor progression by modulating the polarization of

a Th1/Th2 inflammatory response to chemical carcinogens. On the basis of these results, we propose that *Mmp1a*-knockout mice provide an excellent *in vivo* model for the functional analysis of human MMP-1 in both physiological and pathological conditions.

INTRODUCTION

The matrix metalloproteinases (MMPs) are a family of structurally related enzymes that can collectively degrade the main protein components of the extracellular matrix and basement membranes (1). On the basis of these degrading activities, MMPs have been considered as essential enzymes in the invasive and metastatic properties of tumor cells (2). These findings, together with multiple clinical and experimental data associating MMPs with tumor progression, stimulated the search for MMP inhibitors with ability to block the activities of these enzymes in cancer. However, most clinical trials with synthetic MMP inhibitors failed to provide appreciable benefits to patients with advanced cancer (3). These negative results have forced a profound re-evaluation of the functional and clinical relevance of MMPs in cancer as well as a reformulation of the MMP inhibition strategies used in these clinical trials (3,4). As a direct consequence of these post-trial studies, new paradigms have recently emerged in relation to the cancer relevance of the different members of this complex family of endoproteases. First, many experimental data have shown that MMPs are not exclusively implicated in the proteolytic breakdown of tissue barriers for metastatic spread. Thus, these enzymes may target a diversity of non-matrix substrates and influence other critical steps in tumor evolution such as cell proliferation, differentiation, angiogenesis or apoptosis (5). Additionally, these new studies have revealed the occurrence of MMPs, such as MMP-8, MMP-12 and MMP-26, which play a protective role during tumor progression (6). Furthermore, other MMPs such as MMP-3, MMP-9 and MMP-19, which were originally recognized as pro-tumorigenic enzymes, may also function as tumor-suppressive proteases in some specific situations (7-10).

These recent experimental findings have provided some explanations for the lack of success of clinical trials based on the use of broad-range MMP inhibitors in patients with advanced stages of cancer, as they would also reduce the host-protective antitumor properties of certain MMPs (3,4). Likewise, the administration of these MMP inhibitors to patients with advanced cancer would be of limited value for those cases in which MMPs play important roles during early stages of the disease (3,4). Accordingly, it is necessary to perform a detailed analysis of the specific role of each individual MMP in the multiple stages of tumor evolution. This is the case for fibroblast or interstitial collagenase (MMP-1), the first member of the MMP family identified in human tissues and widely associated with cancer, but whose functional relevance in the progression of the disease is still largely unknown (11,12).

Human MMP-1 is produced by a variety of tumor cells as well as by adjacent stromal fibroblasts in response to factors derived from transformed cells. Clinical studies have reported that MMP-1 is overexpressed in a number of malignant tumors and its presence is associated with poor prognosis in different cancers such as colorectal, breast and lung carcinomas (13-15). Moreover, *MMP1* has been identified as one of the four key genes required for lung metastatic colonization in breast cancer (16). Additionally, MMP-1 together with ADAMTS-1 proteolytically engage EGF-like growth factors in an osteolytic signaling cascade which facilitates bone metastasis (17). Furthermore, MMP-1 produced in the stromal-tumor microenvironment activates the proinvasive functions of protease-activated receptor 1 and promotes invasion and tumorigenesis of breast cancer cells (18). Likewise, experimental manipulation of the expression levels of this protease alters the metastatic behavior of melanoma, breast and prostate cancer cells (19-21). However, functional and mechanistic studies on the relevance of MMP-1 in cancer have been hampered by the absence of an *in vivo* model of *MMP1*-deficiency. To address this question, we have undertaken studies to generate mutant mice deficient in *Mmp1a*, the mouse orthologous gene of human *MMP1* (22). In this work, we describe the generation of *Mmp1a*$^{-/-}$ mice and analyze their cancer susceptibility, with the finding that loss of *Mmp1a* partially protects mice against

development of lung carcinomas induced by chemical carcinogens. We have also performed a series of histopathological and proteomic analysis that have provided information about the mechanisms underlying Mmp-1a implication in lung cancer development. Finally, we propose that *Mmp1a*$^{-/-}$ mice represent a novel *in vivo* model to elucidate the functional relevance of human MMP-1 in the context of the large complexity and diversity of proteolytic enzymes.

EXPERIMENTAL PROCEDURES

Animals-To generate *Mmp1a*$^{-/-}$ mice, we first isolated a genomic PAC clone encoding *Mmp1a* from a mouse 129/SvJ library (HGMP Resource Centre) by using a murine *Mmp1a* cDNA fragment as a probe. Then, we used the plasmid pKO scrambler V916 (Lexicon Genetics) to construct the *Mmp1a* targeting vector. A 1.4 kb *HindIII* fragment from the 5'-flanking containing exon 2, 3 and part of exon 4 was used as the 5'-homologous region, whereas a 6.8 kb *EcoRI-RsrII* fragment containing part of the exon 6 and exon 7 was used as the 3'-region of homology. The PGK-neo cassette was subcloned into an *AscI* site of the vector with the transcriptional orientation opposite to that of *Mmp1a* and replaced a 1.7 kb fragment containing exons 4, 5 and part of the exon 6 of the gene. The targeting vector was linearized by digestion with *NotI* and electroporated into HM-1 (129/Ola) embryonic stem cells. Resistant clones were selected for homologous recombination with G418 and ganciclovir, and screened by Southern blot analysis. The heterozygous stem cells were aggregated to CD1 morulas and transferred into uteri of pseudopregnant females to generate chimeras. Chimeric males were mated with C57BL/6J females and the offspring was screened by Southern blot analysis of tail genomic DNA. The heterozygous littermates were mated to generate homozygous mutant mice.

Northern blot analysis-Total RNA was isolated from frozen placenta samples obtained from wild-type and knock-out female mice at 13.5 days of embryonic development by using a commercial kit (RNeasy Mini Kit; Qiagen). A total of 15 µg of denatured RNA was separated by electrophoresis on 1.2% agarose gels and transferred to Hybond N+ (Amersham Pharmacia Biotech). Blots were prehybridized at 42 °C for 3 h in 50% formamide, 5X SSPE (1X = 150 mM NaCl, 10 mM NaH_2PO_4, 1 mM EDTA, pH 7.4), 10X Denhardt's solution, 2% SDS, and 100 µg /ml denatured herring sperm DNA, and then hybridized with a random primed ^{32}P-labeled cDNA probe for mouse *Mmp1a* (40090601, Geneservice) for 20 h under the same conditions. Blots were washed with 0.1X SSC, 0.1% SDS for 2 h at 50 °C and exposed to autoradiography. RNA integrity and equal loading was assessed by hybridization with a β-actin cDNA probe.

RT-PCR- Total RNA was reverse-transcribed using the Thermoscript RT-PCR system (Invitrogen). A PCR reaction was then performed with the following *Mmp1a*-specific primers: *Mmp1a*-Exon4, 5′-GGACCTAACTATAAGCTT GCTCACA-3′; *Mmp1a*-Exon7, 5′-CTGGAAGA TTTGGCCAGAGAATAC-3′. The PCR reaction was performed in a GeneAmp 9700 PCR system from Applied Biosystems for 35 cycles of denaturation (95 ºC, 30 s), annealing (60 ºC, 30 s), and extension (72 ºC, 1 min). As a control, *β*-actin was PCR amplified from all samples under the same conditions. Induction of cancer or other pathologies in mice was performed as indicated in the corresponding references: B16F10 and LLC lung cancer cell models (23), MCA-induced fibrosarcoma and DMBA-induced skin cancer (24), DEN-induced hepatocarcinoma (25), 4-NQO induced oral squamous carcinoma (26), CCl_4-induced hepatic fibrosis (27), for bleomycin-induced lung fibrosis (28), MMTV-PyMT breast cancer (29), and K14-HPV16 skin cancer (30).

Urethane carcinogenesis model-Mouse experimentation was done in accordance with the guidelines of the Universidad de Oviedo (Spain), regarding the care and use of laboratory animals. For urethane (ethylcarbamate; Sigma) chemical carcinogenesis, 12-week-old mice were injected intraperitoneally with two doses (separated by 48 h) of a freshly prepared solution of 1 mg of urethane/g body weight, dissolved in sterile 0.9% NaCl (saline). Mice were sacrificed 32 weeks after urethane exposure, and their lungs were either snap-frozen in liquid nitrogen for further RNA and protein analysis or fixed in 4% paraformaldehyde and processed for histological studies. After conventional staining with hematoxylin and eosin, cells were

morphologically identified by an expert pathologist with no previous knowledge of mice genotypes.

Immunohistochemistry-Lungs samples were fixed in 4% paraformaldehyde and embedded in paraffin. Deparaffined and rehydrated sections were rinsed in PBS (pH 7.5). Endogenous peroxidase activity and nonspecific binding were blocked with peroxidase block buffer (DakoCytomation) and 1% bovine serum albumin, respectively. Sections were incubated overnight at 4 ºC with a rabbit polyclonal antibody anti-mouse CD31 (Abcam), diluted 1:100. Then, sections were incubated with an anti-rabbit EnVision system labeled polymer-HRP (DakoCytomation) for 30 min, washed and visualized with diaminobenzidine. Sections were counterstained with Mayer's hematoxylin, dehydrated and mounted in Entellan®. Sections were examined using a Nikon Eclipse E400 microscope and images were acquired with a Nikon DS-Si1 camera and Nikon NIS-Elements F2.20 software.

Difference gel electrophoresis-Lungs from WT and KO mice were rinsed in TAM (10 mM Tris pH 8.5, 5 mM magnesium acetate) and homogenized in TUCT (2 M thiourea, 7 M urea, 4% CHAPS, 30 mM Tris pH 8.5). 50 µg of each sample were labeled with 400 pmol of a specific fluorophore (GE Healthcare): CyDye 3 (WT sample), CyDye 5 (KO sample) and CyDye 2 (pool of WT and KO sample 1:1). Labeled samples were combined and UCDA (8 M urea, 4% CHAPS, 130 mM DTT, 2% IEF buffer) was added in a 1:1 ratio. UCda (8 M urea, 4% CHAPS, 13 mM DTT, 1% IEF buffer) was used to reach 450 µL of final volume. Samples were loaded in a strip holder and 24 cm IPG strips, non linear pH gradient 3–11 (GE Healthcare), were placed over them. After strip rehydration, protein isoelectrofocusing was allowed to proceed for 26 h on an IPGphor Unit (GE Healthcare) in the dark at 18 ºC. Then, strips were equilibrated for 15 min in SES-DTT (6 M urea, 30% glycerol, 2% SDS, 75 mM Tris pH 6.8, 0.5% DTT and bromophenol blue) and 15 min in SES-IA (SES with 4.5% iodoacetamide), mounted on top of a 13% SDS–PAGE and electrophoresed at 80 V overnight in the dark at 18 ºC. After SDS–PAGE, cyanine dye-labeled proteins were visualized directly by scanning using a Typhoon^{TM} 9400 imager (GE Healthcare), and analyzed with Progenesis SameSpots software (Nonlinear dynamics) and stained with SYPRO Ruby (Molecular Probes).

Tryptic digestion and MALDI-ToF analysis-Differential spots were manually excised over a transilluminator. Gel pieces were washed twice with 25 mM ammonium bicarbonate/acetonitrile (70:30), dried for 15 min at 90 ºC, and incubated with 12 ng/µL trypsin (Promega) in 25 mM ammonium bicarbonate for 1 h at 60 ºC. Peptides were purified with ZipTip C18 (Millipore) and eluted with 1 µL of CHCA (α-cyano-4-hydroxycinnamic acid) to be placed onto MALDI-ToF´s plate. Once dried, they were analyzed by mass spectrometry on a time-of-flight mass spectrometer equipped with a nitrogen laser source (Voyager-DE STR, Applied Biosystems). Data from 200 laser shots were collected and analyzed with data explorer version 4.0.0.0 (Applied Biosystems).

Western blotting- Samples were electrophoresed and transferred to PVDF (0.45 µm pore size) membranes (Millipore). Blots were blocked with 5% non-fat dry milk in TBS-T buffer (20 mM Tris-HCl pH 7.4, 150 mM NaCl and 0.05% Tween-20), for 1 h at room temperature and incubated overnight at 4 ºC with 3% BSA in TBS-T with either 0.2 µg /mL anti-CHI3L3, 0.2 µg/ mL anti-S100A8 (R&D Systems) and 1:1000 anti RAGE (Cell Signaling). Finally, the blots were incubated for 1 h at room temperature in 2.5% non-fat dry milk in TBS-T buffer with 10 ng/mL of goat anti-rat horseradish peroxidase (GE Healthcare), rabbit anti-goat (Thermo Scientific), and donkey anti-rabbit (GE Healthcare), respectively. Then, blots were washed with TBS-T and developed with Immobilon Western chemiluminescent HRP substrate (Millipore). Chemiluminescent images were taken with a Fujifilm LAS3000 mini apparatus.

Enzymatic assays-For *in vitro* proteolysis assays, we used recombinant S100A8 and S100A9 kindly provided by Dr. Philippe Tessier, and recombinant CHI3L3 and MMP-1 from R&D Systems. Briefly, 100 ng of rMMP-1 per reaction was activated with 4-aminophenylmercuric acetate (APMA) at 37 ºC for 2 h. Then, purified CHI3L3, S100A8 and S100A9 (1 µg) were

incubated with activated MMP-1 at 37 ºC for 24 h, and analyzed by SDS-PAGE and Western-blot.

Analysis of cytokine levels-To evaluate the levels of different Th1/Th2 cytokines, we used a Mouse Th1/Th2/Th17/Th22 13plex FlowCytomix Multiplex kit and a TGF-β1 kit (eBioscience), following manufacturer instructions. Briefly, snap-frozen lungs were homogenized at 4 ºC in T-PER containing Complete Mini Protease Inhibitor Cocktail tablets (1 tablet/50 mL of T-PER stock reagent) and centrifuged at 9,000 x g for 15 min. Total protein concentration in supernatant was determined using BCA kit. A total of 100 µg of each homogenate was incubated with antibody-coated bead complexes and biotinylated secondary antibody for 2 h. After washing, 100 µL streptavidin-phycoerythrin was added to each well and incubated for 1 h. Samples were then transferred to appropriate cytometry tubes and analyzed using the FC500 Celular Cytomics analyzer (Beckman Coulter). A minimum of 300 events (beads) were collected for each cytokine/sample and median fluorescence intensities were obtained. Cytokine concentrations were calculated based on standard curve data using FlowCytomix Pro 3.0 Software (eBioscience). The results were expressed as mean ± SE (n = 5).

RESULTS

Generation and phenotype analysis of Mmp1a-deficient mice- To analyze the *in vivo* role in cancer of Mmp-1a, the murine counterpart of human MMP-1, we generated mutant mice deficient in *Mmp1a* by replacing exons 4, 5 and 6, encoding the catalytic domain, with a PGK-neomycin cassette (Fig. 1A). Following heterozygote intercrossing, *Mmp1a*-null, heterozygous and wild-type mice were obtained in the expected Mendelian ratios. We verified homozygosity with respect to the mutated allele by Southern-blot and the absence of functional transcripts by Northern-blot analysis of placenta, a positive control for expression of this gene (Fig. 1B,C). Despite the *Mmp1a* deficiency, these mutant mice developed normally, were fertile and their long-term survival rates were indistinguishable from those of their wild-type littermates. Furthermore, histopathological analysis of multiple tissues from *Mmp1a*$^{-/-}$ adult animals did not reveal any differences with wild-type tissues (data not shown). Taken together, these results demonstrate that Mmp-1a is absolutely dispensable for embryonic and adult mouse development as well as for normal growth and fertility.

Analysis of cancer susceptibility of Mmp1a-deficient mice- The dispensability of Mmp-1a for mouse development, growth and fertility opened the possibility to perform long-term studies aimed at analyzing cancer susceptibility in mice deficient in this metalloproteinase. For this purpose, and because previous results had suggested that the expression of mouse *Mmp1a* in normal and pathological conditions could be more restricted than that of human *MMP1* (22), we first performed an RT-PCR expression analysis of *Mmp1a* in samples from wild-type mice in which cancer and other pathologies had been induced. As can be seen in Fig. 2, *Mmp1a* expression was clearly detected in samples from lung carcinomas induced by chemical carcinogens or by Lewis cancer cells, in skin tumors induced by DMBA/TPA or MCA, in oral carcinomas induced by 4-nitroquinoline 1-oxide and in some acute pulmonary lesions induced by bleomycin-treatment. In contrast, no significant expression of this mouse metalloproteinase gene was detected in mammary tumors induced by MMTV-PyMT or in their metastasis (Fig. 2). According to these results, we focused our study on the analysis of the susceptibility of *Mmp1a*-mutant mice to lung cancer.

To this end, *Mmp1a*$^{-/-}$ mice and their wild-type littermates were subjected to a chemical carcinogenesis protocol with urethane and, after 8 months, mice were sacrificed and the number and histopathological characteristics of their pulmonary lesions were examined. As can be seen in Fig. 3, the number of lung tumors per mouse was higher in wild-type than in mutant mice, especially in the case of male mice, a gender difference which we had already observed in our previous studies with *Mmp8*-mutant mice (24). Therefore, we can conclude that the loss of Mmp-1a protects against lung cancer induced by chemical carcinogens such as urethane. To try to extend these observations, we next performed a histopathological analysis of tumors generated in both genetic backgrounds with the finding that the

size of tumors present in *Mmp1a*-mutant mice was smaller than that of wild-type mice (Fig. 4A). Likewise, we could observe the presence of many inflammatory infiltrate foci in the lungs of knock-out mice (Fig. 4B). Furthermore, tumors of *Mmp1a*$^{-/-}$ mice were less angiogenic as assessed by CD31 immunostaining (Fig. 4C). These characteristics are fully consistent with the idea that the absence of Mmp-1a hampers tumor progression.

Proteomic analysis of lung tissues from Mmp1a-deficient mice-As a first step to elucidate the molecular mechanisms underlying the above described tumor-promoting properties of Mmp-1a, we performed a proteomic analysis by difference gel electrophoresis (DiGE) of lung samples from urethane-treated mutant mice and the corresponding controls. After these DiGE experiments coupled to mass-spectrometry analysis, we could identify a series of differential proteins between tissues from normal and mutant mice (Supplementary Table 1). Specifically, we focused on chitinase-3 like protein 3 (CHI3L3) and the receptor for advanced glycation end-products (RAGE), which were upregulated in wild-type and knock-out mice, respectively (Fig. 5A and Supplementary Fig. 1A). To further validate these results, we performed bi-dimensional Western-blot analysis with antibodies specific against the differential proteins identified by DiGE in the urethane-treated mice lungs (Supplementary Fig.1B). These analyses, together with those performed with other urethane-treated littermates, corroborated that both CHI3L3 and RAGE protein levels were increased in lung samples from wild-type and *Mmp1a*$^{-/-}$ mice, respectively (Fig. 5B). Additionally, we observed that CHI3L3 was the target of a processing event in the urethane-treated lung samples from wild-type that was not present in the equivalent samples from *Mmp1a*$^{-/-}$ mice (Fig. 5B). By using mass spectrometry analysis, we identified these different forms of CHI3L3 as the complete protein or fragments thereof corresponding to the N-terminal and C-terminal region (Supplementary Fig. 1A).We next evaluated the possibility that levels of the S100A8 and S100A9 ligands of the RAGE receptor could also be altered in the lung samples from knock-out mice. To this purpose, we performed a bi-dimensional Western-blot analysis which demonstrated the accumulation of high levels of S100A8, as well as the occurrence of a differential processing event of this chemotactic protein in samples from *Mmp1a*$^{-/-}$ mice (Fig. 5C). By contrast, S100A9 levels did not exhibit any significant difference in mice from both genotypes (not shown). To investigate if any of these proteins could be a substrate for MMP-1, we performed an *in vitro* digestion with the recombinant protease and found that S100A8, but not S100A9 nor CHI3L3, is cleaved by this collagenolytic enzyme (Fig. 5D). Taken together, these results could indicate the occurrence of an imbalance in the inflammatory response induced in wild-type and *Mmp1a*$^{-/-}$ mice by chemical carcinogens.

Inflammatory response evaluation after urethane-lung carcinogenesis-Since the high levels of CHI3L3 in wild-type mice could be indicative of a Th2 pro-tumoral inflammatory response (31,32) and the increased levels of RAGE and its ligand S100A8 in mutant mice could point to the occurrence of a Th1 anti-tumoral response (32,33), we next evaluated the levels of Th1 and Th2 cytokines in lungs from wild-type and *Mmp1a*-knockout mice. To this aim, a total of 14 different mouse cytokines were simultaneously analysed by flow cytometry. As can be seen in Fig. 6A, levels of well-established Th1-associated cytokines such as IL-1α, IL-2, IL-27 and IFN-γ, are increased in lungs from *Mmp1a*$^{-/-}$ mice compared with their corresponding controls. Likewise, levels of IL-5, IL-10, IL-13 and TGF-β1, which are archetypal Th2-response cytokines, are higher in wild-type mice than in *Mmp1a*-deficient mice. Then, and because IL-17 has been described to be highly dependent on IFN-γ (34), we evaluated the levels of both cytokines at different time-points during the development of the urethane-induced lung cancer models, with the finding that IL-17 and IFN-γ showed a parallel increase in *Mmp1a*$^{-/-}$ mice in the course of the carcinogenesis experiment (Fig. 6B).

To further evaluate the putative Th1-polarized inflammatory response occurring in *Mmp1a*$^{-/-}$ mutant mice during urethane carcinogenesis, we analyzed levels of most significant cytokines found at increased levels in lung from *Mmp1a*-knockout mice. Thus, we measured IL-17, IL-27 and IFN-γ levels in the

lungs from two different groups of mutant mice based on the lung inflammatory phenotype presented by them. To this end, we compared mutant mice showing a high number of inflammatory infiltrate foci in the lungs with those animals that did not present any of these foci. Interestingly, the levels of these Th1-related cytokines displayed by the group with inflammatory infiltrate were higher than those found in the group in which that infiltrate was not observed (Fig. 6C). Taken together all these results, it seems that *Mmp1a*$^{-/-}$ mice develop a Th1 antitumoral response which in turn would contribute to explain the significantly low number of chemically-induced lung carcinomas observed in mice deficient in this metalloproteinase.

DISCUSSION

In this work, we have generated mutant mice deficient in *Mmp1a* and demonstrated that they represent a new and valuable *in vivo* model for the functional analysis of MMP-1 in cancer. Over the last years, evidence has accumulated that MMP-1 is associated with tumor progression and metastasis (16,17,19). However, and somewhat surprisingly, very limited information is available about the putative functions mediated by MMP-1 during cancer development and progression. This is especially puzzling if we consider that MMP-1 was the first human MMP cloned and characterized at the biochemical level, and its correlative links with tumor invasion and metastasis were first reported more than 20 years ago (11,35). One possibility to explain this lack of functional information about MMP-1 in cancer is the absence of an *in vivo* model of MMP-1 deficiency, an aspect which has been largely attributed to the wide assumption that no MMP-1 ortholog was present in rodents. However, our finding of two murine genes (*Mmp1a* and *Mmp1b*, also known as *McolA* and *McolB*) similar to human MMP-1 opened a series of further studies which allowed us to conclude that *Mmp1a* is a *bona fide* counterpart of human MMP-1 (22). This finding was the starting point of a long-term work which has now led us to the generation and analysis of mutant mice deficient in *Mmp1a*.

Similar to most cases of *Mmp*-deficiency (1), *Mmp1a*$^{-/-}$ mice are viable and fertile which has facilitated studies aimed at evaluating their cancer susceptibility. These studies first focused on lung carcinomas, because our previous *Mmp1a* expression analysis in tissues from mice subjected to several carcinogenesis protocols revealed high expression levels of this murine metalloproteinase in different samples of lung cancer. After application of a urethane-based protocol of lung cancer induction, we observed that *Mmp1a*$^{-/-}$ mice showed a lower incidence of lung carcinomas than their corresponding wild-type littermates. Interestingly, this difference was more marked in male than in female mutant mice, indicating the occurrence of a gender difference that has been previously reported in other models of *Mmp*-deficiency (24). Histopathological analysis showed that tumors generated in *Mmp1a*$^{-/-}$ mice are smaller and less angiogenic than those of wild-type mice, both characteristics being consistent with the idea that the absence of Mmp-1a hampers tumor progression. These *in vivo* findings agree perfectly with very recent *in vitro* data showing that silencing *Mmp1a* suppresses invasive growth of lung cancer cells in three-dimensional matrices, whereas ectopic expression of this murine metalloproteinase confers invasive properties to epithelial cells (36).

The pro-tumorigenic role of MMPs was originally ascribed to their ability to breakdown tissue barriers for metastatic spread. The fact that both human MMP-1 and mouse Mmp-1a are potent collagenases with ability to degrade different types of fibrillar collagens, would be consistent with a role for these metalloproteinases in promoting tumor progression (16,17,19). Nevertheless, the growing evidence that virtually all MMPs, including MMP-1, target many other proteins distinct from extracellular matrix components (37-39), prompted us to perform comparative proteomic studies between samples of *Mmp1a*-mutant and wild-type mice to try to identify putative *in vivo* substrates of Mmp-1a. Among the identified proteins, it is remarkable the finding of high levels of CHI3L3 and RAGE in lung samples from *Mmp1a*-wild type and mutant mice respectively, after treatment with urethane. Further studies demonstrated that the S100A8 ligand for the RAGE receptor is also elevated in samples from *Mmp1a*-mutant mice. Accordingly, this chemotactic protein could be a substrate directly targeted by Mmp1a, a proposal that we

further assessed by performing a series of enzymatic assays which demonstrated that the recombinant collagenase cleaves S100A8, but no other related proteins such as S100A9. The impaired degradation of this immunoregulatory protein in *Mmp1a*-deficient mice could also contribute to the generation of marked differences in the inflammatory response induced by chemical carcinogens in *Mmp1a* wild-type and mutant mice. Thus, the increased levels of CHI3L3 together with high levels of several Th2-related cytokines in wild-type mice strongly suggests that urethane is inducing the archetypical Th2-polarized inflammatory response which operates under protumoral stimuli (40). In contrast, the absence of increased levels of CHI3L3 in *Mmp1a*-mutant mice together with the presence of high levels of RAGE and its ligand S100A8, which are markers of Th1-polarized responses (32,33), as well as high levels of the well characterized Th1-response IFN-γ, together with some other antitumoral activity cytokines such IL-1α, IL-2, should be consistent with the possibility that the lack of this metalloproteinase hampers the development of the Th2-response triggered by carcinogen injection in *Mmp1a*$^{-/-}$ mice. In this sense, and according to the antiangiogenic effect of IL-27 (41), the notably difference between levels of mutant and control mice could explain the reduced angiogenic phenotype showed by *Mmp1a*$^{-/-}$ mice. Likewise, our data should be consistent with the possibility that IL-17 acts as a tumor-inhibiting cytokine in the lung carcinogenesis model used in this work.

MMPs have been associated with inflammatory responses in a wide variety of diseases (42). Likewise, several reports have described that cytokines released from different Th1/Th2 cell types can modulate MMP expression. Thus, it is well-established that Th2 responses are associated with an increased expression of matrix degradative MMPs, including human MMP-1 (43). Moreover, MMPs may also act as direct inducers of this process, modulating chemokine gradients or processing specific cytokines, and finally switching the balance between both types of responses. This is the case of MMP-2, which is overexpressed in multiple cancers and induces a Th2 polarization through the degradation of type I IFN receptor in dendritic cells (44). In addition, MMP-9 proteolytically activates TFG-β, which in turn promotes differentiation towards the Th2 pro-tumorigenic phenotype (45). Accordingly, lungs from *Mmp1a*-deficient mice exhibit lower levels of active TFG-β1 than controls suggesting that these mutant mice lack the capacity to proteolytically activate TFG-β1. Finally, the fact that human MMP-1 also cleaves the latent form of TGF-β and facilitates tumor invasion and angiogenesis (38) would agree very well with our proposal that its mouse ortholog Mmp-1a acts *in vivo* as a switching protease, which changes the Th1/Th2 balance towards a protumoral state.

In summary, the generation of the first mouse model of MMP-1 deficiency has contributed to the *in vivo* validation of this enzyme as a pro-tumorigenic protease with potential impact in different stages of tumor progression, including growth, angiogenesis and regulation of inflammatory responses. These studies have also validated the concept that human MMP-1 is a target protease, at least in some types of cancer, in which its expression is profoundly deregulated. Nevertheless, further studies aimed at inducing other tumor types in *Mmp1a*$^{-/-}$ mice will be necessary to define the precise *in vivo* role of this protease in different malignancies, since it could have dual roles in tumor development (46). Likewise, studies involving mice simultaneously deficient in *Mmp1a* and other pro-tumorigenic MMPs will be required to evaluate the functional redundancy and relative relevance of MMP-1 in different stages of cancer progression. Hopefully, these studies will contribute to the appropriate targeting of this proteolytic enzyme as part of novel and combined targets for the treatment of malignant tumors (47).

REFERENCES

1. Fanjul-Fernandez, M., Folgueras, A. R., Cabrera, S., and Lopez-Otin, C. (2010) Matrix metalloproteinases: evolution, gene regulation and functional analysis in mouse models *Biochim. Biophys. Acta* **1803**, 3-19
2. Kessenbrock, K., Plaks, V., and Werb, Z. (2010) Matrix metalloproteinases: regulators of the tumor microenvironment *Cell* **141**, 52-67
3. Coussens, L. M., Fingleton, B., and Matrisian, L. M. (2002) Matrix metalloproteinase inhibitors and cancer: trials and tribulations *Science* **295**, 2387-2392
4. Overall, C. M., and Lopez-Otin, C. (2002) Strategies for MMP inhibition in cancer: innovations for the post-trial era *Nat. Rev. Cancer* **2**, 657-672
5. Egeblad, M., and Werb, Z. (2002) New functions for the matrix metalloproteinases in cancer progression *Nat. Rev. Cancer* **2**, 161-174
6. Lopez-Otin, C., and Matrisian, L. M. (2007) Emerging roles of proteases in tumour suppression *Nat. Rev. Cancer* **7**, 800-808
7. McCawley, L. J., Crawford, H. C., King, L. E., Jr., Mudgett, J., and Matrisian, L. M. (2004) A protective role for matrix metalloproteinase-3 in squamous cell carcinoma *Cancer Res.* **64**, 6965-6972
8. Garg, P., Sarma, D., Jeppsson, S., Patel, N. R., Gewirtz, A. T., Merlin, D., and Sitaraman, S. V. (2010) Matrix metalloproteinase-9 functions as a tumor suppressor in colitis-associated cancer *Cancer Res.* **70**, 792-801
9. Jost, M., Folgueras, A. R., Frerart, F., Pendas, A. M., Blacher, S., Houard, X., Berndt, S., Munaut, C., Cataldo, D., Alvarez, J., Melen-Lamalle, L., Foidart, J. M., Lopez-Otin, C., and Noel, A. (2006) Earlier onset of tumoral angiogenesis in matrix metalloproteinase-19-deficient mice *Cancer Res.* **66**, 5234-5241
10. Lopez-Otin, C., Palavalli, L. H., and Samuels, Y. (2009) Protective roles of matrix metalloproteinases: from mouse models to human cancer *Cell Cycle* **8**, 3657-3662
11. Goldberg, G. I., Wilhelm, S. M., Kronberger, A., Bauer, E. A., Grant, G. A., and Eisen, A. Z. (1986) Human fibroblast collagenase. Complete primary structure and homology to an oncogene transformation-induced rat protein *J. Biol. Chem.* **261**, 6600-6605
12. Ala-aho, R., and Kahari, V. M. (2005) Collagenases in cancer *Biochimie* **87**, 273-286
13. Murray, G. I., Duncan, M. E., O'Neil, P., Melvin, W. T., and Fothergill, J. E. (1996) Matrix metalloproteinase-1 is associated with poor prognosis in colorectal cancer *Nat. Med.* **2**, 461-462
14. Poola, I., DeWitty, R. L., Marshalleck, J. J., Bhatnagar, R., Abraham, J., and Leffall, L. D. (2005) Identification of MMP-1 as a putative breast cancer predictive marker by global gene expression analysis *Nat. Med.* **11**, 481-483
15. Sauter, W., Rosenberger, A., Beckmann, L., Kropp, S., Mittelstrass, K., Timofeeva, M., Wolke, G., Steinwachs, A., Scheiner, D., Meese, E., Sybrecht, G., Kronenberg, F., Dienemann, H., Chang-Claude, J., Illig, T., Wichmann, H. E., Bickeboller, H., and Risch, A. (2008) Matrix metalloproteinase 1 (MMP1) is associated with early-onset lung cancer *Cancer Epidemiol. Biomarkers Prev.* **17**, 1127-1135
16. Gupta, G. P., Nguyen, D. X., Chiang, A. C., Bos, P. D., Kim, J. Y., Nadal, C., Gomis, R. R., Manova-Todorova, K., and Massague, J. (2007) Mediators of vascular remodelling co-opted for sequential steps in lung metastasis *Nature* **446**, 765-770

17. Lu, X., Wang, Q., Hu, G., Van Poznak, C., Fleisher, M., Reiss, M., Massague, J., and Kang, Y. (2009) ADAMTS1 and MMP1 proteolytically engage EGF-like ligands in an osteolytic signaling cascade for bone metastasis *Genes Dev.* **23**, 1882-1894
18. Boire, A., Covic, L., Agarwal, A., Jacques, S., Sherifi, S., and Kuliopulos, A. (2005) PAR1 is a matrix metalloprotease-1 receptor that promotes invasion and tumorigenesis of breast cancer cells *Cell* **120**, 303-313
19. Blackburn, J. S., Rhodes, C. H., Coon, C. I., and Brinckerhoff, C. E. (2007) RNA interference inhibition of matrix metalloproteinase-1 prevents melanoma metastasis by reducing tumor collagenase activity and angiogenesis *Cancer Res.* **67**, 10849-10858
20. Wyatt, C. A., Geoghegan, J. C., and Brinckerhoff, C. E. (2005) Short hairpin RNA-mediated inhibition of matrix metalloproteinase-1 in MDA-231 cells: effects on matrix destruction and tumor growth *Cancer Res.* **65**, 11101-11108
21. Pulukuri, S. M., and Rao, J. S. (2008) Matrix metalloproteinase-1 promotes prostate tumor growth and metastasis *Int. J. Oncol.* **32**, 757-765
22. Balbin, M., Fueyo, A., Knauper, V., Lopez, J. M., Alvarez, J., Sanchez, L. M., Quesada, V., Bordallo, J., Murphy, G., and Lopez-Otin, C. (2001) Identification and enzymatic characterization of two diverging murine counterparts of human interstitial collagenase (MMP-1) expressed at sites of embryo implantation *J. Biol. Chem.* **276**, 10253-10262
23. Gutierrez-Fernandez, A., Fueyo, A., Folgueras, A. R., Garabaya, C., Pennington, C. J., Pilgrim, S., Edwards, D. R., Holliday, D. L., Jones, J. L., Span, P. N., Sweep, F. C., Puente, X. S., and Lopez-Otin, C. (2008) Matrix metalloproteinase-8 functions as a metastasis suppressor through modulation of tumor cell adhesion and invasion *Cancer Res.* **68**, 2755-2763
24. Balbin, M., Fueyo, A., Tester, A. M., Pendas, A. M., Pitiot, A. S., Astudillo, A., Overall, C. M., Shapiro, S. D., and Lopez-Otin, C. (2003) Loss of collagenase-2 confers increased skin tumor susceptibility to male mice *Nat. Genet.* **35**, 252-257
25. Im, Y. H., Kim, H. T., Kim, I. Y., Factor, V. M., Hahm, K. B., Anzano, M., Jang, J. J., Flanders, K., Haines, D. C., Thorgeirsson, S. S., Sizeland, A., and Kim, S. J. (2001) Heterozygous mice for the transforming growth factor-beta type II receptor gene have increased susceptibility to hepatocellular carcinogenesis *Cancer Res.* **61**, 6665-6668
26. Korpi, J. T., Kervinen, V., Maklin, H., Vaananen, A., Lahtinen, M., Laara, E., Ristimaki, A., Thomas, G., Ylipalosaari, M., Astrom, P., Lopez-Otin, C., Sorsa, T., Kantola, S., Pirila, E., and Salo, T. (2008) Collagenase-2 (matrix metalloproteinase-8) plays a protective role in tongue cancer *Br. J. Cancer* **98**, 766-775
27. Nabeshima, Y., Tazuma, S., Kanno, K., Hyogo, H., Iwai, M., Horiuchi, M., and Chayama, K. (2006) Anti-fibrogenic function of angiotensin II type 2 receptor in CCl4-induced liver fibrosis *Biochem. Biophys. Res. Commun.* **346**, 658-664
28. Garcia-Prieto, E., Gonzalez-Lopez, A., Cabrera, S., Astudillo, A., Gutierrez-Fernandez, A., Fanjul-Fernandez, M., Batalla-Solis, E., Puente, X. S., Fueyo, A., Lopez-Otin, C., and Albaiceta, G. M. (2010) Resistance to bleomycin-induced lung fibrosis in MMP-8 deficient mice is mediated by interleukin-10 *PLoS ONE* **5**, e13242
29. Nielsen, B. S., Egeblad, M., Rank, F., Askautrud, H. A., Pennington, C. J., Pedersen, T. X., Christensen, I. J., Edwards, D. R., Werb, Z., and Lund, L. R. (2008) Matrix metalloproteinase 13 is induced in fibroblasts in polyomavirus middle T antigen-driven mammary carcinoma without influencing tumor progression *PLoS ONE* **3**, e2959

30. Masset, A., Maillard, C., Sounni, N. E., Jacobs, N., Bruyere, F., Delvenne, P., Tacke, M., Reinheckel, T., Foidart, J. M., Coussens, L. M., and Noel, A. (2011) Unimpeded skin carcinogenesis in K14-HPV16 transgenic mice deficient for plasminogen activator inhibitor *Int. J. Cancer* **128**, 283-293
31. Cai, Y., Kumar, R. K., Zhou, J., Foster, P. S., and Webb, D. C. (2009) Ym1/2 promotes Th2 cytokine expression by inhibiting 12/15(S)-lipoxygenase: identification of a novel pathway for regulating allergic inflammation *J. Immunol.* **182**, 5393-5399
32. Sandler, N. G., Mentink-Kane, M. M., Cheever, A. W., and Wynn, T. A. (2003) Global gene expression profiles during acute pathogen-induced pulmonary inflammation reveal divergent roles for Th1 and Th2 responses in tissue repair *J. Immunol.* **171**, 3655-3667
33. Chen, Y., Akirav, E. M., Chen, W., Henegariu, O., Moser, B., Desai, D., Shen, J. M., Webster, J. C., Andrews, R. C., Mjalli, A. M., Rothlein, R., Schmidt, A. M., Clynes, R., and Herold, K. C. (2008) RAGE ligation affects T cell activation and controls T cell differentiation *J. Immunol.* **181**, 4272-4278
34. Marshall, N. A., Galvin, K. C., Corcoran, A. M., Boon, L., Higgs, R., and Mills, K. H. (2012) Immunotherapy with PI3K inhibitor and Toll-like receptor agonist induces IFN-gamma+IL-17+ polyfunctional T cells that mediate rejection of murine tumors *Cancer Res.* **72**, 581-591
35. Liotta, L. (1990) The role of cellular proteases and their inhibitors in invasion and metastasis. Introductionary overview *Cancer Metastasis Rev.* **9**, 285-287
36. Foley, C. J., Luo, C., O'Callaghan, K., Hinds, P. W., Covic, L., and Kuliopulos, A. (2012) Matrix metalloprotease-1a promotes tumorigenesis and metastasis *J. Biol. Chem.* **287**, 24330-24338
37. Trivedi, V., Boire, A., Tchernychev, B., Kaneider, N. C., Leger, A. J., O'Callaghan, K., Covic, L., and Kuliopulos, A. (2009) Platelet matrix metalloprotease-1 mediates thrombogenesis by activating PAR1 at a cryptic ligand site *Cell* **137**, 332-343
38. Iida, J., and McCarthy, J. B. (2007) Expression of collagenase-1 (MMP-1) promotes melanoma growth through the generation of active transforming growth factor-beta *Melanoma Res.* **17**, 205-213
39. Agarwal, A., Tressel, S. L., Kaimal, R., Balla, M., Lam, F. H., Covic, L., and Kuliopulos, A. (2010) Identification of a metalloprotease-chemokine signaling system in the ovarian cancer microenvironment: implications for antiangiogenic therapy *Cancer Res.* **70**, 5880-5890
40. Wang, H. W., and Joyce, J. A. (2010) Alternative activation of tumor-associated macrophages by IL-4: priming for protumoral functions *Cell Cycle* **9**, 4824-4835
41. Shimizu, M., Shimamura, M., Owaki, T., Asakawa, M., Fujita, K., Kudo, M., Iwakura, Y., Takeda, Y., Luster, A. D., Mizuguchi, J., and Yoshimoto, T. (2006) Antiangiogenic and antitumor activities of IL-27 *J. Immunol.* **176**, 7317-7324
42. Van Lint, P., and Libert, C. (2007) Chemokine and cytokine processing by matrix metalloproteinases and its effect on leukocyte migration and inflammation *J. Leukoc. Biol.* **82**, 1375-1381
43. Chizzolini, C., Rezzonico, R., De Luca, C., Burger, D., and Dayer, J. M. (2000) Th2 cell membrane factors in association with IL-4 enhance matrix metalloproteinase-1 (MMP-1) while decreasing MMP-9 production by granulocyte-macrophage colony-stimulating factor-differentiated human monocytes *J. Immunol.* **164**, 5952-5960
44. Godefroy, E., Manches, O., Dreno, B., Hochman, T., Rolnitzky, L., Labarriere, N., Guilloux, Y., Goldberg, J., Jotereau, F., and Bhardwaj, N. (2011) Matrix metalloproteinase-

2 conditions human dendritic cells to prime inflammatory T(H)2 cells via an IL-12- and OX40L-dependent pathway *Cancer Cell* **19**, 333-346

45. Yu, Q., and Stamenkovic, I. (2000) Cell surface-localized matrix metalloproteinase-9 proteolytically activates TGF-beta and promotes tumor invasion and angiogenesis *Genes Dev.* **14**, 163-176
46. Jawad, M. U., Garamszegi, N., Garamszegi, S. P., Correa-Medina, M., Diez, J. A., Wen, R., and Scully, S. P. (2010) Matrix metalloproteinase 1: role in sarcoma biology *PLoS ONE* **5**, e14250
47. Lopez-Otin, C., and Hunter, T. (2010) The regulatory crosstalk between kinases and proteases in cancer *Nat. Rev. Cancer* **10**, 278-292

Acknowledgments: We thank A. Moncada-Pazos for helpful comments, M. S. Pitiot for histopathological studies, M. Etzlstorfer and E. Colado for FACS analysis, and D. Puente for excellent technical assistance.

Grant support: This work was supported by grants from Ministerio de Economía y Competitividad-Spain and Fundación M. Botín. The Instituto Universitario de Oncología is supported by Obra Social Cajastur-Asturias, Spain.

Conflict of interest-All authors certify that there is no conflict of interest with any financial organization regarding the material discussed in the manuscript.

FIGURES

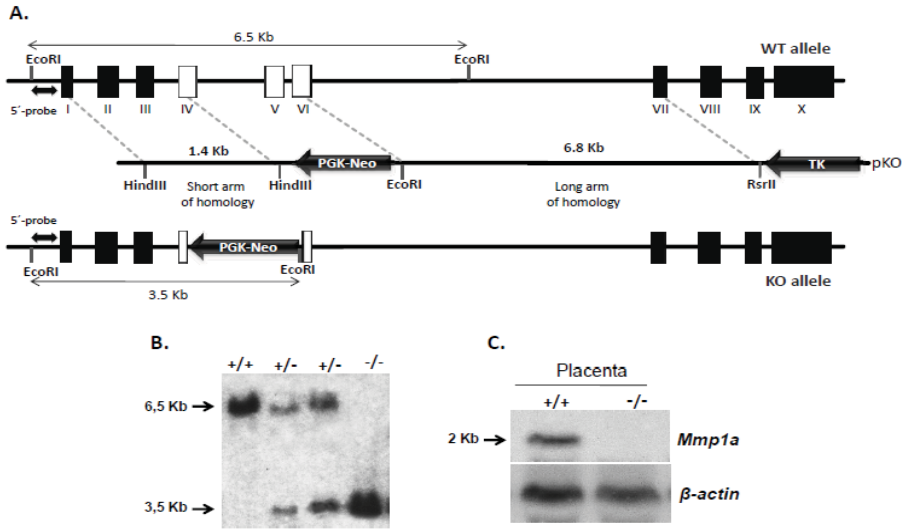

Figure 1. Targeted disruption of mouse *Mmp1a* gene. (A) Restriction maps of the *Mmp1a* gene region of interest (top), the targeting construct (center), and the mutant locus after homologous recombination (bottom). (B) *Eco*RI Southern-blot analysis of *Mmp1a*$^{+/+}$, *Mmp1a*$^{+/-}$ and *Mmp1a*$^{-/-}$ mice. (C) Detection of *Mmp1a* mRNA in placenta by Northern-blot analysis.

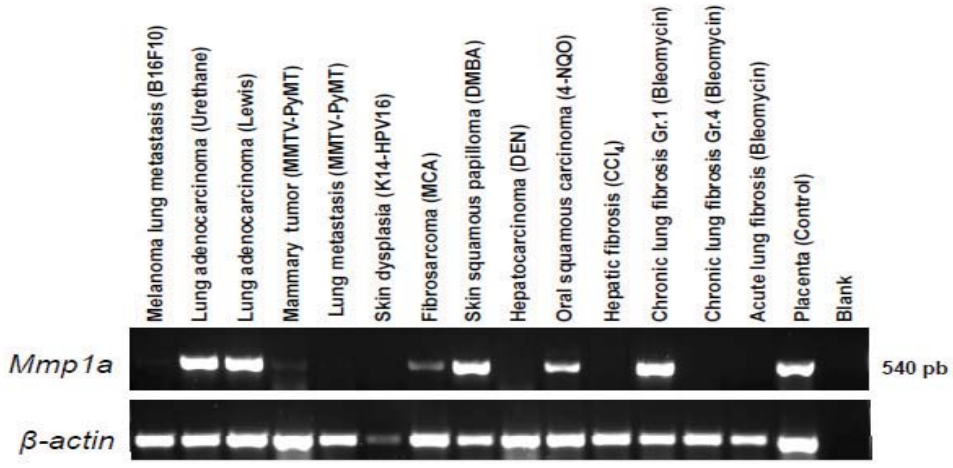

Figure 2. *Mmp1a* mRNA expression levels in tissues from wild-type mice subjected to different experimental protocols. MMTV-PyMT, mouse mammary tumor virus-polyoma middle T antigen; *K14*-HPV16, keratin 14-human papillomavirus type 16; MCA, 3-methyl-cholanthrene; DMBA, 9,10-dimethyl-1,2-benzanthracene. DEN, N,N-diethylnitrosamine; 4-NQO, 4-Nitroquinoline 1-oxide; CCl_4, carbon tetrachloride.

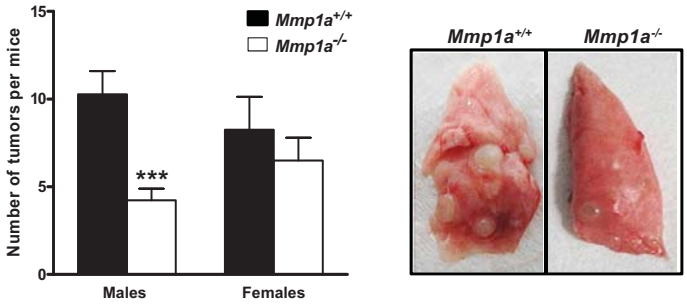

Figure 3. Susceptibility of *Mmp1a*-knockout mouse to urethane-induced lung tumorigenesis. (A) Number of total lung tumors per mouse after 8 months of urethane intraperitoneal treatment. (B) Representative images of lungs from mutant and control mice (n= 15 per group; ***, P < 0.001 by Student´s *t*-test).

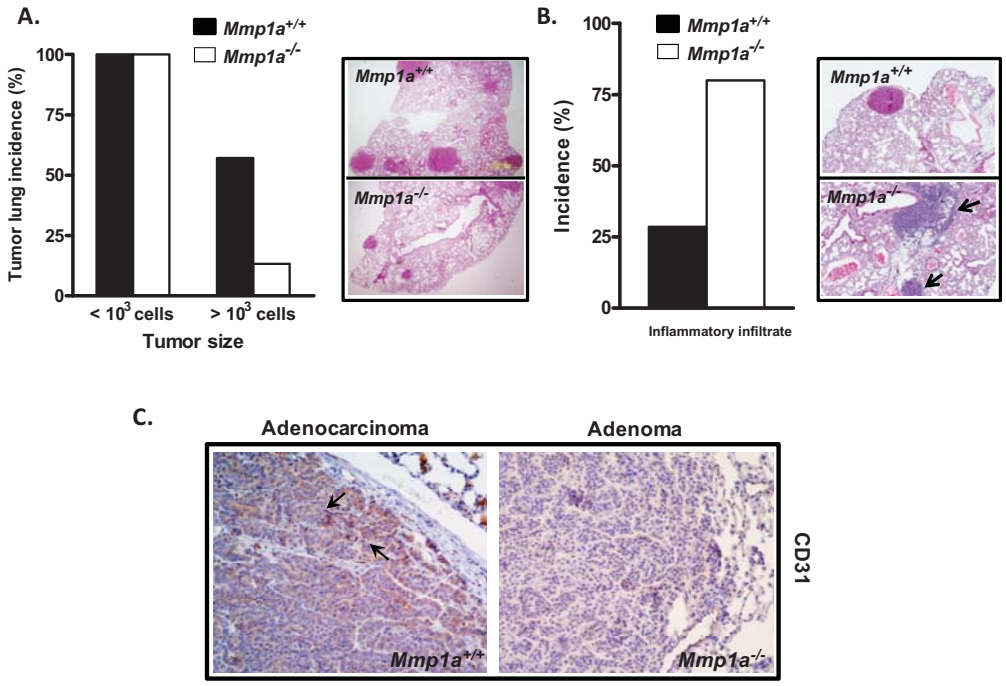

Figure 4. Phenotypic features of wild-type and knock-out urethane-induced tumors. (A) Graphic representation of size tumor incidence in males. Knock-out mice show a lower incidence of tumors with more than 10^3 cells. (B) Inflammatory infiltrate incidence in both sexes. We represent the number of mice which present inflammatory infiltrate foci in their lungs, showing an increased presence of inflammatory foci in lungs from knock-out mice. (C) Representative CD31 immunohistochemistry analysis of the tumor type most frequently found in mouse lung lesions. Adenocarcinomas with higher endothelial infiltrate were found in greater proportion in wild-type than in mutant mice.
.

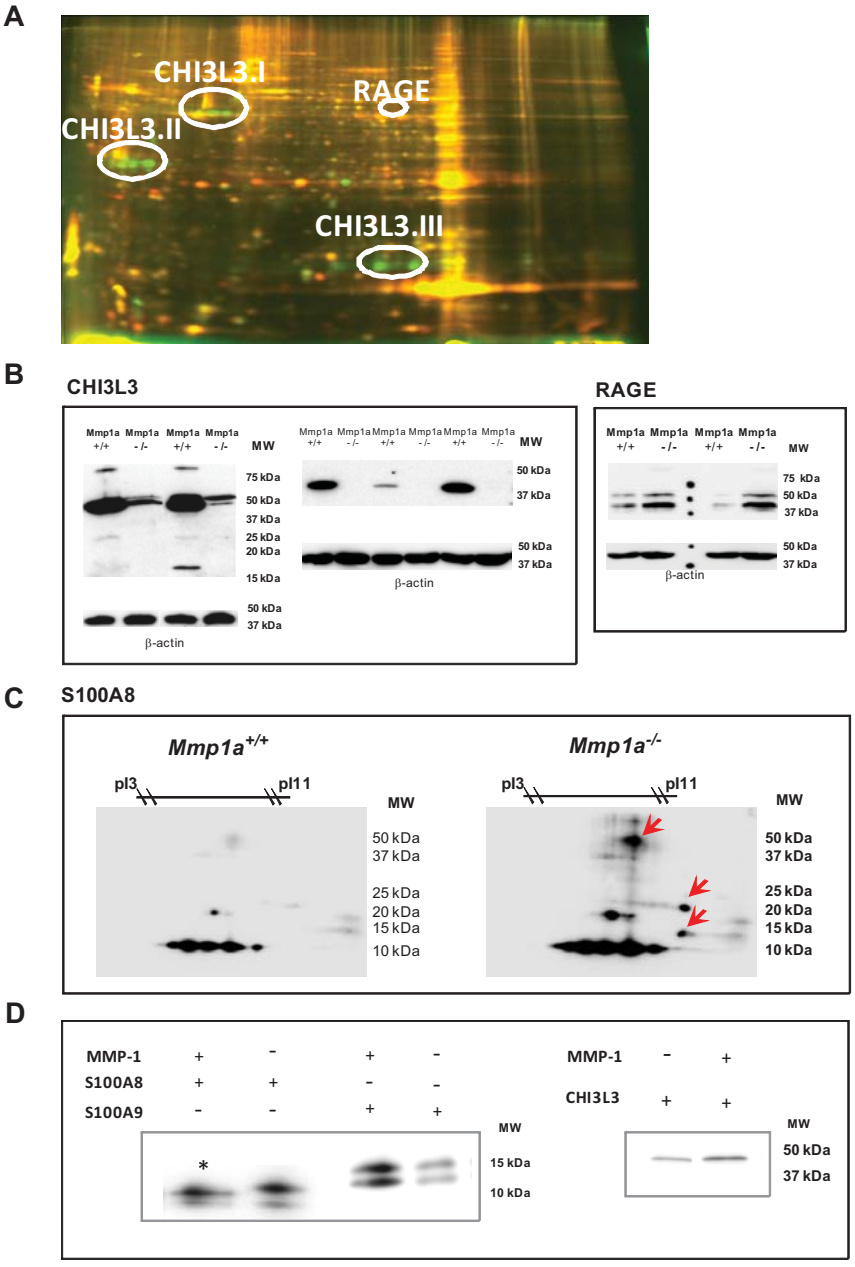

Figure 5. (A) DiGE analysis of lung tissue from urethane-treated mice. Overlaying green and red image highlights differences between wild-type and *Mmp1a*$^{-/-}$ mice. Yellow indicates no change, red spots, more abundant in knock-out mice, and green spots more abundant in wild-type mice. Selected proteins are labeled with white circles and bi-dimensional validation analysis is shown in Supplementary Fig.1. All differential analyzed spots are listed in Supplementary Table 1. (B) Western-blot analysis extended to other urethane-treated littermates showing the increased

CHI3L3 and RAGE levels in wild-type and knock-out mice, respectively, as well as the differential processing of CHI3L3 in wild-type lungs no present in the mutant lungs. Load control is shown at the bottom of each panel. (C) Western-blot analysis of the RAGE ligand S100A8 showing accumulation of different isoforms of this chemokine in lung from knock-out mice. (D) In vitro cleavage assays with human MMP-1. Purified S100A8, S100A9 and CHI3L3 (1 μg) were incubated with 100 ng of activated MMP-1, which resulted in specific cleavage of S100A8 (*), but not S100A9 and CHI3L3.

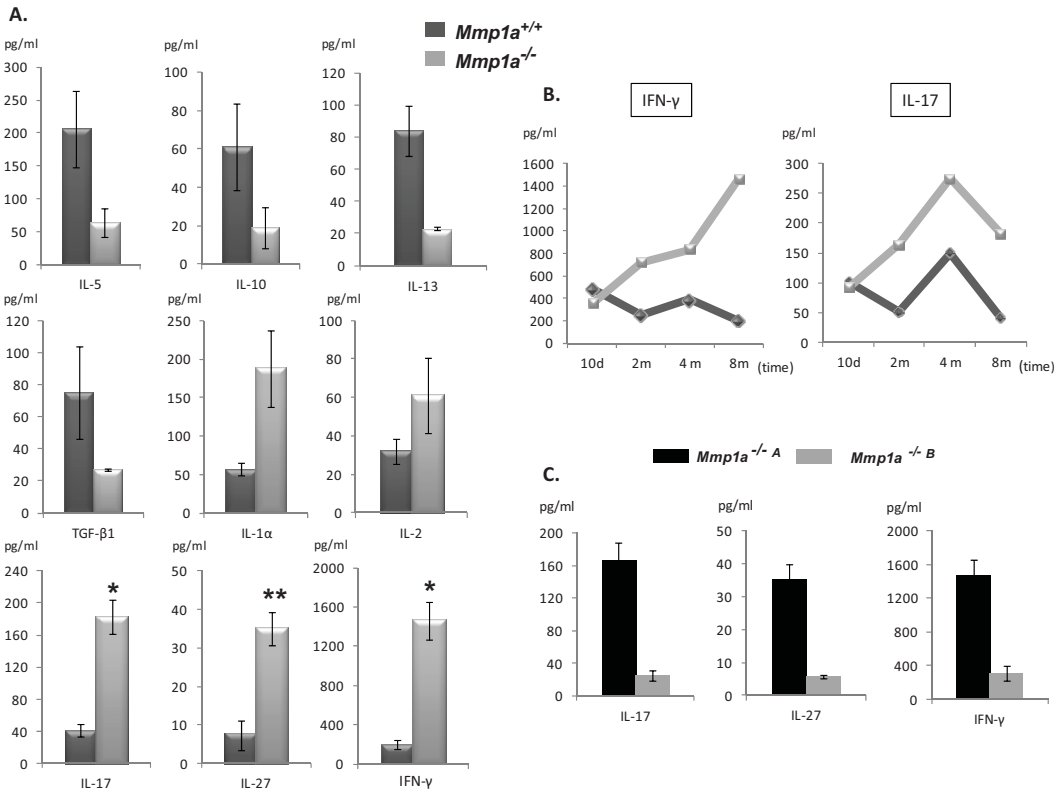

Figure 6. Analysis of cytokine levels in lung from *Mmp1a* wild-type and *knockout* mice treated with urethane. (A) Cytokine levels measured in lung mice after 8 months of urethane intraperitoneal treatment. (B) Measurement of IFN-γ and IL-17 in the lungs of mutant and control mice at several time points along the urethane carcinogenesis model. (C) Levels of Th1 cytokines in lungs from two different groups of *Mmp1a*-deficient mice separated on the basis of their inflammatory phenotype. *Mmp1a* $^{-/-}$ group A (*Mmp1a* $^{-/- A)}$ represents those mutant mice showing a notably high number of inflammatory infiltrate foci in the lungs while *Mmp1a* $^{-/-}$ group B (*Mmp1a* $^{-/- B)}$ represents those mutant mice with no overt infiltrate foci in their lungs. IL-, interleukin; IFN-, interferon, TGF-, transforming growth factor. (*, $P < 0.001$; **, $P < 0.001$ by Student´s *t*-test).

SUPPLEMENTARY DATA

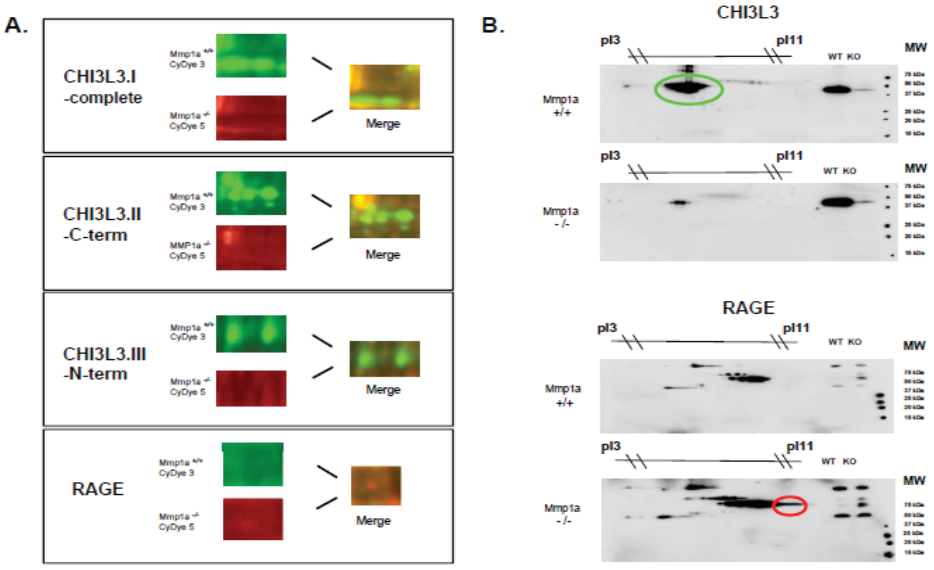

Supplementary Figure 1.Validation of selected proteomic alterations. (A) DiGE selected CHI3L3 and RAGE spot proteins of lung tissues from urethane-treated wild-type (green) and knock-out (red) mice. (B) Bi-dimensional Western-blot analysis with anti-CHI3L3 and anti-RAGE specific antibodies of the lung urethane-treated mice confirming the increased protein levels of these proteins in the lungs of *Mmp1a*$^{+/+}$ (green) and *Mmp1a*$^{-/-}$ (red) mice, respectively.

SupplementaryTable 1. Differential proteins in urethane-treated lungs of *Mmp1a*$^{+/+}$ (green) *and Mmp1a*$^{-/-}$ (red) mice, identified by DiGE analysis.

Name	SwissProt name	kDa	pI	Hits	% sequence coverage	Slope (ppm)
Actin, cytoplasmic 1	ACTB_MOUSE	41.696	5.29	10	33	7
Actin, cytoplasmic 1	ACTB_MOUSE	41.696	5.29	7	26	19
Actin, cytoplasmic 2	ACTG_MOUSE	41.962	5.3	4	14	-29
Advanced glycosylation end product-specific product	RAGE_MOUSE	41.768	6.4	6	28	-20
Alpha-2-macroglobulin 35 kDa subunit	A2M_MOUSE	28.226	7.08	10	40	-6
Carbonyl reductase [NADPH]2	CBR2_MOUSE	25.958	9.09	6	15	22
Chitinase-3 like protein 3 (101-384)	CH3L3_MOUSE	42.322	5.33	5	15	26
Chitinase-3 like protein 3 (117-384)	CH3L3_MOUSE	42.322	5.33	5	13	10
Chitinase-3 like protein 3 (165-384)	CH3L3_MOUSE	42.322	5.33	7	26	-6
Chitinase-3 like protein 3 (178-384)	CH3L3_MOUSE	42.322	5.33	6	22	-2
Chitinase-3 like protein 3 (76-160)	CH3L3_MOUSE	42.322	5.33	6	18	26
Chitinase-3 like protein 3 (76-160)	CH3L3_MOUSE	42.322	5.33	4	11	-13
Chitinase-3 like protein 3 (92-278)	CH3L3_MOUSE	42.322	5.33	5	16	-20
Complement C1q tumor necrosis factor-related protein 4	C1QT4_MOUSE	33.387	9.18	5	22	43
Cytochrome c oxidase subunit 5B, mitochondrial	COX5B_MOUSE	10.718	5.74	5	58	-2
Dihydropyrimidase-related protein 2	DPYL2_MOUSE	62.278	5.95	19	41	23
Fatty acid-binding protein,epidermal	FABP5_MOUSE	15.006	6.19	4	27	32
Glutathione S-transferase A3	GSTA3_MOUSE	25.229	8.77	4	15	0
Heat shock protein beta-1	HSPB1_MOUSE	23.014	6.11	5	30	-30
Hemoglobin subunit beta-1	HBB1_MOUSE	15.709	7.26	8	66	26
Kelch-like protein 9	KLHL9_MOUSE	69.400	6.00	5	7	-27
L-lactate dehydrogenase B chain	LDHB_MOUSE	36.441	5.7	8	25	29
Macrophage-capping protein	CAPG_MOUSE	39.241	6.73	6	18	13
Myosin light chain 4	MYL4_MOUSE	21.028	4.96	6	33	-6
Myosin regulatory light chain 2, atrial isoform	MLRA_MOUSE	19.450	4.75	8	50	-9
Nuclease-sensitive element-binding protein-1	YBOX_MOUSE	35.599	9.88	4	11	16
Peroxiredoxin 1	PRDX1_MOUSE	22.177	8.26	7	33	2
Peroxiredoxin 6	PRDX6_MOUSE	24.740	5.71	11	51	10
Peroxiredoxin 6	PRDX6_MOUSE	24.740	5.71	5	25	29
Peroxiredoxin 6	PRDX6_MOUSE	24.740	5.71	8	38	-13
Phosphoglycerate mutase-1	PGAM1_MOUSE	28.701	6.75	2	11	16
Protein disulfide-isomerase A3	PDIA3_MOUSE	54.268	5.69	16	36	16
S100-A6	S10A6_MOUSE	10.051	5.30	2	17	15
Serpin A12	SPA12_MOUSE	45.490	9.14	6	14	26
Thimet oligopeptidase	THOP1_MOUSE	77.895	5.71	3	4	16
Tropomyosin alpha-3 chain	TPM3_MOUSE	32.863	4.67	14	32	-26

IV. Molecular analysis of cancer susceptibility in *Mmp1a*$^{-/-}$ mice

MMP-1 expression has been associated with a poor prognosis in a variety of human tumors. Nevertheless, the cellular source of MMP-1, either stromal or tumor cells, seems to be an important predictor factor for the outcome of the disease. Thus, MMP-1 expression in stromal cells has been associated with increased risk of metastasis in breast cancer. In addition, MMP-1 undergoes different processing depending on the cell origin. Based on these premises, we decided to evaluate the contribution of Mmp-1a to tumor progression according to the cell source. To this aim, we employed an orthotopic-lung cancer model to analyze the oncogenic relevance of tumor cells expressing *Mmp1a* in a genetic background proficient or deficient in Mmp-1a.

Article 3: Caitlin J. Foley, **Miriam Fanjul-Fernández**, Andrew Bohm, Anika Agarwal, Karyn Austin, Georgios Koukos, Lidija Covic, Carlos López-Otín, and Athan Kuliopulos. "Matrix metalloprotease 1a-deficiency suppresses tumor growth and angiogenesis"

Oncogene (2012, under revision).

Personal contribution to this work

In this work, I was responsible for the management and genotyping of the mice colony used for the experimental work aimed at evaluating the functional relevance of Mmp-1a in cancer. Likewise, I contributed to the discussion of the experiments performed in Dr. Athan Kuliopulos laboratory and participated in the writing of the manuscript.

Matrix Metalloprotease 1a-Deficiency Suppresses Tumor Growth and Angiogenesis

Caitlin J. Foley[a,b], Miriam Fanjul-Fernández[c], Andrew Bohm[d], Anika Agarwal[a,e], George Koukos[a,e], Lidija Covic[a,d,e], Carlos López-Otín[c], and Athan Kuliopulos[a,b,d,e]

From the [a]Molecular Oncology Research Institute, Tufts Medical Center, and Departments of [b]Genetics, [d]Biochemistry and [e]Medicine, Tufts University School of Medicine, Boston, MA 02111, USA, and [c]Departamento de Bioquímica y Biología Molecular, Facultad de Medicina, Instituto Universitario de Oncología, Universidad de Oviedo, 33006 Oviedo, Spain.

Running Title: Deficiency of Mmp1a suppresses lung tumorigenesis

Correspondence: Athan Kuliopulos, Molecular Oncology Research Institute, Tufts Medical Center, Box 7510, 750 Washington St, Boston, MA 02111
E-mail: athan.kuliopulos@tufts.edu

ABSTRACT

Matrix metalloprotease-1 (MMP1) is an important mediator of tumorigenesis and metastasis through its ability to degrade critical matrix components including fibrillar collagen, and cleave bioactive proteins such as the oncogenic receptor, protease-activated receptor-1 (PAR1). MMP1 is secreted as a proenzyme and is regulated in the extracellular milieu by enzyme activation and stability. Although MMP1 has been identified as a key pathogenic factor in multiple human diseases, the study of MMP1 in disease models has been greatly hindered because little is known regarding the function of its rodent homologue, Mmp1a. Here, we describe the role of stromal-produced Mmp1a in the growth of lung tumors using mice deficient in *Mmp1a*. Stromal *Mmp1a*-deficiency resulted in significantly decreased growth and angiogenesis of Lewis lung carcinoma (LLC1) allograft tumors. Co-implantation of LLC1 lung cancer cells with wild-type Mmp1a$^{+/+}$ fibroblasts restored tumor growth in *Mmp1a*-deficient animals. Silencing of PAR1 expression in the LLC1 carcinoma cells phenocopied

stromal *Mmp1a*-deficiency, demonstrating the importance of PAR1 as an Mmp1a target in promoting tumorigenesis. Exchange of the mouse Mmp1a prodomain with that of human MMP1 or introduction of a human point mutation predicted to stabilize interactions between the Mmp1a pro- and catalytic domains, significantly increased Mmp1a secretion and decreased auto-cleavage. Together, these data demonstrate that stromal Mmp1a promotes *in vivo* tumorigenesis and that production of Mmp1a/MMP1 is controlled by the stability of prodomain-catalytic domain interactions.

INTRODUCTION

MMP1 is a zinc-dependent endopeptidase that is frequently overexpressed in a large number of human cancers (1-3). High MMP1 levels in patient tumor samples has been associated with metastasis and decreased progression-free survival in melanoma, colorectal and esophageal cancers (4-6). Fibroblast MMP1 was originally defined as an interstitial collagenase due to its ability to cleave fibrillar collagens (7), but more recent studies found it also cleaves a variety of other substrates (8), including the oncogenic receptor, protease-activated receptor-1 (PAR1) (9-11). MMP1 is produced by many sources in tumors, including cancer cells, fibroblasts, inflammatory cells, and the endothelium, and because it is a secreted enzyme, can have both paracrine and autocrine effects in the microenvironment (10, 12-16). In a clinical study of patients with lung cancer, 35% of tumors had MMP1 expressed on the carcinoma cells, whereas 70% had MMP1 overexpressed in the stromal cells (17). MMP1 expression in stromal cells has also been associated with increased risk of metastasis in breast cancer patients, highlighting the importance of tumor versus stromal MMP1 production (18). Fibroblast-derived and cancer cell-derived MMP1 have been shown to be differentially processed, suggesting that there may be functional differences in MMP1 depending on the source (19).

In order to effectively study the role of MMP1 in cancer and other diseases, it is important to develop a relevant rodent model. The rodent genome contains an *MMP1* gene duplication, resulting in the *Mmp1a* and *Mmp1b* genes which are 82% identical (20). Mmp1a is the most likely MMP1 homologue because unlike Mmp1a, Mmp1b has no known enzymatic activity (20, 21). Mouse Mmp1a, is 58% identical to human MMP1 but is expressed less ubiquitously in healthy mouse tissue than in

humans (20, 22). Elevated Mmp1a expression has been described in a number of inflammatory conditions in mice, including wound healing, lung injury, collagen-induced arthritis, and sepsis (16, 23-25). Mmp1a is induced in the mouse stroma of human breast and renal cell carcinoma xenografts (9, 25), suggesting that like MMP1, Mmp1a is upregulated in the tumor microenvironment.

In order to investigate the role of stromal-derived MMP1 in tumorigenesis, we generated *Mmp1a*-deficient mice. *Mmp1a*$^{-/-}$ mice are grossly normal and born in Mendelian ratios. However, *Mmp1a*-deficiency caused significantly decreased LLC1 lung tumor growth and angiogenesis. This stromal defect was rescued by co-implantation of *Mmp1a*$^{+/+}$ fibroblasts with LLC1 cells in the *Mmp1a*-deficient mice. Biochemical analysis indicated that Mmp1a secretion is limited by the ability of the Mmp1a prodomain to suppress auto-cleavage, whereas human MMP1 is efficiently secreted due to stable pro- and catalytic domain interactions. Together, these data demonstrate that stromal Mmp1a strongly promotes tumorigenesis *in vivo* and that MMP1/Mmp1a secretion is controlled by the stability of prodomain-catalytic domain interactions.

RESULTS

Mmp1a-Deficient Mice Exhibit Impaired Tumorigenesis and Angiogenesis. *Mmp1a*$^{-/-}$ mice were generated by targeted replacement of *Mmp1a* exon 5 with a PGK-neomycin cassette (26). Exon 5 encodes the zinc-coordination motif and a major portion of the catalytic domain and is essential for metalloprotease activity. Mmp1a-deficient mice were back-crossed 10 generations into the C57BL/6 background and *Mmp1a*-null animals were born within close range of expected ratios from heterozygote parents (Supplemental Fig. S1). Adult *Mmp1a*$^{-/-}$ males and females had no obvious abnormalities and were fertile (26). This indicates that *Mmp1a* (collagenase-1) expression is dispensable for normal mouse development, as has been observed with individual deficiency of the two other secreted mouse collagenases, *Mmp8* (collagenase-2) and *Mmp13* (collagenase-3) (27, 28).

Given that Mmp1a is often upregulated in the stroma of tumor xenografts (9, 25), we examined tumor growth in *Mmp1a*-deficient animals using LLC1 cells, a highly aggressive C57BL/6-derived lung cancer cell line (29). LLC1 cells ($2x10^5$) were implanted into the

abdominal fat pads of *Mmp1a*$^{-/-}$ and wild-type (WT) mice. The tumors in *Mmp1a*$^{-/-}$ (KO) mice grew at a significantly slower rate relative to WT mice over the course of the entire experiment (Fig. 1*A*). The tumors from the KO mice also had significantly smaller tumor mass as compared to WT mice at terminal necropsy (Fig. 1*B*), thereby implicating stromal-derived Mmp1a as an important factor in promoting lung cancer tumorigenesis.

The human homolog, MMP1 has been shown to be a pro-angiogenic factor by activating endothelial proliferation and migration through PAR1 (15, 30, 31). LLC1 tumors were assessed for possible defects in angiogenesis in the Mmp1a-deficient mice. Immunohistochemical staining of the tumors for von Willebrand Factor (vWF), a specific marker of endothelial cells, revealed a significant decrease in angiogenesis in both the tumor edges and tumor centers in the *Mmp1a*-knockout mice as compared to wild-type mice (Figure 2*A* and *B*). When human endothelial cells were stimulated with media from day 12.5 mouse embryonic fibroblasts (MEFs) isolated from wild type or *Mmp1a*-knockout mice, the Mmp1a-deficient media resulted in significantly less tube formation, and tubes that formed had decreased complexity (Fig. 2*C*-*E*). Together, these data indicate that stromal-derived Mmp1a is also a proangiogenic factor in tumors and in nascent vessel formation.

Restoration of Fibroblast Mmp1a Rescues Tumor Formation in Mmp1a-knockout Mice. Tumor stroma is a complex tissue composed of multiple cell types that could potentially produce Mmp1a, especially stromal fibroblasts and other mesenchymal cells (13). The human homolog, stromal-derived MMP1, is a potent inducer of cancer cell migration, invasion and mitogenesis, in large part through its activation of the PAR1 oncogene (9, 10). To determine whether stromal fibroblasts expressing Mmp1a could rescue tumorigenesis in *Mmp1a*-null animals, we isolated MEFs at embryonic day 12.5 from WT and *Mmp1a*-deficient mice. Media produced from KO MEFs resulted in >2-fold less chemoinvasion of LLC1 cells as compared to media from wild-type MEFs (Fig. 3*A*). Likewise, an almost identical reduction in the migration of A549 human lung cancer cells towards media from *Mmp1a*-deficient MEFs was observed (Fig. 3*B*). Migration of MCF7 breast cancer cells ectopically expressing PAR1 was four-fold higher towards media from WT MEFs as compared to *Mmp1a*-KO MEFs and inhibition of PAR1 with a small

molecule antagonist, RWJ-58259, caused a decrease in migration by 50% towards WT MEF media (Fig. 3*C*). The PAR1 antagonist did not completely reduce migration to the level observed with *Mmp1a*-KO conditioned media, suggesting PAR1-independent effects for Mmp1a in migration. Conversely, there was a small additional decrease in migration following treatment of knockout MEF conditioned media with the PAR1 inhibitor RWJ-58259. This could be due to suppression of constitutive activity of PAR1-chemokinesis (32).

Given the differences we observed in tumor growth *in vivo*, we also examined the ability of MEF conditioned media to induce LLC1 proliferation *in vitro*. Wild type MEF conditioned media induced a significant 2.2-fold induction of LLC1 proliferation (Fig. 3*D*). Conditioned media from *Mmp1a*-KO mice MEFs resulted in a significant reduction in proliferation to LLC1 cells as compared to wild type MEF conditioned media. These data demonstrate that MEFs, like cancer-associated fibroblasts, can induce cancer cell migration, invasion, and proliferation and that these tumor-promoting functions are reduced in MEFs from *Mmp1a*-KO mice.

To confirm that the reduced tumorigenesis seen in *Mmp1a*-KO mice is due to a stromal defect, we next performed co-implantation experiments with LLC1 cells and MEFs. WT and *Mmp1a*-KO mice were injected in their abdominal fat pads with $2x10^5$ LLC1 cells mixed with $1x10^5$ wild type or *Mmp1a*-KO MEFs. LLC1/*Mmp1a*-KO MEF co-implants in *Mmp1a*-KO mice formed significantly smaller tumors (Fig. 3*E*). However, this phenotype was completely rescued by co-implantation of LLC1 cells with WT *Mmp1a* MEFs in the *Mmp1a*-KO mice, thus demonstrating the importance of a stromal source of Mmp1a in promoting tumorigenesis. Co-implantation with WT *Mmp1a* MEFs did not result in supergrowth of the LLC1 tumors in WT mice suggesting a maximal effect of stromal Mmp1a on tumor growth.

Stromal Mmp1a Promotes Tumorigenesis Through PAR1 in LLC1 Lung Cancer. Lung carcinoma cells from patients and tumors from mice, including LLC1 (21, 33), express high levels of the oncogenic receptor for MMP1, namely PAR1 (9). We assessed whether the observed protumorigenic properties of stromal-produced Mmp1a were dependent on PAR1

expression in the lung tumors. Tumor xenograft experiments in WT and *Mmp1a*-KO mice were performed with LLC1 cells that were stably tranduced with a short hairpin-RNA (shPAR1) that silenced PAR1 expression. LLC1 cells silenced for PAR1 expression were injected into the abdominal fat pads of WT mice and tumor growth monitored over 26 days. shPAR1 knockdown tumors grew slower than control shLuc LLC1 tumors at all time points in WT mice (Fig. 4*A*). At the day 26 endpoint, shPAR1 tumors weighed less than control shLuc tumors in WT mice (Fig. 4*B*), indicating that the growth rate of the lung tumors was dependent at least in part on the expression of PAR1. LLC1 cells silenced for PAR1 expression were then injected into the abdominal fat pads of *Mmp1a*-KO mice and tumor growth monitored over 26 days. The relative decreases in lung tumor growth rates and mass were essentially identical between tumors that had PAR1 silenced on the lung carcinoma cells and those that grew in mice that lacked Mmp1a expression in the stroma (Fig. 4*A-B*). Double loss of Mmp1a in the stroma and PAR1 in the LLC1 cells (KO+shPAR1) did not result in further decreases in lung tumor growth and mass (Fig. 4*A-B*) indicating that stromal-Mmp1a and PAR1 on the carcinoma cells act on the same, e.g. paracrine, pathway in promoting tumorigenesis.

The Prodomains of Mmp1a and MMP1 have Divergent Effects on Protein Secretion and Autocatalysis. As human and mouse collagenases exert their tumorigenic effects as secreted factors, we next compared the efficiency of protein secretion of human MMP1 with mouse Mmp1a, Mmp1b and the two other related collagenases from mice, Mmp8 and Mmp13. Three heterologous expression systems, HEK293T, CHO-K1, and COS7, were used to compare protein levels of all the secreted collagenases. Surprisingly, secreted Mmp1a protein levels were markedly lower than human MMP1 or mouse Mmp1b, Mmp8, and Mmp13 across the three expression systems (Supplementary Fig. S2*A*). We tested the possibility that the Mmp1a signal peptide was responsible for its low secretion efficiency. Mmp1b, which was highly secreted across all the tested expression systems, has a signal peptide identical to that of Mmp1a except for a serine residue at position 2 instead of proline. However, mutation of the Mmp1a signal peptide to that of Mmp1b (P2S Mmp1a) had no effect on secretion of Mmp1a (Supplementary Fig. S2*B*), indicating that the signal peptide

of Mmp1a was not responsible for its low levels of secretion.

We next examined the prodomains of mouse Mmp1a and human MMP1 which are 53% identical to each other (Fig. 5*A-C*). A hPro-Mmp1a chimera was generated in which the prodomain of Mmp1a (residues 1-95) was exchanged with the prodomain of human MMP1 (residues 1-98). We also generated the complementary mPro-MMP1 chimera for human MMP1, with residues 1-96 of Mmp1a replacing human MMP1 residues 1-99. Replacement of the mouse Mmp1a prodomain with that of human MMP1 resulted in massive secretion of soluble hPro-Mmp1a (Fig. 5*D*). Conversely, replacement of the human prodomain with mouse prodomain eliminated secretion of the mPro-MMP1 chimera. These data indicate that the mouse and human prodomains have widely divergent and dominant effects on secretion of MMP1 and Mmp1a from cells.

We next tested the hypothesis that the prodomain of Mmp1a might associate less stably with its catalytic domain and thereby be less effective in maintaining Mmp1a in the zymogen or proteolytic-'off' state as compared to human MMP1. A structural model of proMmp1a (Fig. 5*A-B*) was created based on the highly homologous proMMP1 structure (34). The cysteine-lock motif which acts as the fourth coordination residue for the catalytic zinc effectively sealing off the catalytic pocket, is critical for the auto-inhibitory effects of MMP prodomains on their catalytic domains (35). The proximal residues and geometry of the cysteine-lock were completely conserved between human MMP1 and Mmp1a (Fig. 5*B-C*). However, Mmp1a residue L67 located at the C-terminal end of helix 2 (H2) at the interface between the prodomain and catalytic domains presents a much small hydrophobic surface than the analogous F70 in human proMMP1, suggesting a potentially weaker interaction with the catalytic domain surface in the active site cleft than the corresponding human counterpart (Fig. 5*B-C*). In the human proMMP1 crystal structure, F70 interacts with the critical $H^{228}S^{229}T^{230}$ of the catalytic domain and this phenylalanine is conserved in the other mouse collagenases and mammalian homologues of MMP1.

To determine whether the L67 residue contributed to the low secretion levels of Mmp1a, we generated a L67F point mutant along with a non-interacting substitution at the opposite end of helix 2, A58V (Fig. 5*B-C*). The humanized L67F mutant exhibited increased Mmp1a

expression, whereas the A58V substitution had no enhancing effect on Mmp1a protein secretion (Fig. 5*D*). The increased Mmp1a expression with L67F was still less than that observed with Mmp1b (Supplementary Fig. S2*B*), which also retains the L67 residue. However, unlike Mmp1a, Mmp1b does not have any identified enzymatic activity, suggesting that the proteolytic activity (e.g. autocleavage) of Mmp1a may reduce Mmp1a secretion. Consistent with this notion, catalytically inactive Mmp1a (E216A) was expressed at much higher levels than WT Mmp1a (Fig. 5*D*). To determine whether autocatalysis of Mmp1a in the cells may be reducing secretion, we examined cell lysates of WT Mmp1a and the point mutants. As shown in Fig. 5*E*, WT Mmp1a had significant zymogen activation (48 kDa active form) and cleavage at the linker separating the catalytic domain from the hemopexin domain as evidenced by appearance of the 26 kDa C-terminal hemopexin domain in the cell lysates. The cleaved hemopexin domain was completely absent in the inactive E216A mutant and the highly secreted hPro-Mmp1a chimera as well as WT hMMP1. Likewise, the humanized Mmp1a L67F point mutant had nearly no hemopexin domain cleavage product and much less 48 kDa active form in the cell lysates, further suggesting that stable prodomain-catalytic domain interactions suppress autocatalysis prior to secretion (Fig. 5*E*).

DISCUSSION

Using mice deficient in the collagenase Mmp1a, we show that Mmp1a is a functional MMP1 homologue in driving lung tumorigenesis with significantly less tumor growth and angiogenesis in *Mmp1a*-deficient animals. Loss of stromal-produced Mmp1a from fibroblasts isolated from *Mmp1a*-deficient mice resulted in decreased invasion, migration, and proliferation of lung carcinoma cells, and defects in angiogenesis. Co-implantation of wild-type Mmp1a fibroblasts with lung cancer cells with completely restored tumor growth in *Mmp1a*-deficient animals. The decrease in tumor growth observed in *Mmp1a*-deficient mice is consistent with observations in patient samples that stromal MMP1 is upregulated in aggressive human cancers (10, 17, 18, 36). Together these results demonstrate the importance of stromal Mmp1a in driving lung tumorigenesis and angiogenesis and suggest that the *Mmp1a*-deficient mouse will be a valuable tool in further interrogating the (patho)physiologic functions of MMP1 in the mouse.

The lack of a phenotype for the *Mmp1a*-deficient mouse in embryonic development and fertility is somewhat surprising yet not entirely unexpected. In this regard, the majority of MMP-deficient animals, including the *Mmp8* and *Mmp13* collagenase-deficient mice, have not exhibited developmental or fertility phenotypes (27, 28). The dispensability of individual MMPs is likely due to redundancy or overlap in enzyme-substrate activity within related members of the MMP family (37). A key exception to this is the *Mmp14*-knockout mouse, which exhibits dwarfism, osteopenia, arthritis, and death shortly after birth (38).

Despite the lack of obvious developmental abnormalties, the *Mmp1a*-deficient mice or media produced from *Mmp1a*-deficient fibroblasts exhibited significant defects in tumor angiogenesis and endothelial tube formation. This is in agreement with previous studies that showed that MMP1 triggers PAR1-dependent breast tumor angiogenesis and endothelial cell activation (9, 15, 16, 31). Endothelial PAR1 has been shown to be critical for angiogenesis in the developing mouse (39) and is an important mediator of proliferation, migration, and tube formation of endothelial cells *in vitro* upon activation by MMP1 (15, 30, 31). MMP1-PAR1 induces an increase in intracellular calcium and vWF exocytosis from HUVECs (15) and causes production of other pro-angiogenic chemokines including growth-regulated oncogene-α, IL-8, and monocyte chemoattractant protein-1 (30). Pharmacologic blockade of MMP1 activity (e.g. Mmp1a) in septic mice suppressed endothelial barrier disruption, disseminated intravascular coagulation, multi-organ failure, systemic cytokine production, and improved survival which was lost in *Par1*-deficient mice (16). As MMP1 small molecule inhibitors have exhibited antagonist effects on related collagenases (40) including negating potentially protective effects by MMP8 (41), this new *Mmp1a*-deficient mouse strain may prove to be a useful tool in studying the specific effects of Mmp1a on endothelial biology in various pathological states such as sepsis.

Another unexpected finding of the present work was the identification of divergent effects of the human MMP1 versus mouse Mmp1a prodomains in suppressing autocatalysis and protein section. Substitution of the prodomain of Mmp1a with that of human MMP1 resulted in major increases in protein secretion of Mmp1a and loss of auto-cleavage inside the

cell. Conversely, the efficient secretion of human MMP1 was ablated upon substitution of its prodomain with that of mouse Mmp1a. Analysis of the amino acids located at the interface between the pro- and catalytic domains revealed a key pro- and catalytic domain interaction site in which a phenylalanine in human MMP1 is substituted for a leucine in Mmp1a. Modification of this residue with the human side-chain resulted in increased Mmp1a protein secretion and improved proteolytic stability of Mmp1a in cell lystates, suggesting that prodomain instability may regulate constitutive Mmp1a secretion. Alternatively, the intrinsic instability of its prodomain may prime Mmp1a for activation, making it more difficult to negatively regulate its activity in the tissue or tumor microenvironment.

Lastly, we found that silencing of PAR1 in the lung carcinoma cells phenocopied stromal *Mmp1a*-deficiency, underscoring the importance of cancer cell-expressed PAR1 as a stromal Mmp1a target in the tumor microenvironment. In addition to activating PAR1, Mmp1a may modulate tumor-stromal interactions, angiogenesis and inflammation through cleavage of other bioactive molecules. For example, MMP1 and several other MMPs cleave membrane bound pro-tumor necrosis factor-alpha (proTNF-α) into its active, soluble form (42). MMP1 degrades insulin-like growth factor binding proteins (IGFBP) thereby increasing bioavailability of IGF and inducing fibroblast proliferation (43). MMP1 cleavage inactivates stromal cell-derived factor 1 alpha (SDF-1α), leading to decreased leukocyte and hematopoietic stem cell chemotaxis (44). Interleukin 1β (IL1β), which is a potent inducer of MMP transcription, is itself a target for both activation and degradation by MMP1, suggesting a regulatory mechanism by which IL1β induces MMP expression and thereby downregulates IL1β signaling once sufficient MMP levels have been reached (45, 46). Thus, it is anticipated that the Mmp1a-deficient mouse will be a highly useful tool to help delineate and validate the many *in vivo* functions ascribed to MMP1 in both tumor biology and other disease processes.

MATERIALS AND METHODS

Plasmid DNA and Reagents. C-terminal Myc-His tagged *MMP1, Mmp1a,* E216A *Mmp1a,* and *Mmp1b* in pCMV6-Entry (Origene) were made as previously described (21). The Mmp1a point mutations, A58V and L67F were generated by

QuickChange site directed mutagenesis (Agilent). Oligonucleotides were purchased from Integrated DNA Technologies. Sequencing was performed by the Tufts University Core Facility. The rabbit monoclonal anti-Myc antibody was from Cell Signaling. Polyethylenimine transfection reagent was purchased from Polysciences, Inc.

Cell Culture. Lewis lung carcinoma LLC1 cells, CHOK1 cells, and HEK293T cells were purchased from American Type Culture Collection. A549 human lung cancer cells were obtained from the National Cancer Institute. Cos7 cells were a gift from Dr. Martin Beinborn. Human PAR1 was ectopically expressed in the PAR1-null human breast carcinoma cell line MCF7, by stable transfection, as described previously (9). LLC1, Cos7, and HEK293T cells were maintained in DMEM supplemented with 10% FBS and 1% penicillin/streptomycin. A549 and MCF7+PAR1 cells were maintained in RPMI supplemented with 10% FBS and 1% penicillin/streptomycin. CHOK1 cells were maintained in F12 media supplemented with 10% FBS and 1% penicillin/streptomycin. To generate mouse embryonic fibroblasts (MEFs), embryos were harvested from *Mmp1a* heterozygote crosses at embryonic day 12.5. Cells were maintained in DMEM supplemented with 10% FBS, 1% Pen-Strep.

***Mmp1a*-deficient Mice.** A targeting vector was generated in pKO scrambler V916 (Lexicon Genetics) that was composed of 1.4 kb short arm encompassing exons 1-4 and introns 1-3 of *Mmp1a* and 6.8 Kb long arm encompassing exons 6 and 7 and intron 6 as detailed elsewhere (26). The PGK-Neo cassette replaced most of introns 4 and 5 and exon 5. The construct was linearized and electroporated into 129/SvJ-derived RW4 embryonic stem cells. Clones were selected for G418 resistance and screened by Southern blot. Heterozygous ES cells were injected into C57BL/6 blastocysts and transferred into the uteri of pseudo-pregnant females. Chimeric males were mated to C57BL/6 females and pups were screened by PCR. Heterozygotes were backcrossed for 10 generations into the C57BL/6 background. Homozygotes and wild type controls were obtained by crossing heterozygous littermates.

Genotyping. Genotyping PCR was performed with a three primer strategy using genomic DNA isolated from tail fragments. The primer sequences used were: Wild type allele primer (5'-3'): acgcattctgcctactgcaagg; Knockout allele primer (5'-3'): tgaccgcttcctcgtgcttta;

Common primer (5'-3'): gcagaccatggtgacaacaacc.

Tumor Xenograft Experiments. All mouse experiments were conducted in accordance with the National Institutes of Health guidelines and were approved by the Tufts University Institutional Animal Care and Use Committee. Six to nine week old female C57BL/6 wild type (bred in house or obtained from Charles River Laboratories) and *Mmp1a*$^{-/-}$ animals were injected with $2x10^5$ LLC1 cells in sterile PBS in the abdominal fat pad (2 inoculations per mouse). Starting at day 12, palpable tumors were measured every other day and tumor volume was calculated using the equation $(LxW^2)/2$. At the day 26 endpoint, animals were humanely sacrificed. Tumors were harvested, weighed, and formalin-fixed for histology.

Tumor-MEF co-implantation experiments were performed by injection of $2x10^5$ LLC1 and $1x10^5$ wild type or knockout MEFs in sterile PBS into the abdominal fat pad of six to nine week old wild type or *Mmp1a* knockout females. Tumor growth was measured every other day starting at day 12. The experiment was terminated at day 22 due to protocol limits being reached.

To stably silence PAR1 expression in the LLC1 cells, *PAR1*-targeted and control *luciferas*e-targeted shRNAs in pLKO.1-Puro were constructed as described previously (21). Briefly, lentiviral particles were generated by triple transfection of pLKO.1-Puro, pMD.G, and pCMV-dR8.9 in HEK293T using the calcium phosphate method. Lentiviral supernatants were harvested 24 h after transfection. Cells were transduced overnight with viral supernatant diluted 1:1000 in the presence of 8 μg/mL polybrene. Cells were selected with 3 μg/mL puromycin for 5 d beginning 48 h after transfection.

Histology. Parafin-embedding, sectioning, and immunohistochemistry for Von Willebrand Factor were performed by the Tufts Medical Center Pathology department. Quantification of the number of vWF-positive blood vessels was performed in a blinded fashion by counting the number of blood vessels per 50 fields at 40X magnification, in viable/non-necrotic regions of the tumors.

Endothelial Tube Formation. MatTek plates were chilled and coated with 100 μl Matrigel. HUVEC cells (3.5×10^4, p2-5) in EBM2 media with 0.5% BSA were plated on top. The cells were stimulated with MEF conditioned media (diluted 1:2, from 1×10^6

MEFs following 24h conditioning in 0.5% BSA DMEM). Endothelial tubes were observed after 6 hours under phase contrast inverted microscopy (4X magnification). ImageJ software was used to quantify tubal length and branch complexity from digital images (n=4).

Migration and Invasion Assays. All migration and invasion assays were performed using Boyden chambers with 8 μm pores (Costar) and all cells were starved overnight in 0.1% FBS (migration) or 1% FBS (invasion). For migration, 5 x 10^4 A549 or MCF7+PAR1 cells in 0.1% FBS were placed in the top chamber and allowed to migrate towards MEF conditioned media (harvested from 1 x 10^6 cells in 0.1% FBS over 24 h) in the lower chamber. After 18h migration, unmigrated cells were removed from the upper chamber and membranes were stained using the Hema3 system (Fisher). Chemo-invasion was performed by crosslinking 50 μg of type I rat tail collagen atop a Boyden membrane. MEF conditioned media was used as a chemoattractant in the lower well. LLC1 cells (2 x 10^4) in 1% FBS DMEM were placed in the upper chamber and allowed to invade for 48 h. Non-invasive cells were removed and membranes stained using the Hema3 system. Both the migration and invasion assays were quantified by counting the number of cells per 9 fields at 16X magnification and this number was multiplied by 9.17 to determine the total number of cells on the membrane (47).

Heterologous Expression System. HEK293T cells were passaged 1-3 h before transfection with C-terminal Myc-His tagged MMP constructs in pCMV6-Entry via calcium phosphate. CHOK1 and Cos7 cells were transfected with polyethylenimine (PEI) using a 1:3 DNA:PEI ratio. The following day, the transfection media was removed and replaced with 0.1% FBS DMEM. After 48 h, the conditioned media and cells were harvested. Protein expression was determined by western blotting of 40 μl conditioned media or 40 μg lysate for Myc-tag expression.

Mmp1a Modeling. Mmp1a was homology modeled using SWISS-MODEL (swissmodel.expasy.org) (48). The human pro-MMP1 structure was used as the template structure (PDB code 1su3). Images were generated using the PyMOL software package.

Statistical Analysis. Significance was determine by two tailed, heteroscedastic T test with significance defined as $p < 0.05$. If multiple cohorts were compared, one-way

ANOVA was performed initially followed by T test using Kaleidagraph software package.

REFERENCES

1. Boström P*, et al.* (2011) MMP-1 expression has an independent prognostic value in breast cancer. *BMC Cancer* 11:348.
2. Smith V, Wirth GJ, Fiebig HH, & Burger AM (2008) Tissue microarrays of human tumor xenografts: characterization of proteins involved in migration and angiogenesis for applications in the development of targeted anticancer agents. *Cancer Genomics Proteomics* 5(5):263-273.
3. Kanamori Y*, et al.* (1999) Correlation between expression of the matrix metalloproteinase-1 gene in ovarian cancers and an insertion/deletion polymorphism in its promoter region. *Cancer Research* 59(17):4225-4227.
4. Nikkola J*, et al.* (2002) High expression levels of collagenase-1 and stromelysin-1 correlate with shorter disease-free survival in human metastatic melanoma. *Int J Cancer* 97(4):432-438.
5. Murray GI, Duncan ME, O'Neil P, Melvin WT, & Fothergill JE (1996) Matrix metalloproteinase-1 is associated with poor prognosis in colorectal cancer. *Nat Med* 2(4):461-462.
6. Murray GI*, et al.* (1998) Matrix metalloproteinase-1 is associated with poor prognosis in oesophageal cancer. *J. Pathol.* 185(3):256-261.
7. Goldberg GI*, et al.* (1986) Human fibroblast collagenase. Complete primary structure and homology to an oncogene transformation-induced rat protein. *J Biol Chem* 261(14):6600-6605.
8. Egeblad M & Werb Z (2002) New functions for the matrix metalloproteinases in cancer progression. *Nat Rev Cancer* 2(3):161-174.
9. Boire A*, et al.* (2005) PAR1 is a matrix metalloprotease-1 receptor that promotes invasion and tumorigenesis of breast cancer cells. *Cell* 120(3):303-313.
10. Agarwal A*, et al.* (2008) Targeting a metalloprotease-PAR1 signaling system with cell-penetrating pepducins inhibits angiogenesis, ascites, and progression of ovarian cancer. *Molecular Cancer Therapeutics* 7(9):2746-2757.
11. Blackburn JS, Liu I, Coon CI, & Brinckerhoff CE (2009) A matrix metalloproteinase-1/protease activated receptor-1 signaling axis promotes melanoma invasion and metastasis. *Oncogene* 28(48):4237-4248.
12. Deryugina EI & Quigley JP (2006) Matrix metalloproteinases and tumor metastasis. *Cancer Metastasis Rev* 25(1):9-34.
13. Eck SM, Blackburn JS, Schmucker AC, Burrage PS, & Brinckerhoff CE (2009) Matrix metalloproteinase and G protein coupled receptors: co-conspirators in the pathogenesis of autoimmune disease and cancer. *J Autoimmun* 33(3-4):214-221.
14. Nguyen N, Kuliopulos A, Graham RA, & Covic L (2006) Tumor-derived Cyr61(CCN1) promotes stromal matrix metalloproteinase-1 production and protease-activated receptor 1-dependent migration of breast cancer cells. *Cancer Res* 66(5):2658-2665.

15. Goerge T*, et al.* (2006) Tumor-derived matrix metalloproteinase-1 targets endothelial proteinase-activated receptor 1 promoting endothelial cell activation. *Cancer Res.* 66(15):7766-7774.
16. Tressel SL*, et al.* (2011) A matrix metalloprotease-PAR1 system regulates vascular integrity, systemic inflammation and death in sepsis. *EMBO Mol Med* 3(7):370-384.
17. Bolon I*, et al.* (1995) Expression of c-ets-1, collagenase 1, and urokinase-type plasminogen activator genes in lung carcinomas. *Am J Pathol* 147(5):1298-1310.
18. Vizoso FJ*, et al.* (2007) Study of matrix metalloproteinases and their inhibitors in breast cancer. *Br J Cancer* 96(6):903-911.
19. Saarinen J, Welgus HG, Flizar CA, Kalkkinen N, & Helin J (1999) N-glycan structures of matrix metalloproteinase-1 derived from human fibroblasts and from HT-1080 fibrosarcoma cells. *Eur. J. Biochem.* 259(3):829-840.
20. Balbín M*, et al.* (2001) Identification and enzymatic characterization of two diverging murine counterparts of human interstitial collagenase (MMP-1) expressed at sites of embryo implantation. *J Biol Chem* 276(13):10253-10262.
21. Foley CJ*, et al.* (2012) Matrix metalloprotease-1a promotes tumorigenesis and metastasis. *J Biol Chem* 287:24330-24338.
22. Nuttall RK*, et al.* (2004) Expression analysis of the entire MMP and TIMP gene families during mouse tissue development. *FEBS Letters* 563(1-3):129-134.
23. Hartenstein B*, et al.* (2006) Epidermal development and wound healing in matrix metalloproteinase 13-deficient mice. *J Invest Dermatol* 126(2):486-496.
24. Tomita M*, et al.* (2007) Mouse model of paraquat-poisoned lungs and its gene expression profile. *Toxicology* 231(2-3):200-209.
25. Pfaffen S, Hemmerle T, Weber M, & Neri D (2010) Isolation and characterization of human monoclonal antibodies specific to MMP-1A, MMP-2 and MMP-3. *Experimental Cell Research* 316(5):836-847.
26. Fanjul-Fernandez M*, et al.* (2012) Mice deficient in matrix metalloproteinase Mmp1a show decreased susceptibiity to chemically-induced lung cancer. *Submitted.*
27. Balbín M*, et al.* (2003) Loss of collagenase-2 confers increased skin tumor susceptibility to male mice. *Nat Genet* 35(3):252-257.
28. Stickens D*, et al.* (2004) Altered endochondral bone development in matrix metalloproteinase 13-deficient mice. *Development* 131(23):5883-5895.
29. Bertram JS & Janik P (1980) Establishment of a cloned line of Lewis Lung Carcinoma cells adapted to cell culture. *Cancer Lett* 11(1):63-73.
30. Agarwal A*, et al.* (2010) Identification of a metalloprotease-chemokine signaling system in the ovarian cancer microenvironment: implications for antiangiogenic therapy. *Cancer Research* 70(14):5880-5890.
31. Blackburn JS & Brinckerhoff CE (2008) Matrix metalloproteinase-1 and thrombin differentially activate gene expression in endothelial cells via PAR-1 and promote angiogenesis. *Am. J. Pathol.* 173(6):1736-1746.
32. Kamath L, Meydani A, Foss F, & Kuliopulos A (2001) Signaling from Protease-activated Receptor-1 Inhibits Migration and Invasion of Breast Cancer Cells. *Cancer Res.* 61:5933-5940.
33. Cisowski J*, et al.* (2011) Targeting protease-activated receptor-1 with cell-penetrating pepducins in lung cancer. *Am J Pathol* 179(1):513-523.

34. Jozic D*, et al.* (2005) X-ray structure of human proMMP-1: new insights into procollagenase activation and collagen binding. *J Biol Chem* 280(10):9578-9585.
35. Van Wart HE & Birkedal-Hansen H (1990) The cysteine switch: a principle of regulation of metalloproteinase activity with potential applicability to the entire matrix metalloproteinase gene family. *Proc Natl Acad Sci USA* 87(14):5578-5582.
36. Heppner KJ, Matrisian LM, Jensen RA, & Rodgers WH (1996) Expression of Most Matrix Metalloprotease Family Members in Breast Cancer Represents a Tumor-Induced Host Response. *Am. J. Pathol.* 149:273-282.
37. Gill SE, Kassim SY, Birkland TP, & Parks WC (2010) Mouse models of MMP and TIMP function. *Methods Mol Biol* 622:31-52.
38. Holmbeck K*, et al.* (1999) MT1-MMP-deficient mice develop dwarfism, osteopenia, arthritis, and connective tissue disease due to inadequate collagen turnover. *Cell* 99(1):81-92.
39. Griffin CT, Srinivasan Y, Zheng Y-W, Huang W, & Coughlin SR (2001) A Role for Thrombin Receptor Signaling in Endothelial Cells During Embryonic Development. *Science* 293:1666-1670.
40. Odake S*, et al.* (1994) Inhibition of matrix metalloproteinases by peptidyl hydroxamic acids. *Biochem. Biophys. Res. Commun.* 199:1442-1446.
41. Vanlaere I & Libert C (2009) Matrix metalloproteinases as drug targets in infections caused by gram-negative bacteria and in septic shock. *Clin Microbiol Rev* 22(2):224-239, Table of Contents.
42. Gearing AJ*, et al.* (1994) Processing of tumour necrosis factor-alpha precursor by metalloproteinases. *Nature* 370(6490):555-557.
43. Fowlkes JL, Enghild JJ, Suzuki K, & Nagase H (1994) Matrix metalloproteinases degrade insulin-like growth factor-binding protein-3 in dermal fibroblast cultures. *J Biol Chem* 269(41):25742-25746.
44. McQuibban GA*, et al.* (2001) Matrix metalloproteinase activity inactivates the CXC chemokine stromal cell-derived factor-1. *J Biol Chem* 276(47):43503-43508.
45. Ito A*, et al.* (1996) Degradation of interleukin 1beta by matrix metalloproteinases. *J Biol Chem* 271(25):14657-14660.
46. Schönbeck U, Mach F, & Libby P (1998) Generation of biologically active IL-1 beta by matrix metalloproteinases: a novel caspase-1-independent pathway of IL-1 beta processing. *J Immunol* 161(7):3340-3346.
47. Kamath L, Meydani A, Foss F, & Kuliopulos A (2001) Signaling from protease-activated receptor-1 inhibits migration and invasion of breast cancer cells. *Cancer Res* 61(15):5933-5940.
48. Schwede T, Kopp J, Guex N, & Peitsch MC (2003) SWISS-MODEL: an automated protein homology-modeling server. *Nucleic Acids Res* 31(13):3381-3385.

ACKNOWLEDGEMENTS. We are grateful to Sheida Sharifi for her expertise in quantifying tumor angiogenesis, and Rutika V. Pradhan and Namrata Nammi for analysis of endothelial tube formation . This work was supported in part by NIH grants F30-HL104835 (to CJF), CA122992, HL64701 (to AK) and CA104406 (to LC).

FIGURES

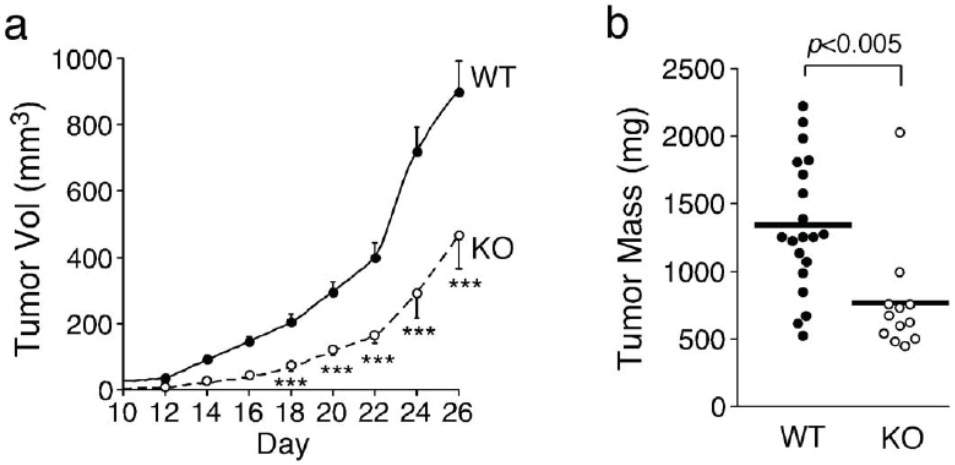

Fig. 1. Stromal Mmp1a-deficiency attenuates growth of lung tumors. *(A) Growth of Lewis lung carcinoma (LLC1) cells (2 x 10^5) implanted subcutaneously into the abdominal fat pad of $Mmp1a^{+/+}$ (n=20) or $Mmp1a^{-/-}$ (n=12) C57BL/6 female mice. (B) Excised tumor mass at the experiment endpoint, day 26. ***p<0.001 by heteroscedastic T-Test at each time point in both genetic backgrounds.*

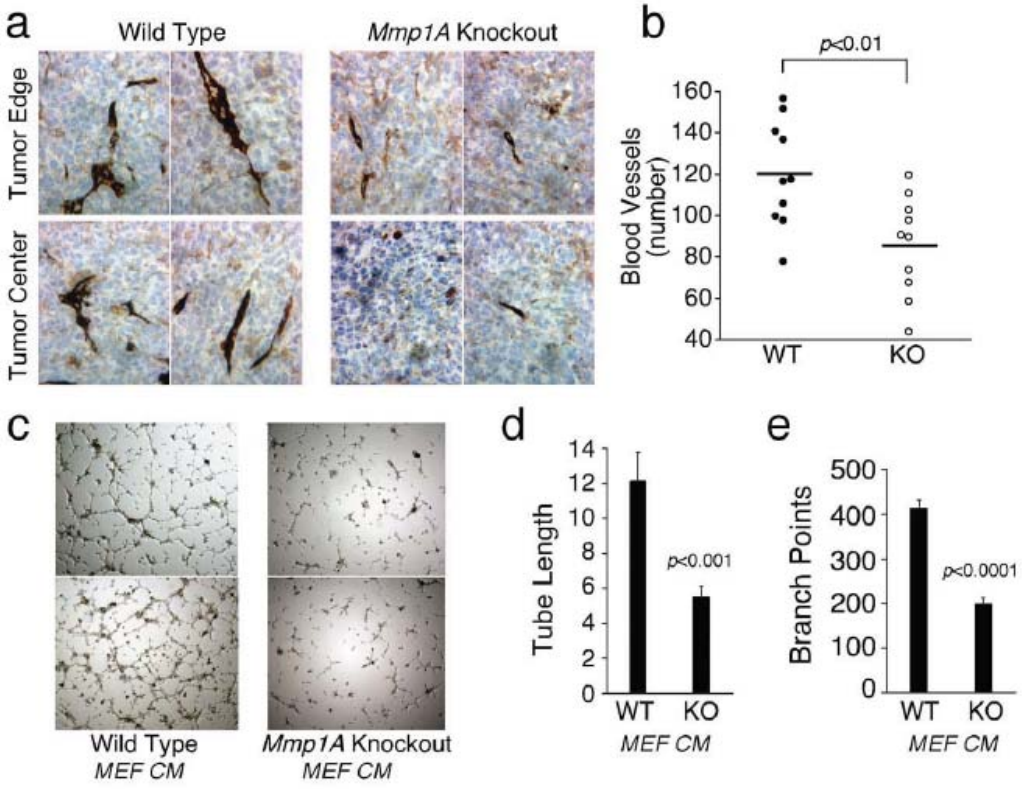

Fig. 2. Tumor angiogenesis is suppressed in Mmp1a-deficient animals *(A) Von Willebrand Factor (vWF) immunohistochemistry on LLC1 subcutaneous tumors from wild type or Mmp1a$^{-/-}$ mice (40X magnification). (B) Number of vWF-positive blood vessels as determined by the sum of 50 fields (40X) per tumor, n=10 per cohort. (C-E) Tube formation of primary human endothelial cells (HUVECs) following 6 h stimulation with media isolated from the embryonic fibroblasts (MEFs) of wild-type or Mmp1a-deficient mice. 4X phase contrast micrographs of representative (C) cultures with corresponding quantification of (D) tubal length and (E) branch point complexity (arbitrary units). All P values were determined by heteroscedastic T-Test.*

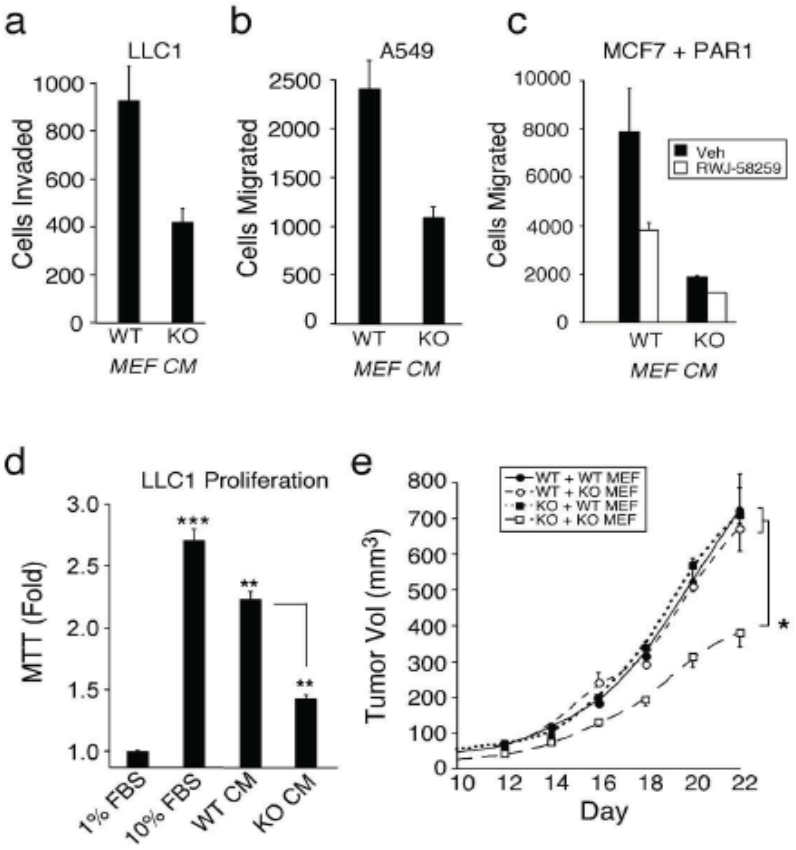

Fig. 3. Stromal Mmp1a promotes proliferation, migration, and tumorigenesis of lung cancer. *(A) LLC1 chemoinvasion through type I collagen towards Mmp1a$^{+/+}$ (WT) or Mmp1a$^{-/-}$ (KO) MEF conditioned media (CM). (B) Migration of the human lung cancer cell line A549 toward WT or KO MEF conditioned media. (C) Migration of MCF7 breast cancer cells ectopically expressing PAR1 towards MEF conditioned media in the absence (black) or presence (white) of the small molecule PAR1 antagonist, RWJ-58259 (3 μM). (D) 96 h MTT proliferation of LLC1 cells in response to 10% FBS or MEF conditioned media. (E), Tumor growth in Mmp1a$^{+/+}$ (WT) or Mmp1a$^{-/-}$ (KO) mice co-implanted with 2 x 10^5 LLC1 and 1 x 10^5 Mmp1a$^{+/+}$ (WT MEF) or Mmp1a$^{-/-}$ (KO MEF) fibroblasts (n=12-16 per cohort). * p<0.05, **p<0.005, ***p<0.001 by heteroscedastic T-Test.*

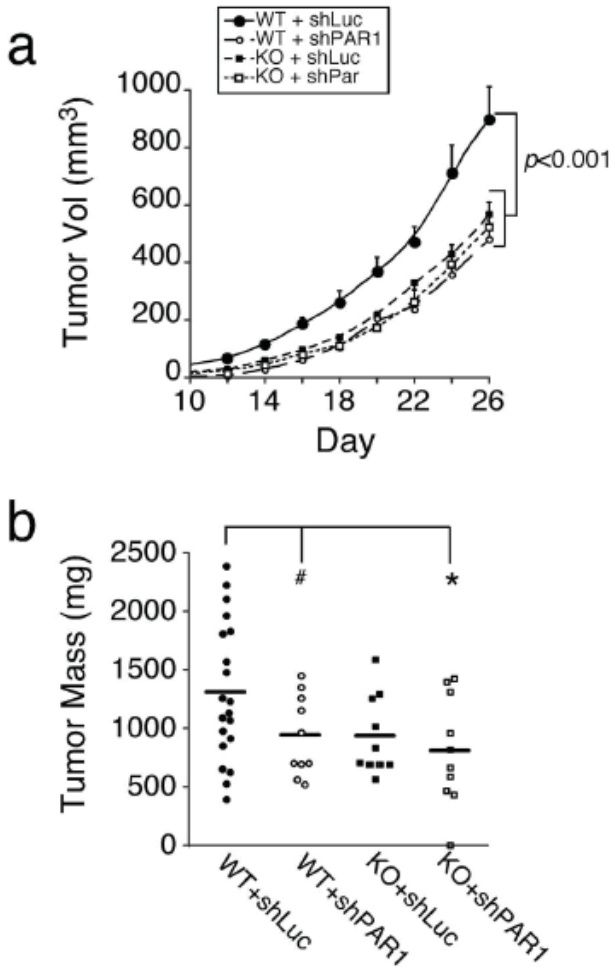

Fig. 4. Stromal Mmp1a promotes the growth of lung cancer through PAR1. *(A) Tumor growth following subcutaneous implantation of 200,000 shLuc control (n=10-20) versus shPAR1 (n=10) transduced LLC1 cells in Mmp1a$^{+/+}$ (WT) or Mmp1a$^{-/-}$ (KO) mice. (B) Mass of excised LLC1 tumors at the day 26 endpoint. # p=0.06, *p<0.05 by one-way ANOVA followed by T-test.*

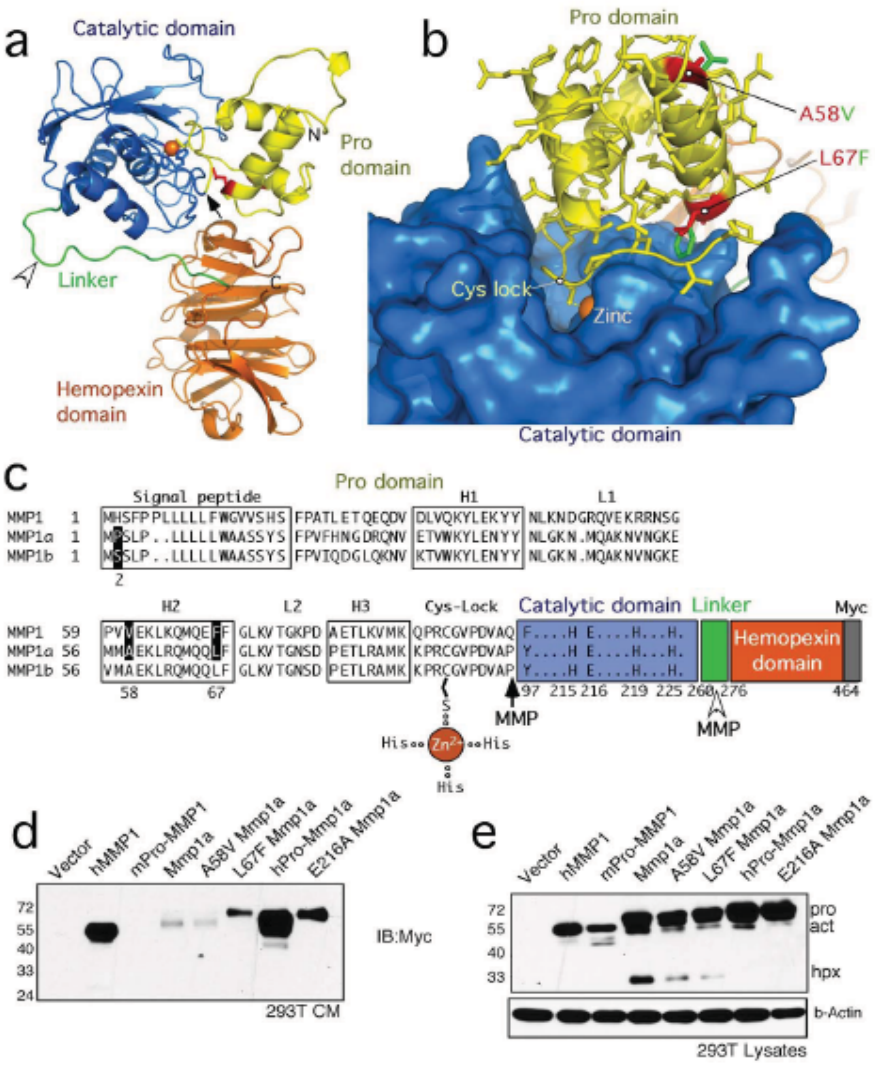

Fig. 5. Mmp1a and MMP1 prodomain-catalytic domain interactions regulate secretion and autocatalysis. *(A) Structure of Mmp1a as predicted by homology modeling with human proMMP1 showing the prodomain (yellow), catalytic domain (blue), linker (green), and hemopexin domain (orange). Black arrow-zymogen activating cleavage site; arrow head-linker cleavage site resulting in loss of hemopexin domain. (B) Docking of the Mmp1a prodomain (yellow) onto the catalytic domain/active site region (blue) of Mmp1a. Residues A58 and L67 in helix 2 (H2) are highlighted in red while the*

corresponding human residues V61 and F70, respectively are depicted in green. (C) Alignment of human MMP1, Mmp1a, and Mmp1b depicting the structural motifs within the prodomain; H=helix, L=linker. Point mutations are highlighted in black. (D) Secretion of Mmp1a and MMP1 prodomain mutants into the media of transfected HEK293T cells as determined by anti-Myc Western blot. (E) MMP expression levels in cell lysates (40 mg) of transfected HEK293T cells, showing proMMP (56 kDa), active MMP (48 kDa), and hemopexin degradation product (26 kDa).

V. The mutational landscape of head and neck carcinomas

HNSCC is an aggressive malignancy but the molecular mechanisms underlying its progression are largely unknown. HNSCC has been described as a multistep cancer process, but the few identified genes associated with the progression of this disease have not resulted in effective therapeutic approaches. Over the last few years, the development of next-generation sequencing techniques has improved our current knowledge of many tumor types. Accordingly, to better understand the molecular pathogenesis of HNSCC, we performed whole-exome sequencing of matched tumor and normal HNSCC samples. Among the more than 500 genes we found mutated in these tumors, we finally pointed to two genes encoding cell-cell adhesion proteins, as novel recurrently mutated genes in this aggressive malignancy.

***Article 5*: Miriam Fanjul-Fernández**, Víctor Quesada, Rubén Cabanillas, Juan Cadiñanos, Tania Fontanil, Álvaro Obaya, José L. Llorente, Aurora Astudillo, Santiago Cal and Carlos López-Otín**. "**Cell-cell adhesion genes *CTNNA2* and *CTNNA3* are novel tumor suppressors frequently mutated in head and neck carcinomas".

Personal contribution to this work

I have been the main responsible of this work along all its different stages. Thus, I have prepared the DNA libraries, analyzed the exome and pooled sequencing results, and performed all experiments for mutation validation. I have also carried out the experimental work focused on the functional analysis of the adhesion genes found to be recurrently mutated in HNSCC. Likewise, I was the main responsible for the integration of the bioinformatic, mechanistic and clinical data derived from this project. Finally, I wrote the manuscript together with Dr. Victor Quesada, and under the supervision of Dr. Carlos López-Otín.

Cell-cell adhesion genes CTNNA2 and CTNNA3 are novel tumor suppressors frequently mutated in head and neck carcinomas

Miriam Fanjul-Fernández*[1], Víctor Quesada*[1], Rubén Cabanillas[2], Juan Cadiñanos[2], Tania Fontanil[1], Álvaro Obaya[3], José L. Llorente[4], Aurora Astudillo[5], Santiago Cal[1] and Carlos López-Otín[1]

[1]Departamento de Bioquímica y Biología Molecular, and [3]Biología Funcional, Facultad de Medicina, Instituto Universitario de Oncología (IUOPA), Universidad de Oviedo, Oviedo, Spain;[2]Instituto de Medicina Oncológica y Molecular de Asturias (IMOMA), Oviedo, Spain; [4]Servicio de Otorrinolaringología and [5]Anatomía Patológica, Hospital Universitario Central de Asturias, Oviedo, Spain.

***MF-F and VQ have contributed equally to this work**

Send correspondence to:

Carlos Lopez-Otin
Departamento de Bioquímica y Biología Molecular
Facultad de Medicina, Universidad de Oviedo
33006 Oviedo-SPAIN
Tel. 34-985-104201; Fax: 34-985-103564
E-mail: clo@uniovi.es

Head and neck squamous cell carcinoma (HNSCC) is the sixth most common malignancy worldwide, representing a significant cause of morbidity and mortality. To explore the biological basis of HNSCC, we performed exome sequencing in four tumor-normal pairs. Among the 569 genes found to present somatic mutations, we selected 40 for further mutational analysis in 86 additional HNSCCs based on their recurrency or their potential cancer relevance. Notably, we detected frequent mutations in the cell-cell adhesion genes *CTNNA2* and *CTNNA3* (8% in each of them). Functional studies revealed a remarkable increase in the migration and invasive ability of HNSCC cells after *CTNNA2* and *CTNNA3* silencing. In addition, HNSCC cells overexpressing mutated forms of each gene show increased migration and invasive ability compared to HNSCC cells overexpressing their wild-type counterparts. Analysis of the clinical relevance of these mutations demonstrated that they are associated with poor prognosis. Taken together, these findings suggest that *CTNNA2* and *CTNNA3* are novel tumor suppressor genes which are commonly mutated in HNSCC.

HNSCC is a frequent human malignancy, being smoking and alcohol abuse the most important risk factors[1]. Several studies have converged in the identification of key HNSCC-genes, which have contributed to a better understanding of the biological basis of this malignancy. Notwithstanding, survival rates for HNSCC have not markedly improved in recent decades and only 40-50% of patients survive over 5 years[2]. The large biological and clinical heterogeneity of this disease hampers accurate prognostication, treatment planning and identification of causative cancer genes. Moreover, given the metastatic potential of HNSCC, a deeper understanding of the molecular mechanisms that lead to invasion and spread of neoplastic cells could be instrumental in improving the clinical management of this disease.

To better understand the molecular pathogenesis of HNSCC, we first performed whole-exome sequencing of matched tumor and normal samples from four individuals with a clinical history of tobacco and alcohol abuse **(Supplementary Table 1)**. We achieved

106-fold mean sequence coverage of targeted exonic regions. On average, 89% of the exome positions were covered by more than 8 reads with Phred quality higher than 30 (callable exome) **(Supplementary Table 2)**. We identified a median of 260 somatic mutations per case, which represents about 7 mutations per Mb of sequenced DNA **(Supplementary Table 3)**. This mutational rate agrees with data recently reported for this type of cancer as well as for other smoking-related malignancies[3-5]. Consistent with other smoker-related tumor studies, the most common substitution was G>T/C>A **(Supplementary Fig. 1)**. Analysis of the identified somatic mutations predicted that 611 of them result in protein-coding changes in 569 genes **(Supplementary Table 4)**. To determine whether any of these genes was recurrently mutated, we next analyzed a validation set of 86 HNSCC cases, in which tumors in most head and neck anatomic sites were represented (oral cavity, oropharynx, hypopharynx, larynx and sinonasal cavity) **(Supplementary Table 5)**. We focused on 40 genes mutated in more than one of the four exome-sequenced HNSCCs, or whose biological function was presumed to be relevant for tumor development **(Supplementary Table 6)**. Then, we used a pooled-sequencing strategy with ability to identify recurrently mutated genes, as assessed in previous genomic studies of chronic lymphocytic leukemia[6]. As a positive control, we used the well-known tumor suppressor *TP53* which is recurrently mutated in HNSCC. Analysis of these 86 HNSCC cases led us to identify *CTNNA2* and *CTNNA3*, encoding cell-cell adhesion α-catenins, as novel recurrently mutated genes in this aggressive malignancy **(Fig. 1)**. We found seven tumors with mutations in *CTNNA2* and six tumors with mutations in *CTNNA3*, including one case harboring two different missense mutations **(Supplementary Table 7)**. These cell-cell adhesion genes were among the most frequently mutated genes (15% when considered together) in our patient series. Only the classical tumor suppressor p53 showed a clearly higher mutational frequency. Interestingly, we found three HNSCC cases harboring mutations in both genes (P=0.005), suggesting that these mutations could have synergic effects **(Supplementary Table 7)**. Analysis of the mutational spectrum in both genes is consistent with the hypothesis that *CTNNA2* and *CTNNA3* might act as HNSCC-tumor suppressor genes **(Fig. 1)**. Thus, thirteen of the identified mutations were predicted to result in damaged protein, three of them through premature stop codons (**Supplementary Table 7**). Additionally, exploration of the COSMIC database revealed that mutations in both α-

catenin genes have been annotated in different malignancies **(Fig. 1)**, thereby expanding the oncological interest of these genes beyond HNSCC.

CTNNA2 and CTNNA3 are key proteins of the adherens junctional complex in epithelial cells and play a crucial role in cellular adherence[7]. To investigate the functional relevance of *CTNNA2* and *CTNNA3* in HNSCC cells, we performed both RNA interference (CT2i and CT3i) and cDNA overexpression (CT2o and CT3o) studies of both genes and interrogated key biological processes for tumor progression. We first carried out a cell adhesion profile assay which revealed that silencing and overexpression of *CTNNA2* and *CTNNA3* mainly affect laminin-dependent adhesion **(Supplementary Fig. 2)**. Subsequently, we analyzed by time-lapse microscopy the capacity of HNSCC cells to migrate through a scratch wound in laminin-coated plates. These experiments revealed that *CTNNA2* and *CTNNA3* silencing confers these malignant cells an enhanced ability to migrate through the wound compared with control cells **(Supplementary Fig. 3, movies 1 and 2)**. Conversely, clones overexpressing these α-catenin genes showed a marked decrease in their migration speed **(Supplementary Fig. 3, movies 3 and 4)**. To study whether silencing of both genes has a synergic effect, as suggested by the relatively high frequency of concurrent somatic mutations in both genes, we generated *CTNNA2* and *CTNNA3* double-interfered HNSCC cells. Time-lapse migration experiments demonstrated that, when both genes are silenced, cells migrate faster than when either single gene is knocked down **(Supplementary Fig. 3, movie 5)**.

We next evaluated the invasive capacity of HNSCC cells with loss- or gain-of-function of these α-catenins. We found that *CTNNA2*- and *CTNNA3*-silenced clones showed enhanced ability to invade a Matrigel matrix, whilst cells overexpressing these α-catenin genes exhibited a considerably reduced invasive ability **(Fig. 2)**. We also observed that changes in the expression levels of both genes did not seem to affect the proliferation rate of HNSCC cells (data not show). To gain insight into the role of the identified mutations in *CTNNA2* and *CTNNA3*, we performed site-directed mutagenesis experiments on some selected residues of both α-T-catenin genes. Cells overexpressing CTNNA2-S132Y, CTNNA2-E266* or CTNNA3-R628P showed enhanced ability to migrate through

the wound compared with cells overexpressing wild-type cDNAs **(Supplementary Fig. 3, movies 6-8)**. Likewise, these mutations increased the capacity of cells to invade a Matrigel matrix **(Fig. 2)**. Collectively, these results are consistent with the hypothesis that *CTNNA2* and *CTNNA3* are tumor suppressor genes, whose genetic inactivation endows HNSCC cells with migration and invasion advantages which may contribute to the progression of these aggressive malignancies.

To further explore the molecular mechanisms underlying the observed alterations caused by *CTNNA2* and *CTNNA3* mutations, we next investigated how changes in these genes affect relevant biochemical pathways involving cell-cell adhesion. Since these α-catenins interact with β-catenin[8], we examined the phosphorylation status of this downstream component of the Wnt/Wingless pathway, which is altered in many types of cancer. We found that overexpression of *CTNNA2* and *CTNNA3* in HNSCC cells grown on laminin causes a substantial decrease in phosphorylation levels of β-catenin at Ser-552 **(Supplementary Fig. 4)**. Conversely, silencing of *CTNNA2* and *CTNNA3* in HNSCC cells increases phosphorylation levels of this β-catenin residue **(Supplementary Fig. 4)**. Phosphorylation of β-catenin at Ser552 results in its translocation from cell-cell contacts into cytosol and nucleus[9]. This loss of β-catenin at cell adherens junctions might cause breaking down of cell-cell contacts, explaining the cell scattering phenotype associated with simultaneous *CTNNA2* and *CTNNA3* down-regulation[10]. It is well established that once β-catenin is translocated into the nucleus, it activates transcription factors of the TCF/LEF-1 family[9]. Therefore, we performed TCF/LEF-1 luciferase reporter assays to evaluate the putative changes in the activity of these transcription factors caused by *CTNNA2* and *CTNNA3* mutations in HNSCC. Silencing of *CTNNA2* and *CTNNA3* led to a significant increase of TCF/LEF-1 transcriptional activity when compared with control cells. In contrast, up-regulation of *CTNNA2* and *CTNNA3* in HNSCC cells was associated with reduced luciferase activity **(Supplementary Fig. 5)**. Likewise, overexpression of S132A and E266* *CTNNA2* mutants as well as that of C622F and R628P *CTNNA3* mutants increased the TCF/LEF-1 transcriptional activity compared with cells overexpressing wild-type genes **(Supplementary Fig. 5)**. Thus, down-regulation of *CTNNA2* and *CTNNA3* increases phosphorylation of β-catenin at Ser552, which might cause its disassociation from

cell-cell contacts, increasing its transcriptional activity and inducing the expression of genes that favor tumor progression.

Finally, to evaluate the impact of *CTNNA2* and *CTNNA3* mutations in the clinical outcome of HNSCC patients, we examined the available clinical data of 86 patients in the validation series, including 7 with mutations in *CTNNA2* and/or *CTNNA3* (**Supplementary Table 5**). Then, we constructed a multivariate Cox proportional hazards model including the stage of each tumor as a co-variable. This analysis showed that patients in a given stage are 4 times more likely to die if they have tumors with *CTNNA2* or *CTNNA3* mutations (hazard ratio 4.209; 95% confidence interval, 1.045–16.949; P=0.027), which suggests that mutations in these genes are associated with worse clinical prognosis.

High-throughput genomic experiments offer unprecedented opportunities to unveil tumor suppressors whose mutational frequencies preclude their identification using traditional techniques. Here, we have used whole-exome and pooled sequencing to identify for the first time *CTNNA2* and *CTNNA3* as moderately frequent and possibly synergic mutational targets in HNSCC. Functional and clinical studies suggest that both genes may act as tumor suppressors in this severe malignancy through their ability to affect cell-cell adhesion pathways. Therefore, these catenins may offer new candidate targets for the development of drugs that may help the treatment of HNSCC.

Acknowledgements. *We thank Drs. J.M.P. Freije and X.S. Puente for helpful comments and D.A. Puente and S. Alvarez for excellent technical support. We acknowledge the Banco Nacional de ADN (University of Salamanca) for sharing tumor and blood samples. HEK-293T and SCC-2 cells were kindly provided by Dr. P.P. Durán (CNIO) and Dr. R. Grenman, respectively. This work was funded by grants from the Spanish Ministry of Economy and Competitiveness, RTICC (Instituto Carlos III, Madrid, Spain), Fundación María Cristina Masaveu Peterson, Fundación Centro Médico de Asturias and Obra Social Cajastur. C.L-O. is an Investigator of the Botín Foundation.*

Author Information. *Sequencing data have been deposited at the Sequence Read Archive (SRA), and can be accessed at http://www.ebi.ac.uk/ena/data/view/PRJEB1136.*

Author Contributions. *M.F. and V.Q. performed the analysis of sequence data; M.F., T.F, A.O. and S.C. performed functional studies; R.C., J.C., J.L. and A.A. obtained the tumor samples and performed histological and clinical analyses; C.L-O conceived and directed the research and together with M.F and V.Q wrote the manuscript which all authors have approved.*

References

1. Bray, F., Ren, J.S., Masuyer, E. & Ferlay, J. Global estimates of cancer prevalence for 27 sites in the adult population in 2008. *Int J Cancer* (2012) in press.
2. Loyo, M. *et al.* Lessons learned from next-generation sequencing in head and neck cancer. *Head Neck* (2012) in press.
3. Stransky, N. *et al.* The mutational landscape of head and neck squamous cell carcinoma. *Science* **333**, 1157-60 (2011).
4. Agrawal, N. *et al.* Exome sequencing of head and neck squamous cell carcinoma reveals inactivating mutations in NOTCH1. *Science* **333**, 1154-7 (2011).
5. Pleasance, E.D. *et al.* A small-cell lung cancer genome with complex signatures of tobacco exposure. *Nature* **463**, 184-90 (2010).
6. Puente, X.S. *et al.* Whole-genome sequencing identifies recurrent mutations in chronic lymphocytic leukaemia. *Nature* **475**, 101-5 (2011).
7. Janssens, B. *et al.* Assessment of the CTNNA3 gene encoding human alpha T-catenin regarding its involvement in dilated cardiomyopathy. *Hum Genet* **112**, 227-36 (2003).
8. Janssens, B. *et al.* alphaT-catenin: a novel tissue-specific beta-catenin-binding protein mediating strong cell-cell adhesion. *J Cell Sci* **114**, 3177-88 (2001).
9. Fang, D. *et al.* Phosphorylation of beta-catenin by AKT promotes beta-catenin transcriptional activity. *J Biol Chem* **282**, 11221-9 (2007).
10. Pan, F.Y. *et al.* Beta-catenin signaling involves HGF-enhanced HepG2 scattering through activating MMP-7 transcription. *Histochem Cell Biol* **134**, 285-95 (2010).

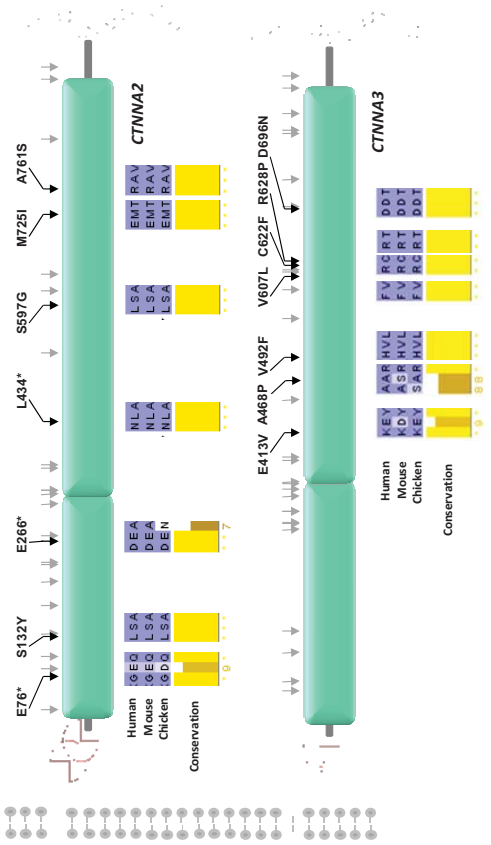

Figure 1. CTNNA2 and CTNNA3 mutations identified in HNSCC. *Schematic representation of the human CTNNA2 and CTNNA3 adhesion proteins with the different somatic alterations found in HNSCC samples (black) and COSMIC (grey). Green blocks identify the two vinculin-like domains in each catenin. Catenins are depicted bound to cadherin (red rectangles) through vinculin (blue arcs) and to actin filaments (gray circles*

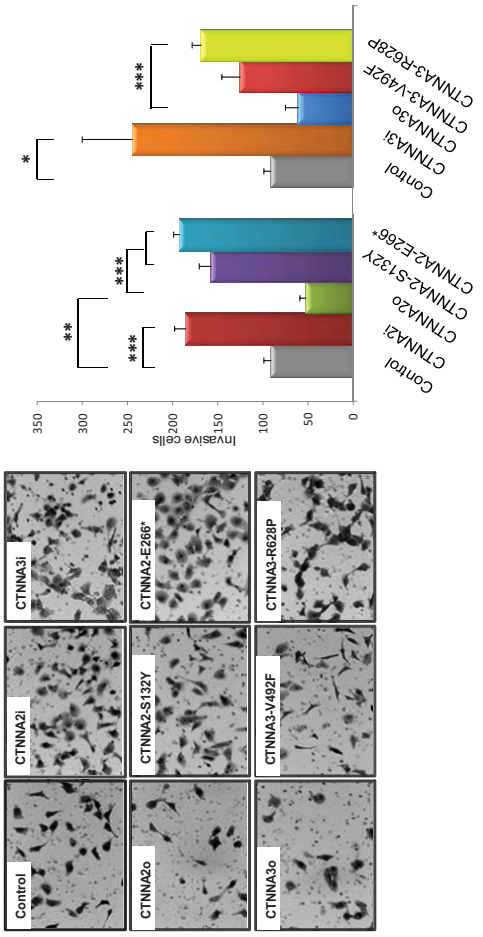

***Figure 2. Invasive capacity of the different SCC lines**. Left, representative microscopic (10x magnification) pictures of cells after silencing (i), overexpression of wild-type (o) or overexpression of mutant forms of CTNNA2 and CTNNA3. Right, number of invasive cells for each cell line. *, $P < 0.05$; **, $P < 0.01$; ***, $P < 0.005$.*

Supplementary Information

(Fanjul-Fernández *et al*. Cell-cell adhesion genes *CTNNA2* and *CTNNA3* are novel tumor suppressors frequently mutated in head and neck carcinomas)

DNA isolation from human specimens

We obtained from each patient **(Supplementary Table 1)** surgically resected tumor samples and matched blood samples. To obtain tumor genomic DNA, approximately 10 mg of fresh-frozen tumor tissue were lysed in 360 µl of ATL buffer supplemented with 40 µl of proteinase K for 2-16 h. After complete macroscopic digestion, the lysate was mixed with 400 µl of AL buffer to homogeneization, and then 400 µl of 100% EtOH were added, followed by thorough vortexing for 15 s and 5 min incubation at room temperature. Genomic DNA was then precipitated by 10 min centrifugation at 4 ºC and 20,000 x g, washed with 70% EtOH, air-dried and resuspended in 50-100 µl of AE buffer. ATL, AL, proteinase K and AE buffer were from Qiagen. Germline genomic DNA was obtained from blood samples using the Flexigene kit (Qiagen), according to manufacturer's instructions. The experiments were conducted in accordance with the Hospital Universitario Central de Asturias Ethics Committee, and written informed consent was obtained from each individual providing biological samples.

Exome-enrichment

Three µg of genomic DNA from each sample were sheared and used for the construction of a paired-end sequencing library as previously described in the Paired-End sequencing sample preparation protocol provided by Illumina[1]. Enrichment of exonic sequences was then performed for each library using the Sure Select Human All Exon Kit 50 Mb (Agilent Technologies) following the manufacturer´s instructions. Exon-enriched DNA was pulled down by magnetic beads coated with streptavidin (Invitrogen), and was followed by washing, elution and 18 additional cycles of amplification of the captured library. Exon enrichment was validated by real-time PCR in a 7300 Real-Time PCR System (Applied Biosystems) using a set of two pairs of primers to amplify exons and one pair to amplify an intron. Enriched libraries were sequenced using two lanes of an Illumina GAIIx.

Read mapping and processing

For exome sequencing, reads from each library were mapped to the human reference genome (GRCh37) using BWA[2] with the sampe option, and a BAM file was generated using SAMtools[3]. Reads from the same paired-end libraries were merged and optical or PCR duplicates were removed using Picard (http://picard.sourceforge.net/index.shtml). Statistics about the number of mapped reads and depth of coverage for each sample are shown in **Supplementary Table 2**. For the identification of somatic substitutions, we used the *Sidrón* algorithm, which has been previously described[4]. The frequencies of machine error were estimated by examining 3 x 10^5 likely homozygous positions (coverage higher than 15, fraction of non-reference bases lower than 0.1). Due to the contamination of tumor samples with normal tissue, the cutoff S values were lowered to 11 for positions with coverage higher than 20. The validation rate of the somatic mutations detected by *Sidrón* was higher than 90% as assessed by Sanger sequencing.

Somatic mutation identification in pooled samples (SMIPS)

To discover recurrent somatic mutations in the validation series, we performed a screening in a set of 86 additional HNSCC cases **(Supplementary Table 5)** using a combination of pooled samples, PCR amplification and high-throughput sequencing. We used a modified method for the analysis of pooled samples[5]. Briefly, we amplified each selected exon from two pools containing equal amounts of tumor and normal DNA respectively from the patients. The primers used in this step are described in **Supplementary Table 8**. To obtain sufficient coverage, we mixed equal amounts of the resulting 466 amplicons in four pools for each sample. Each pool was sequenced in one lane of an Illumina GAIIx sequencer for an average coverage of about 10^5 over 225,698 bases.

Mutation validation

To deconvolute the sequencing data generated by SMIPS, we analyzed each tumor DNA from the validation set by using SNaPShot (Life Technnologies), according to

manufacturer's instructions. We performed two separate SNaPShot reactions per tumor DNA, one for *CTNNA2* and one for *CTNNA3*, using the primers shown in **Supplementary Table 9**. The presence of the corresponding mutation identified by SNaPShot was verified by Sanger sequencing using a 3130XL Genetic Analyzer and the primers described in **Supplementary Table 8**.

Cells and cell culture conditions

The human squamous cell carcinoma cell line SCC-2 was cultured in complete medium Dulbecco´s Modified Eagle Medium (DMEM, Invitrogen) containing 10% fetal bovine serum (FBS), 2% Hepes, 1% non-essential amino acids and 1% penicillin-streptomycin-glutamine. For overexpression experiments, cells at 80% confluence were transfected using Lipofectamine 2000 (Invitrogene) with the full-length human cDNA of *CTNNA2* and/or *CTNNA3* (Origene, RC208731 and RC226241, respectively). For knockdown experiments, cells were transduced with a set of four retroviral short-hairpin RNA (shRNA) vectors based on the pLKO.1 vector and designed to specifically target human *CTNNA2* and/or *CTNNA3* transcripts (Origene, TG313667 and TG313666 respectively), using HEK-293T cells for virus packaging. *CTNNA2* and *CTNNA3* mutant DNAs were created using a Stratagene QuikChange II Site-Directed Mutagenesis kit (Agilent Technologies). Transfected clones were selected during 5-7 days with 400 µg/ml of G418 for overexpressing clones and 1.1 µg/mL puromycin for silencing clones. All cell lines were analyzed by Western blot to confirm expression or silencing.

Cell adhesion assays

The adhesion capacity of different cell pools was analyzed with the ECM Cell Adhesion Array kit (Colorimetric) (EMD Biosciences, ECM540 96 wells) following manufacturer's instructions. Briefly, 6 x 10^5 cells were incubated in the ECM Array during 3 hours. After cell lysis, the absorbance was measured at 485 nm using a Synergy H4 Hybrid reader. All data are the mean of three independent experiments.

Time-lapse migration assays

For cell migration assays, laminin (15 µg/ml; Sigma L2020) were coated for 2 h at 37 ºC on Ibidi uncoated µ-Dishes (Ibidi 81151). 6 x 10^5 cells were seeded 6 h before performance of the experiment on coated dishes with culture inserts (Ibidi 80209) until complete adhesion. Inserts were removed defining a cell free gap of around 500 µm, and cells were overlayed with 2 ml of culture media. Migration of cells were time-lapse recorded in a Zeiss Axiovert 200 microscope during 12 h, with a XL-multi S1 incubator and using Axiovision software. Migration areas at different time points were calculated using ImageJ.

In vitro invasion assays

The *in vitro* invasion potential of different SCC-2 cell lines was evaluated using Matrigel-coated invasion chambers with an 8-Am pore size (BD Biosciences). For each experiment, 2.5 x 10^5 cells per well were allowed to migrate for 27h through the Matrigel-coated membranes using 3% FBS as chemoattractant. Cells that reached the lower surface of the membrane were stained. The total number of cells in the lower chamber was determined by visible microscopy (magnification 4x).

Cell proliferation assays

To quantitate cell proliferation, we used a CellTiter96AQ nonradioactive cell proliferation kit (Promega Corp.). For each experiment, one hundred B16F10 cells were seeded in triplicate in 96-well plates and incubated at 37 ºC, 5% CO_2 for 4 days. Cell proliferation was quantified by measuring the conversion of 3-(4,5-dimethyl thiazol-2-yl)-5-(3-carboxyme-thoxyphenyl)-2-(4-sulfophenyl)-2H-tetrazolium, inner salt (MTS) into water-soluble formazan catalyzed by dehydrogenase in living cells. The reaction was monitorized by measuring the absorbance at 490 nm using a Synergy H4 Hybrid reader. All experiments were repeated three times independently.

Luciferase reporter gene assays

To measure the transcriptional activity of the β-catenin/Wnt signalling pathway, SCC-2 cell lines transfected with different constructs were seeded in 24-well plates at 1 x 10^5 cells/well. After 24 h, 0.6 µg of TCF/LEF-1 reporter (pTOP-FLASH) or control vector

(pFOP-FLASH) were transiently cotransfected with 0.06 μg of TLRK vector and 0.2 μg of each DNA construction (shRNAs, full-length wild-type and mutated cDNAs, respectively for both CTNNA2 and CTNNA3) following the standard Lipofectamine 2000 protocol (Invitrogen). Cells were incubated for 24 h, and then 10 μl out of the 100 μl cell extract were used for measuring luciferase activity using the Dual Luciferase Reporter Assay System kit (Promega).

Western blot

Samples were subjected to SDS-PAGE and transferred to PVDF (0.45 μm pore size) membranes (Millipore). Blots were blocked with 5% non-fat dry milk in TBS-T buffer (20 mM Tris-HCl pH 7.4, 150 mM NaCl and 0.05% Tween-20), for 1 h at room temperature and incubated overnight at 4 ºC with 5% BSA in TBS-T with either 0.2 μg/ml anti-CTNNA2 (TA300943, Origene) or 0.2 μg/ml anti-CTNNA3 (13974-1-AP, Proteintech Europe) and 1:1000 anti α-actin (A5441, Sigma). To evaluate the phosphorylation status of β-catenin, we used β-catenin Antibody Sampler Kit (2951S, Cell Signaling). Finally, the blots were incubated for 1 h at room temperature in 2.5% non-fat dry milk in TBS-T buffer with 10 ng/ml of goat anti-mouse (115-035-062, Jackson Inmunores) and donkey anti-rabbit (NA934V, GE Healthcare), respectively. Then, blots were washed with TBS-T and developed with Immobilon Western chemiluminescent HRP substrate (Millipore). Chemiluminescent images were taken with a Fujifilm LAS3000 mini apparatus.

Statistical analysis

The SPSS Statistics 17.0 (SPSS Inc) package was employed to correlate clinical and biological variables by means of Fisher's test or non-parametric test when necessary. Survival curves were analyzed according to the Kaplan and Meier method and compared using the log-rank test[6]. All statistical tests were two-sided and the level of statistical significance was 0.05. The probability of concurrent *CTNNA2* and *CTNNA3* mutations in the validation series was estimated with a Monte Carlo simulation. A stochastic process where 86 random individuals were assigned 7 *CTNNA2* and 7 *CTNNA3* mutations was simulated ten thousand times. The reported *P*-value was the frequency of three or more individuals with both mutations in those simulations.

References

1. Bentley, D.R. *et al.* Accurate whole human genome sequencing using reversible terminator chemistry. *Nature* **456**, 53-9 (2008).
2. Li, H. & Durbin, R. Fast and accurate short read alignment with Burrows-Wheeler transform. *Bioinformatics* **25**, 1754-60 (2009).
3. Li, H. *et al.* The Sequence Alignment/Map format and SAMtools. *Bioinformatics* **25**, 2078-9 (2009).
4. Puente, X.S. *et al.* Whole-genome sequencing identifies recurrent mutations in chronic lymphocytic leukaemia. *Nature* **475**, 101-5 (2011).
5. Druley, T.E. *et al.* Quantification of rare allelic variants from pooled genomic DNA. *Nat Methods* **6**, 263-5 (2009).
6. Peto, R. & Pike, M.C. Conservatism of the approximation sigma (O-E)2-E in the logrank test for survival data or tumor incidence data. *Biometrics* **29**, 579-84 (1973).

SUPPLEMENTARY DATA

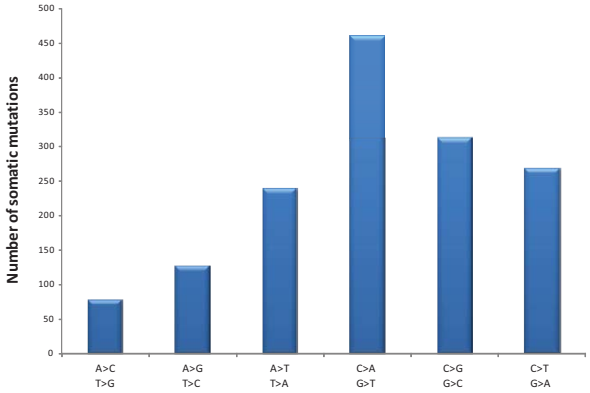

Figure S1. Mutational profile of whole-exome sequenced samples. *Each mutational type is expressed as reference base > mutated base in either strand. The number in each group is the aggregate of all four exomes.*

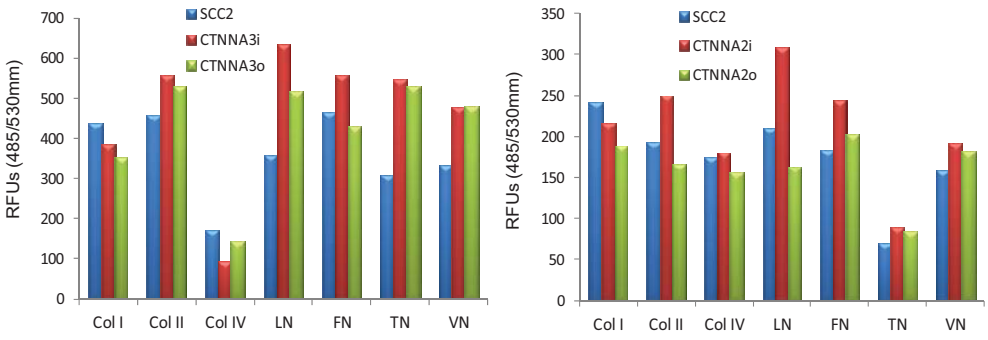

Figure S2. Adhesion profile of cell lines after silencing (i) or overexpression (o) of CTNNA2 and CTNNA3. *Affinity is expressed as relative fluorescence units (RFU). Col, collagen; LN, laminin; FN, fibronectin; TN, tenascin; VN, vitronectin.*

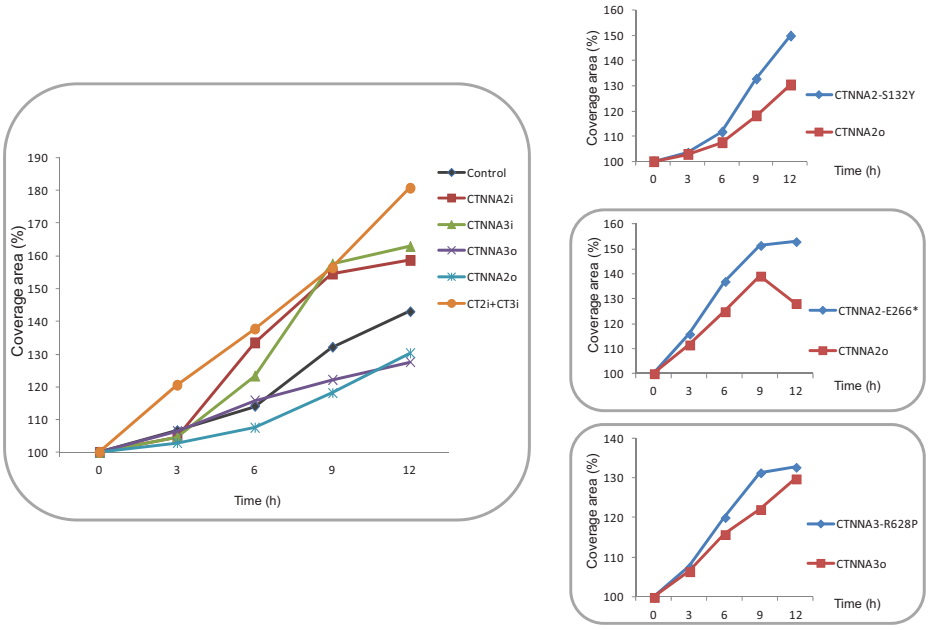

Figure S3. Migration of cell lines after silencing (i), overexpression of wild-type (o) or overexpression of mutant forms of CTNNA2 and CTNNA3. *Cell migration is represented as the percentage of the wound area covered by the cells at different time points.*

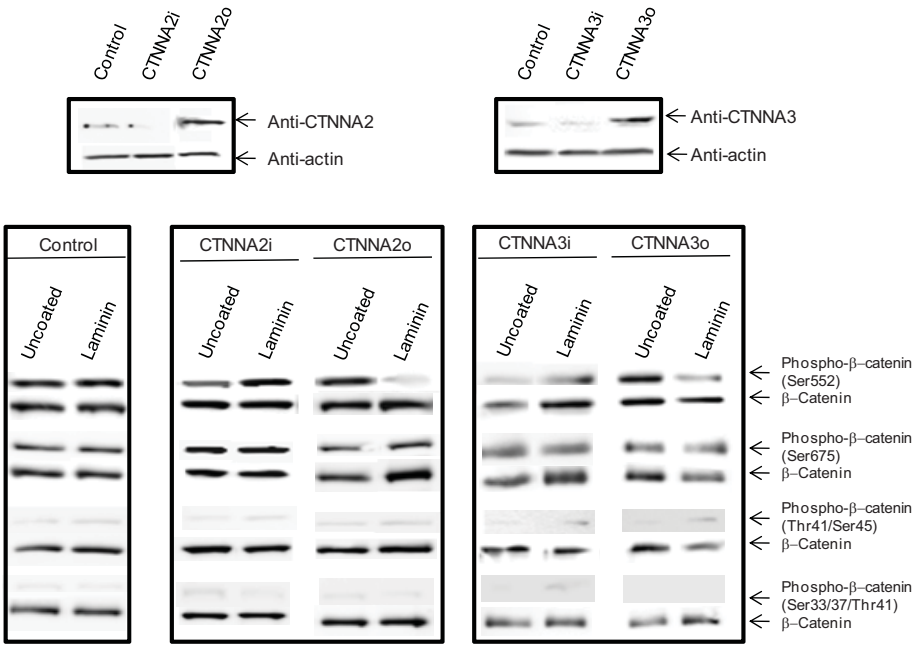

Figure S4. Phosphorylation levels of β-catenin in cell lines after silencing (i) or overexpression (o) of CTNNA2 and CTNNA3. *Each cell line was plated onto uncoated or laminin-coated wells, and the levels of phospho-β-catenin and total β-catenin were assessed by Western-blot. CTNNA2 and CTNNA3 levels in each cell line are shown on top.*

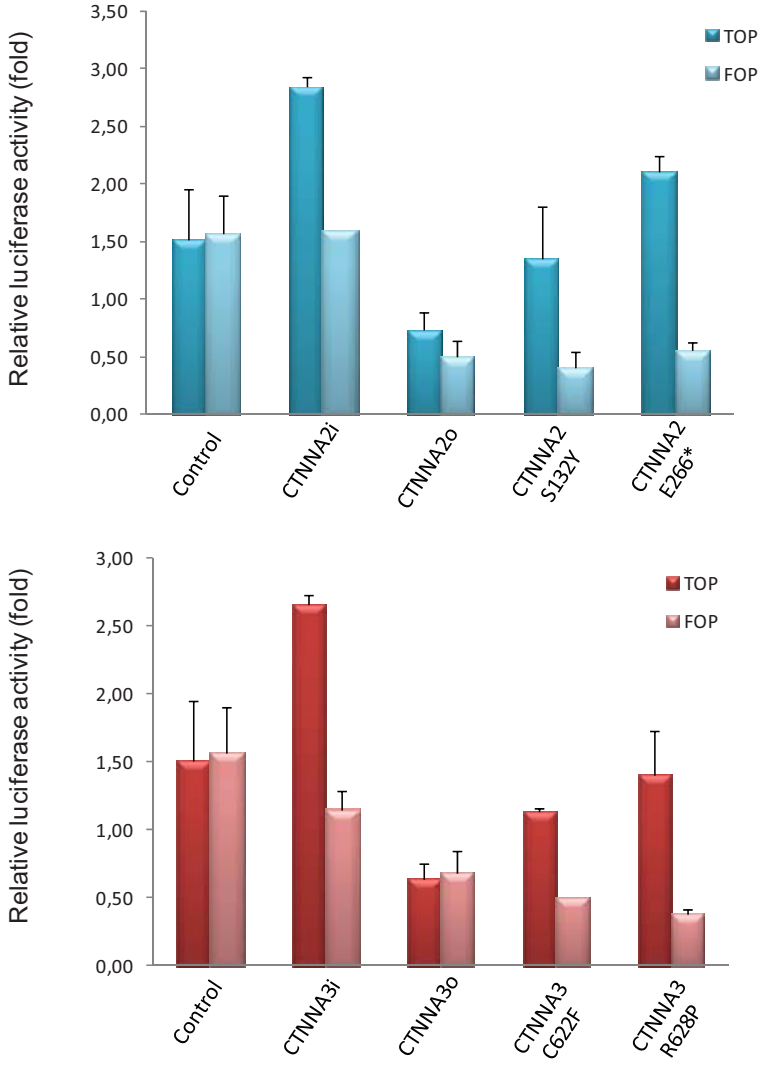

Figure S5. β-catenin transcriptional activity in cell lines after silencing (i), overexpression of wild-type (o) or overexpression of mutant forms of CTNNA2 (top panel) and CTNNA3 (bottom panel). *TOP, reporter with optimal Tcf-binding site; FOP, background assessed with Far-from-optimal Tcf-binding site.* *******, $P < 0.05$;* *********, $P < 0.005$.

Supplementary Table 1. Biological characteristics of HNSCC samples included in whole-exome analysis

Code	Age	Location	pTNM	Stage	Surgery	Status	OS
L000	71	Supraglottic	T4 N2c M0 G2 R0	4A	T+BND	Dead	6
L004	64	Supraglottic	T4a N0 M0 G1 R0	4A	T+BND	Alive	26
L005	56	Supraglottic	T4a N2c M0 G2 R0	4A	P+BND	Dead	26
L006	65	Glottic	T4a N2b M0 G3 R0	4A	T+BND	Dead	18

pTNM, Pathological tumor-node-metastasis stage; T, Total laryngectomy; P, Partial laryngectomy; BND, Bilateral neck disection; OS, Overall survival (months)

Supplementary Table 2. Statistics for whole-exome sequencing

Case	Sample	Number of mapped reads	Average depth	Callable exome
L000	Tumor	133558862	185	91,2%
	Normal	77271946	107	82,8%
L004	Tumor	68741551	93	90,6%
	Normal	75567031	102	90,9%
L005	Tumor	59100524	80	89,4%
	Normal	66920489	91	90,2%
L006	Tumor	62927897	87	85,1%
	Normal	44830623	62	82,8%

The callable exome includes all positions covered by more than 8 reads with Phred quality higher than 30

Supplementary Table 4. Somatic mutations in HNSCC with predicted functional consequences

Case	Symbol	Mutation Type	Effect	Chr	Position	Ref	Obs
L006	ABCA2	non_synonymous	W1464G	9	139908431	T	K
L000	ABCA9	non_synonymous	S1136G	17	67003929	A	R
L005	ABCB5	non_synonymous	F958L	7	20778612	T	W
L000	ABCB7	non_synonymous	S544R	X	74288872	C	S
L000	ABCD1	non_synonymous	R381P	X	153001626	G	S
L004	AC003682.1	non_synonymous	H333R	19	58058614	A	R
L005	ACAD11	non_synonymous	G730R	3	132278717	G	R
L000	ACADS	non_synonymous	A276P	12	121176366	G	S
L005	ACAT2	non_synonymous	E83Q	6	160184055	G	S
L000	ACCN5	non_synonymous	R57L	4	156784777	G	K
L000	ACCSL	non_synonymous	M78I	11	44069820	G	R
L005	ACMSD	non_synonymous	V68E	2	135619542	T	W
L004	ADAM18	non_synonymous	S132Y	8	39468098	C	M
L000	ADAMTS3	non_synonymous	K823E	4	73164117	A	R
L000	AFF2	non_synonymous	E774Q	X	148037895	G	S
L000	AHCYL2	non_synonymous	G404R	7	129046222	G	S
L004	AKAP9	non_synonymous	W2984C	7	91714916	G	K
L005	AMPD1	non_synonymous	K593N	1	115217493	G	K
L000	AMPH	non_synonymous	S117F	7	38530696	C	Y
L000	AMPH	non_synonymous	E79D	7	38534096	G	K
L004	ANK1	non_synonymous	R1257L	8	41550254	G	K
L000	ANK2	non_synonymous	R1865I	4	114275368	G	K
L005	ANK2	non_synonymous	R3441*	4	114280095	C	Y
L000	ANKRD18B	non_synonymous	D749Y	9	33558156	G	K
L005	ANKRD26P1	non_synonymous	Q108E	16	46598141	C	S
L000	ANO5	non_synonymous	K535E	11	22281260	A	R
L000	APOB	non_synonymous	E1334Q	2	21236248	G	S
L000	APOB	non_synonymous	K745*	2	21249671	A	W
L006	APOB	non_synonymous	E120*	2	21263835	G	K
L000	ARAP2	non_synonymous	W1036S	4	36149262	G	S
L005	ARHGAP20	non_synonymous	S1162I	11	110450185	G	K
L000	ARHGEF19	non_synonymous	E799K	1	16525096	G	R
L005	ARHGEF2	non_synonymous	R228*	1	155935127	C	Y
L005	ARID2	non_synonymous	G301C	12	46230652	G	K
L000	ARMCX2	non_synonymous	G266A	X	100911778	G	S
L004	ARRDC3	non_synonymous	D279N	5	90670774	G	R

L000	ATP11C	non_synonymous	D823Y	X	138845511	G	K
L005	ATP2C1	non_synonymous	E393Q	3	130683842	G	S
L005	ATP8A1	non_synonymous	T482A	4	42554597	A	R
L000	ATRNL1	non_synonymous	Q354*	10	116925373	C	Y
L005	AZIN1	non_synonymous	G84*	8	103851904	G	K
L000	BANK1	non_synonymous	R218G	4	102783710	A	R
L004	BCHE	non_synonymous	S356*	3	165547878	C	M
L004	BCL11A	non_synonymous	K736E	2	60687841	A	R
L004	BCL2L12	non_synonymous	R45G	19	50169213	C	S
L000	BCORL1	non_synonymous	A429D	X	129148034	C	M
L000	BCS1L	non_synonymous	K34N	2	219525812	G	K
L004	BEST3	non_synonymous	Y181H	12	70072614	T	Y
L000	BEX1	non_synonymous	R54P	X	102318042	G	S
L000	BRWD3	non_synonymous	D755N	X	79971718	G	R
L006	BTBD10	non_synonymous	I265V	11	13435116	A	R
L000	C10orf137	non_synonymous	D157N	10	127412464	G	R
L005	C10orf90	non_synonymous	E216*	10	128193414	G	K
L000	C10orf93	non_synonymous	A2587P	10	134622314	G	S
L006	C14orf177	non_synonymous	L47M	14	99182667	C	M
L000	C14orf50	non_synonymous	G85S	14	65031539	G	R
L000	C15orf2	non_synonymous	E284D	15	24921866	G	K
L000	C15orf2	non_synonymous	P958H	15	24923887	C	M
L005	C16orf61	splice	-	16	81015410	C	M
L006	C17orf47	non_synonymous	S179Y	17	56621012	C	M
L004	C18orf54	non_synonymous	G36D	18	51887049	G	R
L000	C1GALT1	non_synonymous	E272K	7	7278455	G	R
L000	C1orf94	non_synonymous	P511T	1	34677817	C	M
L000	C2orf85	non_synonymous	G498S	2	242815199	G	R
L000	C2orf85	non_synonymous	G498V	2	242815200	G	K
L005	C3AR1	non_synonymous	P213L	12	8212144	C	Y
L000	C3orf20	non_synonymous	P308R	3	14745888	C	S
L000	C4orf31	non_synonymous	E218*	4	121958474	G	K
L004	C4orf37	non_synonymous	R411K	4	98633938	G	R
L000	C5orf42	non_synonymous	E1519K	5	37183728	G	R
L000	C6	non_synonymous	R850L	5	41149444	G	K
L000	C6orf118	non_synonymous	A99S	6	165715516	G	K
L004	C8A	non_synonymous	P145T	1	57341851	C	M
L004	C8orf34	non_synonymous	H209N	8	69380944	C	M
L005	C8orf80	non_synonymous	A186E	8	27925185	C	M
L000	C9orf79	fs_del_1	A1125fs	9	90502775	GCC	GC
L000	CACNG1	non_synonymous	I119F	17	65051269	A	W

L000	CAPRIN2	indel_splice	-	12	30869440	ACC	AC
L004	CARD11	non_synonymous	D486V	7	2974148	A	W
L006	CASC3	non_synonymous	N120Y	17	38318066	A	W
L000	CCDC114	non_synonymous	D269H	19	48806979	G	S
L000	CCDC27	non_synonymous	P85L	1	3669299	C	Y
L000	CCDC40	non_synonymous	T50K	17	78013666	C	M
L006	CCDC41	non_synonymous	E322*	12	94763782	G	K
L004	CCNE1	non_synonymous	E408*	19	30314673	G	K
L005	CD109	non_synonymous	A1253S	6	74521982	G	K
L005	CD22	non_synonymous	L672V	19	35832847	C	S
L000	CD226	non_synonymous	H67L	18	67614152	A	W
L006	CD300LG	non_synonymous	S214P	17	41931333	T	Y
L005	CD37	non_synonymous	P158Q	19	49841982	C	M
L005	CD96	non_synonymous	D421E	3	111342635	T	W
L004	CDH10	non_synonymous	S250T	5	24535287	T	W
L000	CDH18	non_synonymous	V235F	5	19612651	G	K
L005	CDH18	non_synonymous	T583N	5	19483544	C	M
L005	CDH2	non_synonymous	V58E	18	25593873	T	W
L004	CDK18	non_synonymous	R206Q	1	205495263	G	R
L000	CELF6	non_synonymous	V422F	15	72580703	G	K
L004	CENPF	non_synonymous	M1506T	1	214816198	T	Y
L000	CEP112	non_synonymous	W122L	17	64171267	G	K
L000	CEP128	non_synonymous	K257*	14	81307106	A	W
L000	CHD3	non_synonymous	G1746V	17	7811245	G	K
L006	CHL1	non_synonymous	E1080K	3	440053	G	R
L000	CHM	non_synonymous	A87P	X	85233826	G	S
L000	CHN2	fs_del_1	E515fs	7	29552263	AGG	AG
L005	CHST1	non_synonymous	N214I	11	45671833	A	W
L006	CHST12	non_synonymous	T282P	7	2473118	A	M
L000	CIT	non_synonymous	G2037W	12	120128033	G	K
L000	CKAP2L	non_synonymous	I76L	2	113514722	A	M
L005	CLCN5	non_synonymous	T727A	X	49855362	A	R
L006	CLDN8	non_synonymous	R146T	21	31587807	G	S
L006	CLGN	non_synonymous	E266Q	4	141320093	G	S
L005	CNGB1	non_synonymous	R552L	16	57954437	G	K
L000	CNPPD1	non_synonymous	V252L	2	220037787	G	K
L000	CNTNAP2	non_synonymous	P1112H	7	147926825	C	M
L000	COL11A1	non_synonymous	P890T	1	103444639	C	M
L000	COL12A1	non_synonymous	R56G	6	75904571	A	R
L000	COL14A1	non_synonymous	I1389F	8	121301934	A	W
L000	COL19A1	non_synonymous	W171C	6	70639439	G	K

L004	COL22A1	non_synonymous	G693D	8	139763708	G	R
L004	COL4A4	non_synonymous	P127S	2	227983471	C	Y
L000	COL5A2	non_synonymous	P857H	2	189917728	C	M
L006	CPEB2	non_synonymous	D685H	4	15018830	G	S
L004	CSMD1	splice	-	8	2815330	C	S
L005	CSMD2	non_synonymous	A815D	1	34192211	C	M
L000	CSMD3	non_synonymous	S78I	8	114326968	G	K
L004	CSMD3	non_synonymous	Y2617N	8	113323243	T	W
L005	CSMD3	non_synonymous	P255T	8	114111139	C	M
L004	CTNNA2	non_synonymous	A761S	2	80831290	G	K
L000	CTNNA3	non_synonymous	R628P	10	68040229	G	S
L000	CTNND2	non_synonymous	V657L	5	11199566	G	S
L000	CXorf66	non_synonymous	V357I	X	139038072	G	R
L004	CYLC1	non_synonymous	K434I	X	83129017	A	W
L006	CYLD	non_synonymous	P757R	16	50826536	C	S
L000	CYP4B1	non_synonymous	R246C	1	47279696	C	Y
L000	DACH2	non_synonymous	L465Q	X	86068137	T	W
L005	DAPK1	non_synonymous	R1410H	9	90322140	G	R
L000	DBF4B	non_synonymous	T549I	17	42828419	C	Y
L006	DCBLD1	non_synonymous	E315G	6	117859966	A	R
L006	DCC	non_synonymous	F918L	18	50923743	C	M
L005	DCP1B	non_synonymous	E287Q	12	2062247	G	S
L006	DGKD	non_synonymous	R599L	2	234357930	G	K
L006	DHDDS	non_synonymous	L283R	1	26795465	T	K
L000	DHX29	non_synonymous	R986S	5	54566441	A	W
L000	DICER1	non_synonymous	N282I	14	95592975	A	W
L000	DMD	fs_ins_1	A648fs	X	32583869	CAAA	CAAAA
L000	DNAH3	non_synonymous	K1435N	16	21061273	G	S
L000	DNAH5	fs_del_1	K3554fs	5	13753554	TCC	TC
L000	DNMT3A	non_synonymous	R488P	2	25468900	G	S
L000	DOK6	non_synonymous	I83S	18	67266693	T	K
L005	DOK7	splice	-	4	3494485	G	R
L005	DTNA	non_synonymous	L307M	18	32400797	C	M
L000	DUSP9	non_synonymous	S325Y	X	152915579	C	M
L006	DYNC1I1	splice	-	7	95499194	G	S
L000	DYRK2	non_synonymous	A432P	12	68051981	G	S
L000	E2F3	non_synonymous	A53P	6	20402620	G	S
L000	EBF1	non_synonymous	A431V	5	158140055	C	Y
L000	EDA2R	non_synonymous	R47G	X	65825017	C	S
L005	EEF1A2	non_synonymous	A92S	20	62127259	G	K
L000	EFCAB4B	non_synonymous	G6R	12	3806150	G	S

L005	EGFLAM	non_synonymous	A872S	5	38451463	G	K
L005	EIF2B5	non_synonymous	I342M	3	183858388	C	S
L004	EIF2C3	non_synonymous	R631G	1	36505439	A	R
L000	ENPP3	splice	-	6	132045178	A	W
L004	ENPP3	non_synonymous	E400*	6	132006581	G	K
L005	EP300	non_synonymous	R335C	22	41523587	C	Y
L005	EP300	non_synonymous	R335L	22	41523588	G	K
L005	EP300	non_synonymous	Y1414C	22	41565575	A	R
L000	EPB41L3	non_synonymous	E21D	18	5489120	G	K
L005	EPB41L3	non_synonymous	A922V	18	5397133	C	Y
L005	EPG5	non_synonymous	H1608R	18	43469892	A	R
L005	ERGIC2	non_synonymous	Q64E	12	29523096	C	S
L004	ERMAP	non_synonymous	R234L	1	43305956	G	K
L004	EYS	fs_del_1	C270fs	6	66200539	GC	G
L005	F13B	non_synonymous	Y460D	1	197021941	T	K
L000	FAM120C	non_synonymous	M917V	X	54112238	A	R
L005	FAM124B	non_synonymous	D33Y	2	225266389	G	K
L005	FAM169A	non_synonymous	M221V	5	74109674	A	R
L005	FAM179B	non_synonymous	S1351*	14	45513971	C	S
L004	FAM192A	non_synonymous	E47Q	16	57206775	G	S
L000	FAM46D	non_synonymous	M215L	X	79698681	A	W
L000	FAM47B	non_synonymous	G615*	X	34962791	G	K
L000	FAM47C	non_synonymous	V483L	X	37027930	G	K
L000	FAM47C	non_synonymous	R710L	X	37028612	G	K
L000	FAM9A	non_synonymous	A183S	X	8763403	G	K
L004	FAT1	non_synonymous	W948*	4	187628138	G	R
L004	FAT4	non_synonymous	H2469Q	4	126367661	C	M
L005	FBN2	non_synonymous	R2822S	5	127595420	G	S
L005	FBN2	non_synonymous	G1906C	5	127640733	G	K
L005	FBXL2	non_synonymous	G78A	3	33406154	G	S
L005	FGA	non_synonymous	E559Q	4	155506906	G	S
L005	FGA	non_synonymous	E481Q	4	155507140	G	S
L006	FGD2	non_synonymous	D606A	6	36995788	A	M
L000	FGF13	non_synonymous	Y132F	X	137785183	A	W
L000	FILIP1	non_synonymous	R1154W	6	76018589	C	Y
L000	FLT3	splice	-	13	28599082	T	W
L005	FMO3	splice	-	1	171077218	A	W
L000	FMOD	non_synonymous	P46Q	1	203317262	C	M
L000	FMR1NB	non_synonymous	G253V	X	147106510	G	K
L006	FOXE1	non_synonymous	R86S	9	100616452	C	M
L006	FTSJD2	non_synonymous	P554R	6	37440235	C	S

L000	FZD10	non_synonymous	M520I	12	130649047	G	K
L005	GABRG2	non_synonymous	D48Y	5	161520868	G	K
L005	GAK	non_synonymous	E825*	4	861143	G	K
L006	GALR2	non_synonymous	Y164S	17	74072839	A	M
L004	GATAD2B	non_synonymous	G561E	1	153782753	G	R
L000	GDF3	non_synonymous	F4I	12	7848315	T	W
L005	GDPD1	non_synonymous	R271P	17	57350187	G	S
L005	GGH	non_synonymous	W252L	8	63930132	G	K
L004	GIPC2	non_synonymous	T234N	1	78585170	C	M
L005	GLP2R	non_synonymous	C330F	17	9765340	G	K
L000	GNAQ	non_synonymous	R166S	9	80412545	C	M
L000	GPATCH8	non_synonymous	G596R	17	42477659	G	S
L000	GPHN	non_synonymous	R644W	14	67626186	A	W
L000	GPR112	non_synonymous	D34V	X	135404967	A	W
L000	GPR50	non_synonymous	P356H	X	150349122	C	M
L004	GPR78	non_synonymous	S49Y	4	8582855	C	M
L000	GRIA1	non_synonymous	Y547F	5	153085414	A	W
L004	GRIA2	non_synonymous	N730K	4	158281194	C	M
L000	GRIPAP1	non_synonymous	H447D	X	48839786	C	S
L000	GRM1	non_synonymous	S1157W	6	146755817	C	S
L005	GRM3	non_synonymous	A299T	7	86416003	G	R
L005	GRM3	non_synonymous	W355C	7	86416173	G	K
L005	GRPR	non_synonymous	A274T	X	16170433	G	R
L004	GTF2F1	non_synonymous	A67E	19	6389581	C	M
L005	GTF2IRD1	non_synonymous	P514S	7	73952500	C	Y
L006	GTF3C3	non_synonymous	N406K	2	197645283	T	W
L000	HDAC10	non_synonymous	F253L	22	50687317	T	W
L000	HDX	non_synonymous	G344E	X	83723700	G	R
L000	HERC5	non_synonymous	V550F	4	89400569	G	K
L000	HERC5	non_synonymous	P902L	4	89425505	C	Y
L000	HFM1	non_synonymous	D367N	1	91844679	G	R
L000	HIF3A	non_synonymous	R244S	19	46812576	C	M
L005	HIST1H1B	non_synonymous	K149*	6	27834863	A	W
L004	HIST1H3A	fs_del_1	G13fs	6	26020756	TGG	TG
L005	HIVEP2	non_synonymous	I556F	6	143094210	A	W
L000	HJURP	non_synonymous	R74I	2	234761230	G	K
L006	HLA-DPA1	non_synonymous	D202A	6	33036819	A	M
L005	HLA-DQB1	non_synonymous	Y62N	6	32632770	T	W
L000	HMCN1	non_synonymous	T2358P	1	186024734	A	M
L000	HSD17B14	non_synonymous	G254V	19	49316484	G	K
L000	HSPG2	non_synonymous	H2677R	1	22173981	A	R

L006	HYAL4	non_synonymous	D445H	7	123517096	G	S
L005	HYDIN	non_synonymous	L2585I	16	70954526	C	M
L006	ID1	non_synonymous	I99M	20	30193487	C	S
L000	IFNE	non_synonymous	E129*	9	21481309	G	K
L006	IFT46	non_synonymous	H50L	11	118428502	A	W
L000	IGF2	non_synonymous	A12V	11	2182167	C	Y
L005	IL23R	non_synonymous	G495*	1	67724404	G	K
L005	IMPG1	non_synonymous	S128N	6	76744423	G	R
L000	IMPG2	non_synonymous	K106N	3	101038444	G	S
L005	ING1	non_synonymous	I23M	13	111366565	C	S
L005	INHBA	non_synonymous	R152S	7	41730075	C	M
L000	IRF4	non_synonymous	K80*	6	394842	A	W
L000	IRS4	non_synonymous	G706V	X	107977458	G	K
L000	IRS4	non_synonymous	G706W	X	107977459	G	K
L000	ITGA2B	non_synonymous	S803N	17	42453493	G	R
L000	ITGBL1	non_synonymous	C455W	13	102366873	C	S
L000	ITIH2	non_synonymous	I21F	10	7745458	A	W
L004	ITIH2	non_synonymous	G653E	10	7780584	G	R
L004	JRKL	non_synonymous	I468T	11	96125216	T	Y
L004	KCNK10	non_synonymous	R424L	14	88652240	G	K
L004	KCNMB4	non_synonymous	Q124K	12	70794022	C	M
L000	KCNV1	non_synonymous	G336W	8	110980814	G	K
L000	KDR	non_synonymous	A1031G	4	55956223	C	S
L004	KDR	non_synonymous	L1272S	4	55948156	T	Y
L004	KIAA1109	non_synonymous	G2067*	4	123176084	G	K
L006	KIAA1109	non_synonymous	R3539C	4	123237962	C	Y
L004	KIAA1217	non_synonymous	R430P	10	24762599	G	S
L000	KIAA1409	non_synonymous	D1205N	14	94069623	G	R
L005	KIF26B	non_synonymous	P405H	1	245704116	C	M
L005	KLHL1	non_synonymous	K222M	13	70549767	A	W
L000	KLHL15	non_synonymous	H73N	X	24024594	C	M
L006	KRBA2	non_synonymous	V308F	17	8273009	G	K
L000	KRTAP11-1	non_synonymous	Q88H	21	32253580	A	W
L000	KRTAP19-4	non_synonymous	G42R	21	31869305	G	S
L006	KTN1	non_synonymous	D628H	14	56106689	G	S
L000	L1CAM	non_synonymous	T677S	X	153132924	C	S
L000	LAIR1	non_synonymous	L186I	19	54868127	C	M
L000	LAMA1	non_synonymous	E1291K	18	7010201	G	R
L000	LBR	non_synonymous	R347L	1	225600200	G	K
L000	LEKR1	non_synonymous	G638W	3	156763372	G	K
L000	LEMD3	non_synonymous	I487M	12	65564837	A	R

L000	LPIN2	non_synonymous	R280*	18	2938020	C	Y
L000	LRAT	non_synonymous	A145T	4	155665911	G	R
L000	LRFN3	non_synonymous	A104P	19	36430637	G	S
L000	LRRC15	non_synonymous	G388E	3	194080628	G	R
L005	LRRC36	non_synonymous	Q352H	16	67401221	G	K
L006	LRRIQ1	non_synonymous	D1499N	12	85546877	G	R
L006	LRRN3	non_synonymous	H564Y	7	110764518	C	Y
L005	LYPD3	non_synonymous	A301S	19	43965643	G	K
L000	MAGEA1	non_synonymous	G193C	X	152482434	G	K
L000	MAGEB1	non_synonymous	Q59K	X	30268785	C	M
L000	MAGEB10	fs_ins_1	G215fs	X	27840068	CAA	CAAA
L005	MAGEB10	non_synonymous	P268T	X	27840225	C	M
L000	MAGEB3	non_synonymous	R67I	X	30254241	G	K
L000	MAGEB4	non_synonymous	N298H	X	30261144	A	M
L000	MAGEB6	non_synonymous	Y229*	X	26212650	C	S
L000	MAGEC1	non_synonymous	D573G	X	140994908	A	R
L006	MAML1	non_synonymous	Y974C	5	179201748	A	R
L000	MAMLD1	non_synonymous	A262D	X	149638705	C	M
L004	MAP2	non_synonymous	P1323T	2	210560861	C	M
L000	MAP7	non_synonymous	R143M	6	136710538	G	K
L000	MAPK4	non_synonymous	Q177E	18	48190857	C	S
L005	MAPK4	non_synonymous	E94K	18	48190608	G	R
L006	MARCH6	fs_del_1	I473fs	5	10405756	AT	A
L005	MARS2	non_synonymous	V255M	2	198570892	G	R
L000	MBOAT1	non_synonymous	Q352L	6	20115540	A	W
L000	MBTPS1	non_synonymous	V1052L	16	84088059	G	K
L000	MBTPS2	non_synonymous	P404H	X	21896760	C	M
L000	MCHR2	non_synonymous	W93L	6	100395752	G	K
L000	MDGA2	non_synonymous	R859S	14	47343266	C	M
L004	MDGA2	non_synonymous	P188T	14	47687257	C	M
L006	MERTK	non_synonymous	E571*	2	112760689	G	K
L000	MINPP1	non_synonymous	R186C	10	89265228	C	Y
L005	MIR299	-	-	14	101490173	T	K
L000	MKS1	non_synonymous	V320F	17	56288341	G	K
L005	MLL3	non_synonymous	E2718Q	7	151874386	G	S
L000	MLLT4	non_synonymous	E1552*	6	168352709	G	K
L000	MON2	non_synonymous	S774Y	12	62932242	C	M
L000	MOSC2	non_synonymous	L94Q	1	220928297	T	W
L004	MRPL51	non_synonymous	R81Q	12	6601582	G	R
L005	MRPL55	non_synonymous	R126Q	1	228294579	G	R
L005	MRPS11	non_synonymous	I133M	15	89018458	A	R

L000	MSH5	non_synonymous	A673G	6	31728969	C	S
L000	MSN	non_synonymous	P22H	X	64936732	C	M
L000	MTF1	non_synonymous	V30L	1	38323243	G	K
L005	MTF1	non_synonymous	K196*	1	38305653	A	W
L004	MTHFD1L	non_synonymous	Y829C	6	151336729	A	R
L000	MTM1	non_synonymous	G378R	X	149826372	G	R
L000	MTMR3	non_synonymous	W215R	22	30398954	T	W
L000	MXRA5	non_synonymous	K919*	X	3241046	A	W
L000	MYADM	non_synonymous	L216Q	19	54377430	T	W
L005	MYBBP1A	non_synonymous	Q1029H	17	4445759	G	S
L004	MYH10	non_synonymous	T763I	17	8422254	C	Y
L000	MYH3	non_synonymous	N603K	17	10545813	C	S
L000	MYH8	non_synonymous	A1156V	17	10303975	C	Y
L005	MYH8	non_synonymous	Q501K	17	10314180	C	M
L005	MYH9	non_synonymous	E1496Q	22	36685202	G	S
L006	NBPF3	non_synonymous	Q601E	1	21809778	C	S
L000	NCAM2	non_synonymous	C734F	21	22881295	G	K
L005	NCAPG	non_synonymous	L407V	4	17824706	C	S
L000	NDST4	non_synonymous	P200T	4	115997595	C	M
L000	NELL1	non_synonymous	R382Q	11	20959395	G	R
L004	NETO1	non_synonymous	T341N	18	70417816	C	M
L000	NID1	non_synonymous	I771K	1	236176803	T	W
L000	NKRF	non_synonymous	P178A	X	118724901	C	S
L000	NLRP12	non_synonymous	L32V	19	54327335	C	S
L000	NLRP13	non_synonymous	L508P	19	56423660	T	Y
L004	NLRP14	non_synonymous	H480R	11	7064696	A	R
L004	NLRP14	non_synonymous	H480Q	11	7064697	C	M
L004	NPBWR1	non_synonymous	Y290*	8	53853337	C	S
L005	NPHS1	non_synonymous	I434T	19	36339169	T	Y
L000	NR2F1	fs_del_1	A223fs	5	92923828	CG	C
L006	NTNG2	non_synonymous	D226N	9	135073815	G	R
L005	NUP43	non_synonymous	L187V	6	150059858	C	S
L000	OCA2	non_synonymous	H285Y	15	28261287	C	Y
L000	ODZ1	non_synonymous	V2421L	X	123517520	G	S
L000	ODZ1	non_synonymous	T1892S	X	123525916	A	W
L004	OGN	non_synonymous	L8I	9	95165668	C	M
L004	OR10AG1	non_synonymous	L292F	11	55735064	G	K
L005	OR10R2	non_synonymous	E252K	1	158450421	G	R
L000	OR10S1	non_synonymous	V112L	11	123848128	G	K
L000	OR14A16	non_synonymous	M21R	1	247978970	T	K
L000	OR2G2	non_synonymous	K310N	1	247752591	G	K

L000	OR2T10	non_synonymous	G233V	1	248756372	G	K
L000	OR4C15	non_synonymous	L20*	11	55321841	T	K
L000	OR4C15	non_synonymous	R39T	11	55321898	G	S
L005	OR4K13	non_synonymous	L107Q	14	20502598	T	W
L006	OR51F2	non_synonymous	S161R	11	4843098	C	M
L000	OR56A3	non_synonymous	Y222D	11	5969240	T	K
L000	OR5A1	non_synonymous	F34S	11	59210742	T	Y
L000	OR5B2	non_synonymous	L185M	11	58190182	C	M
L000	OR5D13	non_synonymous	S66N	11	55541110	G	R
L000	OR5D16	non_synonymous	P192T	11	55606801	C	M
L000	OR5T1	non_synonymous	G3V	11	56043122	G	K
L005	OR6B1	non_synonymous	A265S	7	143701882	G	K
L004	OR6F1	non_synonymous	P283A	1	247875211	C	S
L000	OR6M1	non_synonymous	N135K	11	123676653	C	S
L006	OR6Q1	non_synonymous	A151G	11	57798876	C	S
L000	OR8J1	non_synonymous	R122L	11	56128087	G	K
L006	P2RY1	non_synonymous	F40L	3	152553691	C	S
L000	PACSIN3	non_synonymous	P338Q	11	47200469	C	M
L000	PARP4	non_synonymous	S577C	13	25051899	A	W
L000	PAX1	non_synonymous	S215I	20	21687433	G	K
L000	PBLD	non_synonymous	F253L	10	70044042	T	W
L000	PCBP2	non_synonymous	P327L	12	53865507	C	Y
L004	PCDH11X	non_synonymous	P967S	X	91134138	C	Y
L000	PCDH12	non_synonymous	P242L	5	141336692	C	Y
L004	PCDH15	non_synonymous	R967C	10	55721637	C	Y
L005	PCDH8	non_synonymous	E888Q	13	53419737	G	S
L006	PCDHB17	non_synonymous	S544R	5	140537208	C	M
L000	PCDHB3	non_synonymous	P206A	5	140480849	C	S
L004	PCDHB7	non_synonymous	Q73*	5	140552633	C	Y
L000	PCNT	non_synonymous	K587*	21	47773980	A	W
L005	PDE4A	non_synonymous	F262L	19	10565507	C	S
L005	PDZD2	non_synonymous	A2658E	5	32098495	C	M
L000	PGRMC1	non_synonymous	W156*	X	118374410	G	R
L000	PHACTR2	non_synonymous	N408H	6	144086925	A	M
L000	PHACTR3	non_synonymous	P220S	20	58342357	C	Y
L004	PHC3	non_synonymous	R296P	3	169854239	G	S
L004	PHF3	non_synonymous	T1456I	6	64421851	C	Y
L000	PHKA2	non_synonymous	D620H	X	18938255	G	S
L006	PHLDB2	non_synonymous	D464H	3	111632220	G	S
L000	PIBF1	non_synonymous	N407I	13	73409503	A	W
L000	PIK3CA	non_synonymous	N345K	3	178921553	T	W

L000	PIKFYVE	non_synonymous	L349H	2	209163499	T	W
L000	PKHD1	non_synonymous	G1122C	6	51897828	G	K
L005	PLCE1	non_synonymous	A1572S	10	96039587	G	K
L000	PLCL1	non_synonymous	S978R	2	198966023	C	M
L004	PLEKHA7	non_synonymous	Q706L	11	16824559	A	W
L000	PLG	non_synonymous	A587S	6	161157996	G	K
L004	PLXNA3	non_synonymous	E1291K	X	153696475	G	R
L000	PLXNC1	non_synonymous	G473V	12	94580228	G	K
L000	POLR1B	splice	-	2	113322077	G	K
L005	POTEC	non_synonymous	G81V	18	14542904	G	K
L005	POU2F2	non_synonymous	L87V	19	42621446	C	S
L000	PPFIBP2	non_synonymous	R527*	11	7663590	C	Y
L005	PPP1R9A	non_synonymous	L1221F	7	94915569	C	Y
L000	PPP2R4	non_synonymous	L201V	9	131897109	C	S
L004	PPP3CB	non_synonymous	D106N	10	75238352	G	R
L006	PQBP1	non_synonymous	E122*	X	48759581	G	K
L005	PRDM2	non_synonymous	V515A	1	14105834	T	Y
L000	PROL1	non_synonymous	T201N	4	71275647	C	M
L004	PRR14	non_synonymous	A372T	16	30666405	G	R
L005	PRTG	non_synonymous	S420G	15	55970118	A	R
L006	PTEN	non_synonymous	Q171*	10	89711893	C	Y
L000	PTER	non_synonymous	M54I	10	16526545	G	K
L004	PTER	non_synonymous	K62*	10	16526567	A	W
L005	PTGS2	non_synonymous	F187L	1	186646859	T	W
L000	PTPRM	non_synonymous	E1315K	18	8384580	G	R
L000	PTPRS	non_synonymous	A812P	19	5225801	G	S
L005	PTPRZ1	non_synonymous	M382V	7	121637964	A	R
L004	PUS10	non_synonymous	E221K	2	61192574	G	R
L006	PXMP4	splice	-	20	32302478	A	M
L004	PYHIN1	non_synonymous	S386T	1	158913733	T	W
L006	RAB22A	non_synonymous	D135E	20	56929239	C	S
L000	RAB2A	non_synonymous	D51N	8	61484637	G	R
L000	RAI2	non_synonymous	P379H	X	17818995	C	M
L000	RALGAPB	non_synonymous	R384L	20	37146248	G	K
L000	RANBP2	non_synonymous	E1384K	2	109381145	G	R
L000	RAPGEF4	non_synonymous	V827I	2	173891908	G	R
L006	RBFOX1	non_synonymous	H314P	16	7703871	A	M
L000	REG3G	non_synonymous	M13I	2	79253258	G	S
L004	RFX4	non_synonymous	S696R	12	107155100	C	M
L000	RFX6	non_synonymous	S201R	6	117215186	T	K
L000	RHOJ	non_synonymous	T76S	14	63735876	C	S

L006	RLIM	fs_del_2	R45fs	X	73815679	CTATA	CTA
L000	RNF213	non_synonymous	R780W	17	78272299	C	Y
L000	RORB	non_synonymous	D414N	9	77286800	G	R
L000	RPP30	non_synonymous	S82*	10	92635830	C	M
L005	RPS6KA3	non_synonymous	G429R	X	20190932	G	R
L000	RPS6KA6	non_synonymous	L644F	X	83351241	G	K
L006	RRN3	non_synonymous	R632Q	16	15155662	G	R
L000	RTN1	non_synonymous	I498N	14	60193909	T	W
L005	RYR3	non_synonymous	Y4122*	15	34130547	C	M
L004	SAMD4A	non_synonymous	S183Y	14	55169131	C	M
L000	SCAND3	non_synonymous	K481N	6	28543039	G	K
L005	SCN2A	non_synonymous	L1036S	2	166210889	T	Y
L005	SCN5A	non_synonymous	E171*	3	38662434	G	K
L005	SDAD1	non_synonymous	V377G	4	76885339	T	K
L005	SDF2	non_synonymous	I92M	17	26982377	C	S
L004	SEC23IP	non_synonymous	M225L	10	121658448	A	W
L000	SELE	non_synonymous	S541T	1	169696514	T	W
L004	SEMA3D	non_synonymous	D256E	7	84685126	T	W
L006	SEMA5B	non_synonymous	E275Q	3	122646826	G	S
L005	SEPN1	non_synonymous	T121M	1	26131693	C	Y
L000	SEPT4	non_synonymous	R359P	17	56598653	G	S
L005	SERINC3	non_synonymous	G147C	20	43139966	G	K
L004	SFMBT2	non_synonymous	V481L	10	7247780	G	S
L005	SGPL1	non_synonymous	E185Q	10	72619194	G	S
L000	SI	non_synonymous	R132S	3	164786597	G	S
L000	SIM1	non_synonymous	V760G	6	100838259	T	K
L005	SIM1	non_synonymous	A450G	6	100841584	C	S
L000	SIPA1L2	non_synonymous	G417R	1	232649837	G	R
L006	SIPA1L3	non_synonymous	E1526Q	19	38682930	G	S
L000	SIRPB1	non_synonymous	L375F	20	1546875	C	Y
L005	SIRPG	non_synonymous	G200E	20	1616983	G	R
L006	SLC12A5	non_synonymous	G1130S	20	44686212	G	R
L000	SLC17A4	non_synonymous	G129C	6	25770382	G	K
L005	SLC18A2	non_synonymous	S80A	10	119003598	T	K
L000	SLC25A14	non_synonymous	H31Y	X	129479180	C	Y
L006	SLC25A24	non_synonymous	I247V	1	108697688	A	R
L005	SLC27A6	non_synonymous	F96L	5	128302118	C	M
L005	SLC30A6	non_synonymous	G2V	2	32396357	G	K
L006	SLC35E4	non_synonymous	S272R	22	31042781	C	S
L004	SLC39A12	non_synonymous	R76L	10	18242432	G	K
L004	SLC39A12	non_synonymous	H284Y	10	18266929	C	Y

L006	SLC7A11	non_synonymous	L388V	4	139101899	C	S
L000	SLC7A14	non_synonymous	W225C	3	170216540	G	S
L000	SLC8A3	non_synonymous	D715E	14	70515746	T	W
L000	SLIT3	non_synonymous	S277F	5	168233556	C	Y
L000	SLITRK2	non_synonymous	G104A	X	144904254	G	S
L000	SLITRK4	non_synonymous	D354N	X	142717865	G	R
L004	SNAPC4	del_1res	E543-	9	139277994	GCT	-
L000	SNCAIP	non_synonymous	C228F	5	121758974	G	K
L000	SNTG1	non_synonymous	D184E	8	51449240	C	M
L005	SNX27	non_synonymous	I202V	1	151630771	A	R
L000	SOX9	non_synonymous	S448C	17	70120341	C	S
L000	SP140	non_synonymous	L601F	2	231155257	A	W
L000	SPAM1	non_synonymous	Y260*	7	123594404	C	S
L000	SPANXN3	non_synonymous	D86Y	X	142596814	G	K
L005	SPATA17	non_synonymous	L284Q	1	217955643	T	W
L000	SPTA1	non_synonymous	Q255*	1	158648240	C	Y
L004	SPTA1	non_synonymous	R2016L	1	158592846	G	K
L004	SRCRB4D	non_synonymous	E136A	7	76029671	A	M
L000	SRPX2	non_synonymous	Y133N	X	99919812	T	W
L006	SRRT	non_synonymous	K343M	7	100482446	A	W
L000	STAC	non_synonymous	S27F	3	36422215	C	Y
L000	STK33	non_synonymous	D299N	11	8462277	G	R
L006	STX3	non_synonymous	M216V	11	59560958	A	R
L005	SUV420H2	non_synonymous	D195N	19	55857593	G	R
L000	SYN3	fs_ins_1	N233fs	22	33260916	TGGGG	TGGGGG
L000	SYNCRIP	non_synonymous	N344S	6	86329113	A	R
L006	SYNPO	non_synonymous	E802D	5	150029511	G	S
L000	SYT3	non_synonymous	P469S	19	51128819	C	Y
L000	SYTL4	fs_ins_1	G300fs	X	99944870	CT	CTT
L000	TACR3	non_synonymous	P228T	4	104579427	C	M
L000	TAF1	non_synonymous	R1163L	X	70617187	G	K
L005	TAF6L	non_synonymous	Y619F	11	62554755	A	W
L000	TAGLN3	non_synonymous	I80V	3	111719676	A	R
L000	TAS1R2	non_synonymous	L559P	1	19166937	T	Y
L000	TBX22	non_synonymous	V325A	X	79286021	T	Y
L005	TDRD3	non_synonymous	R395I	13	61102543	G	K
L005	TECPR2	non_synonymous	E450Q	14	102898396	G	S
L000	TECTA	non_synonymous	G502C	11	120996311	G	K
L006	TGFB2	non_synonymous	S403F	1	218614583	C	Y
L000	TGFBR2	non_synonymous	D440G	3	30713811	A	R
L005	TGFBR3	non_synonymous	K425N	1	92185588	G	K

L000	THNSL2	non_synonymous	D39H	2	88472784	G	S
L000	THOC2	non_synonymous	T1049I	X	122758432	C	Y
L006	TIAM2	non_synonymous	Q52E	6	155154383	C	S
L006	TIPIN	non_synonymous	D291N	15	66629331	G	R
L000	TKTL2	non_synonymous	T132I	4	164394492	C	Y
L000	TMLHE	non_synonymous	S94C	X	154754195	A	W
L000	TMPRSS11F	non_synonymous	Q90*	4	68956255	C	Y
L005	TNFAIP8L3	non_synonymous	T39K	15	51397258	C	M
L006	TOX	non_synonymous	S241C	8	59750842	C	S
L006	TOX	non_synonymous	Q11H	8	60031514	G	S
L004	TP53	non_synonymous	E204*	17	7578239	G	K
L006	TP53	non_synonymous	H193L	17	7578271	A	W
L004	TRAPPC1	non_synonymous	S136F	17	7833955	C	Y
L000	TRIM58	non_synonymous	G442D	1	248039655	G	R
L000	TRIM60	non_synonymous	D300Y	4	165962122	G	K
L004	TRIM6-TRIM34	non_synonymous	R268L	11	5626766	G	K
L000	TRO	non_synonymous	S752R	X	54955411	A	M
L006	TRPA1	non_synonymous	I735V	8	72951192	A	R
L006	TRPM4	non_synonymous	Q1007R	19	49705287	A	R
L004	TRRAP	non_synonymous	E850D	7	98515230	G	S
L004	TSHZ1	non_synonymous	T138P	18	72997909	A	M
L005	TTN	non_synonymous	E10070V	2	179542905	A	W
L004	TYW1	non_synonymous	V582M	7	66648158	G	R
L006	U2AF1	non_synonymous	S34Y	21	44524456	C	M
L006	UGDH	non_synonymous	R114T	4	39512405	G	S
L000	UGGT2	non_synonymous	D387H	13	96624859	G	S
L000	UMPS	non_synonymous	T77A	3	124454012	A	R
L000	UNC5CL	non_synonymous	R211P	6	41001674	G	S
L006	UPF1	non_synonymous	K881N	19	18974289	G	S
L000	USH2A	non_synonymous	G1192C	1	216373206	G	K
L004	USH2A	non_synonymous	R3538*	1	215955512	C	Y
L005	USP8	non_synonymous	Q490H	15	50773929	G	S
L000	VCAN	non_synonymous	Q2823K	5	82837289	C	M
L000	VCL	non_synonymous	R246H	10	75834615	G	R
L005	VCP	non_synonymous	S748N	9	35057445	G	R
L004	VEPH1	non_synonymous	W697L	3	157004384	G	K
L004	VIPR2	non_synonymous	I434T	7	158827273	T	Y
L000	VN1R1	non_synonymous	F125L	19	57967480	T	W
L000	WBSCR17	non_synonymous	E144Q	7	70853228	G	S
L000	WBSCR27	non_synonymous	K177N	7	73249280	G	S
L006	WDFY3	non_synonymous	S17R	4	85781694	C	S

L006	WDR6	non_synonymous	L631P	3	49050769	T	Y
L000	WDR77	non_synonymous	E188V	1	111986677	A	W
L000	XIAP	non_synonymous	R131M	X	123019904	G	K
L004	XIRP2	non_synonymous	S2663L	2	168105890	C	Y
L004	XIRP2	non_synonymous	E3180D	2	168107442	A	W
L004	ZBBX	non_synonymous	N359K	3	167035292	C	S
L006	ZBBX	non_synonymous	P541A	3	167023535	C	S
L004	ZBED4	non_synonymous	A943V	22	50280138	C	Y
L000	ZBTB16	non_synonymous	A96E	11	113934309	C	M
L000	ZBTB33	non_synonymous	G455W	X	119388633	G	K
L000	ZBTB33	non_synonymous	G455V	X	119388634	G	K
L004	ZCCHC7	non_synonymous	S504*	9	37357144	C	M
L000	ZDHHC4	non_synonymous	Y273C	7	6628324	A	R
L000	ZMYM3	non_synonymous	P1283H	X	70461155	C	M
L000	ZMYM3	non_synonymous	C1075F	X	70464214	G	K
L005	ZNF19	non_synonymous	A421S	16	71509189	G	K
L000	ZNF217	non_synonymous	E201*	20	52198765	G	K
L000	ZNF229	non_synonymous	P260T	19	44934178	C	M
L006	ZNF248	non_synonymous	G383D	10	38121135	G	R
L000	ZNF254	non_synonymous	G141A	19	24309224	G	S
L006	ZNF33A	non_synonymous	E83Q	10	38306290	G	S
L006	ZNF384	non_synonymous	H335P	12	6781606	A	M
L000	ZNF425	non_synonymous	G644C	7	148801033	G	K
L004	ZNF425	non_synonymous	K484M	7	148801512	A	W
L004	ZNF43	non_synonymous	T343S	19	21991812	A	W
L000	ZNF45	non_synonymous	R604S	19	44417776	G	K
L000	ZNF460	non_synonymous	R292S	19	57802783	C	M
L005	ZNF480	non_synonymous	R416L	19	52825750	G	K
L000	ZNF493	non_synonymous	Y685*	19	21607516	C	M
L004	ZNF507	non_synonymous	E685*	19	32845789	G	K
L000	ZNF521	non_synonymous	V535F	18	22806279	G	K
L005	ZNF544	non_synonymous	E299*	19	58772867	G	K
L000	ZNF551	non_synonymous	I659V	19	58199618	A	R
L006	ZNF583	non_synonymous	F249L	19	56934772	T	Y
L005	ZNF593	non_synonymous	R132T	1	26497103	G	S
L005	ZNF611	non_synonymous	R199S	19	53209711	G	K
L000	ZNF645	non_synonymous	Q301H	X	22292011	G	S
L000	ZNF665	non_synonymous	W22R	19	53678776	T	W
L006	ZNF770	non_synonymous	I159V	15	35275161	A	R
L000	ZNF81	non_synonymous	C503F	X	47775553	G	K
L000	ZNF814	non_synonymous	C247S	19	58386019	T	W

L004	ZSCAN4	non_synonymous	G213V	19	58189609	G	K

Supplementary Table 5. Biological characteristics of HNSCC samples in the validation series

Code	Age	Location	pTNM	Stage	Surgery	Status	OS
HN01	60	Supraglottic	T2 N2b M0 G2 R1	4A	P+BND	Alive	60
HN02	63	Supraglottic	T4a N2b M0 G2 R0	4A	T+BND	Alive	68
HN03	57	Supraglottic	T3 N2c M0G3 R0	4A	P+BND	Alive	36
HN04	62	Glottic	T3 N2c M0 G2 R0	4A	T+BND	Alive	24
HN05	61	Glottic	T3 N0 M0 G1 R0	3	T	Dead*	2
HN06	64	Supraglottic	T3 N0 M0 G1 R0	3	P+BND	Alive	14
HN08	75	Supraglottic	T3 N1 M0 G3 R0	3	T+UND	Alive	33
HN09	65	Supraglottic	T2 N0 M0 G1 R1	2	P+BND	Alive	108
HN10	77	Glottic	T1 N0 M0 G1 R0	1	P	Dead	72
HN11	50	Supraglottic	T3 N1 M G1 R0	3	P+BND	Dead	48
HN12	79	Supraglottic	T3 N2c M0 G3 R0	4A	P+BND	Alive	48
HN13	56	Supraglottic	T3 N2b M0 G2 R0	4A	T+BND	Dead	50
HN14	64	Supraglottic	T2 N3 M0 G2 R1	4B	T+UND	Dead	2
HN16	57	Glottic	T3 N0 M0 G2 R0	3	T+BND	Alive	26
HN17	86	Supraglottic	T3 N2c MoG3 R0	4A	T+BND	Censored	9
HN18	67	Supraglottic	T1 N0 M0 G1 R0	1	P	Censored	4
HN19	56	Supraglottic	T2 N2b M0 G3 R0	4A	P+BND	Alive	25
HN20	69	Supraglottic	T2 N0 M0 G1 R1	4A	P+BND	Alive	43
HN21	55	Supraglottic	T2 N0 M0 G1 R0	2	P	Alive	17
HN22	55	Supraglottic	T1 N0 M0 G2 R0	1	P	Censored	15
HN23	71	Glottic	T3 N2a M0 G2 R0	4A	T+BND	Censored	36
HN24	72	Glottic	T2 N0 M0 G3 R0	2	P	Alive	32
HN25	69	Glottic	T4 N0 M0 G1 R0	4A	P	Alive	84
HN26	79	Supraglottic	T3 N1 M0 G3 R0	3	T+BND	Alive	72
HN27	59	Supraglottic	T2 N3 M0 G3 R0	4B	T+BND	Alive	27
HN28	68	Supraglottic	T4a N2b M0 G3 R0	4A	T+BND	Alive	76
HN29	77	Glottic	T2 N1 M0 G1 R0	3	T+UND	Alive	21
HN30	50	Supraglottic	T2 N0 M0 G2 R0	2	P+BND	Alive	48
HN31	51	Supraglottic	T2 N2c M0 G3 R0	4A	P+BND	Alive	21
HN32	72	Supraglottic	T2 N0 M0 G3 R0	2	P+BND	Dead	36
HN33	54	Supraglottic	T3 N1 MO G1 R0	3	P+BND	Dead	6
HN34	74	Supraglottic	T3 N0 M0 G1 R0	3	T+BND	Censored	1
HN35	59	Supraglottic	T3 N2c M0 G1 R2	4A	T+BND	Alive	25

HN36	65	Glottic	T2 N0 M0 G1 R0	2	P+UND	Alive	24
HN37	44	Supraglottic	T2 N3 M0 G1 R0	4B	T+BND	Alive	44
HN38	63	Glottic	T3 N0 M0 G2 R0	3	T+BND	Alive	72
HN39	53	Glottic	T3 N0 M0 G1 R0	3	T+BND	Alive	48
HN40	51	Supraglottic	T2 N0 M0 G1 R0	2	P+UND	Alive	14
HN41	63	Supraglottic	T2 N0 M0 G1 R0	2	P+BND	Alive	120
HN42	65	Supraglottic	T2 N0 M0 G1 R0	2	P	Alive	18
HN43	69	Glottic	T3 N2a M0 G3 R0	4A	T+BND	Alive	29
HN44	77	Glottic	T4 N0 M0 G1 R0	4A	T	Alive	53
HN46	46	Supraglottic	T1 N2c M0 G2 R1	4A	P+BND	Alive	48
HN47	54	Glottic	T1 N0 M0 G1 R0	1	P	Alive	25
HN48	65	Supraglottic	T3 N0 M0 G1 R0	3	T+BND	Alive	24
HN49	54	Supraglottic	T2 N3 M0 G2 R0	4B	P+BND	Dead	8
HN50	82	Supraglottic	T3 N0 M0 G2 R0	3	T+BND	Dead*	48
HN51	65	Supraglottic	T2 Nx M0 G2 R0	2	P+BND	Dead	68
HN52	70	Glottic	T1 N0 M0 G2 R0	1	P	Dead	38
HN53	79	Glottic	T2 N0 M0 G2 R0	2	P	Alive	16
HN54	67	Glottic	T2 Nx M0 G1 R0	2	P	Dead	84
HN55	57	Supraglottic	T4a N2c M0 G2 R1	4A	T+BND	Dead	8
HN56	57	Supraglottic	T3 Nx M0 G2 R1	3	P	Censored	9
HN57	53	Glottic	T1 N0 M0 G1 R0	1	P	Alive	60
HN58	54	Glottic	T3 N0 M0 G3 R0	3	T+BND	Alive	50
HN59	49	Glottic	T2 N0 M0 G2 R0	2	P	Alive	55
HN60	61	Supraglottic	T2 N0 M0 G2 R0	2	T+BND	Alive	43
HN61	59	Supraglottic	T2 N1 M0 G1 R0	3	P+BND	Alive	68
HN62	46	Supraglottic	T2 N2b M0 G2 R0	4A	P+BND	Alive	19
HN63	56	Supraglottic	T3 N0 M0 G3 R0	3	P+BND	Alive	42
HN64	57	Supraglottic	T2 N0 M0 G3 R0	2	P+BND	Alive	24
HN65	52	Glottic	T1 N0 M0 G1 R0	1	P	Alive	192
HN66	57	Supraglottic	T2 N2b M0 G2 R0	4A	P	Dead	72
HN67	90	Supraglottic	T1 N0 M0 G3 R0	1	P	Censored	36
HN68	61	Supraglottic	T1 N2c M0 G3 R0	4A	P+BND	Alive	60
HN69	82	Supraglottic	T4 Nx M0 G2 R0	4A	T+BND	Dead*	48
HN70	59	Supraglottic	T3 N2b M0 G2 R0	4A	T+BND	Dead*	16
HN71	63	Supraglottic	T2 N0 M0 G3 R0	2	P+BND	Alive	34
HN72	45	Supraglottic	T2 N2b M0 G3 R0	4A	P+UND	Alive	45
HN73	58	Glottic	T1 N0 M0 G2 R0	1	P	Alive	72
HN74	64	Supraglottic	T1 N2c M0 G3 R0	4A	P+BND	Alive	52
HN75	69	Supraglottic	T3 N0 M0 G1 R0	3	P+UND	Dead	41
HN76	72	ND	ND	ND	P	ND	ND
HN77	87	ND	ND	ND	T	ND	ND

HN78	71	ND	ND	ND	P	ND	ND
HN79	64	ND	ND	ND	P+BND	ND	ND
HN80	43	ND	ND	ND	P	ND	ND
HN81	82	ND	ND	ND	P	ND	ND
HN82	70	ND	ND	ND	T	ND	ND
HN83	86	ND	ND	ND	P	ND	ND
HN84	75	ND	ND	ND	T	ND	ND
HN85	57	ND	ND	ND	P	ND	ND
HN86	73	ND	ND	ND	P	ND	ND
HN87	49	ND	ND	ND	T	ND	ND
HN88	62	ND	ND	ND	P	ND	ND
HN89	48	ND	ND	ND	T	ND	ND

*Death by other causes; pTNM, Pathological tumor-node-metastasis stage; T, Total laryngectomy; P, Partial laryngectomy; UND, Unilateral neck disection; BND, Bilateral neck disection; OS, Overall survival (months)

Supplementary Table 6. SMIPS analysis of the validation set

Symbol	Amplified exons	Amplicons (bp)	Muts	N
ARHGEF2	11	7846	R608W	1
			R573*	1
			V564L	1
			S387N	1
			R228*	1
BCORL1	16	8697	A429D	1
			G492V	1
			L512P	1
			Q838L	1
			P873L	1

			D1198Y	2
CIT	19	8507	A1120T	1
COMP	13	5588	C387Y	1
CSMD3	10	4210	T3366A	1
			R3105W	2
			splice_site	2
			G414W	1
			D413E	1
			Q397K	1
			H360N	2
			D277E	1
			P255T	1
			S78I	1
CTNNA2	17	6642	E76*	1
			S132Y	1
			E266*	1
			L434*	2
			S597G	1
			A761S	2
CTNNA3	17	6757	D696N	1
			C622F	1
			V607L	2
			V492F	1
			A468P	1
			E413V	1
CTNND2	22	8850	P860L	1
			C766Y	1
			A530V	1
			S517R	1
			R435S	1
			Q430*	1
			Y399F	1
DAPK1	21	9738	I90N	1
			S738F	1
DGKD	23	10545	splice_site	1
DYRK2	4	2679	-	0
EBF1	16	6058	P350H	2
ENPP3	20	8160	G52D	1
			A61E	2
			Y196*	1
			E400*	1

			G500A	1
			G534*	1
FOXL1	2	1913	-	0
GDF10	3	1944	N156K	1
LOXL2	13	5385	-	0
MAML1	13	8716	Y974C	1
MAP2	16	9025	R293S	1
			A374S	1
			G430E	1
			P1323T	1
MAP3K10	8	5168	D860N	1
MAPK4	4	2077	-	0
MDGA2	12	5417	S907I	1
			R859S	1
			A857V	2
			Q750*	1
			splice_site	2
			D319Y	1
			D279H	1
MTF1	10	5060	-	0
NID1	20	8173	R1100L	1
			E713K	1
NLRP12	10	5090	A1010T	1
			V583L	1
PAX1	5	2522	A336T	1
			A396G	1
			P399T	1
PCDHB7	3	3010	-	-
PIKFYVE	25	12059	L349H	1
			Q1146H	1
PPP2R4	10	3461	-	0
PTER	4	1811	M54I	1
			K62*	1
PTPRS	22	10442	-	-
RAB22A	6	2421	N118S	1
RAB2A	8	2928	G210C	1
RHOJ	5	1825	-	-
SELE	8	4295	P556T	1
SIM1	9	5017	D676Y	2
			S541L	1
			R69W	2

SUV420H2	4	2753	G279S	1
			R284W	1
TGFBR2	7	3215	-	0
TP53	5	2033	splice_site	1
			E298*	4
			E286*	1
			R280T	1
			R280G	1
			R273L	2
			R273C	2
			G262V	1
			G245C	5
TMPRSS11F	10	3914	Y364C	1
			Q90*	1
VCAN	19	13780	S617L	1
			K745T	1
			R3188H	1

Shaded genes were excluded due to sub-optimal alignment of reads

Supplementary Table 7. Somatic mutations affecting CTNNA2 and CTNNA3 in the validation series

Gene	Case	Mutation	Condel score	Condel prediction
CTNNA2	HN05	E76*	-	truncating
CTNNA2	HN35	S132Y	0,942	deleterious
CTNNA2	HN22	E266*	-	truncating
CTNNA2	HN03	L434*	-	truncating
CTNNA2	HN24	S597G	0,792	deleterious
CTNNA2	HN45	M725I	0,645	deleterious
CTNNA2	HN15	A761S	0,367	neutral
CTNNA3	HN03	E413V	0,652	deleterious
CTNNA3	HN67	A468P	0,76	deleterious
CTNNA3	HN51	V492F	0,591	deleterious
CTNNA3	HN56	V607L	0,585	deleterious
CTNNA3	HN22	C622F	0,689	deleterious
CTNNA3	HN45	R628P	0,645	deleterious
CTNNA3	HN56	D696N	0,622	deleterious

VI. Other works related with this Thesis

Article 6. Alicia R. Folgueras, Antonio Fueyo, Olivia García-Suárez, Jennifer Cox, Aurora Astudillo, Paolo Tortorella, Cristina Campestre, Ana Gutiérrez-Fernández, **Miriam Fanjul-Fernández**, Caroline J. Pennington, Dylan R Edwards, Christopher M. Overall and Carlos López-Otín. "Collagenase-2 deficiency or inhibition impairs experimental autoimmune encephalomyelitis in mice".

Journal of Biological Chemistry 283: 9465-74 (2008)

Personal contribution to this work: This work represents my first approach to the experimental work with mutant mice. Thus, during this work I learnt the different methodological approaches for generation, care and management of genetically-engineered mutant mice colonies, and then, I contributed to perform the encephalomyelitis protocol in *Mmp8*-deficient mice and their corresponding controls as well as to evaluate the severity of the disease developed by the animals.

Article 7: Xose S. Puente, Víctor Quesada, Fernando G. Osorio, Rubén Cabanillas, Juan Cadiñanos, Julia M. Fraile, Gonzalo R. Ordóñez, Ana Gutiérrez-Fernández, **Miriam Fanjul-Fernández**, Diana A. Puente, Nicolas Lévy, José M. P. Freije. and Carlos López-Otín. "Mutation of BANF1 causes a new form of hereditary progeria".

American Journal of Human Genetics. 88: 650-6 (2011).

Personal contribution to this work: This work represented my introduction to the experimental approaches required to address the second main objective of this Thesis, focused on the application of next-generation sequencing for cancer genome analysis. Accordingly, I contributed to the preparation of the exome capture DNA library together with Dr. Gonzalo R. Ordóñez and Diana A. Puente.

THE JOURNAL OF BIOLOGICAL CHEMISTRY VOL. 283, NO. 14, pp. 9465–9474, April 4, 2008

Collagenase-2 Deficiency or Inhibition Impairs Experimental Autoimmune Encephalomyelitis in Mice*

Received for publication, November 20, 2007, and in revised form, January 28, 2008 Published, JBC Papers in Press, February 1, 2008, DOI 10.1074/jbc.M709522200

Alicia R. Folgueras[‡], Antonio Fueyo[§], Olivia García-Suárez[¶], Jennifer Cox[‖], Aurora Astudillo[¶], Paolo Tortorella[**], Cristina Campestre[‡‡], Ana Gutiérrez-Fernández[‡], Miriam Fanjul-Fernández[‡], Caroline J. Pennington[§§], Dylan R. Edwards[§§], Christopher M. Overall[‖], and Carlos López-Otín[‡1]

*From the [‡]Departamento de Bioquímica y Biología Molecular, and [§]Biología Funcional, Facultad de Medicina, Instituto Universitario de Oncología, Universidad de Oviedo, and [¶]Servicio de Anatomía Patológica, Hospital Central de Asturias, Oviedo 33006, Spain, the [‖]Departments of Oral Biological and Medical Sciences, and Biochemistry and Molecular Biology, Centre for Blood Research, University of British Columbia, Vancouver, V6T 1Z3 Canada, the **Dipartimento Farmaco-Chimico, Università degli Studi di Bari, Bari 70125, Italy, the [‡‡]Dipartimento di Scienze del Farmaco, Università G. d'Annunzio, Chieti 66013, Italy, and the [§§]School of Biological Sciences, University of East Anglia, Norwich, NR4 7TJ United Kingdom*

Matrix metalloproteinases (MMPs) have been implicated in a variety of human diseases, including neuroimmunological disorders such as multiple sclerosis. However, the recent finding that some MMPs play paradoxical protective roles in these diseases has made necessary the detailed study of the specific function of each family member in their pathogenesis. To determine the relevance of collagenase-2 (MMP-8) in experimental autoimmune encephalomyelitis (EAE), an animal model for multiple sclerosis, we have performed two different analyses involving genetic and biochemical approaches. First, we have analyzed the development of EAE in mutant mouse deficient in MMP-8, with the finding that the absence of this proteolytic enzyme is associated with a marked reduction in the clinical symptoms of EAE. We have also found that *MMP-8*$^{-/-}$ mice exhibit a marked reduction in central nervous system-infiltrating cells and demyelinating lesions. As a second approach, we have carried out a pharmacological inhibition of MMP-8 with a selective inhibitor against this protease (IC_{50} = 0.4 nM). These studies have revealed that the administration of the MMP-8 selective inhibitor to mice with EAE also reduces the severity of the disease. Based on these findings, we conclude that MMP-8 plays an important role in EAE development and propose that this enzyme may be a novel therapeutic target in human neuro-inflammatory diseases such as multiple sclerosis.

Multiple sclerosis (MS)[2] is an inflammatory disease of the central nervous system (CNS) characterized by autoreactive T-cell infiltration that causes myelin sheath destruction and axonal loss (1, 2). Although the origin of MS remains unclear, CD4+ Th1 cells are believed to be the main mediators of the autoimmune reaction (3, 4). According to this, the injection of myelin peptides into susceptible mice generates experimental autoimmune encephalomyelitis (EAE), a murine model of human multiple sclerosis, and leads to myelin-specific recruitment of T cells that subsequently differentiate into Th1-type effector cells (5). The extravasation of reactive leukocytes into the CNS parenchyma across the blood-brain barrier correlates with the appearance of clinical symptoms (6).

Matrix metalloproteinases (MMPs) have been largely implicated in MS and EAE progression due to their ability to degrade the main extracellular matrix components that maintain the integrity of the blood-brain barrier (7, 8). Consistent with this putative role of MMPs in the development or progression of MS, several members of this metalloproteinase family have been shown to be up-regulated in serum, cerebrospinal fluid, and brain samples of MS patients (9, 10) as well as in murine models of demyelinating lesions (11, 12). Likewise, expression of MMPs has been detected in diverse cell types involved in the pathogenesis of the disease (13, 14). Interestingly, the administration of MMP inhibitors has reduced the severity of the disease in different EAE murine models (15–18). Furthermore, young MMP-9-deficient mice and MMP-2/MMP-9 double knock-out mice are more resistant to the development of the disease than wild-type animals (19, 20). However, and somewhat unexpectedly, *MMP-2*$^{-/-}$ and *MMP-12*$^{-/-}$ mice are more susceptible to EAE induction than their wild-type counterparts suggesting that these metalloproteinases could play protective roles in the course of MS (21, 22). These findings, together with the variety of processes in which MMPs are involved (23, 24), suggest that the contribution of these enzymes to the progression of neuro-inflammatory diseases is much more complex than originally anticipated. Thus, and besides the degradative action of MMPs during blood-brain barrier disruption, these enzymes may also contribute to the progression of MS through their ability to degrade myelin components releasing encephalitogenic peptides (25, 26). Likewise, MMPs may play important roles in the regulation of the inflammatory stimuli responsible for autoreactive T cell recruitment

* This work was supported by grants from Ministerio de Educación y Ciencia-Spain, Fundación M. Botín, Fundación Lilly, and European Union (Cancer Degradome-FP6). The Instituto Universitario de Oncología is supported by Obra Social Cajastur-Asturias. The costs of publication of this article were defrayed in part by the payment of page charges. This article must therefore be hereby marked "*advertisement*" in accordance with 18 U.S.C. Section 1734 solely to indicate this fact.

[1] To whom correspondence should be addressed. Tel.: 34-985-104-201; Fax: 34-985-103-564; E-mail: clo@uniovi.es.

[2] The abbreviations used are: MS, multiple sclerosis; CNS, central nervous system; EAE, experimental autoimmune encephalomyelitis; MMP, Matrix metalloproteinase; MOG, myelin oligodendrocyte glycoprotein; PBS, phosphate-buffered saline; TNF, tumor necrosis factor; IFN, interferon; IL, interleukin; TGF, transforming growth factor; WT, wild type.

and infiltration (27). In fact, MMPs have been demonstrated to modulate inflammation through the proteolytic cleavage of a number of cytokines and chemokines that have been implicated in the pathobiology of MS (27, 28). This functional diversity of MMPs makes necessary the detailed analysis of the specific role that each individual member of this complex family of metalloproteinases might play in the pathogenesis of MS.

Our study in this regard has focused on the analysis of the putative implication of collagenase-2 (MMP-8) in the development and progression of neuro-inflammatory diseases such as MS. MMP-8 is a potent collagenolytic enzyme frequently associated with inflammatory conditions, including asthma, hepatitis, ulcerative colitis, atherosclerosis, periodontitis, and rhinosinusitis (29–34). Interestingly, several works have also evidenced the up-regulation of MMP-8 in EAE, and its expression has been correlated with disease severity (12, 14). To further explore the possibility that this metalloproteinase could play a role in MS pathogenesis, we have used mutant mice deficient in MMP-8 and analyzed their susceptibility to EAE. In this work, we report that *MMP-8*$^{-/-}$ mice are more resistant to EAE than their wild-type counterparts, and show a marked reduction in CNS-infiltrating cells and demyelinating lesions. On this basis, we propose that MMP-8 plays an important role in EAE development and can be a therapeutic target in human neuro-inflammatory diseases such as MS.

EXPERIMENTAL PROCEDURES

EAE Induction and Clinical Evaluation—Wild-type (*MMP-8*$^{+/+}$) and MMP-8-null mice (*MMP-8*$^{-/-}$) were generated in a C57BL6/129Sv background, as previously described (35). Control and mutant mice used in all experiments were littermates derived from interbreeding of *MMP-8*$^{+/-}$ heterozygotes. For EAE induction, 8- to 10-week-old female mice were injected subcutaneously in the flank on days 0 and 7 with 300 μg of myelin oligodendrocyte glycoprotein (MOG_{35-55}) peptide. The peptide was thoroughly emulsified in 100 μl of complete Freund's adjuvant containing 500 μg of heat-inactivated *Mycobacterium tuberculosis* H37Ra (Difco Laboratories). Mice were also injected intraperitoneally on days 0 and 2 with 200 μl of PBS containing 500 ng of Pertussis toxin (List Biologicals Laboratories). After immunization with MOG, mice were observed daily, and the disease severity was scored on a scale of 0–5 with graduations of 0.5 for intermediate clinical signs. The score was defined as follows: 0, no detectable clinical signs; 1, weakness of the tail; 2, hind limb weakness or abnormal gait; 3, complete paralysis of the hind limbs; 4, complete hind limb paralysis with forelimb weakness or paralysis; 5, moribund or death. Paralyzed mice were given easy access to food and water. Mouse experimentation was done according to the guidelines of the Universidad de Oviedo, Oviedo-Spain.

In Vivo MMP-8 Inhibition Studies—The cyclohexylamine salt of (*R*)-1-(3′-methylbiphenyl-4-sulfonylamino)methylpropyl phosphonic acid, a new phosphonate inhibitor with potent (IC_{50} = 0.4 nM) and selective action against MMP-8 (36), was dissolved in PBS with 5% Me_2SO at 2.5 mg/ml. Treated mice were injected intraperitoneally daily with a dose of 25 mg/kg body weight of the inhibitor, starting at the time of MOG immunization. All mice were monitored daily until the time of sacrifice.

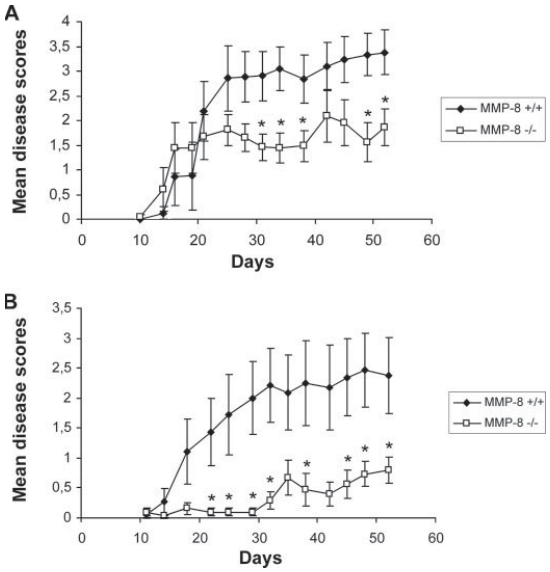

FIGURE 1. **Clinical severity of EAE is reduced in *MMP-8*$^{-/-}$ mice.** Wild-type and *MMP-8*$^{-/-}$ female mice were immunized with the encephalitogenic peptide MOG_{35-55} and scored daily according to the severity of their symptoms. The experiment was performed with 8- to 10-week-old *MMP-8*$^{+/+}$ and *MMP-8*$^{-/-}$ mice (n = 6 mice per group) (*A*) and 4-week-old *MMP-8*$^{+/+}$ (n = 7) and *MMP-8*$^{-/-}$ (n = 8) mice (*B*). Results are expressed as mean disease score ± S.E. *, $p \leq 0.05$.

Analysis of Expression of MMPs, TIMPs, ADAMs, and ADAMTSs—Spinal cords from immunized wild-type and *MMP-8*$^{-/-}$ mice were isolated during the chronic phase of the disease. Tissues were homogenized and total RNA was extracted by using a commercial kit (RNeasy MiniKit, Qiagen). One microgram of RNA was reverse transcribed to make cDNA. TaqMan PCR was used to profile mRNA levels of all members of the MMP family and the four TIMPs and several members of the ADAM and ADAMTS families, as previously described (14). The 18 S rRNA gene was used as an endogenous internal control.

Isolation of Splenocytes and Cytokine Assays—Spleens from immunized wild-type and *MMP-8*$^{-/-}$ mice were isolated and dispersed into a single cell suspension. After lysis of red blood cells, the splenocytes were washed and resuspended in Dulbecco's modified Eagle's medium supplemented with 10% fetal calf serum, L-glutamine, sodium pyruvate, 2-mercaptoethanol, and streptomycin/penicillin. Cells were plated at 4×10^6 cells/well in 24-well plates containing 1 ml of culture medium with 0, 5, or 50 μg/ml MOG_{35-55}. Supernatants were collected at 48 h for cytokine analysis. Quantitative enzyme-linked immunosorbent assay was performed for TNF-α, IFN-γ (R&D), IL-4, IL-10 (BD Biosciences), and TGF-β (Promega) according to the protocol supplied by the manufacturer.

Splenocyte Proliferation Assay—Spleens from wild-type and *MMP-8*$^{-/-}$ mice were removed 21 days after immunization and processed as described above. Cells were plated in tripli-

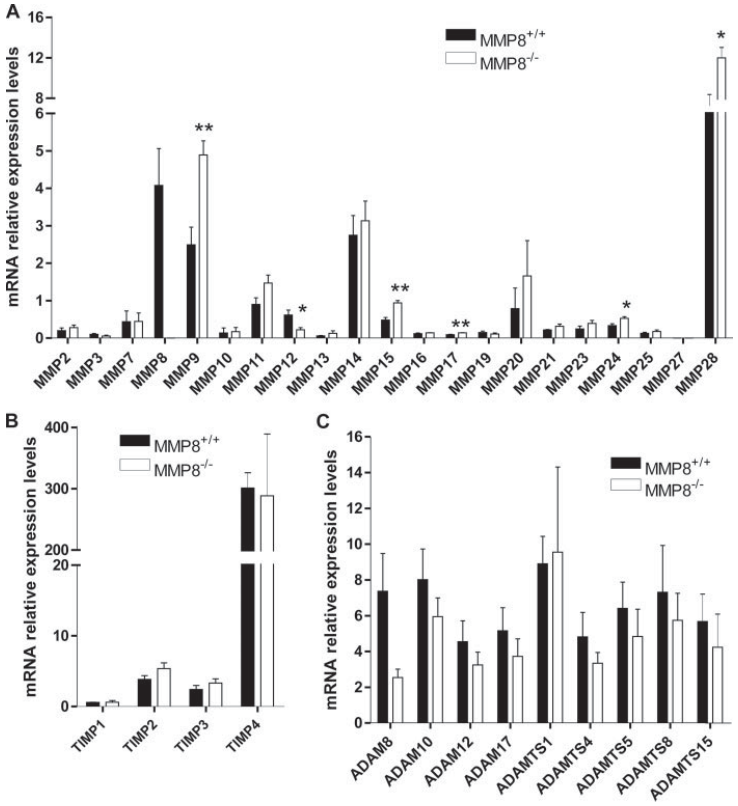

FIGURE 2. **Analysis of MMP, ADAM, ADAMTS, and TIMP expression levels in 8-week-old wild-type and *MMP-8*$^{-/-}$ immunized mice.** TaqMan real-time PCR analysis of MMPs (*A*), TIMPs (*B*), and ADAMs and ADAMTSs (*C*) expressed in spinal cord samples from wild-type (*black bar*) and MMP-8$^{-/-}$ immunized mice (*white bar*). mRNA levels on the *y*-axis are expressed relative to 18 S rRNA levels. Both forms of murine *MMP-1* (43) were undetectable. Values are means ± S.E. *, $p \leq 0.05$; **, $p \leq 0.01$. $n = 4$ mice per group.

cates at 7×10^5 cells/well in 96-well microtiter plates containing 200 μl of culture medium with 0, 5, or 50 μg/ml MOG_{35-55}. They were cultured for 48 h and then pulsed with 1 μCi/well [*methyl*-^{3}H]thymidine for the last 16 h. Cells were collected and precipitated with 5% trichloroacetic acid for 4 h at 4 °C. The precipitated DNA was filtered using G/C glass fiber filters and radioactivity was determined in a scintillation counter.

Histological Analysis and Immunofluorescence—Wild-type and *MMP-8*$^{-/-}$ immunized mice with representative clinical scores were selected from each group. Brains and spinal cords were isolated, fixed in 4% paraformaldehyde, and embedded in paraffin. Each sample was serially sectioned 5-μm thick at 100-μm intervals and stained with hematoxylin and eosin. To evaluate the degree of inflammation, the "depth" of inflammatory infiltrates was measured in serial sections of spinal cord samples and quantified using Image Tool HUCA software. To assess the degree of demyelinization, an immunohistochemical analysis was performed using a primary antibody against myelin basic protein. To perform immunohistochemistry, deparaffined, and rehydrated sections were rinsed in PBS (pH 7.5). Endogenous peroxidase activity and nonspecific binding were blocked with peroxidase block buffer (DakoCytomation) and 1% bovine serum albumin, respectively. Sections were incubated overnight at 4 °C with a monoclonal antibody anti-myelin basic protein (a gift from Dr. Sternberger), diluted 1:1500. Then, sections were incubated with an anti-mouse EnVision system-labeled polymer (DakoCytomation) for 30 min, washed in buffer solution, and visualized with diaminobenzidine. Sections were counterstained with Mayer's hematoxylin, dehydrated, and mounted in Entellan®. Inflammatory and demyelinating lesions were evaluated by a neuropathologist. To quantify the different cellular profiles, sampling was systematically randomized, and two sections of the spinal cord from wild-type and *MMP-8*$^{-/-}$ immunized mice, with representative clinical scores, were selected to perform the immunohistochemical analysis. To detect T lymphocytes, deparaffined and rehydrated sections were heated in 10 mM citrate buffer solution (pH 6.5) in a pressure cooker for 7 min. Antibody nonspecific binding was blocked using 1% bovine serum albumin in PBS. Samples were incubated overnight at 4 °C with a rabbit anti-human CD3 antibody (Aton Pharma Inc.), diluted 1:100. Then, slides were incubated with an anti-rabbit EnVision system-labeled polymer for 30 min, washed in buffer solution, and visualized with diaminobenzidine. To perform macrophage and polymorphonuclear (PHN) immunohistochemistry, sections were incubated for 2 h at 37 °C and overnight at 4 °C with a rat anti-mouse neutrophils (Serotec) or a rat anti-mouse F4/80 (Serotec), diluted 1:50. After that, slides were incubated with a goat anti-rat secondary antibody diluted 1:50. Sections were counterstained with Mayer's hematoxylin, dehydrated, and mounted in Entellan®. The total number of each cellular profile was referred to the area of white matter analyzed. This area was calculated in each section using Image Tool HUCA software. For double immunofluorescence, spinal cords were isolated, fixed in 4% paraformaldehyde, and embedded in OCT. Cryosections were blocked with 20% serum in PBS and 0.2% Triton X-100 for 30 min. Then, slides were incubated overnight at 4 °C with a rat monoclonal antibody to mouse Ly6G (BD Pharmingen) diluted 1:25. After washing with PBS, samples were incubated for 1 h at room temperature with Alexa Fluor 488-goat anti-rat IgG secondary antibody diluted 1:100. A primary antibody against MMP-8 (35) was added to the slides diluted 1:3000 in blocking buffer and incubated for 1 h. Finally,

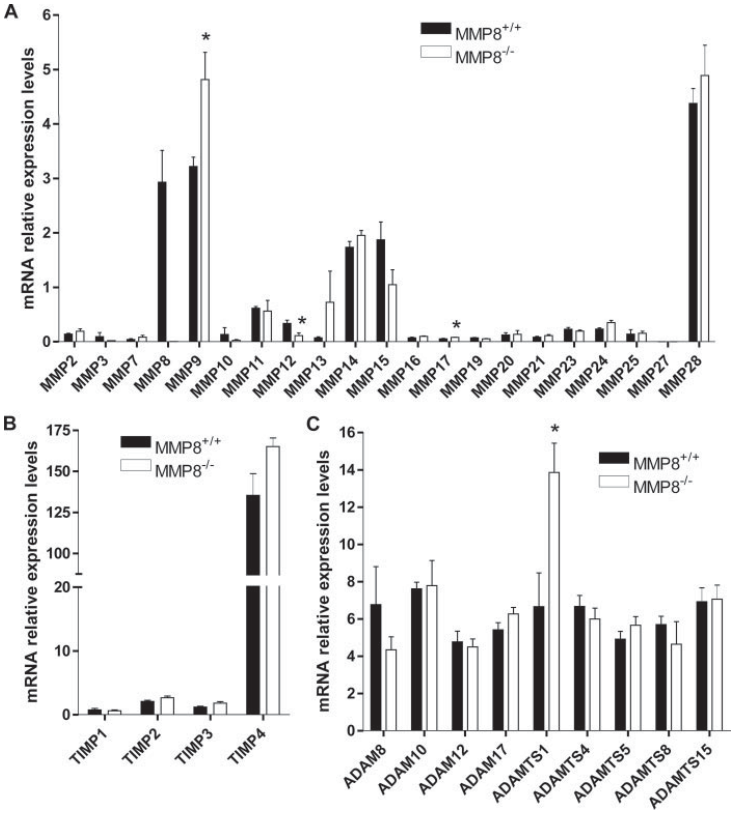

FIGURE 3. **Analysis of MMP, ADAM, ADAMTS, and TIMP expression levels in 4-week-old wild-type and *MMP-8*$^{-/-}$ immunized mice.** TaqMan real time PCR analysis of MMPs (*A*), TIMPs (*B*), and ADAMs and ADAMTSs (*C*) expressed in spinal cord samples from wild-type (*black bar*) and MMP-8$^{-/-}$ immunized mice (*white bar*). mRNA levels on the *y*-axis are expressed relative to 18 S rRNA levels. Both forms of murine *MMP-1* were undetectable. Values are means ± S.E. *, $p \leq 0.05$; **, $p \leq 0.01$. $n = 4$ mice per group.

samples were incubated for 1 h at room temperature with Alexa Fluor 594-goat anti-rabbit IgG secondary antibody diluted 1:2000. Nuclei were counterstained with 4′,6-diamidino-2-phenylindole. Sections were examined using a Confocal-Ultra Espectral Leica TCS-SP2-AOBS microscope.

MMP and ADAM Inhibition Assays—MMP inhibition assays have been previously described (36). Recombinant ADAM-10 and ADAM-17 were purchased from R&D Systems. For assaying ADAMs, the inhibitor (*R*)-1-(3′-methylbiphenyl-4-sulfonylamino)methylpropylphosphonic acid stock solution (100 mM) was further diluted at six different concentrations (0.01 nM to 10 μM) in the fluorometric assay buffer (25 mM Tris, pH 8.0, 25 μM $ZnCl_2$, 0.005% Brij-35). The enzyme (final concentration of 19 nM for ADAM-10 and 1.4 nM for ADAM-17) and inhibitor solutions were incubated in the assay buffer for 4 h at 25 °C. After addition of 5 μM (final concentration) of the fluorogenic substrate Mca-Pro-Leu-Ala-Gln-Ala-Val-Dap (Dpn)-Arg-Ser-Ser-Ser-Arg-NH_2 (Bachem), the hydrolysis was monitored recording the increase of fluorescence (λ_{ex} = 320 nm, λ_{em} = 405 nm) using a LS55 spectrofluorometer from PerkinElmer Life Sciences. The assays were performed in duplicate in a total volume of 100 μl per well in 96-well microtiter plates (Nunc). The percentage of inhibition was calculated from control reactions without the inhibitor. IC_{50} was determined using the formula: $V_i/V_0 = 1/(1 + [I]/IC_{50})$, where V_i is the initial velocity of substrate cleavage in the presence of the inhibitor at concentration [*I*] and V_0 is the initial velocity in the absence of the inhibitor. Results were analyzed using GraphPad Software.

Statistical Analysis—Values shown are mean ± S.E. Comparison of clinical scores, cytokine production levels, and cellular profiles between the various treatment groups were analyzed by using two-tailed Student's *t* test. A value of $p \leq 0.05$ was considered significant. Statistically significant differences are shown with *asterisks*.

RESULTS

MMP-8$^{-/-}$ Mice Are More Resistant to EAE—To investigate the possible contribution of MMP-8 to the initiation and progression of EAE, wild-type and MMP-8-deficient mice were immunized with the encephalitogenic peptide MOG_{35-55} and scored according to the severity of their symptoms. A total of 66 female mice (8–10 weeks old, *MMP-8$^{+/+}$*, $n = 32$, *MMP-8$^{-/-}$*, $n = 34$) were immunized in three independent experiments, and the results of a representative experiment are shown in Fig. 1*A*. Although the disease onset is similar in both groups, after day 20 from the immunization, the clinical scores observed in *MMP-8$^{-/-}$* mice were significantly reduced during the chronic phase of the disease. Also, the maximal disease score was diminished in *MMP-8$^{-/-}$* mice compared with wild type (wild type = 3.4 *versus* knock-out = 2.1, $p = 0.09$). Considering that the lack of MMP-8 could be compensated in the adult life by other members of the MMP family or by alternative proteolytic pathways, we also induced EAE in 4-week-old wild-type ($n = 7$) and *MMP-8$^{-/-}$* mice ($n = 8$). As shown in Fig. 1*B*, the severity and the onset of the disease were significantly reduced in young *MMP-8$^{-/-}$* compared with young wild-type mice. As expected, the maximal disease severity score of young *MMP-8$^{-/-}$* mice (wild type = 2.5 *versus* knock-out = 0.8, $p \leq 0.05$) was also diminished in comparison to that obtained with *MMP-8$^{+/+}$* young mice. The greatest differences between wild-type and *MMP-8$^{-/-}$* mice EAE susceptibility obtained in this experiment suggest the existence of a compensatory mech-

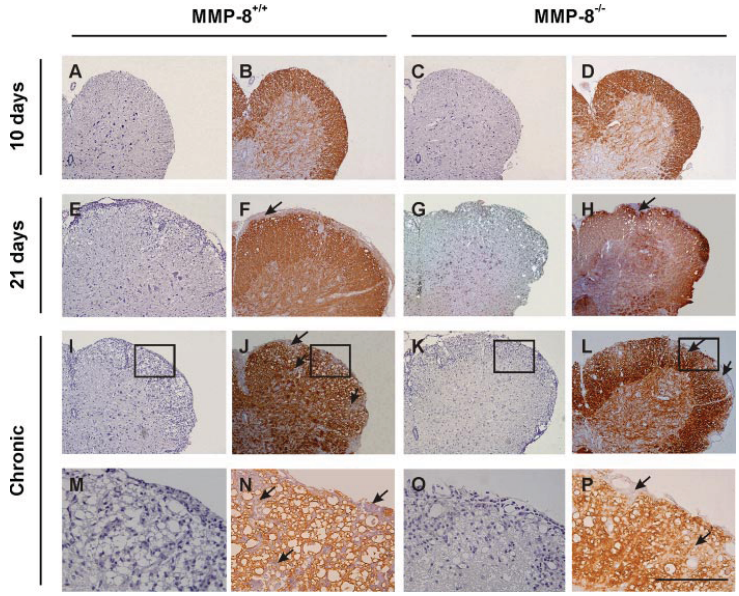

FIGURE 4. **Diminished CNS inflammation during the chronic phase of EAE in *MMP-8*$^{-/-}$ mice immunized with MOG$_{35-55}$.** Hematoxylin and eosin staining (*A*, *C*, *E*, *G*, *I*, *K*, *M*, and *O*) and myelin basic protein immunohistochemistry (*B*, *D*, *F*, *H*, *J*, *L*, *N*, and *P*) of spinal cords from 8-week-old *MMP-8*$^{+/+}$ and *MMP-8*$^{-/-}$ mice immunized with MOG$_{35-55}$. There is no inflammation in CNS samples from *MMP-8*$^{+/+}$ and *MMP-8*$^{-/-}$ mice sacrificed on day 10 post-immunization (*top panel*). Typical multifocal inflammation in the leptomeninges, around blood vessels, and incipient demyelinating lesions (indicated by *arrows*) are observed in *MMP-8*$^{+/+}$ and *MMP-8*$^{-/-}$ mice sacrificed on day 21 post-immunization. Representative tissue sections from *MMP-8*$^{+/+}$ and *MMP-8*$^{-/-}$ mice sacrificed during the chronic phase of the disease (*I–L*) show vacuolization in the white matter, parenchymal inflammation, and severe demyelination in *MMP-8*$^{+/+}$ mice, whereas inflammatory lesions are reduced in *MMP-8*$^{-/-}$ mice. Magnification, 10×. *Scale bar*,100 μm. A higher magnification image of the tissue lesion, indicated by a *rectangle*, is shown (*M–P*). Magnification, 40×. *Scale bar*, 100 μm.

anism in the adult life. To evaluate this possibility, we analyzed the expression levels of all murine MMPs and their endogenous inhibitors (TIMPs), as well as selected members of the structurally related families of ADAMs and ADAMTSs, in the spinal cords of 8-week-old (n = 4 mice per group) and 4-week-old (n = 4 mice per group) wild-type and *MMP-8*$^{-/-}$ immunized mice, sacrificed during the chronic phase of the disease. Interestingly, the relative expression level of *MMP-8* was one of the highest in the wild-type diseased mice (Figs. 2*A* and 3*A*). This analysis revealed that there are six genes, *MMP-9*, *MMP-12*, *MMP-15*, *MMP-17*, *MMP-24*, and *MMP-28*, whose expression levels were significantly different between *MMP-8*$^{+/+}$ and *MMP-8*$^{-/-}$ 8-week-old mice. However, three of them, *MMP-9*, *MMP-12*, and *MMP-17*, also showed different expression patterns in young mice (Figs. 2*A* and 3*A*). These results suggest that the occurrence of compensatory events, elicited by the lack of MMP-8, may have appeared during earlier stages of knock-out mice development. By contrast, there are certain genes whose expression pattern is markedly different between 8- and 4-week-old *MMP-8*$^{-/-}$ mice. Thus, *MMP-15*, *MMP-24*, and *MMP-28* were significantly up-regulated in adult *MMP-8*$^{-/-}$ mice compared with wild type, whereas there were not significant differences between their expression levels in *MMP-8*$^{+/+}$ and *MMP-8*$^{-/-}$ 4-week-old mice (Figs. 2*A* and 3*A*). In an opposite way, *ADAMTS1* expression levels were significantly up-regulated in *MMP-8*$^{-/-}$ 4-week-old mice compared with wild-type, whereas no difference was observed between *MMP-8*$^{+/+}$ and *MMP-8*$^{-/-}$ adult mice. The relative expression levels of the four *TIMPs* and the analyzed *ADAMs* remained unaltered in both groups (Figs. 2*B*, 2*C*, 3*B*, and 3*C*). Altogether, these findings confirm the existence of different expression patterns between 8- and 4-week-old *MMP-8*$^{-/-}$ mice that may contribute to explain the differences observed between the EAE susceptibility of adult and young *MMP-8*$^{-/-}$ mice.

Reduced Inflammation and Demyelination in MMP-8$^{-/-}$ *EAE Mice*—To evaluate whether MMP-8 may contribute to activated cell recruitment and CNS inflammation, histopathological examination of spinal cord and brain samples from 8-week-old wild-type and *MMP-8*$^{-/-}$ immunized mice was performed at different times in the course of the disease. We first analyzed samples extracted 10 days after the initiation of the experiment, before any clinical symptoms were observed. As expected, no detectable lesions were present at this time point in both wild-type and *MMP-8*$^{-/-}$ mice (Fig. 4, *A–D*). In contrast, samples extracted during the acute phase of the disease (21 days) showed a marked increase in the number of infiltrating cells, although the demyelinating lesions were still very limited. Despite the fact that this time marks the point of divergence in EAE progression between wild-type and *MMP-8*$^{-/-}$ mice, as the severity of EAE symptoms continues to increase in wild-type animals while is maintained in *MMP-8*$^{-/-}$ mice, no histological differences were observed between both groups (Fig. 4, *E–H*).

Finally, we analyzed CNS tissues from wild-type and *MMP-8*$^{-/-}$ mice sacrificed at the chronic phase of the disease. Interestingly, although animals were chosen with similar clinical symptoms in both genotypes, the extent of the inflammatory infiltrates were significantly reduced in knock-out tissues compared with wild-type counterparts (wild type = 334.1 ± 57.2 μm, n = 3, *versus* knock-out = 125.0 ± 39.5 μm, n = 3, $p \leq 0.05$) (Fig. 4, *I*, *K*, *M*, and *O*). In addition, myelin basic protein immunohistochemistry revealed extensive demyelinating lesions in the wild-type tissues, while demyelination was less severe in *MMP-8*$^{-/-}$ mice (Fig. 4, *J*, *L*, *N*, and *P*). A detailed analysis of the cellular types present in the inflammatory lesions revealed that, despite the fact that T lymphocytes were the predominant subpopulation in the parenchyma infiltrates, a great number of macrophages and neutrophils were also detected in

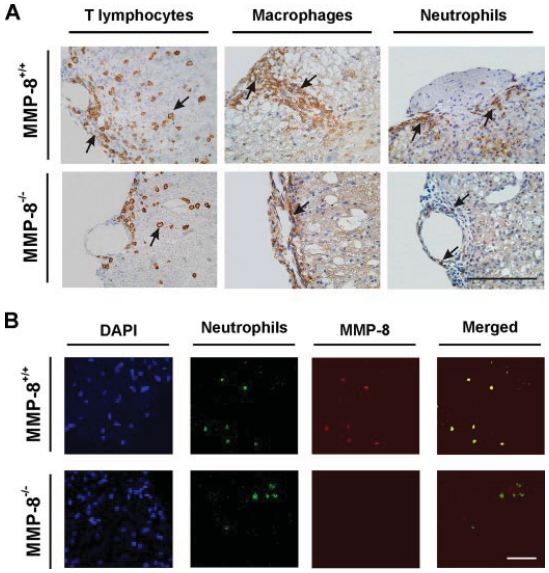

FIGURE 5. **Cellular profiles and specific localization of MMP-8 in the inflammatory infiltrates of mice subjected to EAE.** *A*, representative immunostaining showing the presence of T lymphocytes (*left panels*), macrophages (*middle panels*), and neutrophils (*right panels*) in spinal cords from 8-week-old *MMP-8*$^{+/+}$ and *MMP-8*$^{-/-}$ mice immunized with MOG_{35-55} and sacrificed during the chronic phase of the disease. Magnification, 40×. *Scale bar*, 100 μm. *B*, immunofluorescence reveals Ly6G-positive neutrophils that colocalize with specific MMP-8 immunostaining in spinal cords from EAE-induced *MMP-8*$^{+/+}$ and *MMP-8*$^{-/-}$ mice sacrificed during the chronic phase of the disease. Magnification, 63×. *Scale bar*, 30 μm.

TABLE 1

Cellular profiles in spinal cords of 8-week-old *MMP-8*$^{+/+}$ and *MMP-8*$^{-/-}$ mice subjected to EAE

Data represent the number of each cell type per mm^2 of white matter. Values are means ± S.E. ($n = 4$ mice per group).

	T lymphocytes	Macrophages	Neutrophils
MMP-8$^{+/+}$	410.2 ± 67.5	102.1 ± 50.6	28.7 ± 11.8
MMP-8$^{-/-}$	265.6 ± 84.9	29.9 ± 9.1	16.9 ± 7.3

wild-type mice. The same cellular profiles were observed in *MMP-8*$^{-/-}$ mice, although the number of inflammatory cells was markedly reduced (Fig. 5*A* and Table 1). To determine the cellular source of MMP-8, we performed immunofluorescence analysis of spinal cord samples obtained from immunized mice. These experiments revealed that neutrophils, present at the sites of inflammation, were the main source of MMP-8 (Fig. 5*B*), whereas no co-localization was observed with lymphocytes or macrophages (data not shown).

Splenocyte Activation in MMP-8$^{-/-}$ *Mice during EAE*—Because *MMP-8*$^{-/-}$ mice exhibit both marked reduction in the extent of inflammatory/demyelinating EAE lesions and less severe clinical symptoms, we further investigated if this phenotype was associated with alterations in the antigen-specific immune response. To this purpose, splenocytes from 8-week-old wild-type ($n = 8$) and *MMP-8*$^{-/-}$ ($n = 8$) immunized mice were isolated at day 21 after immunization and cultured in the presence or absence of different concentrations of MOG_{35-55} peptide. Then, the secretion of TNF-α and IFN-γ, two pro-inflammatory Th1 cytokines involved in EAE pathogenesis, was evaluated. As shown in Fig. 6 (*A* and *B*), there was no defect in the ability of splenocytes derived from *MMP-8*$^{-/-}$ mice to secrete TNF-α or IFN-γ when compared with those from wild-type mice. In addition, we analyzed the production of Th2 cytokines such as IL-10 or IL-4 (Fig. 6, *C* and *D*) and TGF-β ($n = 4$) (Fig. 6*E*). However, no significant differences were seen in the secretion of these cytokines. In addition, we determined if the proliferative response was altered in *MMP-8*$^{-/-}$ mice, but the culture of stimulated splenocytes with [*methyl*-^{3}H]thymidine did not reveal significant differences between both groups (Fig. 6*F*). We next evaluated the possibility that this pattern of secretion could change during the chronic phase of the disease. Thus, we isolated splenocytes from 8-week-old wild-type ($n = 4$) and *MMP-8*$^{-/-}$ ($n = 3$) immunized mice at day 50, and cells were stimulated as described above. As can be seen in Fig. 7, no significant differences in cytokine production were observed between wild-type and knock-out mice. However, as shown Fig. 7*F*, when we analyzed the relative increase in cytokine production during the chronic phase *versus* the average levels obtained in each group during the acute phase of the disease, we observed certain differences in the pattern of cytokine secretion between wild-type and knock-out splenocytes. Thus, IL-4 and IL-10 levels were markedly increased in splenocytes derived from *MMP-8*$^{-/-}$ mice during the chronic phase compared with the increased production observed in the cultures derived from wild-type mice. Considering that the relative secretion of TNF-α and IFN-γ was maintained, these results suggest a greater ability of *MMP-8*$^{-/-}$ splenic cells to increase the Th2-type response during the chronic phase of the disease.

MMP-8 Inhibition Reduces the EAE Symptoms in the Acute Phase of the Disease—To investigate whether the administration of a selective MMP-8 inhibitor (Table 2) would reduce the clinical symptoms of EAE disease, we designed an experimental procedure based on previously published results obtained with broad spectrum MMP inhibitors. To this purpose, wild-type female mice (8–10 weeks old) were subjected to EAE induction as described above. The control group was composed of 9 mice that were compared with 11 mice injected with the MMP-8 inhibitor. Treated mice were injected intraperitoneally daily with a dose of 25 mg/kg body weight of the inhibitor, starting at the time of MOG immunization. Wild-type mice daily injected with the vehicle reached similar disease scores as untreated mice (data not shown), thus ruling out any significant influence of the experimental procedure on the observed results. As shown in Fig. 8*A*, which is representative of two independent experiments, MMP-8 inhibitor treatment markedly reduces the disease severity during the early stages of EAE. This was apparent by day 21 post induction, where the mean clinical disease score of the control group was 2.6 ± 0.6 *versus* 0.9 ± 0.4 of the treated mice ($p \leq 0.05$). However, during the chronic phase of the disease, the severity of EAE progressively increased in the treated mice showing that MMP-8 inhibition was not effective at later time points. At this time point, mice were sacrificed and CNS tissues were histopathologically evaluated. No differences were observed in

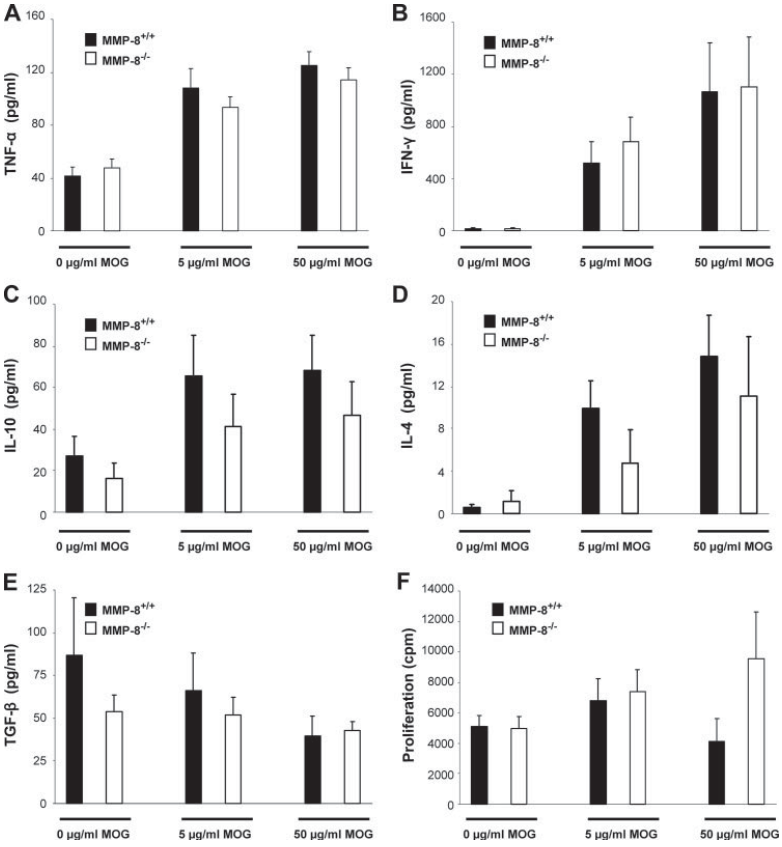

FIGURE 6. **Antigen-specific cytokine production and proliferative responses of splenic cells from 8-week-old *MMP-8*$^{+/+}$ and *MMP-8*$^{-/-}$ mice.** Splenocytes were isolated on day 21 post-immunization and stimulated *in vitro* with 0, 5, and 50 μg/ml MOG_{35-55}. Supernatants were collected at 48 h and TNF-α (*A*), IFN-γ (*B*), IL-10 (*C*), IL-4 (*D*), and TGF-β (*E*) concentrations were determined by enzyme-linked immunosorbent assay. To determine the proliferative responses, [^{3}H]methylthymidine was added after 72 h of antigen stimulation, and its incorporation was measured 16 h later (*F*). Values are means ± S.E. $n = 8$ mice per group.

the severity of the inflammatory and demyelinating lesions (Fig. 8*B*).

DISCUSSION

The pathogenesis of multiple sclerosis is characterized by the massive entry of inflammatory auto-reactive T cells in the parenchyma of the CNS. Several reports have directly related the degradative actions of MMPs with the disruption of the blood-brain barrier (20, 37, 38). Thus, it has been demonstrated that the administration of MMP inhibitors reduces the transmigration of leukocytes in EAE. However, despite this pathogenic role classically attributed to the MMP family of proteases, the availability of murine models deficient in specific MMPs has demonstrated that certain members of this group of enzymes may play protective roles in neuro-inflammatory diseases (21, 22). This fact is likely a consequence of the great variety of bioactive substrates that the MMPs can proteolytically process, including cytokines, chemokines, or adhesion molecules that modulate the recruitment of inflammatory infiltrating cells into the CNS parenchyma (27, 28). These previous findings make of special interest the analysis of the putative role of MMP-8 in MS. Interestingly, MMP-8 combines a potent collagenolytic activity with a reported ability to cleave several chemokines involved in inflammatory processes (39, 40), thereby having the potential to modulate the evolution of the disease in different ways.

To determine the beneficial or detrimental functions that MMP-8 may play in the progression of MS, we have analyzed the susceptibility of MMP-8-deficient mice to EAE. Our results have demonstrated that these mutant mice have attenuated clinical symptoms during the chronic phase of the disease when compared with their wild-type counterparts. Thus, and despite the fact that *MMP-8*$^{-/-}$ and wild-type mice show similar disease scores during the onset and the acute phase of the disease, we have observed that *MMP-8*$^{-/-}$ mice manifest a clear recovery at later time points. Moreover, considering the possibility that a compensatory mechanism may act in the adult life as a consequence of the absence of a certain MMP (19, 21), we performed the same study with younger mice. Interestingly, we found several differences in the expression levels of certain MMPs and ADAMTSs between wild-type and *MMP-8*$^{-/-}$ mice, suggesting the existence of alternative proteolytic pathways that can restore some functions of this collagenolytic MMP. One of the main candidates to perform these activities was *MMP-9*, which was markedly up-regulated in 8-week-old *MMP-8*$^{-/-}$ mice compared with wild types, and its relevance in the pathogenesis of EAE has been largely demonstrated (15, 19, 20). However, we observed that its expression level was also increased in 4-week-old *MMP-8*$^{-/-}$ mice, indicating that there are compensatory mechanisms but they may have appeared earlier during *MMP-8*$^{-/-}$ mice development. These results suggest that the differences observed in EAE susceptibility between adult and young *MMP-8*$^{-/-}$ mice derive from the differences found in the expression pattern of other genes, such as *MMP-15*, *MMP-24*, *MMP-28*, or *ADAMTS1*; however, to date, the particular contribution of these genes to the development of this disease remains unclear.

Impaired Autoimmune Encephalomyelitis in MMP-8$^{-/-}$ Mice

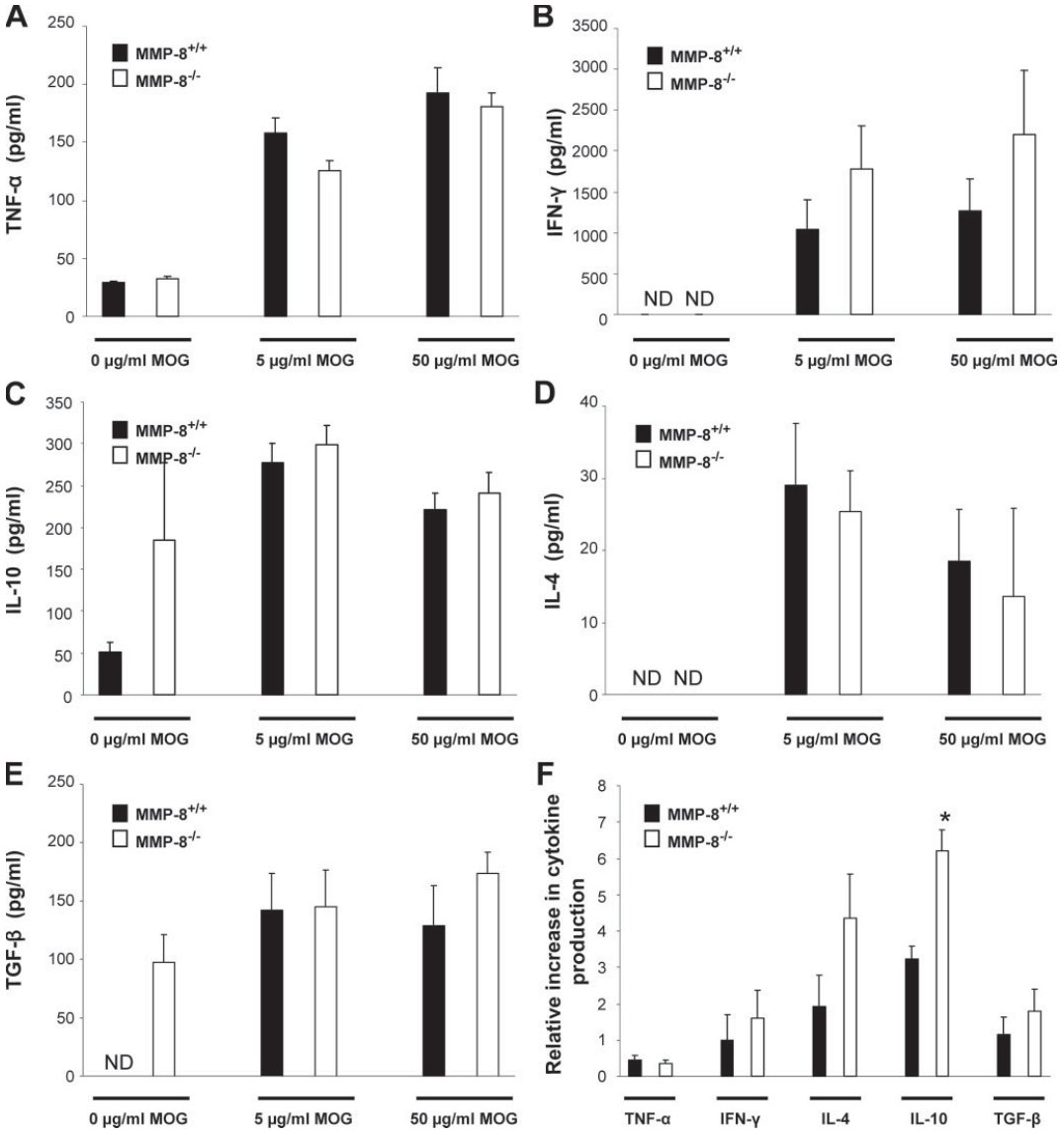

FIGURE 7. **Increased Th2-type cytokine production in splenocytes from *MMP-8*$^{-/-}$ mice during the chronic phase of EAE.** Spleens from 8-week-old *MMP-8*$^{+/+}$ ($n = 4$) and *MMP-8*$^{-/-}$ ($n = 3$) mice with representative disease scores were isolated during the chronic phase of the disease. Splenic cells were cultured and stimulated *in vitro* with 0, 5, and 50 μg/ml MOG_{35-55}. Supernatants were collected at 48 h and the production of TNF-α (*A*), IFN-γ (*B*), IL-10 (*C*), IL-4 (*D*), and TGF-β (*E*) was determined by enzyme-linked immunosorbent assay. *ND*, not detectable. The relative increase in cytokine production during the chronic phase was calculated by comparison with the average of cytokine production obtained in each group during the acute phase of the disease. These results correspond to the values obtained with cultured splenocytes stimulated with 5 μg/ml MOG_{35-55} (*F*). Values are means ± S.E. *, $p \leq 0.05$.

The histopathological analysis of the spinal cord and brain parenchyma revealed a marked correlation between the observed clinical symptoms and the degree of inflammation. Thus, samples taken during the acute phase of the disease showed similar meningeal inflammatory foci in both wild-type and *MMP-8*$^{-/-}$ mice. However, during the chronic phase of the disease, the severity of the infiltrating and demyelinating lesions was markedly reduced in *MMP-8*$^{-/-}$ mice. Considering that a large number of neutrophils was present at the sites of inflammation and that it has been reported that these cells play a key role in the recruitment of inflammatory cells during the effector phase of the disease (41), our results suggest that MMP-8 may contribute to this regulatory function of the immune response once the inflammation has been initiated.

TABLE 2
Inhibitory activity of (*R*)-1-(3′-methylbiphenyl-4-sulfonylamino)methylpropylphosphonic acid against MMPs and ADAMs
IC_{50} (nM); errors are in the range of 5–10% of the reported value.

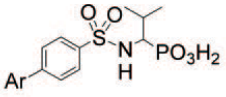

No.	Ar	MMP-1	MMP-2	MMP-3	MMP-7	MMP-8	MMP-9	MMP-13	MMP-14	ADAM-10	ADAM-17
(*R*)-14i		320	24	230	1100	0.4	64	15	26	>10000	>10000

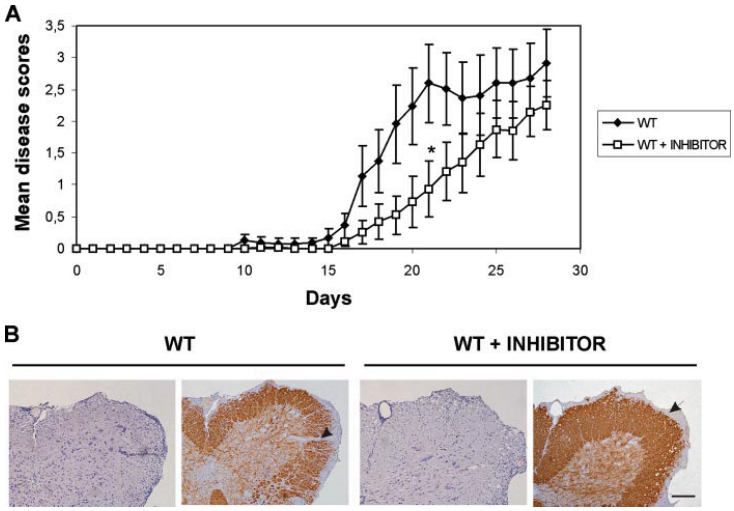

FIGURE 8. **Pharmacological inhibition of MMP-8 attenuates clinical severity of EAE during the acute phase of the disease.** Eight-week-old wild-type mice were immunized with MOG_{35-55} and injected intraperitoneally daily with a dose of 25 mg/kg body weight of an MMP-8 inhibitor, starting at the time of MOG immunization ($n = 9$). This group was compared with a control group of wild-type mice immunized with MOG_{35-55} ($n = 11$). Mice were monitored daily and scored for clinical symptoms of EAE. Results are expressed as mean disease score ± S.E. *, $p \leq 0.05$. *A*, representative hematoxylin and eosin staining (*first* and *third panels*) and myelin basic protein immunohistochemistry (*second* and *fourth panels*) of spinal cords from control and treated mice sacrificed during the chronic phase of the disease (*B*). The data shown are representative of two independent experiments. Magnification, 10×. *Scale bar*, 100 μm.

Consistent with this possibility, the analysis of the antigen-specific responses of splenocytes isolated from wild-type and *MMP-8*$^{-/-}$ mice revealed a greater increase in certain immunomodulatory cytokines in the *MMP-8*$^{-/-}$ cultures during the chronic phase of the disease, compared with the response observed in wild-type samples. Thus, levels of IL-10, which is critical in the regulation of EAE progression (42), are significantly increased in splenocytes from *MMP-8*$^{-/-}$ mice at this chronic phase, suggesting that the absence of MMP-8 may affect Th1/Th2 polarization responses in *MMP-8*$^{-/-}$ splenic cells during the chronic phase of EAE.

The results described herein with *MMP-8*$^{-/-}$ mice and the EAE model should be consistent with the idea that therapeutic inhibition of MMP-8 may reduce the clinical symptoms of the treated mice. In agreement with this proposal, we have demonstrated in this work that the administration of an MMP-8-selective inhibitor markedly reduces the severity of EAE. Interestingly, the protective effect of the inhibitor was more pronounced in the early stages of the disease, whereas data from mutant mice indicate a critical role for the protease at later stages during the disease development. A possible explanation for these results derives from the temporal window in which the proteolytic function of MMP-8 is targeted. Thus, in *MMP-8*$^{-/-}$ mice, the absence of the protease encoded by the targeted gene can induce compensatory or adaptive mechanisms during the embryonic development until adult life in an attempt to replace the functions provided by this enzyme. However, this response is limited when the inhibition is performed in a particular moment during the adult life, as is the case of pharmacological interventions like that based on the administration of the MMP-8-selective inhibitor used in this study. We have also to consider that this inhibitor, although it mainly targets MMP-8, can also block the activity of other related MMPs. Accordingly, additional studies with MMP-8-specific inhibitors currently unavailable as well as with animal models deficient in other MMPs will be necessary to define the precise relevance of MMP-8 in the pathogenesis of MS.

In conclusion, our results provide the first causal evidence that MMP-8 plays an important role in EAE development and open a novel therapeutic possibility to reduce the clinical symptoms of human neuro-inflammatory diseases by specific targeting of this member of the large and complex family of matrix metalloproteinases.

Acknowledgments—We thank Drs. S. Shapiro, C. Gallina, A. M. Pendás, and M. Balbín for support and helpful comments and F. Rodríguez and C. Garabaya for excellent technical assistance.

REFERENCES

1. Steinman, L., Martin, R., Bernard, C., Conlon, P., and Oksenberg, J. R. (2002) *Annu. Rev. Neurosci.* **25,** 491–505

2. Hafler, D. A., Slavik, J. M., Anderson, D. E., O'Connor, K. C., De Jager, P., and Baecher-Allan, C. (2005) *Immunol. Rev.* **204,** 208–231
3. Sospedra, M., and Martin, R. (2005) *Annu. Rev. Immunol.* **23,** 683–747
4. Hemmer, B., Archelos, J. J., and Hartung, H. P. (2002) *Nat. Rev. Neurosci.* **3,** 291–301
5. Bernard, C. C., Johns, T. G., Slavin, A., Ichikawa, M., Ewing, C., Liu, J., and Bettadapura, J. (1997) *J. Mol. Med.* **75,** 77–88
6. Muller, D. M., Pender, M. P., and Greer, J. M. (2005) *J. Neuroimmunol.* **160,** 162–169
7. Yong, V. W., Power, C., Forsyth, P., and Edwards, D. R. (2001) *Nat. Rev. Neurosci.* **2,** 502–511
8. Rosenberg, G. A. (2002) *Glia* **39,** 279–291
9. Lindberg, R. L., De Groot, C. J., Montagne, L., Freitag, P., van der Valk, P., Kappos, L., and Leppert, D. (2001) *Brain* **124,** 1743–1753
10. Yong, V. W., Zabad, R. K., Agrawal, S., Goncalves Dasilva, A., and Metz, L. M. (2007) *J. Neurol. Sci.* **259,** 79–84
11. D'Souza, C. A., Mak, B., and Moscarello, M. A. (2002) *J. Biol. Chem.* **277,** 13589–13596
12. Nygardas, P. T., and Hinkkanen, A. E. (2002) *Clin. Exp. Immunol.* **128,** 245–254
13. Bar-Or, A., Nuttall, R. K., Duddy, M., Alter, A., Kim, H. J., Ifergan, I., Pennington, C. J., Bourgoin, P., Edwards, D. R., and Yong, V. W. (2003) *Brain* **126,** 2738–2749
14. Toft-Hansen, H., Nuttall, R. K., Edwards, D. R., and Owens, T. (2004) *J. Immunol.* **173,** 5209–5218
15. Brundula, V., Rewcastle, N. B., Metz, L. M., Bernard, C. C., and Yong, V. W. (2002) *Brain* **125,** 1297–1308
16. Giuliani, F., Fu, S. A., Metz, L. M., and Yong, V. W. (2005) *J. Neuroimmunol.* **165,** 83–91
17. Opdenakker, G., Nelissen, I., and Van Damme, J. (2003) *Lancet Neurol.* **2,** 747–756
18. Liedtke, W., Cannella, B., Mazzaccaro, R. J., Clements, J. M., Miller, K. M., Wucherpfennig, K. W., Gearing, A. J., and Raine, C. S. (1998) *Ann. Neurol.* **44,** 35–46
19. Dubois, B., Masure, S., Hurtenbach, U., Paemen, L., Heremans, H., van den Oord, J., Sciot, R., Meinhardt, T., Hammerling, G., Opdenakker, G., and Arnold, B. (1999) *J. Clin. Invest.* **104,** 1507–1515
20. Agrawal, S., Anderson, P., Durbeej, M., van Rooijen, N., Ivars, F., Opdenakker, G., and Sorokin, L. M. (2006) *J. Exp. Med.* **203,** 1007–1019
21. Esparza, J., Kruse, M., Lee, J., Michaud, M., and Madri, J. A. (2004) *FASEB J.* **18,** 1682–1691
22. Weaver, A., Goncalves da Silva, A., Nuttall, R. K., Edwards, D. R., Shapiro, S. D., Rivest, S., and Yong, V. W. (2005) *FASEB J.* **19,** 1668–1670
23. Folgueras, A. R., Pendás, A. M., Sánchez, L. M., and López-Otín, C. (2004) *Int. J. Dev. Biol.* **48,** 411–424
24. Brinckerhoff, C. E., and Matrisian, L. M. (2002) *Nat. Rev. Mol. Cell. Biol.* **3,** 207–214
25. Gijbels, K., Proost, P., Masure, S., Carton, H., Billiau, A., and Opdenakker, G. (1993) *J. Neurosci. Res.* **36,** 432–440
26. Proost, P., Van Damme, J., and Opdenakker, G. (1993) *Biochem. Biophys. Res. Commun.* **192,** 1175–1181
27. Parks, W. C., Wilson, C. L., and López-Boado, Y. S. (2004) *Nat. Rev. Immunol.* **4,** 617–629
28. Zhang, K., McQuibban, G. A., Silva, C., Butler, G. S., Johnston, J. B., Holden, J., Clark-Lewis, I., Overall, C. M., and Power, C. (2003) *Nat. Neurosci.* **6,** 1064–1071
29. Balbín, M., Fueyo, A., Knauper, V., Pendás, A. M., López, J. M., Jiménez, M. G., Murphy, G., and López-Otín, C. (1998) *J. Biol. Chem.* **273,** 23959–23968
30. Owen, C. A., Hu, Z., López-Otín, C., and Shapiro, S. D. (2004) *J. Immunol.* **172,** 7791–7803
31. Gueders, M. M., Balbín, M., Rocks, N., Foidart, J. M., Gosset, P., Louis, R., Shapiro, S., López-Otín, C., Noël, A., and Cataldo, D. D. (2005) *J. Immunol.* **175,** 2589–2597
32. Sorsa, T., Tjaderhane, L., and Salo, T. (2004) *Oral Dis.* **10,** 311–318
33. Van Lint, P., Wielockx, B., Puimege, L., Noël, A., López-Otín, C., and Libert, C. (2005) *J. Immunol.* **175,** 7642–7649
34. Pirila, E., Ramamurthy, N. S., Sorsa, T., Salo, T., Hietanen, J., and Maisi, P. (2003) *Dig. Dis. Sci.* **48,** 93–98
35. Balbín, M., Fueyo, A., Tester, A. M., Pendás, A. M., Pitiot, A. S., Astudillo, A., Overall, C. M., Shapiro, S. D., and López-Otín, C. (2003) *Nat. Genet.* **35,** 252–257
36. Biasone, A., Tortorella, P., Campestre, C., Agamennone, M., Preziuso, S., Chiappini, M., Nuti, E., Carelli, P., Rossello, A., Mazza, F., and Gallina, C. (2007) *Bioorg. Med. Chem.* **15,** 791–799
37. Graesser, D., Mahooti, S., and Madri, J. A. (2000) *J. Neuroimmunol.* **109,** 121–131
38. Wang, X., Jung, J., Asahi, M., Chwang, W., Russo, L., Moskowitz, M. A., Dixon, C. E., Fini, M. E., and Lo, E. H. (2000) *J. Neurosci.* **20,** 7037–7042
39. Gutiérrez-Fernández, A., Inada, M., Balbín, M., Fueyo, A., Pitiot, A. S., Astudillo, A., Hirose, K., Hirata, M., Shapiro, S. D., Noel, A., Werb, Z., Krane, S. M., López-Otín, C., and Puente, X. S. (2007) *FASEB J.* **21,** 2580–2591
40. Tester, A. M., Cox, J. H., Connor, A. R., Starr, A. E., Dean, R. A., Puente, X. S., López-Otín, C., and Overall, C. M. (2007) *PLoS ONE* **2,** e312
41. McColl, S. R., Staykova, M. A., Wozniak, A., Fordham, S., Bruce, J., and Willenborg, D. O. (1998) *J. Immunol.* **161,** 6421–6426
42. Bettelli, E., Das, M. P., Howard, E. D., Weiner, H. L., Sobel, R. A., and Kuchroo, V. K. (1998) *J. Immunol.* **161,** 3299–3306
43. Balbín, M., Fueyo, A., Knauper, V., López, J. M., Álvarez, J., Sánchez, L. M., Quesada, V., Bordallo, J., Murphy, G., and López-Otín, C. (2001) *J. Biol. Chem.* **276,** 10253–10262

REPORT

Exome Sequencing and Functional Analysis Identifies *BANF1* Mutation as the Cause of a Hereditary Progeroid Syndrome

Xose S. Puente,[1] Victor Quesada,[1] Fernando G. Osorio,[1] Rubén Cabanillas,[2] Juan Cadiñanos,[2] Julia M. Fraile,[1] Gonzalo R. Ordóñez,[1] Diana A. Puente,[1] Ana Gutiérrez-Fernández,[1] Miriam Fanjul-Fernández,[1] Nicolas Lévy,[3] José M.P. Freije,[1] and Carlos López-Otín[1,*]

Accelerated aging syndromes represent a valuable source of information about the molecular mechanisms involved in normal aging. Here, we describe a progeroid syndrome that partially phenocopies Hutchinson-Gilford progeria syndrome (HGPS) but also exhibits distinctive features, including the absence of cardiovascular deficiencies characteristic of HGPS, the lack of mutations in *LMNA* and *ZMPSTE24*, and a relatively long lifespan of affected individuals. Exome sequencing and molecular analysis in two unrelated families allowed us to identify a homozygous mutation in *BANF1* (c.34G>A [p.Ala12Thr]), encoding barrier-to-autointegration factor 1 (BAF), as the molecular abnormality responsible for this Mendelian disorder. Functional analysis showed that fibroblasts from both patients have a dramatic reduction in BAF protein levels, indicating that the p.Ala12Thr mutation impairs protein stability. Furthermore, progeroid fibroblasts display profound abnormalities in the nuclear lamina, including blebs and abnormal distribution of emerin, an interaction partner of BAF. These nuclear abnormalities are rescued by ectopic expression of wild-type *BANF1*, providing evidence for the causal role of this mutation. These data demonstrate the utility of exome sequencing for identifying the cause of rare Mendelian disorders and underscore the importance of nuclear envelope alterations in human aging.

Aging is a very complex process that affects most biological functions of the organism, but its molecular basis remain largely unknown.[1] Over the last few years, our knowledge of the molecular mechanisms underlying human aging has gained new insights from studies on premature aging syndromes that cause the early development of multiple phenotypes normally associated with advanced age.[2,3] Most of these human progeroid syndromes are caused by defects in DNA repair systems, but recent studies have shown that alterations in nuclear envelope formation and dynamics are involved in the development of accelerated aging syndromes.[4] Thus, patients with Hutchinson-Gilford progeria syndrome (HGPS [MIM 176670]) carry mutations in *LMNA* (MIM 150330), which encodes two major components of the nuclear envelope, the lamins A and C.[5,6] In addition, other progeroid syndromes, such as restrictive dermopathy (RD [MIM 275210]) and mandibuloacral dysplasia (MADB [MIM 608612]), are caused by mutations in *ZMPSTE24* (also known as *FACE1* [MIM 606480]),[7,8] which encodes a metalloprotease involved in prelamin A maturation.[9] However, there may still be other classes of genetic mutations responsible for the development of accelerated aging in patients who lack mutations in all previously described genes associated with these devastating diseases.

The recent availability of high-throughput sequencing technologies has now made it feasible to address personal genome projects that could uncover the precise genetic causes of human diseases.[10,11] In addition to whole-genome sequencing, exome sequencing has been successfully used to identify mutations responsible for genetic disorders of unknown cause.[12–15] In this work, we have used this approach to identify the disease-causing mutations in patients who were originally diagnosed with a progeroid syndrome that phenocopies features of HGPS and mandibuloacral dysplasia but whose mutational analysis of candidate genes did not reveal any change in *LMNA* or *ZMPSTE24*.

To gain insights into the molecular mechanisms implicated in putative accelerated aging, we studied patients with progeroid syndromes without mutations in known candidate genes. Affected individuals are members of two unrelated Spanish families, from distant regions of the country (family A is from Gran Canaria; family B is from Castilla). DNA samples were isolated from peripheral-blood leukocytes via standard techniques. The experiments were conducted in accordance with the guidelines of the Comité Científico de la Fundación Centro Médico de Asturias, and written informed consent was obtained from each individual providing biological samples. The pedigrees for both families are shown in Figure 1. The first patient studied (II-1, family A; Figure 1) was the second child born to consanguineous third cousins (coefficient of inbreeding, $F = 1/64$). Both parents and his four siblings were healthy, and there was no significant clinical family history. The patient exhibited normal development until 2 years of age. From that age, he experienced failure to thrive and his skin became dry and atrophic with small light-brown

[1]Departamento de Bioquímica y Biología Molecular, Facultad de Medicina, Instituto Universitario de Oncología, Universidad de Oviedo, 33006-Oviedo, Spain; [2]Instituto de Medicina Oncológica y Molecular de Asturias, Centro Médico de Asturias, 33193-Oviedo, Spain; [3]Université de la Méditerranée, INSERM, UMR_S910, Faculté de Médecine la Timone, 13385-Marseille, France
*Correspondence: clo@uniovi.es
DOI 10.1016/j.ajhg.2011.04.010.

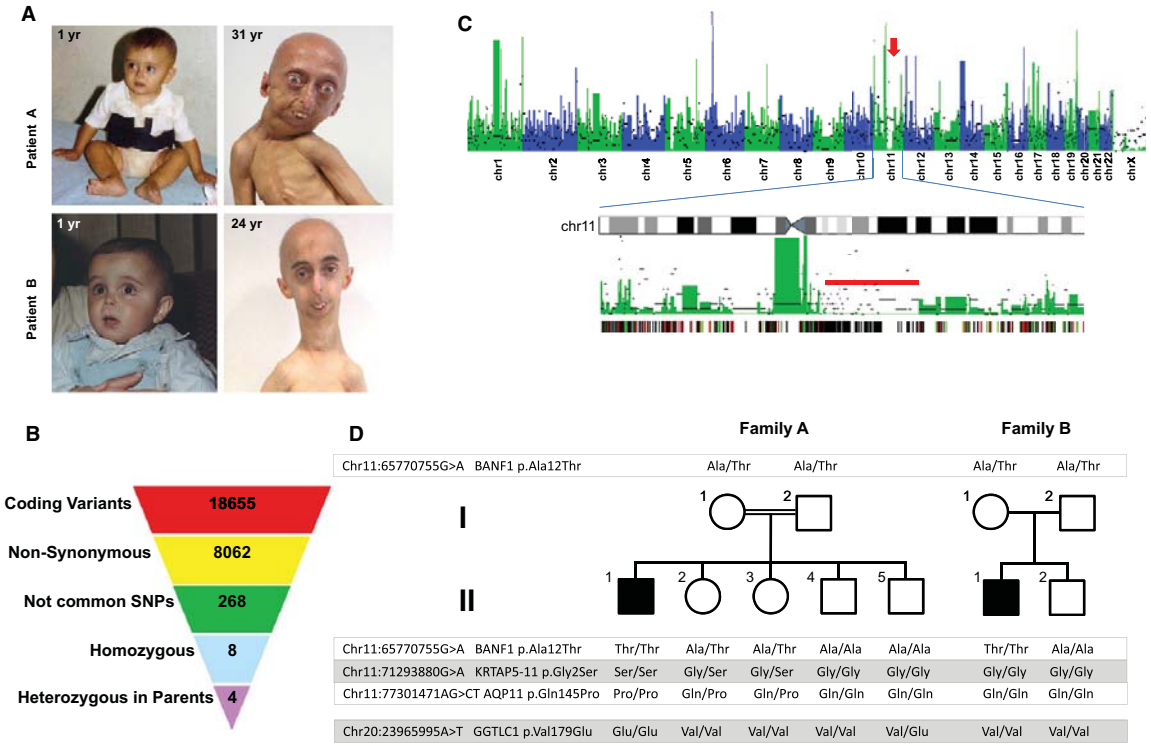

Figure 1. Identification of a Mutation in *BANF1* by Exome Sequencing in a Patient with Atypical Progeria
(A) The appearance of both patients included in the study at 1 year of age (left), evidence of progeroid features in patient A at 31 years of age (top), and evidence of such features in patient B at 24 years (bottom). Clinical characteristics include facial abnormalities due to severe bone changes, small chin, convex nasal ridge, and prominent eyes. The presence of eyebrows and eyelashes are characteristics of atypical progeria.
(B) Scheme showing the filtering procedure used for identifying candidate genes in study of this progeroid syndrome, assuming a recessive inheritance model. Coding variants were filtered by retaining only those causing amino acid substitution. Common polymorphisms present in either dbSNP131 or in ten unrelated individual genomes were excluded. Homozygous variants that were present in heterozygosity in both parents were finally selected.
(C) Manhattan plot showing the density of heterozygous variants obtained from exome sequencing data in 50 Kb nonoverlapping windows of coding-sequence. The density of homozygous variants per window is indicated by black bars. An arrow indicates the presence of a homozygosity track on chromosome 11. Below is a detailed view of chromosome 11, showing a long stretch of homozygosity (red bar), and a plot showing mutations present in the patient and the mother (red lines), in the patient and the father (green lines), and in the patient and both parents (black lines).
(D) Pedigrees and results from sequencing of the four candidate gene variants in both families.

spots over the thorax, scalp, and limbs. He also developed a generalized lipoatrophy, severe osteoporosis, and marked osteolysis. The atrophic facial subcutaneous fat pad and the marked osteolysis of the maxilla and mandible result in a typical pseudosenile facial appearance with micrognatia, prominent subcutaneous venous patterning, a convex nasal ridge, and proptosis (Figure 1A and Figure S1 available online). His cognitive development was completely normal. Despite an initial diagnosis of HGPS or MAD, some of the clinical features suggested that this patient could have a distinct progeroid syndrome. The age of the patient (31 years, which is very unusual given that most HGPS patients die in their teenage years), his height (145 cm, underestimated as a result of his scoliosis), the presence of eyebrows and eyelashes, the persistence of scalp hair until the age of 12 (which never disappeared completely), the very severe osteolysis (of the mandible, clavicles, ribs, distal phalanges, and radius), and the absence of coronary dysfunction, atherosclerosis, or metabolic anomalies finally led to the diagnosis of atypical progeria. A second patient (II-1, family B; Figure 1), a 24-year-old man showing a phenotype almost identical to the index case (Figure 1A and Figure S2), was also analyzed. Despite thorough cardiovascular examination (echocardiogram, stress test, cardiac computed tomography, Doppler study of supra-aortic trunks), neither of the patients showed signs of ischemia or atherosclerosis, both cardinal features of HGPS.[16] Moreover, the lack of mutations in *LMNA* and *ZMPSTE24* would also be consistent with the hypothesis that these patients have a different progeroid syndrome.

To evaluate this possibility at the molecular level, we first performed exon enrichment, followed by massively

parallel sequencing on DNA samples from the proband (II-1, family A; Figure 1) and both parents. Three micrograms of genomic DNA was fragmented and hybridized with the use a SureSelect Human All Exon Kit (Agilent, Palo Alto, CA) together with the Paired-End Sample Preparation Kit from Illumina in accordance with the manufacturers' protocols. The captured DNA fragments were sequenced with the Genome Analyzer *IIx* (Illumina, San Diego, CA), with the use of two lanes per sample and 52 cycles, resulting in more than 60 million paired reads per sample. Reads were aligned to the reference genome (GRCh37) with the Burrows-Wheeler Aligner (BWA 0.5.7),[17] and SAMtools 0.1.7[18] was used for removal of PCR duplicates and initial SNP calling. All single-nucleotide variants were required to have a minimum SNP quality of 40, supported by reads in both orientations, and to be no fewer than three bases from an indel. Common variants present in either dbSNP131 or in ten personal genomes of Spanish origin were filtered. Homozygous variants were identified with the use of custom scripts and verified by visual inspection. More than 98% of the coding exome was covered by at least one read in the three individuals, and more than 90% was covered by at least ten reads. Although these extremely rare diseases can be caused by dominant de novo mutations, we first assumed an autosomal-recessive mode of inheritance because of the consanguinity of healthy parents. We first searched for homozygous variants and applied a model of identity by descent (IBD). Out of the 18,655 coding variants found in the proband, 8062 produced nonsynonymous changes, from which 96% were present either in dbSNP131 or in several unrelated individuals from whom genomic data were available at our group (Figure 1B). Only four of the uncommon remaining variants were homozygous in the proband and heterozygous in the parents. Interestingly, three of the four candidate genes (*BANF1* [MIM 603811], *KRTAP5-11*, and *AQP11* [MIM 609914]) were located in a long contiguous stretch of homozygosity on chromosome 11q13 (Figure 1C), whereas the fourth one (*GGTLC1* [MIM 612338]) was located on chromosome 20p11. SNP array analysis revealed that the first region contained two copies in the proband, precluding the occurrence of a large deletion in this patient. In addition, all nucleotide variants detected in this region were also present in both the father and the mother, indicating that this homozygosity track was not due to uniparental disomy but was independently inherited from the parents.

The presence of three candidate genes in a small locus of less than 13 Mb would likely result in linkage disequilibrium between the three variants, thus making difficult the identification of the individual alteration responsible for this disease. Therefore, we performed PCR amplification and capillary sequencing of the four variants mentioned above in the studied family and in the second family, with a similar progeroid syndrome and without mutations in either *LMNA* or *ZMPSTE24*. We found that the affected individual from the second family (II-1, family B; Figure 1) had the same homozygous mutation (chr11:65770755G>A) in *BANF1* (NM_001143985.1, c.34G>A [p.Ala12Thr]) that was originally identified in the patient from family A, although sequencing of the coding regions of *AQP11*, *KRTAP5-11*, and *GGTLC1* did not reveal additional mutations (Figure 1D and Figure S3). Even though both families are of different geographical origins and they did not report any known relationship with each other, both patients shared a common homozygous haplotype comprising four SNPs in *BANF1* (rs14157, G/G; rs1786171, C/C; rs1786172, G/G; rs56984820, −/−), which suggests the occurrence of a founder mutation. All nonaffected members from both families were either heterozygous or did not have the *BANF1* mutation, and sequencing of more than 400 chromosomes from individuals of the Spanish population failed to detect this variant, confirming that it is not a common polymorphism. Together, these data strongly support the causal role of this mutation in *BANF1* as the genetic alteration responsible for this progeroid syndrome.

BANF1 encodes a protein of 89 amino acids called barrier-to-autointegration factor 1 (BAF), which forms dimers and is implicated in nuclear envelope assembly.[19] The affected residue (Ala12) has been highly conserved through evolution from fish to humans (Figure 2A), suggesting an important role in the structure or function of this small protein. BAF interacts with DNA as well as with different proteins,[19–21] including lamin A, which is mutated in HGPS, reinforcing the role of BAF in the segmental progeroid syndrome exhibited by the patients described herein. A three-dimensional model of mutant BAF shows that the mutated residue is located on the surface of the protein[22,23] (Figure 2B). Nevertheless, the p.Ala12Thr mutation is not predicted to affect BAF dimerization or its binding to either DNA or emerin, raising the possibility that this amino acid substitution could impair the interaction with other proteins, its subcellular localization, or its stability. For examination of the effect of the BAF p.Ala12Thr mutation at the protein level, a skin biopsy was obtained from both patients and from a parent (I-1, family A) and used to establish cell cultures of primary dermal fibroblasts. Control cells (AG10803 human skin fibroblasts) were obtained from the Coriell Cell Repository. We analyzed BAF expression in primary fibroblasts from both patients (homozygous for the mutation), from a heterozygous carrier (I-1, family A), and from control fibroblasts, using immunoblotting with mouse monoclonal anti-BAF (ab88464, Abcam), which recognizes two bands corresponding to phosphorylated (slower migrating) and nonphosphorylated (faster migrating) BAF.[24] Fibroblasts homozygous for the p.Ala12Thr mutation had very low levels of BAF protein as compared to control fibroblasts, whereas heterozygous fibroblasts had intermediate levels (Figure 2C). Quantitative RT-PCR experiments using a specific TaqMan expression assay for *BANF1* (Applied Biosystems, Foster City, CA) revealed that *BANF1* mRNA levels were not significantly

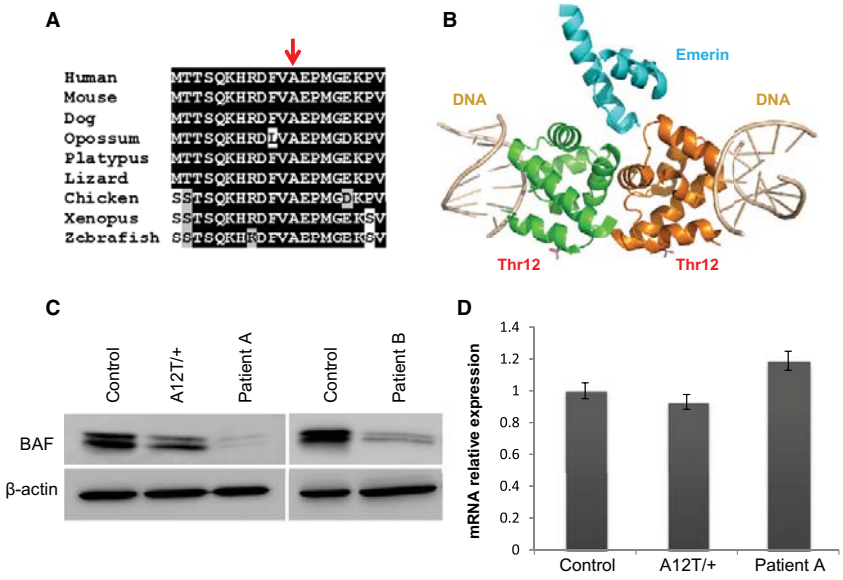

Figure 2. Alteration of BAF Structure in Cells Homozygous for the p.Ala12Thr Mutation
(A) Sequence alignment of the first 20 residues of human BAF to its orthologs from the indicated species, showing the evolutionary conservation of the Ala12 residue (indicated with an arrow).
(B) Three-dimensional model of a BAF dimer (green and orange in the figure) in complex with emerin (blue) and DNA (gray). To generate the model, the structure of the BAF dimer-emerin complex (PDB 2ODG) was aligned with the structure of a BAF-DNA complex (PDB 2BZF) with the use of PyMOL. The position of the Thr residue in mutant BAF is indicated.
(C) Immunoblot analysis of BAF in control human fibroblasts along with fibroblasts from patients homozygous for the p.Ala12Thr mutation and from the mother (heterozygous carrier) of the family A patient. The immunoblots shown are representative of three independent experiments.
(D) *BANF1* mRNA relative levels in fibroblasts homozygous or heterozygous for the p.Ala12Thr mutation, determined by qRT-PCR. Values correspond to the mean of triplicates. Error bars represent standard deviation of the mean.

downregulated in the mutant cells, indicating that this mutation affects the stability of the protein rather than having an effect at the mRNA level (Figure 2D).

A morphological analysis of the nuclei from mutant fibroblasts revealed profound nuclear abnormalities, including blebs and aberrations previously described in other laminopathies[5–8,25,26] (Figure 3). Immunofluorescence analysis using antibodies against lamin A/C and emerin, interaction partners of BAF and structural constituents of the nuclear lamina,[27,28] revealed significant differences in the subcellular distribution of emerin between control cells and fibroblasts from these patients (Figure 3), whereas alterations in lamin A/C distribution were not evident under the same conditions (Figure S4). Emerin was specifically located in the nuclear lamina of normal fibroblasts, whereas in fibroblasts homozygous for the p.Ala12Thr mutation, emerin lost its nuclear distribution and was found predominantly in the cytoplasm, with some minor staining in the nuclear lamina.

To further confirm the causal role of the BAF p.Ala12Thr mutation in this process, we generated an EGFP-BAF protein by cloning the coding sequence of human BAF in the polylinker region of pEGFP-C1 (Clontech, Palo Alto, CA). We transiently transfected mutant fibroblasts with this expression vector encoding an EGFP-BAF fusion protein, and confocal microscopy analysis revealed that ectopic expression of EGFP-BAF in these progeroid fibroblasts rescued the nuclear abnormalities. Thus, EGFP-BAF-positive cells recovered a normal nuclear morphology, in contrast to the aberrations observed in control cells transfected with EGFP (Figure 4). These findings are consistent with the reported relevance of BAF in nuclear lamina dynamics.[29,30] In fact, experimental reduction of BAF by RNAi in human cells results in the formation of nuclear envelope alterations and abnormal localization of emerin,[29] similar to the findings observed in these progeroid patients. Together, these results show that the p.Ala12Thr mutation in BAF identified in patients with this progeroid syndrome causes an abnormal distribution of components of the nuclear lamina, which are likely responsible for the nuclear abnormalities observed in this laminopathy. The phenotypic expression of laminopathies is highly variable, and although our two patients have features that are also exhibited in HGPS and mandibuloacral dysplasia, their clinical findings differ in several aspects. Neither of our patients has signs of atherosclerosis or cardiac ischemia (fatal heart attacks and strokes at a mean age of 13 years are a common feature of HGPS). Additionally, our patients do not have insulin resistance, diabetes mellitus, or hypertriglyceridemia, all of which are usual features of mandibuloacral dysplasia. Finally, it is remarkable

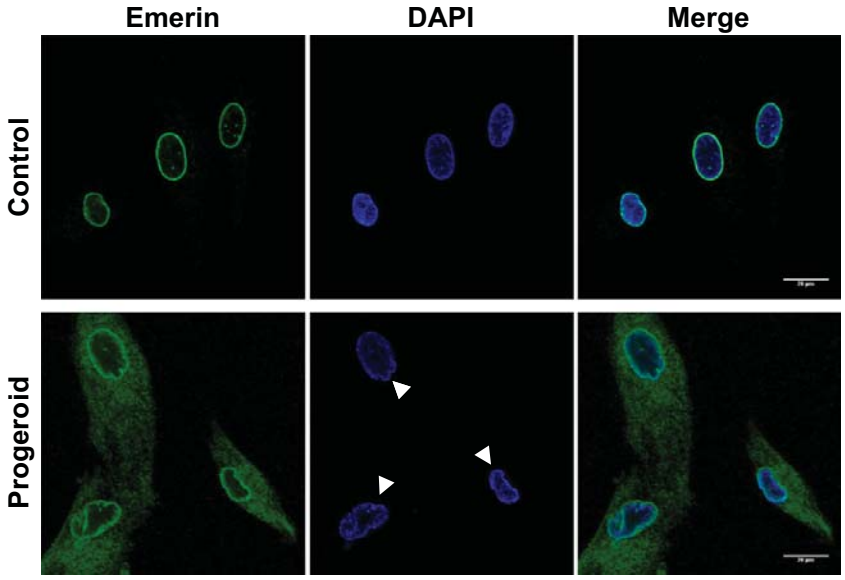

Figure 3. Nuclear Envelope Alterations in Fibroblasts Homozygous for the p.Ala12Thr Mutation in BAF
Emerin distribution was analyzed by immunofluorescence with the use of an anti-emerin rabbit polyclonal antibody (ab14208, Abcam) and by confocal microscopy (Leica SP2) in primary fibroblasts from the progeroid patient II-1 (family A) and in control fibroblasts. Nuclei with structural abnormalities can be observed in progeroid fibroblasts.

that despite the phenotypic overlapping between patients with HGPS or mandibuloacral dysplasia and those with the segmental progeria described herein, the observed differences are of utmost importance to patients and their families. Thus, it seems that those patients with the progeroid syndrome caused by *BANF1* mutation are not at increased risk of acute myocardial infarcts, cerebrovascular accidents, or diabetes mellitus. In contrast, they suffer profound skeletal abnormalities that affect their quality of life (both patients experience pain, dysfunction, and disability) and occasionally may result in life-threatening complications, such as pulmonary hypertension secondary to severe scoliosis. Therefore, palliation of osseous manifestations is a priority in our patients, given their relatively long lifespan.

In summary, the finding of mutations in *BANF1* associated with a progeroid syndrome may open therapeutic approaches for patients with this condition, as has been the case for children with HGPS (ClinicalTrials.gov; NCT00731016, NCT00425607, NCT00916747).[31–33] Furthermore, the fact that BAF is functionally connected to the nuclear envelope, together with the previous finding that prelamin A isoforms are accumulated during normal and pathological aging,[5,6,34–36] underscores the importance of the nuclear lamina for human aging and may provide new mechanistic insights about this complex, multifactorial, and universal process.

Supplemental Data

Supplemental Data include four figures and can be found with this article online at http://www.cell.com/AJHG/.

Acknowledgments

We thank the atypical progeria patients and their families for participating in this study, and especially N.M.O. and G.R.P. for their courage and enthusiasm. We also thank Y. Español for help with confocal microscopy; A. Ramsay and G. Velasco for helpful comments; S. Álvarez, M. Fernández, and R. Álvarez for excellent technical assistance; and the staff of the Centro Médico de Asturias for their kind assistance. This work has been supported by grants from Ministerio de Ciencia e Innovación-Spain, PCTI-FICYT Asturias, Fundación Centro Médico de Asturias, Fundación María Cristina Masaveu Peterson, and the European Union (FP7 Micro-EnviMet). C.L-O. is an investigator in the Botin Foundation. The Instituto Universitario de Oncología is supported by Obra Social Cajastur and Acción Transversal del Cáncer-RTICC.

Received: March 22, 2011
Revised: April 13, 2011
Accepted: April 13, 2011
Published online: May 5, 2011

Web Resources

The URLs for data presented herein are as follows:

ClinicalTrials.gov, http://clinicaltrials.gov
Online Mendelian Inheritance in Man (OMIM), http://www.omim.org

References

1. Vijg, J., and Campisi, J. (2008). Puzzles, promises and a cure for ageing. Nature *454*, 1065–1071.

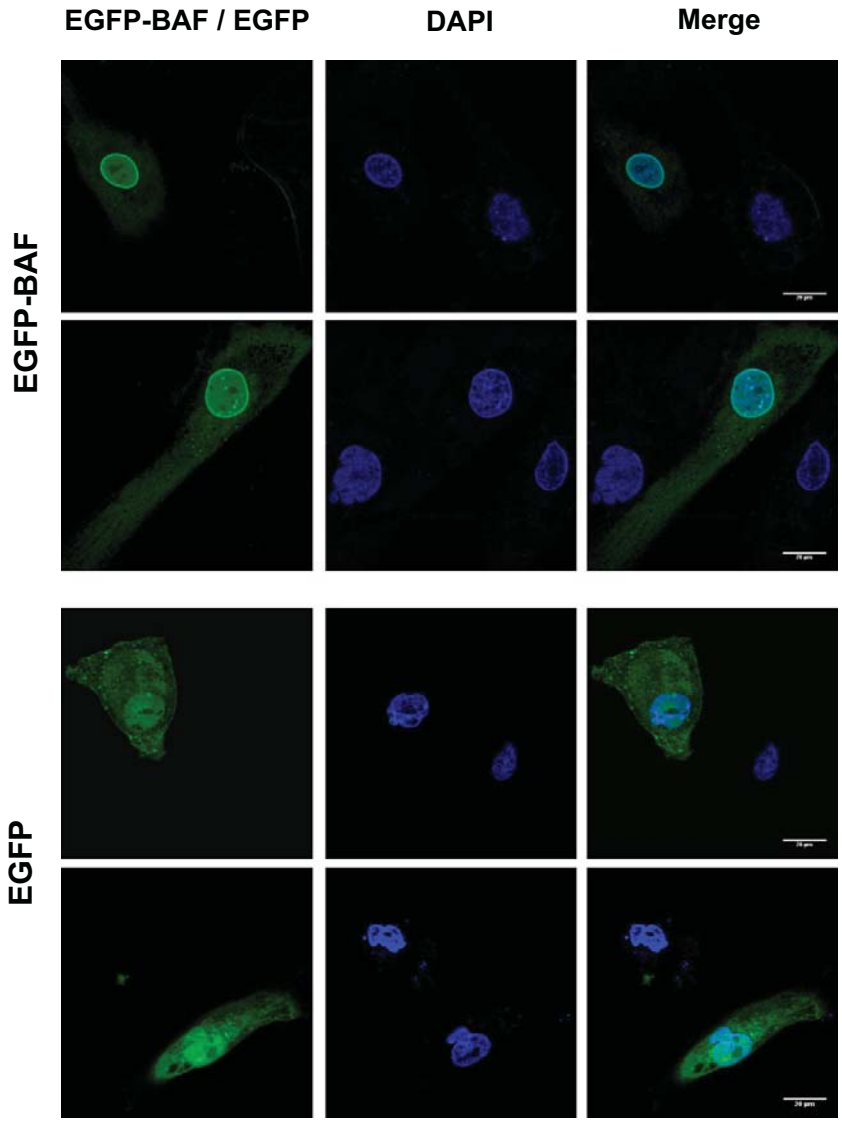

Figure 4. Rescue of the Nuclear Abnormalities by *BANF1* Ectopic Expression
Fibroblasts from patient II-1 (family A) were transiently transfected with an expression vector encoding EGFP-BAF or EGFP alone as control and were analyzed by confocal microscopy. Untransfected progeroid cells present in the same preparation show frequent nuclear abnormalities (arrowheads). These structural alterations are rescued by *BANF1* ectopic expression. Two independent representative fields are shown.

2. Martin, G.M., and Oshima, J. (2000). Lessons from human progeroid syndromes. Nature *408*, 263–266.
3. Burtner, C.R., and Kennedy, B.K. (2010). Progeria syndromes and ageing: what is the connection? Nat. Rev. Mol. Cell Biol. *11*, 567–578.
4. Ramírez, C.L., Cadiñanos, J., Varela, I., Freije, J.M., and López-Otín, C. (2007). Human progeroid syndromes, aging and cancer: new genetic and epigenetic insights into old questions. Cell. Mol. Life Sci. *64*, 155–170.
5. De Sandre-Giovannoli, A., Bernard, R., Cau, P., Navarro, C., Amiel, J., Boccaccio, I., Lyonnet, S., Stewart, C.L., Munnich, A., Le Merrer, M., and Lévy, N. (2003). Lamin a truncation in Hutchinson-Gilford progeria. Science *300*, 2055.
6. Eriksson, M., Brown, W.T., Gordon, L.B., Glynn, M.W., Singer, J., Scott, L., Erdos, M.R., Robbins, C.M., Moses, T.Y., Berglund, P., et al. (2003). Recurrent de novo point mutations in lamin A cause Hutchinson-Gilford progeria syndrome. Nature *423*, 293–298.
7. Navarro, C.L., Cadiñanos, J., De Sandre-Giovannoli, A., Bernard, R., Courrier, S., Boccaccio, I., Boyer, A., Kleijer, W.J., Wagner, A., Giuliano, F., et al. (2005). Loss of ZMPSTE24 (FACE-1) causes autosomal recessive restrictive dermopathy

and accumulation of Lamin A precursors. Hum. Mol. Genet. *14*, 1503–1513.
8. Agarwal, A.K., Fryns, J.P., Auchus, R.J., and Garg, A. (2003). Zinc metalloproteinase, ZMPSTE24, is mutated in mandibuloacral dysplasia. Hum. Mol. Genet. *12*, 1995–2001.
9. Pendás, A.M., Zhou, Z., Cadiñanos, J., Freije, J.M., Wang, J., Hultenby, K., Astudillo, A., Wernerson, A., Rodríguez, F., Tryggvason, K., and López-Otín, C. (2002). Defective prelamin A processing and muscular and adipocyte alterations in Zmpste24 metalloproteinase-deficient mice. Nat. Genet. *31*, 94–99.
10. Roach, J.C., Glusman, G., Smit, A.F., Huff, C.D., Hubley, R., Shannon, P.T., Rowen, L., Pant, K.P., Goodman, N., Bamshad, M., et al. (2010). Analysis of genetic inheritance in a family quartet by whole-genome sequencing. Science *328*, 636–639.
11. Lupski, J.R., Reid, J.G., Gonzaga-Jauregui, C., Rio Deiros, D., Chen, D.C., Nazareth, L., Bainbridge, M., Dinh, H., Jing, C., Wheeler, D.A., et al. (2010). Whole-genome sequencing in a patient with Charcot-Marie-Tooth neuropathy. N. Engl. J. Med. *362*, 1181–1191.
12. Ng, S.B., Buckingham, K.J., Lee, C., Bigham, A.W., Tabor, H.K., Dent, K.M., Huff, C.D., Shannon, P.T., Jabs, E.W., Nickerson, D.A., et al. (2010). Exome sequencing identifies the cause of a mendelian disorder. Nat. Genet. *42*, 30–35.
13. Ng, S.B., Turner, E.H., Robertson, P.D., Flygare, S.D., Bigham, A.W., Lee, C., Shaffer, T., Wong, M., Bhattacharjee, A., Eichler, E.E., et al. (2009). Targeted capture and massively parallel sequencing of 12 human exomes. Nature *461*, 272–276.
14. Becker, J., Semler, O., Gilissen, C., Li, Y., Bolz, H.J., Giunta, C., Bergmann, C., Rohrbach, M., Koerber, F., Zimmermann, K., et al. (2011). Exome Sequencing Identifies Truncating Mutations in Human SERPINF1 in Autosomal-Recessive Osteogenesis Imperfecta. Am. J. Hum. Genet. *88*, 362–371.
15. Walsh, T., Shahin, H., Elkan-Miller, T., Lee, M.K., Thornton, A.M., Roeb, W., Abu Rayyan, A., Loulus, S., Avraham, K.B., King, M.C., and Kanaan, M. (2010). Whole exome sequencing and homozygosity mapping identify mutation in the cell polarity protein GPSM2 as the cause of nonsyndromic hearing loss DFNB82. Am. J. Hum. Genet. *87*, 90–94.
16. Merideth, M.A., Gordon, L.B., Clauss, S., Sachdev, V., Smith, A.C., Perry, M.B., Brewer, C.C., Zalewski, C., Kim, H.J., Solomon, B., et al. (2008). Phenotype and course of Hutchinson-Gilford progeria syndrome. N. Engl. J. Med. *358*, 592–604.
17. Li, H., and Durbin, R. (2009). Fast and accurate short read alignment with Burrows-Wheeler transform. Bioinformatics *25*, 1754–1760.
18. Li, H., Handsaker, B., Wysoker, A., Fennell, T., Ruan, J., Homer, N., Marth, G., Abecasis, G., and Durbin, R.; 1000 Genome Project Data Processing Subgroup. (2009). The Sequence Alignment/Map format and SAMtools. Bioinformatics *25*, 2078–2079.
19. Margalit, A., Brachner, A., Gotzmann, J., Foisner, R., and Gruenbaum, Y. (2007). Barrier-to-autointegration factor—a BAFfling little protein. Trends Cell Biol. *17*, 202–208.
20. Montes de Oca, R., Shoemaker, C.J., Gucek, M., Cole, R.N., and Wilson, K.L. (2009). Barrier-to-autointegration factor proteome reveals chromatin-regulatory partners. PLoS ONE *4*, e7050.
21. Segura-Totten, M., and Wilson, K.L. (2004). BAF: roles in chromatin, nuclear structure and retrovirus integration. Trends Cell Biol. *14*, 261–266.
22. Cai, M., Huang, Y., Suh, J.Y., Louis, J.M., Ghirlando, R., Craigie, R., and Clore, G.M. (2007). Solution NMR structure of the barrier-to-autointegration factor-Emerin complex. J. Biol. Chem. *282*, 14525–14535.
23. Bradley, C.M., Ronning, D.R., Ghirlando, R., Craigie, R., and Dyda, F. (2005). Structural basis for DNA bridging by barrier-to-autointegration factor. Nat. Struct. Mol. Biol. *12*, 935–936.
24. Nichols, R.J., Wiebe, M.S., and Traktman, P. (2006). The vaccinia-related kinases phosphorylate the N′ terminus of BAF, regulating its interaction with DNA and its retention in the nucleus. Mol. Biol. Cell *17*, 2451–2464.
25. Espada, J., Varela, I., Flores, I., Ugalde, A.P., Cadiñanos, J., Pendás, A.M., Stewart, C.L., Tryggvason, K., Blasco, M.A., Freije, J.M., and López-Otín, C. (2008). Nuclear envelope defects cause stem cell dysfunction in premature-aging mice. J. Cell Biol. *181*, 27–35.
26. Goldman, R.D., Shumaker, D.K., Erdos, M.R., Eriksson, M., Goldman, A.E., Gordon, L.B., Gruenbaum, Y., Khuon, S., Mendez, M., Varga, R., and Collins, F.S. (2004). Accumulation of mutant lamin A causes progressive changes in nuclear architecture in Hutchinson-Gilford progeria syndrome. Proc. Natl. Acad. Sci. USA *101*, 8963–8968.
27. Bengtsson, L., and Wilson, K.L. (2004). Multiple and surprising new functions for emerin, a nuclear membrane protein. Curr. Opin. Cell Biol. *16*, 73–79.
28. Haraguchi, T., Koujin, T., Segura-Totten, M., Lee, K.K., Matsuoka, Y., Yoneda, Y., Wilson, K.L., and Hiraoka, Y. (2001). BAF is required for emerin assembly into the reforming nuclear envelope. J. Cell Sci. *114*, 4575–4585.
29. Haraguchi, T., Koujin, T., Osakada, H., Kojidani, T., Mori, C., Masuda, H., and Hiraoka, Y. (2007). Nuclear localization of barrier-to-autointegration factor is correlated with progression of S phase in human cells. J. Cell Sci. *120*, 1967–1977.
30. Haraguchi, T., Kojidani, T., Koujin, T., Shimi, T., Osakada, H., Mori, C., Yamamoto, A., and Hiraoka, Y. (2008). Live cell imaging and electron microscopy reveal dynamic processes of BAF-directed nuclear envelope assembly. J. Cell Sci. *121*, 2540–2554.
31. Capell, B.C., Olive, M., Erdos, M.R., Cao, K., Faddah, D.A., Tavarez, U.L., Conneely, K.N., Qu, X., San, H., Ganesh, S.K., et al. (2008). A farnesyltransferase inhibitor prevents both the onset and late progression of cardiovascular disease in a progeria mouse model. Proc. Natl. Acad. Sci. USA *105*, 15902–15907.
32. Varela, I., Pereira, S., Ugalde, A.P., Navarro, C.L., Suárez, M.F., Cau, P., Cadiñanos, J., Osorio, F.G., Foray, N., Cobo, J., et al. (2008). Combined treatment with statins and aminobisphosphonates extends longevity in a mouse model of human premature aging. Nat. Med. *14*, 767–772.
33. Worman, H.J., Fong, L.G., Muchir, A., and Young, S.G. (2009). Laminopathies and the long strange trip from basic cell biology to therapy. J. Clin. Invest. *119*, 1825–1836.
34. Dechat, T., Pfleghaar, K., Sengupta, K., Shimi, T., Shumaker, D.K., Solimando, L., and Goldman, R.D. (2008). Nuclear lamins: major factors in the structural organization and function of the nucleus and chromatin. Genes Dev. *22*, 832–853.
35. Scaffidi, P., and Misteli, T. (2006). Lamin A-dependent nuclear defects in human aging. Science *312*, 1059–1063.
36. Varela, I., Cadiñanos, J., Pendás, A.M., Gutiérrez-Fernández, A., Folgueras, A.R., Sánchez, L.M., Zhou, Z., Rodríguez, F.J., Stewart, C.L., Vega, J.A., et al. (2005). Accelerated ageing in mice deficient in Zmpste24 protease is linked to p53 signalling activation. Nature *437*, 564–568.

The American Journal of Human Genetics, Volume *88*

Supplemental Data

Exome Sequencing and Functional Analysis Identifies *BANF1* Mutation as the Cause of a Hereditary Progeroid Syndrome

Xose S. Puente, Victor Quesada, Fernando G. Osorio, Rubén Cabanillas, Juan Cadiñanos, Julia M. Fraile, Gonzalo R. Ordóñez, Diana A. Puente, Ana Gutiérrez-Fernández, Miriam Fanjul-Fernández, Nicolas Lévy, José M. P. Freije, and Carlos López-Otín

Figure S1. Clinical Characteristics of Atypical Progeria in Patient II-1 from Family A

Frontal and dorsal view of the patient, and detailed pictures of head, ears, feet and hands, illustrating progeroid features and severe skeletal abnormalities.

Figure S2. Clinical Characteristics of Atypical Progeria in Patient II-1 from Family B

Frontal and dorsal view of the patient, and detailed pictures of head, ears, feet and hands, illustrating progeroid features and severe skeletal abnormalities.

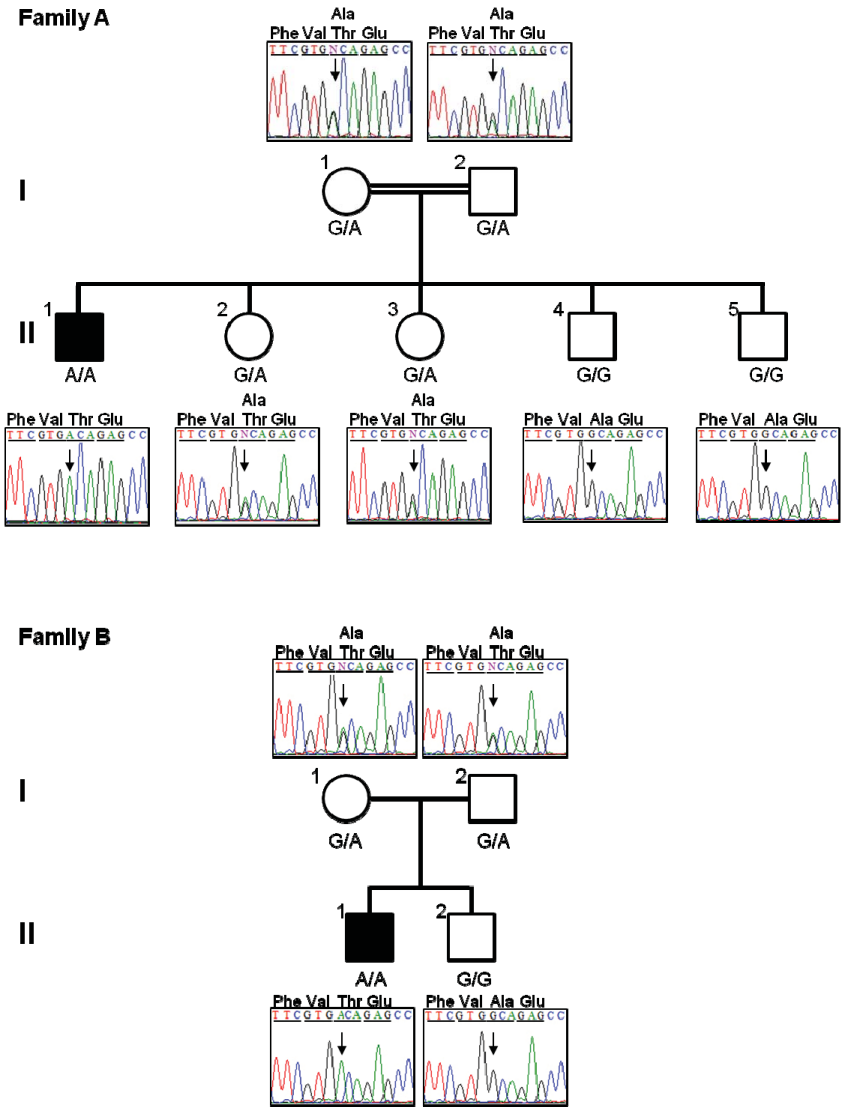

Figure S3. Pedigrees and Electropherograms Corresponding to the p.Ala12Thr Mutation in BAF

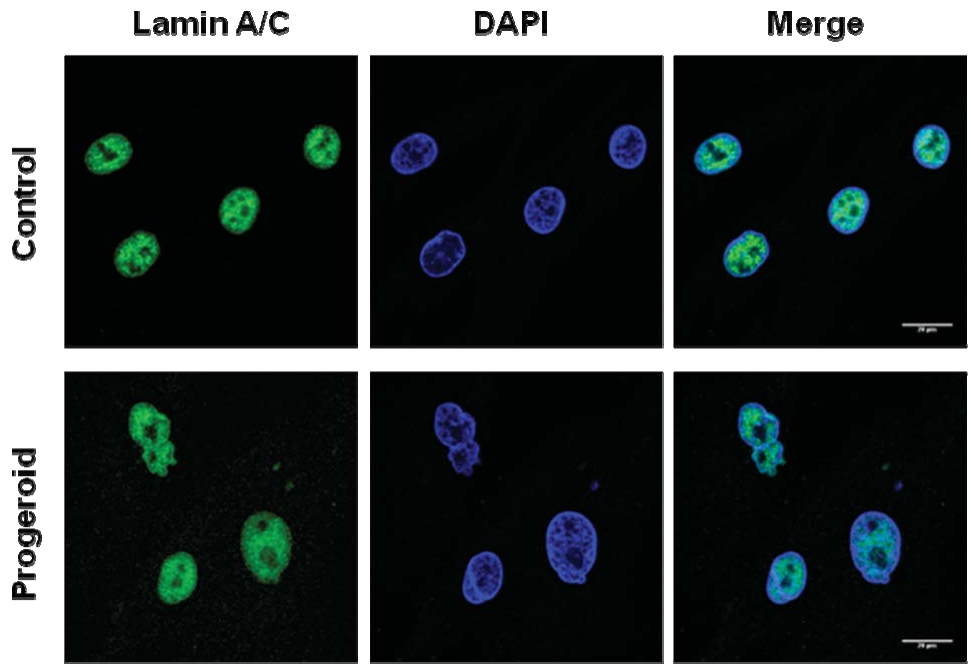

Figure S4. Lamin A/C in Fibroblasts Homozygous for the p.Ala12Thr Mutation in BAF

Lamin A/C distribution was analyzed by immunofluorescence and confocal microscopy in primary fibroblasts from the progeroid patient II-1 (family A) as well as in control fibroblasts.

DISCUSSION

During the past decade, cancer research has generated a complex landscape of the genetic and epigenetic changes occurring within the genome of transformed cells. We have also learnt that these changes influence the expression and function of numerous proto-oncogenes and tumor suppressor genes implicated in regulatory circuits governing cell proliferation, differentiation, and homeostasis. These data have consolidated the idea that tumorigenesis is a multistage process bearing certain analogy to classical evolutionary events and leading to the progressive conversion of normal cells into cancer cells. Hanahan and Weinberg brilliantly integrated an immense body of literature and proposed that the vast majority of cancer cell genotypes arise as a consequence of the alteration of eight essential biological processes in cell physiology. These combined changes finally result in sustaining proliferative signaling, the evasion of growth suppressors, the circumvention of programmed cell death and immune system, unlimited replication potential, sustained angiogenesis and tissue, reprogramming of energy metabolism and invasion and metastasis (1).

The experimental approaches aimed to unmask the molecular mechanisms underlying these powerful advantages acquired by tumor cells were largely focused on the study of individual genes of oncological relevance. However, the recent development of new high-throughput techniques for sequencing and analysis of whole genomes has represented a radical change in the strategies aimed at gaining insights into the complex genetic landscape of cancer. In this Thesis, we have taken advantage of the experience of our laboratory in both technical and methodological approaches to try to provide new insights into the complex mechanisms governing tumor development and progression. Thus, we have moved from the *in vivo* and *in vitro* functional study of an individual gene, presumably associated with cancer invasion, to the global analysis of the molecular alterations present in the genome of cancer patients.

As we mentioned above, cancer originates from mutations in genes that regulate essential pathways of cell function leading to uncontrolled outgrowth of tissue cells. Nevertheless, solid cancers are not only autonomous masses of transformed tumor cells, but also consist of multiple cell types such as fibroblast, epithelial, immune and endothelial cells, which create a tumor-specific

microenvironment. Understanding the complex crosstalk between malignant cells and the surrounding stroma represents one of the major challenges in cancer research. In this regard, a large body of evidence supports the view that extracellular proteinases, such as matrix metalloproteinases (MMPs), mediate many of the changes in the microenvironment during tumor progression. On this basis, the first part of this doctoral work has been focused on the study of the MMP family **(I-IV)**.

MMPs are a family of zinc-dependent endopeptidases first described almost half century ago **(I)**. They play a crucial role in various physiological processes, including tissue remodeling and organ development, but also in aggressive diseases such as cancer. The notion that MMP-mediated ECM degradation leads to cancer cell invasion and metastasis has been a guiding principle in MMP research. However, these enzymes play more specific and subtle roles than just being potent excavators of surrounding tissue. Hence, MMPs may be critically involved in disrupting the balance between proliferative and anti-proliferative signals in the tumor microenvironment, as they potently influence the bioavailability or functionality of many important factors that regulate growth **(I)**. Evading programmed cell death is another strategy which increases the cell number and size of tumors, and that is normally mediated via extracellular receptors exposed to selective degradation by MMPs. Likewise, MMPs are key players in angiogenesis, regulation of the inflammation and pre-metastac niche formation, evidencing that MMP function is more complex than initially thought **(I)**. In fact, although the current understanding in this field is that extracellular proteolysis is mostly implicated in cancer promotion, it has also been well-established that MMPs exhibit tumor-suppressing effects in several circumstances. This dual role is well illustrated in the case of MMP-19 **(II)**.

MMP19 is up-regulated during the later stages of melanoma progression, facilitating the vertical migration of tumor cells (132). However, *MMP19* is down-regulated in basal and squamous cell carcinoma during neoplastic dedifferentiation, as well as in colon and nasopharyngeal cancers (133-135). Different *in vivo* studies of cancer susceptibility performed in *Mmp19*-deficient mice generated in our laboratory have confirmed the dual role of this

metalloproteinase in cancer. Thus, in a methylcholanthrene-induced fibrosarcoma model, *Mmp19*-null mice develop less fibrosarcomas and with longer latency period than their control littermates whereas, conversely, they exhibit an early onset of angiogenesis and tumor invasion after transplantation of malignant murine keratinocytes (50,51). Altogether, these data suggest that MMP-19 negatively regulates the early stages of tumor cell invasion, but cancer cells could become less sensitive to MMP-19 activity once tumor develops. These apparently paradoxical results may reflect different roles for MMP-19 in the evolution of various cancer types as well as throughout different steps of cancer progression, highlighting the requirement to understand the individual functions of each MMP in order to improve anticancer strategies **(II)**.

It is precisely in this context of the need of *in vivo* analysis of MMP functions, in which we addressed the first experimental objective for the present doctoral Thesis, which has been focused on the generation of mice deficient in Mmp-1a, the closest murine ortholog of human MMP-1 **(III)**. This metalloproteinase has been described in a wide variety of advanced cancers, and, in nearly all instances, there has been a significant negative correlation between MMP-1 expression and survival (136). Likewise, it has been demonstrated that overexpression of this enzyme is associated with tumor initiation, invasion and metastasis (137). However, despite the relevant role attributed to MMP-1 in tumor progression, these cancer-related functions have not been formally demonstrated *in vivo*. This is even more surprising if we realize that Mmp-1a was first identified and cloned more than 10 years ago (85). The technical difficulties derived from the large complexity of the *Mmp* cluster located at mouse chromosome 9, which even contains a duplicated *Mmp1* gene absent in human, together with the doubts regarding the functional relevance of these mouse orthologs of human MMP-1 hampered the progress of this project. Fortunately, the successive work initiated by Drs. M. Balbín and A. R. Folgueras and continued in this Thesis, has finally resulted in the generation of the first *in vivo* model of MMP-1 deficiency and its utilization for the analysis of the functional relevance of this metalloproteinase in cancer **(III)**.

Similar to most cases of *Mmp* deficiency (138), *Mmp1a*$^{-/-}$ mice were viable and fertile and showed no overt abnormalities, which facilitated those studies aimed at evaluating their cancer susceptibility. After analyzing *Mmp1a* expression levels in a battery of tissues subjected to different mouse carcinogenesis protocols, we concluded that lung cancer could represent a proper scenario to study the contribution of this murine metalloproteinase in cancer, since high *Mmp1a* expression levels were found in lung tumors **(III)**. On this basis, we decided to use a well-established urethane-based protocol of lung cancer induction, and observed that *Mmp1a*$^{-/-}$ mice showed a lower incidence of lung carcinomas than their corresponding wild-type littermates. Interestingly, this difference was more marked in male than in female mutant mice, indicating the occurrence of a gender difference, which has been previously reported in other models of *Mmp* deficiency (29). Histopathological analysis showed that tumors generated in *Mmp1a*$^{-/-}$ mice were smaller and less angiogenic than those from wild-type mice, both characteristics being consistent with the idea that the absence of Mmp-1a hampers tumor progression. These *in vivo* findings agree perfectly with very recent *in vitro* data showing that silencing *Mmp1a* suppresses invasive growth of lung cancer cells in three-dimensional matrices, whereas ectopic expression of this murine metalloproteinase confers invasive properties to epithelial cells (139).

The pro-tumorigenic role of MMPs was originally ascribed to their ability to breakdown tissue barriers during metastatic spread. The fact that both human MMP-1 and mouse Mmp-1a are potent collagenases with ability to degrade different types of fibrillar collagens, would be consistent with a role for these metalloproteinases in promoting tumor progression (83,140,141). Nevertheless, the growing evidence that virtually all MMPs, including MMP-1, target many other proteins distinct from extracellular matrix components (142-144), prompted us to perform comparative proteomic studies between samples of *Mmp1a*-mutant and wild-type mice to try to identify putative *in vivo* substrates of Mmp-1a **(III)**. Among the identified proteins, it is remarkable the finding of high levels of CHI3L3 and RAGE in lung samples from *Mmp1a*-wild type and mutant mice respectively, after treatment with urethane. Further studies demonstrated that the S100A8 ligand for

the RAGE receptor is also elevated in samples from *Mmp1a*-mutant mice. Accordingly, this chemotactic protein could be a substrate directly targeted by Mmp-1a, a proposal that we further assessed by performing a series of enzymatic assays which demonstrated that the recombinant collagenase cleaves S100A8, but no other related proteins such as S100A9. The impaired degradation of this immunoregulatory protein in *Mmp1a*-deficient mice could also contribute to the generation of marked differences in the inflammatory response induced by chemical carcinogens in *Mmp1a* wild-type and mutant mice. Thus, the increased levels of CHI3L3 together with high levels of several Th2-related cytokines in wild-type mice strongly suggests that urethane is inducing the archetypical Th2-polarized inflammatory response that operates under pro-tumorigenic stimuli (145). In contrast, the absence of increased levels of CHI3L3 in *Mmp1a*-mutant mice, together with the presence of high levels of RAGE and its ligand S100A8, which are markers of Th1-polarized responses (146,147), might be consistent with the possibility that the lack of this metalloproteinase hampers the development of the Th2-response triggered by carcinogen injection in *Mmp1a*$^{-/-}$ mice. Also, in agreement with this proposal, we detected in these mutant mice high levels of interferon gamma (IFN-γ), another well- characterized Th1-response factor, as well as some antitumor cytokines such IL-1α and IL-2. Additionally, the relative high levels of the anti-angiogenic cytokine IL-27 (148) found in *Mmp1a*$^{-/-}$ mice could explain the reduced angiogenic phenotype showed by tumors generated in these animals **(III)**.

MMPs have been associated with inflammatory responses in a wide variety of diseases (149). Likewise, several reports have described that cytokines released from different Th1/Th2 cell types can modulate MMP expression. Thus, it is well-established that Th2 responses are associated with an increased expression of matrix degradative MMPs, including human MMP-1 (150). Moreover, MMPs may also act as direct inducers of this process, modulating chemokine gradients or processing specific cytokines, and finally switching the balance between both types of responses. This is the case of MMP-2, which is overexpressed in multiple cancers and induces a Th2 polarization through the degradation of type I IFN receptor in dendritic cells (151). In addition, MMP-9

proteolytically activates TFG-β, which in turn promotes differentiation towards the Th2 pro-tumorigenic phenotype (152). Accordingly, lungs from *Mmp1a*-deficient mice exhibit lower levels of active TFG-β1 than controls, suggesting that these mutant mice lack the capacity to proteolytically activate TFG-β1. Finally, the fact that human MMP-1 also cleaves the latent form of TGF-β and facilitates tumor invasion and angiogenesis (143) would agree very well with our proposal that its mouse ortholog Mmp-1a acts *in vivo* as a switching protease, which changes the Th1/Th2 balance towards a pro-tumorigenic state **(III)**.

The relevance of Mmp-1a in lung cancer has been further demonstrated in additional experiments performed in collaboration with the group of Dr. A. Kuliopulos **(IV)**. As we already mentioned, human MMP-1 is produced by a variety of cell types present in malignant tumors, including cancer cells, fibroblasts, inflammatory cells, and endothelial cells (136). MMP-1 expression in stromal cells has been associated with increased risk of metastasis in breast cancer patients, highlighting the importance of tumor *versus* stromal MMP-1 production. In addition, it has been shown that fibroblast-derived and cancer cell-derived MMP-1 are differentially processed, suggesting that there may be functional differences in MMP-1 depending on the cell of origin (153). To investigate the role of stromal Mmp-1a in tumorigenesis and after demonstrating that this protease displays an important role in lung carcinogenesis **(III)**, we decided to employ an orthotopic-lung cancer model to combine tumor-*Mmp1a* expression with genetic backgrounds proficient or deficient in Mmp-1a. Thus, after implantation of Lewis lung carcinoma cells (LLC1) in animals from both genotypes, we observed that the growth of tumors in *Mmp1a*$^{-/-}$ mice was lower than in control mice. These results confirm our previous findings on the pro-tumorigenic activity of Mmp-1a during lung tumor evolution **(III)** and demonstrate that stromal-derived Mmp-1a is an important factor in promoting lung tumorigenesis **(IV)**. Consistent with these findings, co-implantation of wild-type Mmp-1a fibroblasts with lung cancer cells completely restored tumor growth in *Mmp1a*-deficient animals. In addition, loss of stroma-produced Mmp-1a from fibroblasts isolated from *Mmp1a*-deficient mice also resulted in decreased invasion, migration and proliferation of lung carcinoma cells, and also caused defects in angiogenesis **(IV)**.

Then, and because endothelial protease-activated receptor 1 (PAR1) is critical for angiogenesis in the developing mouse (154) and an important mediator of proliferation, migration and tube formation of endothelial cells upon activation by MMP-1 (155-157), we next investigated the interrelation between tumoral PAR-1 and stromal Mmp-1a **(IV)**. We found that *PAR1* silencing in lung carcinoma cells phenocopied stromal *Mmp1a* deficiency, underscoring the importance of cancer cell-expressed PAR1 as a stromal Mmp-1a target for tumor promotion. Likewise, loss of both Mmp-1a in the stroma and PAR1 in LLC1 cancer cells did not result in a further decrease in lung tumor growth, indicating that stromal Mmp-1a and PAR1 produced by the carcinoma cells act on the same pathway in tumorigenesis **(IV)**.

In summary, and taking collectively these findings, we can conclude that the generation of the first mouse model of MMP-1 deficiency has contributed to the *in vivo* validation of this enzyme as a pro-tumorigenic protease with potential impact in different stages of tumor progression, including growth, angiogenesis and regulation of inflammatory responses. These studies have also validated the concept that human MMP-1 is a target protease, at least in some types of cancer, in which its expression is profoundly deregulated. Nevertheless, further studies aimed at inducing other tumor types in *Mmp1a*$^{-/-}$ mice will be necessary to define the precise *in vivo* role of this protease in different malignancies, since it could have dual roles in tumor development, as discussed above for the paradigmatic case of MMP-19 (**II)**. In this regard, we have recently performed preliminary studies to analyze the role of Mmp-1a in different tumor scenarios. Thus, by using an oral squamous cell carcinogenesis model induced by 4-NQO in drinking water, we have observed that tumors from wild-type mice develop more papillomas than *Mmp1a*-null mice. Interestingly, these papillomas progress to invasive carcinomas in wild-type mice but not in mutant animals. Likewise, wild-type mice showed more MCA-induced fibrosarcomas than *Mmp1a*-deficient mice. In contrast, no significant differences between both genotypes were found in azoxymethane-induced colon carcinomas or DEN-induced hepatocarcinomas (Fanjul-Fernández *et al*., unpublished results). These results reveal tissue specificity as a silencing accomplice in Mmp1a-related carcinogenesis and reflect the diversity hidden

behind each tumor type, emphasizing the importance of carefully characterizing the specific role of each individual MMP family member in human malignancies.

This growing awareness of cancer complexity and diversity also highlights the necessity of adopting a wider perspective of the tumor landscape. Fortunately, this "zoom out" of the tumor picture is now increasingly available due to the recent development of high-throughput techniques that facilitate the acquisition of a global view of the key molecular pathways employed by each particular cancer along its progression. Among these new approaches, next-generation sequencing strategies have become an extremely useful tool to better understand cancer evolution (158). Based on these considerations, the second general objective of this Thesis has been based on the study of head and neck carcinomas from a genomic perspective.

HNSCC is an aggressive cancer which arises from epithelial mucosa of upper aerodigestive track and frequently progresses to higher pathological grades of malignancy. Over the last years, many research projects have tried to gain a comprehensive view about this disease. However, and contrary to the results obtained in other human malignancies, survival has decreased among HNSCC patients during the past two decades (159). In addition, it is noteworthy that HNSCC has a high incidence in our region, which provides an additional dimension to the study of this malignancy (122). Remarkably, at the beginning of this Thesis, no genomic analysis had been performed on this type of tumor. However, two recent works from the very prestigious laboratories directed by Drs. B. Vogelstein and E. Lander have reported the first mutational studies of HNSCC (130,131). Despite their unquestionable interest, these works have not revealed any novel gene related to the progression of this disease and have only reported the occurrence of recurrent mutations in a series of genes widely known in cancer biology, such as *TP53, PIK3CA* and *PTEN*. Accordingly, we reformulated our initial aims in this regard and directed our main efforts not only to the global genomic analysis of HNSCC, but also to the identification and functional analysis of new genes that could be recurrently mutated in these carcinomas **(V).**

To this aim, and as a first global approach to HNSCC, we performed exome-sequencing of matched normal and tumor samples from 4 individuals with this disease. Somewhat predictably, we found that tobacco signature was printed in the tumor DNA from these patients since most base changes were G>T/C>A substitutions, which have been already reported to be associated with tobacco abuse (96). We identified a median of 260 somatic mutations per case, which agrees with data recently reported for this type of cancer, as well as for other smoking-related malignancies (130). According with aforementioned data, classical *TP53*, *PIK3CA* and *PTEN* HNSCC-related genes were found in the somatic mutation list. Among all the 569 genes that underwent protein-coding changes, we focused on 40 genes whose biological function was presumed to be relevant for tumor development to further analyze its mutational status in 86 additional HNSCC cases. Two of these selected genes, encoding the cell-cell adhesion proteins named CTNNA2 and CTNNA3, caught our attention as novel recurrently mutated genes since they were found mutated in about 15% of the HNSCC cases **(V)**. Detailed analysis of the mutational profile of these genes demonstrated that mutations were distributed along the entire gene in both cases, a situation that resembles that occurring in tumor suppressor genes and differs from the mutational hotspots characteristic of oncogenes. To evaluate the hypothesis that *CTNNA2* and *CTNNA3* are novel tumor suppressor genes, we were prompted to perform a series of cell functional studies in HNSCC cells, in which we performed the silencing and overexpression of these α-catenins. These studies revealed an increase in the migration and invasion capacities of cells in which these catenins had been interfered. Moreover, cells in which both *CTNNA2* and *CTNNA3* had been silenced, showed an enhanced migration ability compared to cells in which either single gene had been knocked down. These findings could reflect a synergistic effect between both genes and would explain the curious fact that three different patients harbour inactivating mutations in both genes. Site-directed mutagenesis experiments corroborated the idea that *CTNNA2* and *CTNNA3* are tumor suppressor genes, since overexpression of mutant isoforms did not increase adhesion properties, nor caused a decrease in the migration and invasion properties of transfected cells, as occurred after overexpression of the

corresponding wild-type cDNAs for *CTNNA2* and *CTNNA3*. Collectively, these results indicate that the identified mutations in these genes in HNSCC patients cause loss of function in both alpha-catenin proteins.

Alpha-catenins are cell-cell adhesion proteins which link β-catenin to the cytoskeleton. On this basis, and to further explore the molecular mechanisms underlying the observed phenotype caused by *CTNNA2* and *CTNNA3* mutations, we next examined the phosphorylation status of β-catenin, a downstream component of the Wnt/Wingless pathway, which is altered in many types of cancer. Interestingly, we found decreased phosphorylation levels at the residue responsible for the translocation of β-catenin from cell-cell contacts into cytosol and nucleus (Ser552) in cells overexpressing *CTNNA2* and *CTNNA3* **(V)**. It is well established that once β-catenin is translocated into the nucleus, it activates transcription factors of the TCF/LEF-1 family (160). Therefore, we performed TCF/LEF-1 luciferase reporter assays to evaluate the putative changes in the activity of these transcription factors caused by *CTNNA2* and *CTNNA3* mutations in HNSCC. We observed that silencing of *CTNNA2* and *CTNNA3* led to a significant increase of TCF/LEF-1 transcriptional activity when compared with control cells. In contrast, up-regulation of *CTNNA2* and *CTNNA3* in HNSCC cells was associated with reduced luciferase activity. Likewise, overexpression of *CTNNA2* and *CTNNA3* mutants increased the TCF/LEF-1 transcriptional activity compared with cells overexpressing wild-type genes. Thus, down-regulation of *CTNNA2* and *CTNNA3* increases the phosphorylation of β-catenin at Ser552, which might cause its disassociation from cell-cell contacts, enhancing its transcriptional activity and inducing the expression of genes that favor tumor invasion, including some members of the MMP family (161-163). Further studies involving microarray-based expression analysis corroborated this assumption after the finding that tumors from patients with *CTNNA2* or *CTNNA3* mutations exhibit high levels of expression of MMP-1 and MMP-13 (Fanjul-Fernández *et al*., unpublished results).

It is also noteworthy that the mutation causing major differences in the above described functional experiments corresponds to a nucleotide change that generates a premature stop codon in *CTNNA2*. Taking into account that cells

overexpressing this truncated protein still have two copies of the wild-type gene, it is tempting to speculate that its effect on tumor cells could be even higher, making mutated cells more invasive and aggressive than the effect we can observe by using an *in vitro* cell system. In addition, the loss of the C-terminal end of CTNNA2 could seriously damage the cell adherence junctions at the cadherin-catenin-actin axis, since this protein region is responsible for the binding of cadherin-catenin complex to cytoskeleton fibers. In this regard, preliminary immunofluorescence experiments showed the presence of actin fibers all across the cytoplasm in cells overexpressing the truncated protein, whilst cells overexpressing the wild-type gene showed actin fibers gently wrapped around the interphase nucleus, after phalloidin staining (data not shown). These different rearrangements of the cytoskeleton in cells overexpressing truncated forms of α-catenin are consistent with a stimuli-response migratory phenotype (164).

Finally, it is remarkable that the clinical analysis of HNSCC patients with mutations in *CTNNA2* and *CTNNA3* demonstrated that these mutations are associated with worse clinical prognosis **(V)**. Taken together all these data, we can conclude that this work has identified for the first time *CTNNA2* and *CTNNA3* as moderately frequent and possibly synergistic mutational targets in HNSCC. Functional and clinical studies strongly suggest that both genes may act as tumor suppressors, which is consistent with the growing idea that the vast majority of HNSCC tumors harbour many inactivating mutations. Accordingly, these catenins may represent new candidate targets for the development of strategies that may contribute to the future treatment of HNSCC.

In summary, in this Thesis we have tried to contribute to a better understanding of the mechanisms underlying cancer progression. To this aim, we have approached to the complexity of cancer through two opposite but complementary perspectives. Thus, in the first part of this work, we have generated genetically-modified *Mmp1a*-deficient mouse, as one of the most powerful strategies to study gene function *in vivo*. Since mice were viable and developed normally, we could perform several cancer-induction protocols to evaluate the implication of this protease in tumor pathogenesis. *Mmp1a*-deficient mice showed decreased susceptibility to lung cancer, corroborating *in vivo* the

classical pro-tumorigenic role largely assumed for human MMP-1 and providing new mechanistic insights on the functional relevance of this enzyme in cancer progression. Nevertheless, cancer is, in essence, a genetic disease caused by accumulation of molecular alterations in the genome of somatic cells. Accordingly, in the second part of this work, and by taking advantage of the recent introduction in our laboratory of new-generation sequencing approaches, we have moved from the functional study of specific genes involved in cancer to the global genomic analysis of HNSCC genomes. This study has allowed us to identify *CTNNA2* and *CTNNA3* as novel recurrently mutated genes in head and neck carcinomas. The integration of these genomic data with the functional analysis of the mutated genes and with the clinical information of the corresponding patients may serve as a representative example of a new and forthcoming era in oncology which hopefully will lead to the development of individualized therapies for cancer patients.

CONCLUSIONS

1. The matrix metalloproteinase Mmp-1a promotes lung cancer progression through regulation of inflammation and angiogenesis.

2. Stroma-derived Mmp-1a contributes to lung tumorigenesis by inducing cancer cell growth, migration and invasion through a mechanism involving cleavage of PAR-1.

3. *CTNNA2* and *CTNNA3* are tumor suppressor genes recurrently mutated in head and neck carcinomas.

4. CTNNA2 and CTNNA3 are implicated in the pathogenesis of head and carcinomas through regulation of the β-catenin/Wnt signaling pathway.

BIBLIOGRAPHY

1 Hanahan, D., and Weinberg, R. A. Hallmarks of cancer: the next generation (2011) *Cell* **144** 646-674

2 Vogelstein, B., and Kinzler, K. W. Cancer genes and the pathways they control (2004) *Nat. Med.* **10** 789-799

3 Comen, E., Norton, L., and Massague, J. Clinical implications of cancer self-seeding (2011) *Nat Rev Clin Oncol* **8** 369-377

4 Pietras, K., and Ostman, A. Hallmarks of cancer: interactions with the tumor stroma (2010) *Exp. Cell Res.* **316** 1324-1331

5 Friedl, P., and Wolf, K. Tube travel: the role of proteases in individual and collective cancer cell invasion (2008) *Cancer Res.* **68** 7247-7249

6 Moncada-Pazos, A., Obaya, A. J., Fraga, M. F., Viloria, C. G., Capella, G., Gausachs, M., Esteller, M., Lopez-Otin, C., and Cal, S. The ADAMTS12 metalloprotease gene is epigenetically silenced in tumor cells and transcriptionally activated in the stroma during progression of colon cancer (2009) *J. Cell Sci.* **122** 2906-2913

7 Llamazares, M., Obaya, A. J., Moncada-Pazos, A., Heljasvaara, R., Espada, J., Lopez-Otin, C., and Cal, S. The ADAMTS12 metalloproteinase exhibits anti-tumorigenic properties through modulation of the Ras-dependent ERK signalling pathway (2007) *J. Cell Sci.* **120** 3544-3552

8 Rucci, N., Sanita, P., and Angelucci, A. Roles of metalloproteases in metastatic niche (2011) *Curr Mol Med* **11** 609-622

9 Heljasvaara, R., Nyberg, P., Luostarinen, J., Parikka, M., Heikkila, P., Rehn, M., Sorsa, T., Salo, T., and Pihlajaniemi, T. Generation of biologically active endostatin fragments from human collagen XVIII by distinct matrix metalloproteases (2005) *Exp. Cell Res.* **307** 292-304

10 Boire, A., Covic, L., Agarwal, A., Jacques, S., Sherifi, S., and Kuliopulos, A. PAR1 is a matrix metalloprotease-1 receptor that promotes invasion and tumorigenesis of breast cancer cells (2005) *Cell* **120** 303-313

11 Gutiérrez-Fernández, A., Fueyo, A., Folgueras, A. R., Garabaya, C., Pennington, C. J., Pilgrim, S., Edwards, D. R., Holliday, D. L., Jones, J. L., Span, P. N., Sweep, F. C., Puente, X. S., and López-Otín, C. Matrix metalloproteinase-8 functions as a metastasis suppressor through modulation of tumor cell adhesion and invasion (2008) *Cancer Res.* **68** 2755-2763

12 Gomis-Ruth, F. X. Catalytic domain architecture of metzincin metalloproteases (2009) *J. Biol. Chem.* **284** 15353-15357

13 Puente, X. S., Sanchez, L. M., Overall, C. M., and Lopez-Otin, C. Human and mouse proteases: a comparative genomic approach (2003) *Nat. Rev. Genet.* **4** 544-558

14 Limb, G. A., Matter, K., Murphy, G., Cambrey, A. D., Bishop, P. N., Morris, G. E., and Khaw, P. T. Matrix metalloproteinase-1 associates with intracellular organelles and confers resistance to lamin A/C degradation during apoptosis (2005) *Am. J. Pathol.* **166** 1555-1563

15 Ruta, A., Mark, B., Edward, B., Jawaharlal, P., and Jianliang, Z. Nuclear localization of active matrix metalloproteinase-2 in cigarette smoke-exposed apoptotic endothelial cells (2009) *Exp. Lung Res.* **35** 59-75

16 Luo, D., Mari, B., Stoll, I., and Anglard, P. Alternative splicing and promoter usage generates an intracellular stromelysin 3 isoform directly translated as an active matrix metalloproteinase (2002) *J. Biol. Chem.* **277** 25527-25536

17 Cuadrado, E., Rosell, A., Borrell-Pages, M., Garcia-Bonilla, L., Hernandez-Guillamon, M., Ortega-Aznar, A., and Montaner, J. Matrix metalloproteinase-13 is activated and is found in the nucleus of neural cells after cerebral ischemia (2009) *J. Cereb. Blood Flow Metab.* **29** 398-410

18 Vincenti, M. P., and Brinckerhoff, C. E. Signal transduction and cell-type specific regulation of matrix metalloproteinase gene expression: can MMPs be good for you? (2007) *J. Cell. Physiol.* **213** 355-364

19 Shukeir, N., Pakneshan, P., Chen, G., Szyf, M., and Rabbani, S. A. Alteration of the methylation status of tumor-promoting genes decreases prostate cancer cell invasiveness and tumorigenesis in vitro and in vivo (2006) *Cancer Res.* **66** 9202-9210

20 Kim, M. K., Shin, J. M., Eun, H. C., and Chung, J. H. The role of p300 histone acetyltransferase in UV-induced histone modifications and MMP-1 gene transcription (2009) *PLoS ONE* **4** e4864

21 Fahling, M., Steege, A., Perlewitz, A., Nafz, B., Mrowka, R., Persson, P. B., and Thiele, B. J. Role of nucleolin in posttranscriptional control of MMP-9 expression (2005) *Biochim. Biophys. Acta* **1731** 32-40

22 Krishnamurthy, P., Rajasingh, J., Lambers, E., Qin, G., Losordo, D. W., and Kishore, R. IL-10 inhibits inflammation and attenuates left ventricular remodeling after myocardial infarction via activation of STAT3 and suppression of HuR (2009) *Circ. Res.* **104** e9-18

23 Liu, L., Wu, J., Wu, C., Wang, Y., Zhong, R., Zhang, X., Tan, W., Nie, S., Miao, X., and Lin, D. A functional polymorphism (-1607 1G-->2G) in the matrix metalloproteinase-1 promoter is associated with development and progression of lung cancer (2011) *Cancer* **117** 5172-5181

24 McColgan, P., and Sharma, P. Polymorphisms of matrix metalloproteinases 1, 2, 3 and 9 and susceptibility to lung, breast and colorectal cancer in over 30,000 subjects (2009) *Int. J. Cancer* **125** 1473-1478

25 Politi, K., and Pao, W. How genetically engineered mouse tumor models provide insights into human cancers (2011) *J Clin Oncol* **29** 2273-2281

26 Lopez-Otin, C., and Bond, J. S. Proteases: multifunctional enzymes in life and disease (2008) *J. Biol. Chem.* **283** 30433-30437

27 Inada, M., Wang, Y., Byrne, M. H., Rahman, M. U., Miyaura, C., López-Otín, C., and Krane, S. M. Critical roles for collagenase-3 (Mmp13) in development of growth plate cartilage and in endochondral ossification (2004) *Proc. Natl. Acad. Sci. U. S. A.* **101** 17192-17197

28 Stickens, D., Behonick, D. J., Ortega, N., Heyer, B., Hartenstein, B., Yu, Y., Fosang, A. J., Schorpp-Kistner, M., Angel, P., and Werb, Z. Altered endochondral bone development in matrix metalloproteinase 13-deficient mice (2004) *Development* **131** 5883-5895

29 Balbin, M., Fueyo, A., Tester, A. M., Pendas, A. M., Pitiot, A. S., Astudillo, A., Overall, C. M., Shapiro, S. D., and Lopez-Otin, C. Loss of collagenase-2 confers increased skin tumor susceptibility to male mice (2003) *Nat. Genet.* **35** 252-257

30 Wiseman, B. S., Sternlicht, M. D., Lund, L. R., Alexander, C. M., Mott, J., Bissell, M. J., Soloway, P., Itohara, S., and Werb, Z. Site-specific inductive and inhibitory activities of MMP-2 and MMP-3 orchestrate mammary gland branching morphogenesis (2003) *J. Cell Biol.* **162** 1123-1133

31 Vu, T. H., Shipley, J. M., Bergers, G., Berger, J. E., Helms, J. A., Hanahan, D., Shapiro, S. D., Senior, R. M., and Werb, Z. MMP-9/gelatinase B is a key regulator of growth plate angiogenesis and apoptosis of hypertrophic chondrocytes (1998) *Cell* **93** 411-422

32 Inoue, K., Mikuni-Takagaki, Y., Oikawa, K., Itoh, T., Inada, M., Noguchi, T., Park, J. S., Onodera, T., Krane, S. M., Noda, M., and Itohara, S. A crucial role for matrix metalloproteinase 2 in osteocytic canalicular formation and bone metabolism (2006) *J. Biol. Chem.* **281** 33814-33824

33 Holmbeck, K., Bianco, P., Caterina, J., Yamada, S., Kromer, M., Kuznetsov, S. A., Mankani, M., Robey, P. G., Poole, A. R., Pidoux, I., Ward, J. M., and Birkedal-Hansen, H. MT1-MMP-deficient mice develop dwarfism, osteopenia, arthritis, and connective tissue disease due to inadequate collagen turnover (1999) *Cell* **99** 81-92

34 Zhou, Z., Apte, S. S., Soininen, R., Cao, R., Baaklini, G. Y., Rauser, R. W., Wang, J., Cao, Y., and Tryggvason, K. Impaired endochondral ossification and angiogenesis in mice deficient in membrane-type matrix metalloproteinase I (2000) *Proc. Natl. Acad. Sci. U. S. A.* **97** 4052-4057

35 Caterina, J. J., Skobe, Z., Shi, J., Ding, Y., Simmer, J. P., Birkedal-Hansen, H., and Bartlett, J. D. Enamelysin (matrix metalloproteinase 20)-deficient mice display an amelogenesis imperfecta phenotype (2002) *J. Biol. Chem.* **277** 49598-49604

36 Martignetti, J. A., Aqeel, A. A., Sewairi, W. A., Boumah, C. E., Kambouris, M., Mayouf, S. A., Sheth, K. V., Eid, W. A., Dowling, O., Harris, J., Glucksman, M. J., Bahabri, S., Meyer, B. F., and Desnick, R. J. Mutation of the matrix metalloproteinase 2 gene (MMP2) causes a multicentric osteolysis and arthritis syndrome (2001) *Nat. Genet.* **28** 261-265

37 Kennedy, A. M., Inada, M., Krane, S. M., Christie, P. T., Harding, B., Lopez-Otin, C., Sanchez, L. M., Pannett, A. A., Dearlove, A., Hartley, C., Byrne, M. H., Reed, A. A., Nesbit, M. A., Whyte, M. P., and Thakker, R. V. MMP13 mutation causes spondyloepimetaphyseal dysplasia, Missouri type (SEMD(MO) (2005) *The Journal of clinical investigation* **115** 2832-2842

38 Kim, J. W., Simmer, J. P., Hart, T. C., Hart, P. S., Ramaswami, M. D., Bartlett, J. D., and Hu, J. C. MMP-20 mutation in autosomal recessive pigmented hypomaturation amelogenesis imperfecta (2005) *J. Med. Genet.* **42** 271-275

39 Oh, J., Takahashi, R., Adachi, E., Kondo, S., Kuratomi, S., Noma, A., Alexander, D. B., Motoda, H., Okada, A., Seiki, M., Itoh, T., Itohara, S., Takahashi, C., and Noda, M. Mutations in two matrix metalloproteinase genes, MMP-2 and MT1-MMP, are synthetic lethal in mice (2004) *Oncogene* **23** 5041-5048

40 Shi, J., Son, M. Y., Yamada, S., Szabova, L., Kahan, S., Chrysovergis, K., Wolf, L., Surmak, A., and Holmbeck, K. Membrane-type MMPs enable extracellular matrix permissiveness and mesenchymal cell proliferation during embryogenesis (2008) *Dev. Biol.* **313** 196-209

41 D'Armiento, J., DiColandrea, T., Dalal, S. S., Okada, Y., Huang, M. T., Conney, A. H., and Chada, K. Collagenase expression in transgenic mouse skin causes hyperkeratosis and acanthosis and increases susceptibility to tumorigenesis (1995) *Mol. Cell. Biol.* **15** 5732-5739

42 Ha, H. Y., Moon, H. B., Nam, M. S., Lee, J. W., Ryoo, Z. Y., Lee, T. H., Lee, K. K., So, B. J., Sato, H., Seiki, M., and Yu, D. Y. Overexpression of membrane-type matrix metalloproteinase-1 gene induces mammary gland abnormalities and adenocarcinoma in transgenic mice (2001) *Cancer Res.* **61** 984-990

43 Sternlicht, M. D., Lochter, A., Sympson, C. J., Huey, B., Rougier, J. P., Gray, J. W., Pinkel, D., Bissell, M. J., and Werb, Z. The stromal proteinase MMP3/stromelysin-1 promotes mammary carcinogenesis (1999) *Cell* **98** 137-146

44 Gutierrez-Fernandez, A., Fueyo, A., Folgueras, A. R., Garabaya, C., Pennington, C. J., Pilgrim, S., Edwards, D. R., Holliday, D. L., Jones, J. L., Span, P. N., Sweep, F. C., Puente, X. S., and Lopez-Otin, C. Matrix metalloproteinase-8 functions as a metastasis suppressor through modulation of tumor cell adhesion and invasion (2008) *Cancer Res.* **68** 2755-2763

45 Gorrin-Rivas, M. J., Arii, S., Furutani, M., Mizumoto, M., Mori, A., Hanaki, K., Maeda, M., Furuyama, H., Kondo, Y., and Imamura, M. Mouse macrophage metalloelastase gene transfer into a murine melanoma suppresses primary tumor growth by halting angiogenesis (2000) *Clin Cancer Res* **6** 1647-1654

46 Lopez-Otin, C., and Matrisian, L. M. Emerging roles of proteases in tumour suppression (2007) *Nat. Rev. Cancer* **7** 800-808

47 Witty, J. P., Lempka, T., Coffey, R. J., Jr., and Matrisian, L. M. Decreased tumor formation in 7,12-dimethylbenzanthracene-treated stromelysin-1 transgenic mice is associated with alterations in mammary epithelial cell apoptosis (1995) *Cancer Res.* **55** 1401-1406

48 Coussens, L. M., Tinkle, C. L., Hanahan, D., and Werb, Z. MMP-9 supplied by bone marrow-derived cells contributes to skin carcinogenesis (2000) *Cell* **103** 481-490

49 Andarawewa, K. L., Boulay, A., Masson, R., Mathelin, C., Stoll, I., Tomasetto, C., Chenard, M. P., Gintz, M., Bellocq, J. P., and Rio, M. C. Dual stromelysin-3 function during natural mouse mammary tumor virus-ras tumor progression (2003) *Cancer Res.* **63** 5844-5849

50 Pendas, A. M., Folgueras, A. R., Llano, E., Caterina, J., Frerard, F., Rodriguez, F., Astudillo, A., Noel, A., Birkedal-Hansen, H., and Lopez-Otin, C. Diet-induced obesity and reduced skin cancer susceptibility in matrix metalloproteinase 19-deficient mice (2004) *Mol. Cell. Biol.* **24** 5304-5313

51 Jost, M., Folgueras, A. R., Frerart, F., Pendas, A. M., Blacher, S., Houard, X., Berndt, S., Munaut, C., Cataldo, D., Alvarez, J., Melen-Lamalle, L., Foidart, J. M., Lopez-Otin, C., and Noel, A. Earlier onset of tumoral angiogenesis in matrix metalloproteinase-19-deficient mice (2006) *Cancer Res.* **66** 5234-5241

52 Egeblad, M., and Werb, Z. New functions for the matrix metalloproteinases in cancer progression (2002) *Nat. Rev. Cancer* **2** 161-174

53 Overall, C. M., and Lopez-Otin, C. Strategies for MMP inhibition in cancer: innovations for the post-trial era (2002) *Nat. Rev. Cancer* **2** 657-672

54 Hu, J., Van den Steen, P. E., Sang, Q. X., and Opdenakker, G. Matrix metalloproteinase inhibitors as therapy for inflammatory and vascular diseases (2007) *Nature reviews* **6** 480-498

55 Itoh, T., Matsuda, H., Tanioka, M., Kuwabara, K., Itohara, S., and Suzuki, R. The role of matrix metalloproteinase-2 and matrix metalloproteinase-9 in antibody-induced arthritis (2002) *J. Immunol.* **169** 2643-2647

56 Clements, K. M., Price, J. S., Chambers, M. G., Visco, D. M., Poole, A. R., and Mason, R. M. Gene deletion of either interleukin-1beta, interleukin-1beta-converting enzyme, inducible nitric oxide synthase, or stromelysin 1 accelerates the development of knee osteoarthritis in mice after surgical transection of the medial collateral ligament and partial medial meniscectomy (2003) *Arthritis. Rheum.* **48** 3452-3463

57 Deguchi, J. O., Aikawa, E., Libby, P., Vachon, J. R., Inada, M., Krane, S. M., Whittaker, P., and Aikawa, M. Matrix metalloproteinase-13/collagenase-3 deletion promotes collagen accumulation and organization in mouse atherosclerotic plaques (2005) *Circulation* **112** 2708-2715

58 Silence, J., Lupu, F., Collen, D., and Lijnen, H. R. Persistence of atherosclerotic plaque but reduced aneurysm formation in mice with stromelysin-1 (MMP-3) gene inactivation (2001) *Arterioscler. Thromb. Vasc. Biol.* **21** 1440-1445

59 Luttun, A., Lutgens, E., Manderveld, A., Maris, K., Collen, D., Carmeliet, P., and Moons, L. Loss of matrix metalloproteinase-9 or matrix metalloproteinase-12 protects apolipoprotein E-deficient mice against atherosclerotic media destruction but differentially affects plaque growth (2004) *Circulation* **109** 1408-1414

60 Kuzuya, M., Nakamura, K., Sasaki, T., Cheng, X. W., Itohara, S., and Iguchi, A. Effect of MMP-2 deficiency on atherosclerotic lesion formation in apoE-deficient mice (2006) *Arterioscler. Thromb. Vasc. Biol.* **26** 1120-1125

61 Agrawal, S., Anderson, P., Durbeej, M., van Rooijen, N., Ivars, F., Opdenakker, G., and Sorokin, L. M. Dystroglycan is selectively cleaved at the parenchymal basement membrane at sites of leukocyte extravasation in experimental autoimmune encephalomyelitis (2006) *J. Exp. Med.* **203** 1007-1019

62 Folgueras, A. R., Fueyo, A., Garcia-Suarez, O., Cox, J., Astudillo, A., Tortorella, P., Campestre, C., Gutierrez-Fernandez, A., Fanjul-Fernandez, M., Pennington, C. J., Edwards, D. R., Overall, C. M., and Lopez-Otin, C. Collagenase-2 deficiency or inhibition impairs experimental autoimmune encephalomyelitis in mice (2008) *J. Biol. Chem.* **283** 9465-9474

63 Buhler, L. A., Samara, R., Guzman, E., Wilson, C. L., Krizanac-Bengez, L., Janigro, D., and Ethell, D. W. Matrix metalloproteinase-7 facilitates immune access to the CNS in experimental autoimmune encephalomyelitis (2009) *BMC Neurosci.* **10** 17

64 Weaver, A., Goncalves da Silva, A., Nuttall, R. K., Edwards, D. R., Shapiro, S. D., Rivest, S., and Yong, V. W. An elevated matrix metalloproteinase (MMP) in an animal model of multiple sclerosis is protective by affecting Th1/Th2 polarization (2005) *FASEB J.* **19** 1668-1670

65 Corry, D. B., Rishi, K., Kanellis, J., Kiss, A., Song Lz, L. Z., Xu, J., Feng, L., Werb, Z., and Kheradmand, F. Decreased allergic lung inflammatory cell egression and increased susceptibility to asphyxiation in MMP2-deficiency (2002) *Nat. Immunol.* **3** 347-353

66 Greenlee, K. J., Corry, D. B., Engler, D. A., Matsunami, R. K., Tessier, P., Cook, R. G., Werb, Z., and Kheradmand, F. Proteomic identification of in vivo substrates for matrix metalloproteinases 2 and 9 reveals a mechanism for resolution of inflammation (2006) *J. Immunol.* **177** 7312-7321

67 Gueders, M. M., Balbin, M., Rocks, N., Foidart, J. M., Gosset, P., Louis, R., Shapiro, S., Lopez-Otin, C., Noel, A., and Cataldo, D. D. Matrix metalloproteinase-8 deficiency promotes granulocytic allergen-induced airway inflammation (2005) *J. Immunol.* **175** 2589-2597

68 Kassim, S. Y., Gharib, S. A., Mecham, B. H., Birkland, T. P., Parks, W. C., and McGuire, J. K. Individual matrix metalloproteinases control distinct transcriptional responses in airway epithelial cells infected with Pseudomonas aeruginosa (2007) *Infect. Immun.* **75** 5640-5650

69 Hautamaki, R. D., Kobayashi, D. K., Senior, R. M., and Shapiro, S. D. Requirement for macrophage elastase for cigarette smoke-induced emphysema in mice (1997) *Science* **277** 2002-2004

70 Zuo, F., Kaminski, N., Eugui, E., Allard, J., Yakhini, Z., Ben-Dor, A., Lollini, L., Morris, D., Kim, Y., DeLustro, B., Sheppard, D., Pardo, A., Selman, M., and Heller, R. A. Gene expression analysis reveals matrilysin as a key regulator of pulmonary fibrosis in mice and humans (2002) *Proc. Natl. Acad. Sci. U. S. A.* **99** 6292-6297

71 Kruger, A. Functional genetic mouse models: promising tools for investigation of the proteolytic internet (2009) *Biol. Chem.* **390** 91-97

72 Goldberg, G. I., Wilhelm, S. M., Kronberger, A., Bauer, E. A., Grant, G. A., and Eisen, A. Z. Human fibroblast collagenase. Complete primary structure and homology to an oncogene transformation-induced rat protein (1986) *J. Biol. Chem.* **261** 6600-6605

73 Pardo, A., and Selman, M. MMP-1: the elder of the family (2005) *Int. J. Biochem. Cell Biol.* **37** 283-288

74 Ala-aho, R., and Kahari, V. M. Collagenases in cancer (2005) *Biochimie* **87** 273-286

75 Poulalhon, N., Farge, D., Roos, N., Tacheau, C., Neuzillet, C., Michel, L., Mauviel, A., and Verrecchia, F. Modulation of collagen and MMP-1 gene expression in fibroblasts by the immunosuppressive drug rapamycin. A direct role as an antifibrotic agent? (2006) *J. Biol. Chem.* **281** 33045-33052

76 Takeuchi, T., Iwasaki, S., Miyazaki, J., Nozaki, Y., Takahashi, M., Ono, M., Saibara, T., and Furihata, M. Matrix metalloproteinase-1 expression in splenic angiosarcoma metastasizing to the serous membrane (2010) *Int J Clin Exp Pathol* **3** 634-639

77 Hadler-Olsen, E., Fadnes, B., Sylte, I., Uhlin-Hansen, L., and Winberg, J. O. Regulation of matrix metalloproteinase activity in health and disease (2011) *FEBS J.* **278** 28-45

78 Zinzindohoue, F., Lecomte, T., Ferraz, J. M., Houllier, A. M., Cugnenc, P. H., Berger, A., Blons, H., and Laurent-Puig, P. Prognostic significance of

MMP-1 and MMP-3 functional promoter polymorphisms in colorectal cancer (2005) *Clin Cancer Res* **11** 594-599

79 Bradbury, P. A., Zhai, R., Hopkins, J., Kulke, M. H., Heist, R. S., Singh, S., Zhou, W., Ma, C., Xu, W., Asomaning, K., Ter-Minassian, M., Wang, Z., Su, L., Christiani, D. C., and Liu, G. Matrix metalloproteinase 1, 3 and 12 polymorphisms and esophageal adenocarcinoma risk and prognosis (2009) *Carcinogenesis* **30** 793-798

80 Nikkola, J., Vihinen, P., Vlaykova, T., Hahka-Kemppinen, M., Kahari, V. M., and Pyrhonen, S. High expression levels of collagenase-1 and stromelysin-1 correlate with shorter disease-free survival in human metastatic melanoma (2002) *Int. J. Cancer* **97** 432-438

81 Zhu, Y., Spitz, M. R., Lei, L., Mills, G. B., and Wu, X. A single nucleotide polymorphism in the matrix metalloproteinase-1 promoter enhances lung cancer susceptibility (2001) *Cancer Res.* **61** 7825-7829

82 Przybylowska, K., Zielinska, J., Zadrozny, M., Krawczyk, T., Kulig, A., Wozniak, P., Rykala, J., Kolacinska, A., Morawiec, Z., Drzewoski, J., and Blasiak, J. An association between the matrix metalloproteinase 1 promoter gene polymorphism and lymphnode metastasis in breast cancer (2004) *J Exp Clin Cancer Res* **23** 121-125

83 Gupta, G. P., Nguyen, D. X., Chiang, A. C., Bos, P. D., Kim, J. Y., Nadal, C., Gomis, R. R., Manova-Todorova, K., and Massague, J. Mediators of vascular remodelling co-opted for sequential steps in lung metastasis (2007) *Nature* **446** 765-770

84 Freije, J. M., Diez-Itza, I., Balbin, M., Sanchez, L. M., Blasco, R., Tolivia, J., and Lopez-Otin, C. Molecular cloning and expression of collagenase-3, a novel human matrix metalloproteinase produced by breast carcinomas (1994) *J. Biol. Chem.* **269** 16766-16773

85 Balbin, M., Fueyo, A., Knauper, V., Lopez, J. M., Alvarez, J., Sanchez, L. M., Quesada, V., Bordallo, J., Murphy, G., and Lopez-Otin, C. Identification and enzymatic characterization of two diverging murine counterparts of human interstitial collagenase (MMP-1) expressed at sites of embryo implantation (2001) *J. Biol. Chem.* **276** 10253-10262

86 Golomb, H. M., Vardiman, J. W., Rowley, J. D., Testa, J. R., and Mintz, U. Correlation of clinical findings with quinacrine-banded chromosomes in 90 adults with acute nonlymphocytic leukemia: an eight-year study (1970-1977) (1978) *N. Engl. J. Med.* **299** 613-619

87 Ley, T. J., Mardis, E. R., Ding, L., Fulton, B., McLellan, M. D., Chen, K., Dooling, D., Dunford-Shore, B. H., McGrath, S., Hickenbotham, M., Cook, L., Abbott, R., Larson, D. E., Koboldt, D. C., Pohl, C., Smith, S., Hawkins, A., Abbott, S., Locke, D., Hillier, L. W., Miner, T., Fulton, L., Magrini, V., Wylie, T., Glasscock, J., Conyers, J., Sander, N., Shi, X., Osborne, J. R., Minx, P., Gordon, D., Chinwalla, A., Zhao, Y., Ries, R. E., Payton, J. E., Westervelt, P., Tomasson, M. H., Watson, M., Baty, J., Ivanovich, J., Heath, S., Shannon, W. D., Nagarajan, R., Walter, M. J., Link, D. C., Graubert, T. A., DiPersio, J. F., and Wilson, R. K. DNA sequencing of a cytogenetically normal acute myeloid leukaemia genome (2008) *Nature* **456** 66-72

88 Hudson, T. J., Anderson, W., Artez, A., Barker, A. D., Bell, C., Bernabe, R. R., Bhan, M. K., Calvo, F., Eerola, I., Gerhard, D. S., Guttmacher, A.,

Guyer, M., Hemsley, F. M., Jennings, J. L., Kerr, D., Klatt, P., Kolar, P., Kusada, J., Lane, D. P., Laplace, F., Youyong, L., Nettekoven, G., Ozenberger, B., Peterson, J., Rao, T. S., Remacle, J., Schafer, A. J., Shibata, T., Stratton, M. R., Vockley, J. G., Watanabe, K., Yang, H., Yuen, M. M., Knoppers, B. M., Bobrow, M., Cambon-Thomsen, A., Dressler, L. G., Dyke, S. O., Joly, Y., Kato, K., Kennedy, K. L., Nicolas, P., Parker, M. J., Rial-Sebbag, E., Romeo-Casabona, C. M., Shaw, K. M., Wallace, S., Wiesner, G. L., Zeps, N., Lichter, P., Biankin, A. V., Chabannon, C., Chin, L., Clement, B., de Alava, E., Degos, F., Ferguson, M. L., Geary, P., Hayes, D. N., Johns, A. L., Kasprzyk, A., Nakagawa, H., Penny, R., Piris, M. A., Sarin, R., Scarpa, A., van de Vijver, M., Futreal, P. A., Aburatani, H., Bayes, M., Botwell, D. D., Campbell, P. J., Estivill, X., Grimmond, S. M., Gut, I., Hirst, M., Lopez-Otin, C., Majumder, P., Marra, M., McPherson, J. D., Ning, Z., Puente, X. S., Ruan, Y., Stunnenberg, H. G., Swerdlow, H., Velculescu, V. E., Wilson, R. K., Xue, H. H., Yang, L., Spellman, P. T., Bader, G. D., Boutros, P. C., Flicek, P., Getz, G., Guigo, R., Guo, G., Haussler, D., Heath, S., Hubbard, T. J., Jiang, T., Jones, S. M., Li, Q., Lopez-Bigas, N., Luo, R., Muthuswamy, L., Ouellette, B. F., Pearson, J. V., Quesada, V., Raphael, B. J., Sander, C., Speed, T. P., Stein, L. D., Stuart, J. M., Teague, J. W., Totoki, Y., Tsunoda, T., Valencia, A., Wheeler, D. A., Wu, H., Zhao, S., Zhou, G., Lathrop, M., Thomas, G., Yoshida, T., Axton, M., Gunter, C., Miller, L. J., Zhang, J., Haider, S. A., Wang, J., Yung, C. K., Cros, A., Liang, Y., Gnaneshan, S., Guberman, J., Hsu, J., Chalmers, D. R., Hasel, K. W., Kaan, T. S., Lowrance, W. W., Masui, T., Rodriguez, L. L., Vergely, C., Bowtell, D. D., Cloonan, N., deFazio, A., Eshleman, J. R., Etemadmoghadam, D., Gardiner, B. B., Kench, J. G., Sutherland, R. L., Tempero, M. A., Waddell, N. J., Wilson, P. J., Gallinger, S., Tsao, M. S., Shaw, P. A., Petersen, G. M., Mukhopadhyay, D., DePinho, R. A., Thayer, S., Shazand, K., Beck, T., Sam, M., Timms, L., Ballin, V., Lu, Y., Ji, J., Zhang, X., Chen, F., Hu, X., Yang, Q., Tian, G., Zhang, L., Xing, X., Li, X., Zhu, Z., Yu, Y., Yu, J., Tost, J., Brennan, P., Holcatova, I., Zaridze, D., Brazma, A., Egevard, L., Prokhortchouk, E., Banks, R. E., Uhlen, M., Viksna, J., Ponten, F., Skryabin, K., Birney, E., Borg, A., Borresen-Dale, A. L., Caldas, C., Foekens, J. A., Martin, S., Reis-Filho, J. S., Richardson, A. L., Sotiriou, C., Thoms, G., van't Veer, L., Birnbaum, D., Blanche, H., Boucher, P., Boyault, S., Masson-Jacquemier, J. D., Pauporte, I., Pivot, X., Vincent-Salomon, A., Tabone, E., Theillet, C., Treilleux, I., Bioulac-Sage, P., Decaens, T., Franco, D., Gut, M., Samuel, D., Zucman-Rossi, J., Eils, R., Brors, B., Korbel, J. O., Korshunov, A., Landgraf, P., Lehrach, H., Pfister, S., Radlwimmer, B., Reifenberger, G., Taylor, M. D., von Kalle, C., Majumder, P. P., Pederzoli, P., Lawlor, R. A., Delledonne, M., Bardelli, A., Gress, T., Klimstra, D., Zamboni, G., Nakamura, Y., Miyano, S., Fujimoto, A., Campo, E., de Sanjose, S., Montserrat, E., Gonzalez-Diaz, M., Jares, P., Himmelbauer, H., Bea, S., Aparicio, S., Easton, D. F., Collins, F. S., Compton, C. C., Lander, E. S., Burke, W., Green, A. R., Hamilton, S. R., Kallioniemi, O. P., Ley, T. J., Liu, E. T., and Wainwright, B. J. International network of cancer genome projects (2010) *Nature* **464** 993-998

89 Comprehensive genomic characterization defines human glioblastoma genes and core pathways (2008) *Nature* **455** 1061-1068

90 Sanger, F., Nicklen, S., and Coulson, A. R. DNA sequencing with chain-terminating inhibitors (1977) *Proc. Natl. Acad. Sci. U. S. A.* **74** 5463-5467

91 Meyerson, M., Gabriel, S., and Getz, G. Advances in understanding cancer genomes through second-generation sequencing (2010) *Nat. Rev. Genet.* **11** 685-696

92 Schadt, E. E., Turner, S., and Kasarskis, A. A window into third-generation sequencing (2010) *Hum. Mol. Genet.* **19** R227-240

93 Ward, P. S., Patel, J., Wise, D. R., Abdel-Wahab, O., Bennett, B. D., Coller, H. A., Cross, J. R., Fantin, V. R., Hedvat, C. V., Perl, A. E., Rabinowitz, J. D., Carroll, M., Su, S. M., Sharp, K. A., Levine, R. L., and Thompson, C. B. The common feature of leukemia-associated IDH1 and IDH2 mutations is a neomorphic enzyme activity converting alpha-ketoglutarate to 2-hydroxyglutarate (2010) *Cancer Cell* **17** 225-234

94 Ley, T. J., Ding, L., Walter, M. J., McLellan, M. D., Lamprecht, T., Larson, D. E., Kandoth, C., Payton, J. E., Baty, J., Welch, J., Harris, C. C., Lichti, C. F., Townsend, R. R., Fulton, R. S., Dooling, D. J., Koboldt, D. C., Schmidt, H., Zhang, Q., Osborne, J. R., Lin, L., O'Laughlin, M., McMichael, J. F., Delehaunty, K. D., McGrath, S. D., Fulton, L. A., Magrini, V. J., Vickery, T. L., Hundal, J., Cook, L. L., Conyers, J. J., Swift, G. W., Reed, J. P., Alldredge, P. A., Wylie, T., Walker, J., Kalicki, J., Watson, M. A., Heath, S., Shannon, W. D., Varghese, N., Nagarajan, R., Westervelt, P., Tomasson, M. H., Link, D. C., Graubert, T. A., DiPersio, J. F., Mardis, E. R., and Wilson, R. K. DNMT3A mutations in acute myeloid leukemia (2010) *N. Engl. J. Med.* **363** 2424-2433

95 Mardis, E. R., Ding, L., Dooling, D. J., Larson, D. E., McLellan, M. D., Chen, K., Koboldt, D. C., Fulton, R. S., Delehaunty, K. D., McGrath, S. D., Fulton, L. A., Locke, D. P., Magrini, V. J., Abbott, R. M., Vickery, T. L., Reed, J. S., Robinson, J. S., Wylie, T., Smith, S. M., Carmichael, L., Eldred, J. M., Harris, C. C., Walker, J., Peck, J. B., Du, F., Dukes, A. F., Sanderson, G. E., Brummett, A. M., Clark, E., McMichael, J. F., Meyer, R. J., Schindler, J. K., Pohl, C. S., Wallis, J. W., Shi, X., Lin, L., Schmidt, H., Tang, Y., Haipek, C., Wiechert, M. E., Ivy, J. V., Kalicki, J., Elliott, G., Ries, R. E., Payton, J. E., Westervelt, P., Tomasson, M. H., Watson, M. A., Baty, J., Heath, S., Shannon, W. D., Nagarajan, R., Link, D. C., Walter, M. J., Graubert, T. A., DiPersio, J. F., Wilson, R. K., and Ley, T. J. Recurring mutations found by sequencing an acute myeloid leukemia genome (2009) *N. Engl. J. Med.* **361** 1058-1066

96 Pleasance, E. D., Stephens, P. J., O'Meara, S., McBride, D. J., Meynert, A., Jones, D., Lin, M. L., Beare, D., Lau, K. W., Greenman, C., Varela, I., Nik-Zainal, S., Davies, H. R., Ordonez, G. R., Mudie, L. J., Latimer, C., Edkins, S., Stebbings, L., Chen, L., Jia, M., Leroy, C., Marshall, J., Menzies, A., Butler, A., Teague, J. W., Mangion, J., Sun, Y. A., McLaughlin, S. F., Peckham, H. E., Tsung, E. F., Costa, G. L., Lee, C. C., Minna, J. D., Gazdar, A., Birney, E., Rhodes, M. D., McKernan, K. J., Stratton, M. R., Futreal, P. A., and Campbell, P. J. A small-cell lung cancer genome with complex signatures of tobacco exposure (2010) *Nature* **463** 184-190

97 Lee, W., Jiang, Z., Liu, J., Haverty, P. M., Guan, Y., Stinson, J., Yue, P., Zhang, Y., Pant, K. P., Bhatt, D., Ha, C., Johnson, S., Kennemer, M. I., Mohan, S., Nazarenko, I., Watanabe, C., Sparks, A. B., Shames, D. S., Gentleman, R., de Sauvage, F. J., Stern, H., Pandita, A., Ballinger, D. G., Drmanac, R., Modrusan, Z., Seshagiri, S., and Zhang, Z. The mutation spectrum revealed by paired genome sequences from a lung cancer patient (2010) *Nature* **465** 473-477

98 Taylor, B. S., Schultz, N., Hieronymus, H., Gopalan, A., Xiao, Y., Carver, B. S., Arora, V. K., Kaushik, P., Cerami, E., Reva, B., Antipin, Y., Mitsiades, N., Landers, T., Dolgalev, I., Major, J. E., Wilson, M., Socci, N. D., Lash, A. E., Heguy, A., Eastham, J. A., Scher, H. I., Reuter, V. E., Scardino, P. T., Sander, C., Sawyers, C. L., and Gerald, W. L. Integrative genomic profiling of human prostate cancer (2010) *Cancer Cell* **18** 11-22

99 Stephens, P. J., Tarpey, P. S., Davies, H., Van Loo, P., Greenman, C., Wedge, D. C., Nik-Zainal, S., Martin, S., Varela, I., Bignell, G. R., Yates, L. R., Papaemmanuil, E., Beare, D., Butler, A., Cheverton, A., Gamble, J., Hinton, J., Jia, M., Jayakumar, A., Jones, D., Latimer, C., Lau, K. W., McLaren, S., McBride, D. J., Menzies, A., Mudie, L., Raine, K., Rad, R., Chapman, M. S., Teague, J., Easton, D., Langerod, A., Lee, M. T., Shen, C. Y., Tee, B. T., Huimin, B. W., Broeks, A., Vargas, A. C., Turashvili, G., Martens, J., Fatima, A., Miron, P., Chin, S. F., Thomas, G., Boyault, S., Mariani, O., Lakhani, S. R., van de Vijver, M., van 't Veer, L., Foekens, J., Desmedt, C., Sotiriou, C., Tutt, A., Caldas, C., Reis-Filho, J. S., Aparicio, S. A., Salomon, A. V., Borresen-Dale, A. L., Richardson, A. L., Campbell, P. J., Futreal, P. A., and Stratton, M. R. The landscape of cancer genes and mutational processes in breast cancer (2012) *Nature* **486** 400-404

100 Puente, X. S., Pinyol, M., Quesada, V., Conde, L., Ordonez, G. R., Villamor, N., Escaramis, G., Jares, P., Bea, S., Gonzalez-Diaz, M., Bassaganyas, L., Baumann, T., Juan, M., Lopez-Guerra, M., Colomer, D., Tubio, J. M., Lopez, C., Navarro, A., Tornador, C., Aymerich, M., Rozman, M., Hernandez, J. M., Puente, D. A., Freije, J. M., Velasco, G., Gutierrez-Fernandez, A., Costa, D., Carrio, A., Guijarro, S., Enjuanes, A., Hernandez, L., Yague, J., Nicolas, P., Romeo-Casabona, C. M., Himmelbauer, H., Castillo, E., Dohm, J. C., de Sanjose, S., Piris, M. A., de Alava, E., San Miguel, J., Royo, R., Gelpi, J. L., Torrents, D., Orozco, M., Pisano, D. G., Valencia, A., Guigo, R., Bayes, M., Heath, S., Gut, M., Klatt, P., Marshall, J., Raine, K., Stebbings, L. A., Futreal, P. A., Stratton, M. R., Campbell, P. J., Gut, I., Lopez-Guillermo, A., Estivill, X., Montserrat, E., Lopez-Otin, C., and Campo, E. Whole-genome sequencing identifies recurrent mutations in chronic lymphocytic leukaemia (2011) *Nature* **475** 101-105

101 Turner, E. H., Lee, C., Ng, S. B., Nickerson, D. A., and Shendure, J. Massively parallel exon capture and library-free resequencing across 16 genomes (2009) *Nat Methods* **6** 315-316

102 Liu, X., Wang, J., and Chen, L. Whole-exome sequencing reveals recurrent somatic mutation networks in cancer (2012) *Cancer Lett.*

103 Quesada, V., Conde, L., Villamor, N., Ordonez, G. R., Jares, P., Bassaganyas, L., Ramsay, A. J., Bea, S., Pinyol, M., Martinez-Trillos, A., Lopez-Guerra, M., Colomer, D., Navarro, A., Baumann, T., Aymerich, M.,

Rozman, M., Delgado, J., Gine, E., Hernandez, J. M., Gonzalez-Diaz, M., Puente, D. A., Velasco, G., Freije, J. M., Tubio, J. M., Royo, R., Gelpi, J. L., Orozco, M., Pisano, D. G., Zamora, J., Vazquez, M., Valencia, A., Himmelbauer, H., Bayes, M., Heath, S., Gut, M., Gut, I., Estivill, X., Lopez-Guillermo, A., Puente, X. S., Campo, E., and Lopez-Otin, C. Exome sequencing identifies recurrent mutations of the splicing factor SF3B1 gene in chronic lymphocytic leukemia (2012) *Nat. Genet.* **44** 47-52

104 Ding, L., Ellis, M. J., Li, S., Larson, D. E., Chen, K., Wallis, J. W., Harris, C. C., McLellan, M. D., Fulton, R. S., Fulton, L. L., Abbott, R. M., Hoog, J., Dooling, D. J., Koboldt, D. C., Schmidt, H., Kalicki, J., Zhang, Q., Chen, L., Lin, L., Wendl, M. C., McMichael, J. F., Magrini, V. J., Cook, L., McGrath, S. D., Vickery, T. L., Appelbaum, E., Deschryver, K., Davies, S., Guintoli, T., Crowder, R., Tao, Y., Snider, J. E., Smith, S. M., Dukes, A. F., Sanderson, G. E., Pohl, C. S., Delehaunty, K. D., Fronick, C. C., Pape, K. A., Reed, J. S., Robinson, J. S., Hodges, J. S., Schierding, W., Dees, N. D., Shen, D., Locke, D. P., Wiechert, M. E., Eldred, J. M., Peck, J. B., Oberkfell, B. J., Lolofie, J. T., Du, F., Hawkins, A. E., O'Laughlin, M. D., Bernard, K. E., Cunningham, M., Elliott, G., Mason, M. D., Thompson, D. M., Jr., Ivanovich, J. L., Goodfellow, P. J., Perou, C. M., Weinstock, G. M., Aft, R., Watson, M., Ley, T. J., Wilson, R. K., and Mardis, E. R. Genome remodelling in a basal-like breast cancer metastasis and xenograft (2010) *Nature* **464** 999-1005

105 Yachida, S., Jones, S., Bozic, I., Antal, T., Leary, R., Fu, B., Kamiyama, M., Hruban, R. H., Eshleman, J. R., Nowak, M. A., Velculescu, V. E., Kinzler, K. W., Vogelstein, B., and Iacobuzio-Donahue, C. A. Distant metastasis occurs late during the genetic evolution of pancreatic cancer (2010) *Nature* **467** 1114-1117

106 Jemal, A., Siegel, R., Ward, E., Hao, Y., Xu, J., Murray, T., and Thun, M. J. Cancer statistics, 2008 (2008) *CA Cancer J Clin* **58** 71-96

107 Gillison, M. L., and Lowy, D. R. A causal role for human papillomavirus in head and neck cancer (2004) *Lancet* **363** 1488-1489

108 Sturgis, E. M., and Cinciripini, P. M. Trends in head and neck cancer incidence in relation to smoking prevalence: an emerging epidemic of human papillomavirus-associated cancers? (2007) *Cancer* **110** 1429-1435

109 Woolgar, J. A., and Triantafyllou, A. Pitfalls and procedures in the histopathological diagnosis of oral and oropharyngeal squamous cell carcinoma and a review of the role of pathology in prognosis (2009) *Oral Oncol.* **45** 361-385

110 van Houten, V. M., Snijders, P. J., van den Brekel, M. W., Kummer, J. A., Meijer, C. J., van Leeuwen, B., Denkers, F., Smeele, L. E., Snow, G. B., and Brakenhoff, R. H. Biological evidence that human papillomaviruses are etiologically involved in a subgroup of head and neck squamous cell carcinomas (2001) *Int. J. Cancer* **93** 232-235

111 Wiest, T., Schwarz, E., Enders, C., Flechtenmacher, C., and Bosch, F. X. Involvement of intact HPV16 E6/E7 gene expression in head and neck cancers with unaltered p53 status and perturbed pRb cell cycle control (2002) *Oncogene* **21** 1510-1517

112 Leemans, C. R., Braakhuis, B. J., and Brakenhoff, R. H. The molecular biology of head and neck cancer (2011) *Nat. Rev. Cancer* **11** 9-22

113 Haddad, R. I., and Shin, D. M. Recent advances in head and neck cancer (2008) *N. Engl. J. Med.* **359** 1143-1154

114 Poeta, M. L., Manola, J., Goldwasser, M. A., Forastiere, A., Benoit, N., Califano, J. A., Ridge, J. A., Goodwin, J., Kenady, D., Saunders, J., Westra, W., Sidransky, D., and Koch, W. M. TP53 mutations and survival in squamous-cell carcinoma of the head and neck (2007) *N. Engl. J. Med.* **357** 2552-2561

115 Reed, A. L., Califano, J., Cairns, P., Westra, W. H., Jones, R. M., Koch, W., Ahrendt, S., Eby, Y., Sewell, D., Nawroz, H., Bartek, J., and Sidransky, D. High frequency of p16 (CDKN2/MTS-1/INK4A) inactivation in head and neck squamous cell carcinoma (1996) *Cancer Res.* **56** 3630-3633

116 Pedrero, J. M., Carracedo, D. G., Pinto, C. M., Zapatero, A. H., Rodrigo, J. P., Nieto, C. S., and Gonzalez, M. V. Frequent genetic and biochemical alterations of the PI 3-K/AKT/PTEN pathway in head and neck squamous cell carcinoma (2005) *Int. J. Cancer* **114** 242-248

117 Braakhuis, B. J., Tabor, M. P., Kummer, J. A., Leemans, C. R., and Brakenhoff, R. H. A genetic explanation of Slaughter's concept of field cancerization: evidence and clinical implications (2003) *Cancer Res.* **63** 1727-1730

118 Virgilio, L., Shuster, M., Gollin, S. M., Veronese, M. L., Ohta, M., Huebner, K., and Croce, C. M. FHIT gene alterations in head and neck squamous cell carcinomas (1996) *Proc. Natl. Acad. Sci. U. S. A.* **93** 9770-9775

119 Qiu, W., Schonleben, F., Li, X., and Su, G. H. Disruption of transforming growth factor beta-Smad signaling pathway in head and neck squamous cell carcinoma as evidenced by mutations of SMAD2 and SMAD4 (2007) *Cancer Lett.* **245** 163-170

120 Morris, L. G., Taylor, B. S., Bivona, T. G., Gong, Y., Eng, S., Brennan, C. W., Kaufman, A., Kastenhuber, E. R., Banuchi, V. E., Singh, B., Heguy, A., Viale, A., Mellinghoff, I. K., Huse, J., Ganly, I., and Chan, T. A. Genomic dissection of the epidermal growth factor receptor (EGFR)/PI3K pathway reveals frequent deletion of the EGFR phosphatase PTPRS in head and neck cancers (2011) *Proc. Natl. Acad. Sci. U. S. A.* **108** 19024-19029

121 Smeets, S. J., Braakhuis, B. J., Abbas, S., Snijders, P. J., Ylstra, B., van de Wiel, M. A., Meijer, G. A., Leemans, C. R., and Brakenhoff, R. H. Genome-wide DNA copy number alterations in head and neck squamous cell carcinomas with or without oncogene-expressing human papillomavirus (2006) *Oncogene* **25** 2558-2564

122 Lopez, F., Llorente, J. L., Oviedo, C. M., Vivanco, B., Marcos, C. A., Garcia-Inclan, C., Scola, B., and Hermsen, M. A. Gene amplification and protein overexpression of EGFR and ERBB2 in sinonasal squamous cell carcinoma (2012) *Cancer* **118** 1818-1826

123 Grandis, J. R., and Tweardy, D. J. Elevated levels of transforming growth factor alpha and epidermal growth factor receptor messenger RNA are early markers of carcinogenesis in head and neck cancer (1993) *Cancer Res.* **53** 3579-3584

124 Murugan, A. K., Hong, N. T., Fukui, Y., Munirajan, A. K., and Tsuchida, N. Oncogenic mutations of the PIK3CA gene in head and neck squamous cell carcinomas (2008) *Int. J. Oncol.* **32** 101-111

125 Tanaka, N., Odajima, T., Ogi, K., Ikeda, T., and Satoh, M. Expression of E-cadherin, alpha-catenin, and beta-catenin in the process of lymph node metastasis in oral squamous cell carcinoma (2003) *Br. J. Cancer* **89** 557-563

126 Shintani, S., Li, C., Mihara, M., Nakashiro, K., and Hamakawa, H. Gefitinib ('Iressa'), an epidermal growth factor receptor tyrosine kinase inhibitor, mediates the inhibition of lymph node metastasis in oral cancer cells (2003) *Cancer Lett.* **201** 149-155

127 George, A., Ranganathan, K., and Rao, U. K. Expression of MMP-1 in histopathological different grades of oral squamous cell carcinoma and in normal buccal mucosa - an immunohistochemical study (2010) *Cancer Biomark* **7** 275-283

128 Yu, T., Wu, Y., Helman, J. I., Wen, Y., Wang, C., and Li, L. CXCR4 promotes oral squamous cell carcinoma migration and invasion through inducing expression of MMP-9 and MMP-13 via the ERK signaling pathway (2011) *Mol. Cancer Res.* **9** 161-172

129 Bhave, S. L., Teknos, T. N., and Pan, Q. Molecular parameters of head and neck cancer metastasis (2011) *Crit. Rev. Eukaryot. Gene Expr.* **21** 143-153

130 Agrawal, N., Frederick, M. J., Pickering, C. R., Bettegowda, C., Chang, K., Li, R. J., Fakhry, C., Xie, T. X., Zhang, J., Wang, J., Zhang, N., El-Naggar, A. K., Jasser, S. A., Weinstein, J. N., Trevino, L., Drummond, J. A., Muzny, D. M., Wu, Y., Wood, L. D., Hruban, R. H., Westra, W. H., Koch, W. M., Califano, J. A., Gibbs, R. A., Sidransky, D., Vogelstein, B., Velculescu, V. E., Papadopoulos, N., Wheeler, D. A., Kinzler, K. W., and Myers, J. N. Exome sequencing of head and neck squamous cell carcinoma reveals inactivating mutations in NOTCH1 (2011) *Science* **333** 1154-1157

131 Stransky, N., Egloff, A. M., Tward, A. D., Kostic, A. D., Cibulskis, K., Sivachenko, A., Kryukov, G. V., Lawrence, M. S., Sougnez, C., McKenna, A., Shefler, E., Ramos, A. H., Stojanov, P., Carter, S. L., Voet, D., Cortes, M. L., Auclair, D., Berger, M. F., Saksena, G., Guiducci, C., Onofrio, R. C., Parkin, M., Romkes, M., Weissfeld, J. L., Seethala, R. R., Wang, L., Rangel-Escareno, C., Fernandez-Lopez, J. C., Hidalgo-Miranda, A., Melendez-Zajgla, J., Winckler, W., Ardlie, K., Gabriel, S. B., Meyerson, M., Lander, E. S., Getz, G., Golub, T. R., Garraway, L. A., and Grandis, J. R. The mutational landscape of head and neck squamous cell carcinoma (2011) *Science* **333** 1157-1160

132 Muller, M., Beck, I. M., Gadesmann, J., Karschuk, N., Paschen, A., Proksch, E., Djonov, V., Reiss, K., and Sedlacek, R. MMP19 is upregulated during melanoma progression and increases invasion of melanoma cells (2010) *Mod. Pathol.* **23** 511-521

133 Impola, U., Jeskanen, L., Ravanti, L., Syrjanen, S., Baldursson, B., Kahari, V. M., and Saarialho-Kere, U. Expression of matrix metalloproteinase (MMP)-7 and MMP-13 and loss of MMP-19 and p16 are associated with malignant progression in chronic wounds (2005) *Br. J. Dermatol.* **152** 720-726

134 Bister, V. O., Salmela, M. T., Karjalainen-Lindsberg, M. L., Uria, J., Lohi, J., Puolakkainen, P., Lopez-Otin, C., and Saarialho-Kere, U. Differential expression of three matrix metalloproteinases, MMP-19, MMP-26, and

MMP-28, in normal and inflamed intestine and colon cancer (2004) *Dig. Dis. Sci.* **49** 653-661

135 Chan KC, K. J., Lung HL, Sedlacek R, Zhang ZF, Luo DZ, Feng ZB, Chen S, Chen H, Chan KW, Tsao SW, Chua DT, Zabarovsky ER, Stanbridge EJ, Lung ML. Catalytic activity of matrix metalloproteinase-19 is essential for tumor suppressor and anti-angiogenic activities in nasopharyngeal carcinoma. (2010) *Int. J. Cancer*

136 Brinckerhoff, C. E., Rutter, J. L., and Benbow, U. Interstitial collagenases as markers of tumor progression (2000) *Clin Cancer Res* **6** 4823-4830

137 Anand, M., Van Meter, T. E., and Fillmore, H. L. Epidermal growth factor induces matrix metalloproteinase-1 (MMP-1) expression and invasion in glioma cell lines via the MAPK pathway (2011) *J Neurooncol* **104** 679-687

138 Fanjul-Fernandez, M., Folgueras, A. R., Cabrera, S., and Lopez-Otin, C. Matrix metalloproteinases: evolution, gene regulation and functional analysis in mouse models (2010) *Biochim. Biophys. Acta* **1803** 3-19

139 Foley, C. J., Luo, C., O'Callaghan, K., Hinds, P. W., Covic, L., and Kuliopulos, A. Matrix metalloprotease-1a promotes tumorigenesis and metastasis (2012) *J. Biol. Chem.* **287** 24330-24338

140 Lu, X., Wang, Q., Hu, G., Van Poznak, C., Fleisher, M., Reiss, M., Massague, J., and Kang, Y. ADAMTS1 and MMP1 proteolytically engage EGF-like ligands in an osteolytic signaling cascade for bone metastasis (2009) *Genes Dev.* **23** 1882-1894

141 Blackburn, J. S., Rhodes, C. H., Coon, C. I., and Brinckerhoff, C. E. RNA interference inhibition of matrix metalloproteinase-1 prevents melanoma metastasis by reducing tumor collagenase activity and angiogenesis (2007) *Cancer Res.* **67** 10849-10858

142 Trivedi, V., Boire, A., Tchernychev, B., Kaneider, N. C., Leger, A. J., O'Callaghan, K., Covic, L., and Kuliopulos, A. Platelet matrix metalloprotease-1 mediates thrombogenesis by activating PAR1 at a cryptic ligand site (2009) *Cell* **137** 332-343

143 Iida, J., and McCarthy, J. B. Expression of collagenase-1 (MMP-1) promotes melanoma growth through the generation of active transforming growth factor-beta (2007) *Melanoma Res.* **17** 205-213

144 Agarwal, A., Tressel, S. L., Kaimal, R., Balla, M., Lam, F. H., Covic, L., and Kuliopulos, A. Identification of a metalloprotease-chemokine signaling system in the ovarian cancer microenvironment: implications for antiangiogenic therapy (2010) *Cancer Res.* **70** 5880-5890

145 Wang, H. W., and Joyce, J. A. Alternative activation of tumor-associated macrophages by IL-4: priming for protumoral functions (2010) *Cell Cycle* **9** 4824-4835

146 Chen, Y., Akirav, E. M., Chen, W., Henegariu, O., Moser, B., Desai, D., Shen, J. M., Webster, J. C., Andrews, R. C., Mjalli, A. M., Rothlein, R., Schmidt, A. M., Clynes, R., and Herold, K. C. RAGE ligation affects T cell activation and controls T cell differentiation (2008) *J. Immunol.* **181** 4272-4278

147 Sandler, N. G., Mentink-Kane, M. M., Cheever, A. W., and Wynn, T. A. Global gene expression profiles during acute pathogen-induced pulmonary

inflammation reveal divergent roles for Th1 and Th2 responses in tissue repair (2003) *J. Immunol.* **171** 3655-3667

148 Shimizu, M., Shimamura, M., Owaki, T., Asakawa, M., Fujita, K., Kudo, M., Iwakura, Y., Takeda, Y., Luster, A. D., Mizuguchi, J., and Yoshimoto, T. Antiangiogenic and antitumor activities of IL-27 (2006) *J. Immunol.* **176** 7317-7324

149 Van Lint, P., and Libert, C. Chemokine and cytokine processing by matrix metalloproteinases and its effect on leukocyte migration and inflammation (2007) *J. Leukoc. Biol.* **82** 1375-1381

150 Chizzolini, C., Rezzonico, R., De Luca, C., Burger, D., and Dayer, J. M. Th2 cell membrane factors in association with IL-4 enhance matrix metalloproteinase-1 (MMP-1) while decreasing MMP-9 production by granulocyte-macrophage colony-stimulating factor-differentiated human monocytes (2000) *J. Immunol.* **164** 5952-5960

151 Godefroy, E., Manches, O., Dreno, B., Hochman, T., Rolnitzky, L., Labarriere, N., Guilloux, Y., Goldberg, J., Jotereau, F., and Bhardwaj, N. Matrix metalloproteinase-2 conditions human dendritic cells to prime inflammatory T(H)2 cells via an IL-12- and OX40L-dependent pathway (2011) *Cancer Cell* **19** 333-346

152 Yu, Q., and Stamenkovic, I. Cell surface-localized matrix metalloproteinase-9 proteolytically activates TGF-beta and promotes tumor invasion and angiogenesis (2000) *Genes Dev.* **14** 163-176

153 Saarinen, J., Welgus, H. G., Flizar, C. A., Kalkkinen, N., and Helin, J. N-glycan structures of matrix metalloproteinase-1 derived from human fibroblasts and from HT-1080 fibrosarcoma cells (1999) *Eur. J. Biochem.* **259** 829-840

154 Griffin, C. T., Srinivasan, Y., Zheng, Y.-W., Huang, W., and Coughlin, S. R. A Role for Thrombin Receptor Signaling in Endothelial Cells During Embryonic Development (2001) *Science* **293** 1666-1670

155 Goerge, T., Barg, A., Schnaeker, E.-M., Poppelmann, B., Shpacovitch, V., Rattenholl, A., Maaser, C., Luger, T. A., Steinhoff, M., and Schneider, S. W. Tumor-derived matrix metalloproteinase-1 targets endothelial proteinase-activated receptor 1 promoting endothelial cell activation (2006) *Cancer Res.* **66** 7766-7774

156 Blackburn, J. S., and Brinckerhoff, C. E. Matrix metalloproteinase-1 and thrombin differentially activate gene expression in endothelial cells via PAR-1 and promote angiogenesis (2008) *Am. J. Pathol.* **173** 1736-1746

157 Agarwal, A., Tressel, S. L., Kaimal, R., Balla, M., Lam, F. H., Covic, L., and Kuliopulos, A. Identification of a metalloprotease-chemokine signaling system in the ovarian cancer microenvironment: implications for antiangiogenic therapy (2010) *Cancer Research* **70** 5880-5890

158 Stratton, M. R. Exploring the genomes of cancer cells: progress and promise (2011) *Science* **331** 1553-1558

159 Hoffman, H. T., Porter, K., Karnell, L. H., Cooper, J. S., Weber, R. S., Langer, C. J., Ang, K. K., Gay, G., Stewart, A., and Robinson, R. A. Laryngeal cancer in the United States: changes in demographics, patterns of care, and survival (2006) *Laryngoscope* **116** 1-13

160 Fang, D., Hawke, D., Zheng, Y., Xia, Y., Meisenhelder, J., Nika, H., Mills, G. B., Kobayashi, R., Hunter, T., and Lu, Z. Phosphorylation of beta-catenin by AKT promotes beta-catenin transcriptional activity (2007) *J. Biol. Chem.* **282** 11221-11229

161 Liu, P., Yang, J., Pei, J., Pei, D., and Wilson, M. J. Regulation of MT1-MMP activity by beta-catenin in MDCK non-cancer and HT1080 cancer cells (2010) *J. Cell. Physiol.* **225** 810-821

162 Brabletz, T., Jung, A., Dag, S., Reu, S., and Kirchner, T. [beta-Catenin induces invasive growth by activating matrix metalloproteinases in colorectal carcinoma] (2000) *Verh Dtsch Ges Pathol* **84** 175-181

163 Pan, F. Y., Zhang, S. Z., Xu, N., Meng, F. L., Zhang, H. X., Xue, B., Han, X., and Li, C. J. Beta-catenin signaling involves HGF-enhanced HepG2 scattering through activating MMP-7 transcription (2010) *Histochem. Cell Biol.* **134** 285-295

164 Tojkander, S., Gateva, G., and Lappalainen, P. Actin stress fibers--assembly, dynamics and biological roles (2012) *J. Cell Sci.* **125** 1855-1864